Discovery and characterisation of host-factors involved in Zika virus infection

University of Glasgow

Jamie Royle, BSc, MBiol

Submitted in the fulfilment for the degree of Doctor of Philosophy in Virology.

MRC-University of Glasgow Centre for Virus Research
Institute of Infection, Immunity and Inflammation
College of Medical, Veterinary and Life Sciences
University of Glasgow

MRC Medical Research Council

University of Glasgow

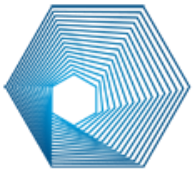

CVR Medical Research Council University of Glasgow Centre for Virus Research

Abstract

Zika virus (ZIKV, *Flaviviridae*), like other emerging arboviruses, poses a considerable threat to human health. It is estimated that approximately half of the world's population is at risk from contracting a mosquito-borne arboviral infection, and this was exemplified during the 2015/16 ZIKV outbreak in the Americas. ZIKV infection is thought to be largely asymptomatic, although ZIKV disease has previously been characterised by mild symptoms such as a maculopapular rash, conjunctivitis, and fever. However, recent outbreaks have been associated with an increased incidence of Guillain-Barré syndrome, and a pattern of neurological and developmental symptoms in neonates which is now termed congenital Zika syndrome. Despite intense efforts, no therapeutic or vaccine has been developed. As such, it is vital that further fundamental research is conducted to discover novel host-virus interactions in both vector and mammalian host systems, which may allow development of targeted interventions.

Here, multiple approaches were used to generate basic tools for ZIKV research, and siRNA screens and data from mass-spectrometry based proteomics were utilised to uncover important host interactors of ZIKV. A study investigating the *Aedes aegypti* immune response was conducted, and the classical RNAi effector Argonaute 2 (Ago2) was not found to be antiviral, whereas PIWI 4 was. Data from a previous proteomics experiment suggested that glucose-regulated protein 78 kDa (GRP78) may interact with ZIKV E. In this study, co-immunoprecipitation and immunofluorescence was used to verify that GRP78 interacts with ZIKV E in both mammalian and *Aedes aegypti* cell culture. GRP78 is a key modulator of the unfolded protein response (UPR), and while small-molecule inhibitors (EGCG and HNK) of the GRP78-mediated UPR did not inhibit ZIKV infection, EGCG was able to inhibit ZIKV entry independent of GRP78, likely through direct binding of the virion. Further study of GRP78 revealed that while it is not important for entry, replication, or egress of ZIKV, it did aid viral translation. Depletion of GRP78 with siRNA resulted in a loss of coordination of viral replication factories and relieved

a virus-specific inhibition of host translation. Furthermore, STRING analysis of GRP78 host-interactors followed by a targeted siRNA screen revealed that DnaJC1 is also a pro-viral factor. DnaJC1 has previously been shown to coordinate GRP78 localisation to ribosome exit tunnels, and so may contribute to ZIKV infection through GRP78, though this was not assessed in this study. Additionally, by using a circular polymerase extension reaction (CPER) system, a reverse genetics ZIKV was generated. This CPER ZIKV represents a genetically stable source of virus which can be easily modified and can support future research.

Collectively, the data herein informs on important ZIKV interactions in both arthropod vector and mammalian systems, and highlights tools and techniques that can be used to conduct future fundamental ZIKV research.

Table of Contents

List of Tables

List of Figures

Abbreviations

A - Alanine
aa – amino acids
Ago2 - Argonaute 2
Arbovirus - Arthropod borne virus
ATF6 - activating transcription factor 6α/ß
ATPase - adenosine triphosphatase
BiP - binding immunoglobulin protein
BVDV – Bovine viral diarrhoea virus
C - capsid
CA – capsid anchor
CHIKV - chikungunya
CID - collision-induced dissociation
CLR – C-type lectin receptors
CPE - cytopathic effects
CPER - circular polymerase extension reaction
CPIV3 - caprine-parainfluenza virus type 3
CS – circularisation signal
CZS - congenital Zika syndrome
Dcr2 - Dicer 2
DC-SIGN - dendritic cell-specific intercellular adhesion molecule-grabbing nonintegrin
DC-SIGNR - DC-SIGN related protein
DCX - doublecortin
DENV – dengue virus
DMEM - Dulbecco Modified Eagle Medium
DMSO - Dimethyl sulphoxide
dsRNA - double-stranded RNA
E – envelope
ED - ectodomains
EGCG - Epigallocatechin gallate
ER - Endoplasmic Reticulum
ERdj1 - ER j domain protein 1
ERN1 - endoplasmic reticulum to nucleus signalling 1
ERSE - ER stress element
ESI - electrospray ionisation
MAP3K - mitogen-activated protein 3x kinase
me^7 – N^7 methylated
MERS - Middle East respiratory syndrome
miRNA - microRNA
MS/MS - Tandem mass spectrometry
MTJ1 - mouse tumour cell DnaJ-like protein 1
N - Asparagine
NA - neuraminidase
Nanoluc - Nanoluciferase
NBD - nucleotide-binding domain
NCAM-1 - Neural Cell Adhesion Molecule 1
NEAA - Non-essential amino acids
NPCs – neuronal progenitor cells
NPro - N-terminal protease
NS – non-structural
$NS3^{hel}$ - NS3 helicase
nt - nucleotide
OASL - Oligoadenylate synthase-like
Opti-MEM - Opti-Minimum Essential Medium
ORF – open reading frame
PAHO - Pan-American health organisation
PBS - Phosphate buffered saline
PDB - Protein data bank
PEI - Polyethyleneimine
PERK - PKR-like ER kinase
PFA - Paraformaldehyde
PHTs - primary human trophoblasts
piRNA - PIWI-interacting RNA
PNS - peripheral nervous system
prM – pre-membrane
R_0 - basic reproduction number
RdRp - RNA-dependent RNA polymerase
RF - replication factories
RG - reverse genetics

exo-siRNA - exogenous small interfering RNA
f/t - freeze/thaw
FA - Formaldehyde
FBS - fetal bovine serum
FMDV - foot and mouth disease virus
FoA - formic acid
G - Glycine
G3BP-1 - Ras-GTPase activating binding protein 1
GBS - Guillain-Barré syndrome
GRP78 - glucose-regulated protein 78kDa
HCV – hepatitis C virus
HDVR - hepatitis D virus ribozyme
HEK - Human embryonic kidney
HiBiT - Nanoluc split-luciferase small subunit
HNK - Honokiol
HSP40 - DnaJ heat shock protein family
HSP70 - heat-shock protein 70
HSP90B1 - heat-shock protein 90 B1
HSPA5 - heat-shock 70kDa protein A5
HTJ1 - human tumour cell DnaJ-like protein 1
IF - immunofluorescence
IFI6 - interferon alpha-inducible protein 6
IFN – interferon
IFN-λ2 - interferon lambda 2
IP - co-immunoprecipitation
IRE1 - inositol requiring enzyme 1α/β
IRF3 – interferon regulatory factor 3
ISF – insect-specific flaviviruses
ISG - interferon stimulated gene
JAK/STAT - Toll and Janus kinase/signal transducer and activator of transcription
JEV – Japanese encephalitis virus
K/O - knockout
KDEL - C-terminal lysine, aspartic acid, glutamic acid and leucine motif
KDELR - KDEL receptor
KUNV – Kunjin virus
RIG-I – retinoic acid-inducible gene 1
RISC - RNA-induced silencing complex
RNAi - RNA interference
RNP – ribonucleoprotein
RSV - respiratory syncytial virus
RT - reverse transcriptase
RTPase - RNA triphosphatase activities
SARS-CoV-2 - severe-acute respiratory syndrome coronavirus 2
SBD - substrate-binding domain
SC - Sertoli cells
SEM - standard error of the mean
SFKs - Src-family kinases
sfRNA – subgenomic flavivirus RNA
siG - anti-GRP78 siRNA
siN - scrambled siRNA
SLA - stem-loop A
STRING - Search Tool for Retrieval of Interacting Genes/Proteins
SV40 - Simian Virus 40
TAM – TYRO3, AXL and MER
TAO1 - thousand and one amino-acid protein 1
TBEV – tick-borne encephalitis virus
TIM- T-cell immunoglobuin and mucin domain
TMD – transmembrane domains
TMUV - duck Tembusu virus
TPB - Tryptose Phosphate Broth
TRIM25 - tripartite motif 25
UPR - unfolded protein response
UTR – untranslated region
V - Valine
VCP - vasolin-containing protein
VLPs - virus like particles
VP - vesicle packets
WNV – West Nile virus
WT - wild type
XBP-1 - X-box-binding protein 1

LC - Leydig cells
LgBiT - Nanoluc split-luciferase large subunit
LQT - linear ion trap
M – membrane
YFV – yellow fever virus
ZIKV – Zika virus
ZIKV Nanoluc – Zika Nanoluciferase virus

Publications

Data published from thesis:

Royle J, Ramirez-Santana C, Akpunarlieva S, Donald CL, Gestuveo RJ, Anaya JM, Merits A, Burchmore R, Kohl A, Varjak M. 'Glucose-Regulated Protein 78 interacts with Zika virus envelope protein and contributes to a productive infection.' *Viruses,* 2020. doi.org/10.3390/v12050524

Data published, not included in thesis:

Royle J, Donald CL, Merits A, Kohl A, Varjak M. 'Differential effects of lipid biosynthesis inhibitors on Zika and Semliki Forest viruses.' *The Veterinary Journal,* 2017. doi.org/10.1016/j.tvjl.2017.10.009

Rihn SJ, Merits A, … Royle J … *et al*. 'A Plasmid DNA-Launched SARS-CoV-2 Reverse Genetics System and Coronavirus Toolkit for COVID-19 Research' *PLoS Biology, 2021.* doi.org/10.1371/journal.pbio.3001091

Gestuveo RJ, Royle J, Donald CL, Lamont D, Hutchinson E, Merits A, Kohl A, Varjak M. 'Analysis of Zika virus capsid-Aedes aegypti mosquito interactome reveals pro-viral host factors critical for establishing infection.' *Nature Communications, 2021.* doi.org/10.1038/s41467-021-22966-8

Acknowledgements

Firstly, I would like to thank both of my supervisors, Professor Alain Kohl and Dr Margus Varjak, for their support throughout my PhD. While I do not think my project ended up where any of us thought it would, I am thankful to Alain for supporting me to set my own course, and for giving me the opportunity to see more of the world than I had before. Margus, while you rightly deserve your own chapter here, I hope you can settle for one sentence and my sincere gratitude for your being there every single step of this PhD, no matter how much I grumbled about it.

To the whole of the Kohl, Brennan and Pondeville labs, past and present, I am grateful for all the kindness and support you have shown over the years. There have been/are far too many of you to list everyone here, but that does not diminish how much I value your contributions throughout this journey. I would however like to especially thank Jordan, and (my ex-landlord) Tim for their friendship (and the cheap rent) over the years. I don't think I'll forget much of our time together anytime soon. Rommel, Claire, and Mel, you have all been great, and without your help I wouldn't have made it this far. Special thanks to Claire, who like Margus helped me no matter what, Rommel for providing the soundtrack to my tissue culture sessions, and to Steven for indulging my 'The Thick Of It' obsession (and to Claire and Steven for reading parts of this thesis), it was greatly appreciated. James, never change.

Natalia and Victor A.K.A, the best Phoenix Bar owners there has or ever will be, those trips to Morrisons and subsequent Fridays were the highlight of my time at the CVR, and I'm glad I got to share it with you. To the patron's past and present, James, Betty, Sam, Ben, and everyone else, thank you so much. All said, I've left one of the chief CVR characters, Jack 'wise' the Brave. Jamie certainly wouldn't have got far without Jack. It goes without saying that I think myself (probably incorrectly) as more of a 'Sam' and you as a 'Frodo,' but then the reference wouldn't work so well... Sincerely, thank you.

To friends from home, Dan, Fiona, Gemma, Jamie and Vicki and thanks for the continued friendship and for still visiting me/each other, despite the long years apart. You all mean a lot to me, thank you!

I would like to thank my family, especially Mum, Dad and Grandma, for all their love and their interest in what I do, and for always wanting the best for me. I will always appreciate it and I hope I've made you proud.

And finally, Vic. You have been absolutely amazing and I'm truly thankful to have met you. You help me strive to be the best I can be, and I know that no matter what we do, it'll be worth it.

Authors Declaration

I declare that all results presented herein are a result of my own work, except for where explicitly stated. Some results and figures have been, or will be published (see Publications), although in these circumstances they have been adapted from what is/will be shown in print.

Printed Name: Jamie Royle

Date: 28/06/2021

Chapter 1. Introduction

1.1 Flaviviridae

1.1.1 Taxonomy

The *Flaviviridae* family of viruses covers 4 separate genera (*Flavivirus, Hepacivirus, Pestivirus and Pegivirus)* and contains approximately 90 known virus species (Simmonds *et al.*, 2017).

The largest genus, *Flavivirus,* consists of over 50 members which are primarily arthropod-borne viruses (arboviruses) (Huang, Higgs and Vanlandingham, 2019). These viruses are generally transmitted to vertebrate hosts by both mosquito and tick species and includes viruses such as Japanese encephalitis virus (JEV), West Nile virus (WNV), dengue virus (DENV), Zika virus (ZIKV), and tick-borne encephalitis virus (TBEV) (Guzman *et al.*, 2010; Petersen, Brault and Nasci, 2013; Petersen *et al.*, 2016; Pulkkinen, Butcher and Anastasina, 2018). The first discovered member of the *Flavivirus* genus was yellow fever virus (YFV), which gave its name to both the family and genus; *flavus* means 'yellow' in Latin, and YFV patients can display a yellow pigmentation of skin (Clements and Harbach, 2017). Many of these viruses are important human and animal pathogens which represent an ongoing threat to health (Pierson and Diamond, 2020). However, some flaviviruses have no known vertebrate target, and as such are termed insect-specific flaviviruses (ISF) (Blitvich and Firth, 2015). These ISF divide into two classes; those which phylogenetically associate to the classical vertebrate/mosquito viruses, and a more genetically dissimilar group; whether these viruses truly lack a vertebrate host remains to be verified. Additionally, some flaviviruses have no known vector and have only been isolated from either rodents or bats (Blitvich and Firth, 2015). These include Yokose virus, a bat virus closely related to YFV, and a rodent-associated virus called Modoc virus (Tajima *et al.*, 2005; Adams *et al.*, 2013). It is thought that these viruses can persist in their host via vertical transmission from mother to progeny, although this has not

been definitely proven (Adams *et al.*, 2013). The relationship between selected flaviviruses is highlighted in a phylogenetic tree shown in Figure 1-1.

The important human pathogen hepatitis C virus (HCV) is the primary member of the *Hepacivirus* genus (Hartlage, Cullen and Kapoor, 2016). There are a large subset of HCV genotypes and subtypes, all of which are derived from human infections and are causative agents of chronic and acute liver disease (Smith *et al.*, 2014). Until 2011, there was only one other known *Hepacivirus*. Since then, a wide range of zoonotic hepaciviruses have been discovered and expanded this genus, though whether these represent a new class of human disease has yet to be elucidated as they cause no known disease (Williams *et al.*, 2020).

Pestivirus is a genus containing viruses currently only known to infect mammals and includes the economically important Bovine viral diarrhoea virus (BVDV) (Houe, 1995). Recently, there have been proposed changes to the naming conventions of pestiviruses to incorporate newly discovered related species (Smith *et al.*, 2017).

The last genus, *Pegivirus,* represent a growing list of viruses that persistently infect a large range of mammals although they have not conclusively been associated with any disease (Berg *et al.*, 2015; Miao *et al.*, 2017).

The following sections will discuss flaviviruses in more detail before focusing on the primary topic of this thesis, Zika virus.

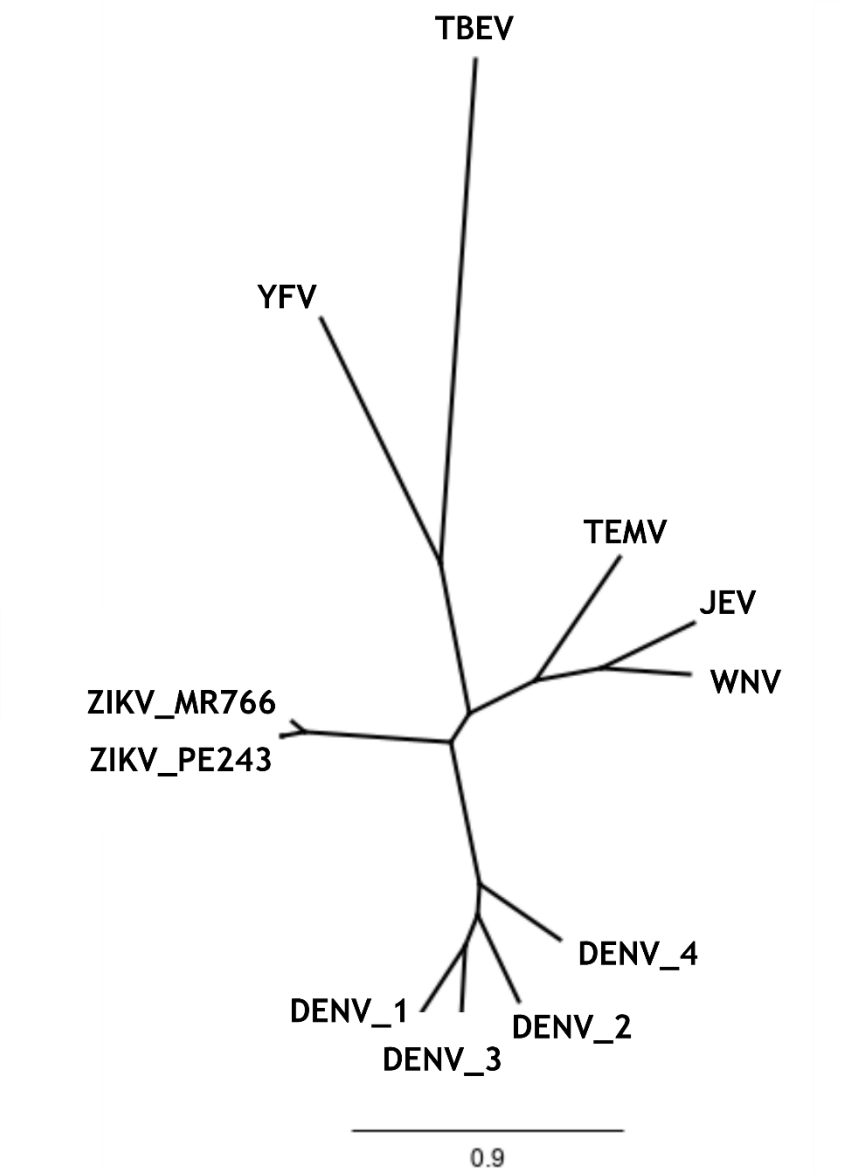

Figure 1-1: Phylogenetic analysis of the flavivirus genus.
A figure highlighting the unrooted phylogenetic relationship between important flaviviruses. The PhyML 3.0 extension for Geneious was used to create a maximum-likelihood tree using the GTR+G substitution model with 4 gamma categories and 100 bootstrap replicates. Results are displayed as a Neighbor-Joining tree and scale-bar represents substitutions per site. Sequences were obtained from GenBank (KJ776791.2, DQ859059.1, KX197192.1, MN869914.1, L48961.1, KF192951.1, M12294.2, JN628279.1, KU725663.1, NC001475.2, NC002640.1) or European Nucleotide Archive (AAB53095).

1.1.2 Flavivirus Genomic RNA

Flaviviruses encode a single-stranded, positive sense RNA genome approximately 11 kb in length which is translated into a single polyprotein as illustrated in Figure 1-2 (Chambers *et al.*, 1990). The genome contains a single open reading frame (ORF) flanked by a 5' and 3' untranslated region (UTR) of approximately 100 bp and 500 bp respectively, although species specific variations in length occur (Ng *et al.*, 2017). The 5' UTR has a N^7 methylated (me^7)-guanosine cap to protect the genome from exonuclease degradation and to enable translation of the polyprotein (Saeedi and Geiss, 2013). Flavivirus genomes are not poly-adenylated, and the 3' UTR contains a series of conserved RNA hairpins that terminates with a stem loop (Saeedi and Geiss, 2013; Göertz *et al.*, 2018). These RNA structures are illustrated in Figure 1-2. The 3' UTR also contains a circularisation signal (CS). This signal can form a long range RNA:RNA interaction with RNA found in the capsid coding region, promoting circularisation of the genome which is essential for minus-strand viral RNA synthesis (Alvarez *et al.*, 2005; Manzano *et al.*, 2011). In Kunjin virus (KUNV, now known as West Nile virus Kunjin subtype (Gray *et al.*, 2011)), the CS is 8 nucleotides long and if mutated will abrogate the elongation of viral RNA, though compensatory mutations can restore replication (Khromykh *et al.*, 2001). While circularised genomes are clearly important, studies of DENV have suggested there needs to be a balance between circular and linear forms of the genome (Villordo, Alvarez and Gamarnik, 2010). The swap between circular and linear genome forms may regulate the production of minus or positive RNA strands (Mazeaud, Freppel and Chatel-Chaix, 2018).

Complex secondary structures in the 3' UTR also protect the RNA from complete 5'-3' digestion by the cellular XRN1 exoribonuclease, which results in the production of subgenomic flavivirus RNA (sfRNA) (Pijlman *et al.*, 2008; Mazeaud, Freppel and Chatel-Chaix, 2018). sfRNA ranges from 300 to 700 nt in length and contains multiple stem-loops and pseudoknots which stall and capture XRN1, inhibiting its cellular function (Mazeaud, Freppel and Chatel-Chaix, 2018). Additionally, sfRNA is a highly abundant RNA molecule in the infected cell which

can function to inhibit type-1 interferon (IFN) responses in many flaviviruses (Schuessler *et al.*, 2012; Manokaran *et al.*, 2015; Donald *et al.*, 2016). There are several potential mechanisms behind this. DENV sfRNA has been shown to inhibit the deubiquitination of tripartite motif 25 (TRIM25), which prevents the activation of retinoic acid-inducible gene 1 (RIG-I) and therefore subsequent type-1 IFN production is inhibited (Manokaran *et al.*, 2015). ZIKV sfRNA has also been shown to inhibit IFN-β activity, likely through a similar mechanism as seen for DENV (Donald *et al.*, 2016). Alternatively, JEV sfRNA can inhibit the phosphorylation and nuclear translocation of the upstream regulator of IFN-β, interferon regulatory factor 3 (IRF3) (Chang *et al.*, 2013). sfRNA is also important for flaviviruses infection in their mosquito vectors as depletion of ZIKV sfRNA reduced viral dissemination in *Aedes aegypti*, and similarly WNV requires sfRNA for efficient transmission in *Culex spp.* mosquitoes (Göertz *et al.*, 2016; Slonchak *et al.*, 2020). This could be in part due to sfRNA-mediated suppression of mosquito RNA interference (RNAi) pathways, as has been demonstrated for DENV and KUNV (Moon *et al.*, 2015).

Figure 1-2: Flavivirus genome organisation

A figure depicting a generalised genome of a flavivirus. A 5' and 3' UTR, complete with signature secondary structures, flank the contiguous protein coding region. The 5' UTR has a N7 methylated (me7)-guanosine cap, as indicated. The images for the 5' and 3' UTR were adapted (Neufeldt *et al.*, 2018)*, and the complete final figure was created in Inkscape.*

1.1.3 Flavivirus protein expression

The polyprotein contains 3 structural proteins (capsid [C], membrane [M] and envelope [E]) and 7 non-structural proteins (NS1, NS2A, NS2B, NS3, NS4A, 2K, NS4B and NS5) (Lindenbach and Rice, 2003). The polyprotein is threaded through the endoplasmic reticulum (ER) membrane via a series of transmembrane domains (TMD) found in several of these proteins. Proteins are liberated from the polyprotein by a combination of viral (NS2B-3) and host-cell (furin, signal peptidase) proteases, though the identity of at least one factor required for complete processing has not yet been discovered (Apte-Sengupta, Sirohi and Kuhn, 2014; Tan *et al.*, 2020). An illustration of the flavivirus polyprotein is shown in Figure 1-3.

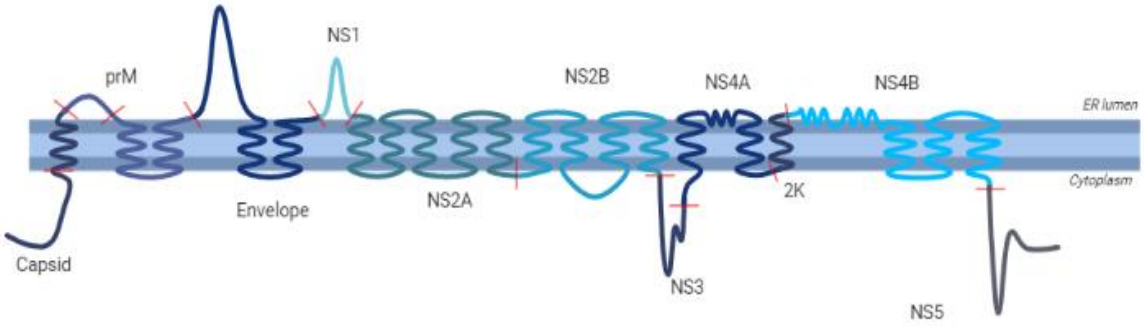

Figure 1-3: A schematic of the polyprotein of flaviviruses.

A figure displaying the constituent parts of the flavivirus polyprotein and generalized topology. Structural proteins (capsid [C], precursor membrane [prM] and envelope [E]) and non-structural proteins (NS1, NS2A, NS2B, NS3, NS4A, 2K, NS4B and NS5) are indicated, and sites of cleavage are indicated with red lines. Created in BioRender.

The C protein performs a structural role for the virus; multiple copies of C encapsulate the viral genome to form the ribonucleoprotein (RNP) complex (otherwise known as the nucleocapsid) which can then be packaged into the virion (Oliveira *et al.*, 2017). C is the first protein to be translated and is formed of a highly-positively charged, disordered loop which precedes 5 α-helices (helix 1-5), the 5th of which is embedded in the ER membrane and is known as the capsid anchor (CA) (Rana *et al.*, 2018). Host signal peptidases in the ER lumen cleave the C-terminus of C from precursor membrane (prM), and the viral protease NS2B-NS3 cuts between α-helices 4 and 5 to liberate the mature C protein, leaving CA behind (Tan *et al.*, 2020). Mature C exists as a homodimer, and in this form it can bridge viral RNA with the ER lipid membranes decorated with prM and E to help form immature virions (Tan, Fibriansah and Lok, 2020). ZIKV C has a longer N-termini disordered loop than other flaviviruses, made possible by 2 additional proline residues that disrupt α-helix 1 and repositions it perpendicular to the helix 2 instead of parallel, as is seen for most other flaviviruses (Shang *et al.*, 2018). Interestingly WNV, another neurotropic flavivirus, also has this unusual helical assembly, though whether this orientation contributes to pathogenicity or disease phenotypes is currently unknown (Dokland *et al.*, 2004).

The M protein is one of two viral proteins, the other being E, which span the host-derived lipid bilayer to make up the viral membrane (Smit *et al.*, 2011). Translation and initial proteolytic cleavage liberates a full length prM protein from the polyprotein. prM is incorporated in immature virions by forming a heterodimer with E, before undergoing a further cleavage event during virus export in the acidic Golgi network to yield a fully matured virus particle (Randolph, Winkler and Stollar, 1990). The initial formation of an immature virion is thought to prevent the pre-emptive fusion of the virus particle in cellular compartments during export, and the conversion of prM to M allows E to form the homodimers that coat the virion surface and prime it for infection (Zhang *et al.*, 2003). prM is one of the least conserved *flavivirus* proteins, and substantial changes to the polarity or structure of amino acid (aa) residues exist between different flaviviruses, and even between different strains of ZIKV (Prasad *et al.*, 2017). In ZIKV, prM is 168

aa long, of which the first 93 aa make up the precursor domain (Cox, Stanton and Schinazi, 2015). Mutations in Zika prM have been associated with an increase in neurovirulence. For example, a S17N mutation found in 2015/16 South American ZIKV isolates (but not in an earlier 2010 Cambodian isolate) significantly enhanced viral infectivity in both human and mouse neuronal progenitor cells (NPCs), and also increased the incidence of microcephaly in fetal mice (Yuan *et al.*, 2017). While the mechanism behind the enhancement of neurovirulence is not known, changes in prM protein sequence could potentially alter the rate of maturation or the final structure of the virion. Additionally, flavivirus particles are known to exist as a pleomorphic population, in part due to varying degrees of prM processing. These immature *flavivirus* particles are known to retain some infectivity through the use of antibody-dependent entry (Rodenhuis-Zybert *et al.*, 2010; Dejnirattisai *et al.*, 2016). Mutations in prM could potentially alter the rate or route of these alternative infection methods.

The E protein is the major structural protein which coats the surface of the virion, and is therefore integral to viral entry, assembly, and egress. E is a class II fusion protein consisting of 3 primarily β-sheet ectodomains (EDI, II and III), and two TMD which serve to anchor E in the membrane and direct NS1 localisation into the ER lumen (White *et al.*, 2008; Zhang *et al.*, 2017). Alhough EDI is formed from the N-terminus of E, it is centrally located in the 3D architecture of the protein and acts to stabilise and facilitate conformational changes in EDII and EDIII (Zhang *et al.*, 2017). Glycosylation often occurs at N154 in EDI; however, this is not conserved between all flaviviruses, or even within strains of the same virus. For example, DENV E is unusual in that it contains two glycosylation signals at N67 and N153, instead of the more common N154 site (Lee *et al.*, 2010). Additionally, Asian lineage strains of ZIKV all seem to share N154 glycosylation, however strains of African lineages do not (Carbaugh and Lazear, 2020). These differing glycosylation states can certainly impact upon cell tropism; simple E glycosylation structures bind either dendritic cell-specific intercellular adhesion molecule-grabbing nonintegrin (DC-SIGN) or DC-SIGN related protein (DC-SIGNR), and more complex glycans preferentially attach to DC-SIGNR (Carbaugh and Lazear, 2020). EDI and

EDII are connected via a flexible hinge, mutations in which can alter the dynamics of conformational changes and pathogenicity of flaviviruses (Goo *et al.*, 2017). EDII contains a highly conserved, small peptide loop with a highly hydrophobic tip known as the fusion loop. The fusion loop is absolutely essential for insertion of E into target membranes, and is therefore required for viral uncoating and genome release (Modis *et al.*, 2004). This fusion loop interacts with, and is hidden by, prM in immature virions to prevent premature interaction with cellular membranes. Following prM maturation in the Golgi, the fusion is loop is said to be activated and is as such available to facilitate binding (Roby *et al.*, 2015). EDIII adopts an immunoglobulin-like fold and contains the cell receptor-binding sites and is therefore vital for entry into host cells. Entry is initiated through receptor-mediated endocytosis following EDIII binding to a cellular receptor (Smit *et al.*, 2011; Zhang *et al.*, 2017). Many different cellular proteins have been identified as entry factors during flavivirus infections including C-type lectin receptors (CLR) (S. T. Chen *et al.*, 2011), $\alpha_v\beta_3$ integrins (Chu and Ng, 2004; Zaitsev *et al.*, 2014; Fan *et al.*, 2017), TYRO3, AXL and MER (TAM), and T-cell immunoglobulin and mucin domain (TIM) (Meertens *et al.*, 2012; Niu *et al.*, 2018; Oliveira and Peron, 2019; Ghosh Roy, 2020). Additionally, EDIII is highly antigenic and most of the host neutralising antibody response is directed against epitopes found in this domain (Volk *et al.*, 2007; Esswein *et al.*, 2020). The antibodies directed against EDIII tend not to be cross-reactive across flaviviruses, perhaps due to relatively low sequence identity in this region (Sun, Chen and Lai, 2018). However, antibodies that are generated to recognise EDI and EDII can be cross-reactive, such as those which neutralise both DENV and ZIKV. This is perhaps due to sequence similarity in highly-conserved epitopes found in EDI and EDII such as the fusion loop. (Barba-Spaeth *et al.*, 2016; Fernandez *et al.*, 2017; Rathore and St. John, 2020).

The non-structural proteins fulfil a variety of roles, ranging from immune antagonism to protease functions and polymerase activities. NS1 is a highly conserved *flavivirus* protein that has diverse functions in the viral life cycle, including as a co-factor in virus replication, as a host immune response antagonist, and in disease pathogenesis (Muller and Young, 2013; Rastogi, Sharma and Singh,

2016). NS1 is translated and translocated into the ER membrane and then proteolytically cleaved by ER-resident host proteases (Falgout and Markoff, 1995). Immediately following this, NS1 is glycosylated at two asparagine residues (N130 and N207) that are conserved across most flaviviruses, although additional sites for glycosylation exist (Yap *et al.*, 2017). Subsequent oligomerisation occurs and is influenced by the glycosylation state of NS1; intracellular NS1 tends to display high-mannose glycosylation, and trimming of these sugars with the addition of complex glycans in the Golgi allows formation of soluble hexameric NS1, which can then be excreted from the cell (Muller and Young, 2013; Rastogi, Sharma and Singh, 2016). Although NS1 lacks a TMD, the β-roll protrusions of dimeric NS1 are hydrophobic and can interact with cellular membranes (Akey *et al.*, 2015). This intracellular, dimeric NS1 can remodel liposome structure and acts as an important co-factor to viral replication. Indeed, NS1 has been shown to be able to remodel ER membranes to form replication factory-like compartments (Ci *et al.*, 2020). While mutations in the hydrophobic β-roll that increase its charge do not alter liposome remodelling kinetics, this modified NS1 is no longer able to aid viral replication and is also exported more readily from the cell (Akey *et al.*, 2015). Hexameric NS1 can be exported from both vertebrate and invertebrate cells, though export from invertebrate cells requires interactions with the chaperone caveolin complex. This interaction is not required in vertebrate systems for NS1 export (Rosales Ramirez and Ludert, 2018). During human infection, a large amount of NS1 can be secreted and so detection of NS1 has been used as an early diagnostic marker. This has primarily used for DENV detection, but assays for other flaviviruses have also been developed (Ricciardi-Jorge *et al.*, 2017; Tan *et al.*, 2019). Secreted NS1 from various flaviviruses have also been shown to increase endothelial membrane permeability *in vitro* and *in vitro*, possibly aiding viral dissemination and contributing to pathogenicity (Puerta-Guardo *et al.*, 2019).

NS2A is a hydrophobic membrane-associated protein which can associate with the viral 3' UTR and is important for replication and immune antagonism (Leung *et al.*, 2008). Cleavage by an unknown protease and the viral NS2B/NS3 protease liberates NS2A from the viral polyprotein, generating a protein of 224 amino acids

with 5 predicted TMD (Xie *et al.*, 2013). While critical sequences of NS2A are conserved between flaviviruses, there is some difference in the predicted membrane topology. For example, ZIKV and DENV may have reversed transmembrane topology to YFV. In the case of the former pair, a vital N-terminal stretch of amino acids can be located in the ER, whereas for the latter these residues are found in the cytoplasm (Barnard *et al.*, 2020). Mutations in ZIKV NS2A have been linked to viral virulence, whereby variations at a single residue (alanine (A) or valine (V) 117) can result in dramatically different infection outcomes in mice models (Ávila-Pérez *et al.*, 2019). Another A to V switch at residue 175 was also shown to attenuate ZIKV in both *in vitro* and *in vivo* systems (Márquez-Jurado *et al.*, 2018). NS2A has been shown to be important for viral RNA synthesis, and virion assembly and maturation (Xie *et al.*, 2013). Specifically, NS2A can selectively bind and recruit prM, E, NS2B/NS3 and viral 3' UTR to sites of assembly, and mutations which disrupt these interactions leads to an abrogation of virion assembly (X. Zhang *et al.*, 2019; Xie *et al.*, 2019). For some flaviviruses, such as YFV, a truncated form of NS2A is generated through partial cleavage by NS2B/NS3 at an internal site producing a 190 amino acid variant which also seems to be essential to infectious virion production, although the mechanism behind this has not yet been fully explored (Kümmerer and Rice, 2002). As such, NS2A is a critical factor in *flavivirus* assembly. In addition to its role in assembly, NS2A has been shown to inhibit innate immune responses by inhibiting IFNß signalling during KUNV infection and blocking TBK1/IKKε signaling in DENV infection (Chen *et al.*, 2017). ZIKV NS2A has also been shown to disrupt RIG-I signaling, providing another mechanism for immune evasion (Ngan *et al.*, 2019).

NS2B is an essential co-factor for NS3 protease activity, and mutations in the central hydrophilic region will abrogate this activity (Li *et al.*, 2016). Indeed, the hydrophilic region alone, which is flanked by TMD, is necessary and sufficient for NS3 protease functions. The TMD may serve to help anchor the viral protease in host membranes and may improve protease efficiency (Chambers *et al.*, 1993). As few solved structures for NS2B exist, the number of TMDs are sometimes reported differently. DENV NS2B reportedly contains 4 TMDs (Y. Li *et al.*, 2015) and JEV

NS2B has 3 (Li *et al.*, 2016). This, like the differences observed in NS2A membrane topology highlights important differences between related viruses. These TMDs, while not required for NS2B/NS3 protease activity, have been implicated in virus replication and virion assembly (Li *et al.*, 2016).

As discussed above, NS3 has protease activity when coordinating with NS2B (NS2B/NS3^{pro}), the action of which is essential for polyprotein processing (Li, Zhang and Li, 2017). Additionally, NS3 is also vital for replication and forms the helicase of the viral polymerase (NS3^{hel}), with which NS5 makes up the RNA-dependent RNA polymerase (RdRp) (Papageorgiou *et al.*, 2016). The trypsin-like serine protease activity of NS3 is encoded in the N-terminus of the protein. This domain contains the catalytic triad (N-Histidine (H)-Serine (S)) conserved through all flaviviruses (Assenberg *et al.*, 2009). The N-terminal protease domain is joined to the larger helicase domain by a short, flexible linker (Luo *et al.*, 2008). Without binding a substrate, NS2B/NS3^{pro} adopts an open conformation. Substrates bind to the NS3 active site before NS2B encloses the NS3-substrate core (Brecher *et al.*, 2017). NMR spectroscopy also revealed that binding of inhibitors to DENV NS2B/NS3^{pro} switched the conformation of the protease from open to closed (Zhu *et al.*, 2015). The *flavivirus* protease is highly conserved and essential, and as such is a promising target for developing therapeutics (Lee *et al.*, 2017; Z. Li *et al.*, 2017; Yao *et al.*, 2019). The larger C-terminal domain has helicase, adenosine triphosphatase (ATPase) and RNA triphosphatase activities (RTPase) and may be required to resolve viral genomic RNA secondary structures to allow NS5-mediated negative-sense RNA synthesis. Additionally, NS5 unwinds duplex RNA using energy generated from ATP hydrolysis (Swarbrick *et al.*, 2017). The RTPase activity of NS3, along with the guanylyltransferase/methyltransferase activities of NS5 are essential for transferring the N^7 methylated (me^7)-guanosine cap to nascent viral RNA (Saeedi and Geiss, 2013). While NS3 does not seem to be packaged in the virion, NS3 may be required to help deliver viral RNA to virions and is important for virus assembly independent of its enzymatic activities (Liu *et al.*, 2002; Patkar and Kuhn, 2008; Barnard *et al.*, 2020).

NS4A is another small, hydrophobic protein containing multiple TMD and is one of the least well understood proteins in the viral lifecycle. It is flanked by NS3 and a small, so called '2K' peptide. Cleavage between 2K and NS4A by NS2B/NS3^{pro} is required for subsequent release of NS4B from 2K (Lin *et al.*, 1993). NS4A has been shown to induce ER membrane rearrangements, and associate with NS1 and the viral replication complex; these interactions are vital for infection (McLean *et al.*, 2011). In DENV, NS1 has also been shown to interact with the NS4A-2K-NS4B precursor molecule, an interaction which was vital for RNA replication but not related to membrane reassortments (Płaszczyca *et al.*, 2019). DENV NS4A has been shown to oligomerise, a feature which is vital for function and is mediated through intermolecular interactions in the first TMD. Mutations in DENV NS4A (such as E50A and G67A) can reduce oligomerisation and stability, and subsequently attenuate viral replication (Lee *et al.*, 2015). NS4A localises to sites coincident with dsRNA staining, and NS4A lacking 2K is sufficient to induce membrane rearrangements to produce structures resembling viral replication compartments. This is most likely achieved through induction of membrane curvature following insertion of TMDs into lipid bilayers and subsequent oligomerisation (Miller *et al.*, 2007). Indeed, the cytosolic N-terminus of NS4A has been shown to preferentially bind curved lipid membranes, and mutations in this region impair viral replication (Hung *et al.*, 2015). As such NS4A is vital for forming the replication factories that are characteristic of *flavivirus* infections. In addition, NS4A has been linked to immune antagonist functions, as ZIKV NS4A is able to suppress type 1 IFN production through RIG-I inhibition (Ma *et al.*, 2018; Ngan *et al.*, 2019). JEV NS4A can also inhibit phosphorylation of STAT1/2, thus suppressing type 1 IFN (Lin *et al.*, 2008).

NS4B is hydrophobic protein of around 30kDa which is predicted to contain 5 integral, transmembrane domains. The 2K signal peptide is required to direct NS4B translocation through the ER membrane, though it is dispensable for most other functions and is cleaved following membrane insertion (Zmurko, Neyts and Dallmeier, 2015). WNV and DENV NS4B has been shown to dimerise, and mutations in regions which mediate dimerisation are lethal to the viruses (Zou *et al.*, 2014). As with NS4A, NS4B has been shown to localise to sites of dsRNA staining and is

likely to be involved in viral RNA replication, although the exact mechanism behind this has yet to be elucidated (Zmurko, Neyts and Dallmeier, 2015). Like other non-structural proteins, NS4B is part of the *flavivirus* anti-immune repertoire. NS4B from DENV has been shown to inhibit STAT1 phosphorylation, a function that is conserved in both WNV and YFV and is generated through the N-terminus of the protein (Muñoz-Jordán *et al.*, 2005). Mutations in this section of ZIKV NS4B have been shown to result in an attenuated virus, which induces stronger type-1 interferon and T-cell immune responses in challenged mice than a wild-type (WT) virus (Li *et al.*, 2019).

NS5 is the largest *flavivirus* protein at around 900 amino acids in length and contains a N-terminal methyl-transferase domain and is connected via a short, flexible linker to the previously mentioned, C-terminal RdRp (Zhou *et al.*, 2007; Zhao *et al.*, 2017). Nascent viral RNAs are capped by NS3 and NS5 to increase stability in the cytoplasm through the prevention of cellular exoribonuclease digestion, and enables efficient translation (Sanford *et al.*, 2019). The NS5 RdRp is loaded onto a conserved viral RNA sequence at the 5'-terminus of the genome termed stem-loop A (SLA), and is then transferred to the 3' end following cyclisation of the RNA genome. Viral RNA can then be copied in the 3' to 5' direction to generate negative-sense template strands to produce more positive-sense RNA for use in translation of virus assembly (Fajardo *et al.*, 2020). The mechanism behind the switch from replication to translation is not well understood, however some evidence suggests the binding of nascent NS5 to SLA following initial translation inhibits further translation, and switches the priority to replication (Fajardo *et al.*, 2020). NS5 has also evolved potent type 1 IFN suppression mechanisms, although different *flavivirus* NS5 proteins have divergent mechanisms for dealing with the immune response (Best, 2017). For example, both ZIKV and DENV NS5 bind to, and prevent activation of, human STAT2 (Wang *et al.*, 2020).

1.1.4 Virus structure

Flaviviruses form icosahedral virions around 500 Å in diameter which, when mature, are coated with 180 copies of E arranged in 90 homodimers, and 180 copies of M which sits just below the surface of the virion as shown in Figure 1-4 (Kuhn *et al.*, 2002). In these particles, E and M are anchored via their C-terminal domains into a lipid bilayer derived from the ER (Zhang *et al.*, 2003). Three E dimers lie parallel to each other and so form a total of 30 rafts. Half of each raft forms each of the 60 asymmetric units that make up the virion (Sirohi and Kuhn, 2017). This encases an internal nucleocapsid core, made up of the RNA genome encapsulated by multiple copies of C. Immature particles are made up of 180 prM:E heterodimers, and furin-mediated (or a furin-like protease) cleavage removes the pre-peptide of prM, generating the mature particle described above (Prasad *et al.*, 2017).

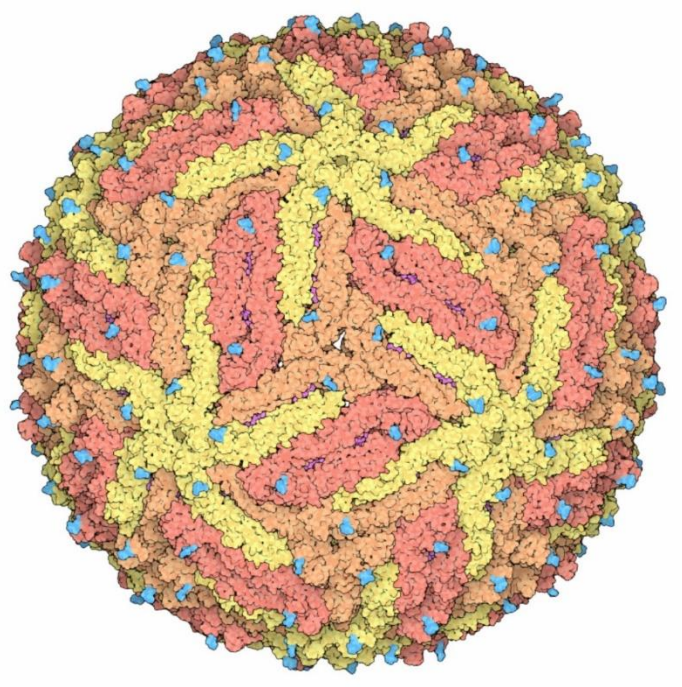

Figure 1-4: Illustration of Zika virus.

Envelope proteins are indicated by red and yellow, and glycosylated asparagine residues are indicated in turquoise. Membrane is coloured purple and mostly hidden beneath the surface. Adapted from an image from the Protein Data Bank (PBD), adapted from (Sirohi *et al.*, 2016).

1.1.5 Geographical distribution and vectors

As mentioned, most members of the *Flavivirus* genus are arboviruses, and as such are generally transmitted to a vertebrate host and limited in geographical range by their vector host (Gould *et al.*, 2003). Dissemination of flaviviruses from a vector to a vertebrate host is termed horizontal transmission, and flaviviruses can be maintained solely in vector populations through transgenerational (vertical) transmission (Rosen, 1988). Vertical transmission has been suggested as a way for flaviviruses to persist in periods unfavourable to transmission, such as during winter, though the importance of this has been questioned (Lequime and Lambrechts, 2014). This controversy has largely stemmed from discrepancies between laboratory and field experiments, and estimated rates of vertical transmission may not be sufficient to maintain arboviruses (Lequime, Paul and Lambrechts, 2016). Nevertheless, recent reviews, such as by Ferreira *et al*, highlight that vertical transmission of viruses such as DENV is widely found in nature (Ferreira-De-Lima and Lima-Camara, 2018). The principal vectors of flaviviruses are blood-feeding mosquitoes and ticks. *Culex* and *Aedes* genera of mosquitoes are the primary vector for the majority of mosquito-borne flaviviruses where, broadly speaking, *Culex* species primarily transmit flaviviruses such as WNV and JEV while *Aedes* species transmit viruses such as DENV, YFV and ZIKV (Huang *et al.*, 2014). Often, these viruses are maintained naturally through sylvatic cycles where humans are considered a dead-end host. A typical cycle will see transmission to, and amplification of the arbovirus in, a susceptible vertebrate host. Subsequent blood-meals taken from an infected host can transfer the virus to the mosquito vector, and the virus can quickly penetrate the mosquito midgut and spread to other tissues such as the salivary gland via the haemolymph in preparation for further transmission (Salas-Benito and De Nova-Ocampo, 2015). So while vector-human transmission is often accidental for some flaviviruses, the increasing urbanisation of tropical regions and the presence of highly anthropophilic mosquitos such as *Aedes aegypti* can results in human-only transmission cycles, as has been seen for DENV, YFV and possibly ZIKV (Weaver

and Reisen, 2010; Gregory *et al.*, 2017; Douam and Ploss, 2018). For ZIKV, gaps in understanding of transmission cycles remain, although the 2015/16 outbreak in the Americas showed that human-only cycles are possible.

These mosquito species are now prevalent over a wide expanse of the globe following recent rapid expansion events. *Aedes aegypti* originates in Africa and is thought to have spread to the Americas through the Atlantic slave trade, while *Aedes albopictus* more recently spread from Asia into the pacific islands and further into the Americas (Kraemer *et al.*, 2015). Additionally, as *Aedes albopictus* can tolerate a wider range of temperatures than *Aedes aegypti* and it has recently expanded into southern Europe. The difference in geographical range between *Aedes aegypti* and *Aedes albopictus* is illustrated in Figure 1-5. A large amount of people are therefore exposed to the diseases borne by *Aedes* mosquitoes. For example, an estimated 53% of the world's population now live in areas that are suitable for DENV transmission, a figure that is likely to increase (Messina *et al.*, 2019). Factors that predict the suitability of an environment to *Aedes* habitation include temperature, precipitation, vegetation and urban coverage (Kraemer *et al.*, 2015). As such, phenomena such as climate change and urbanisation are rendering large areas of the tropics more amenable to mosquito survival and propagation.

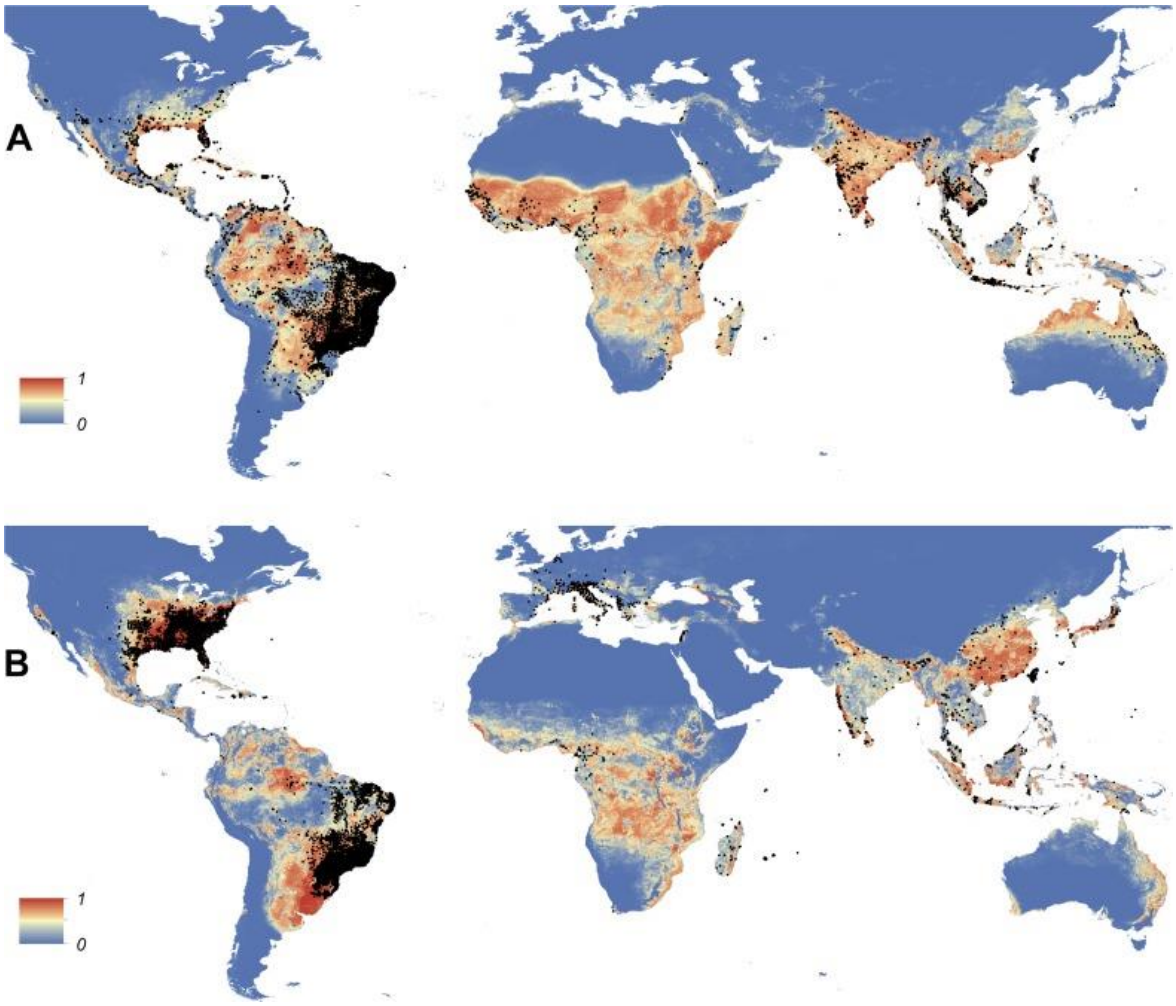

Figure 1-5: Global distribution of *Aedes* species mosquitoes.
Figure showing the global distribution of ***Aedes aegypti*** *(A) and* ***Aedes albopictus*** *(B). The heatmap represents predicted range of the selected mosquitoes, with block dots representing confirmed mosquito isolations as identified in the literature. Adapted from* (Kraemer *et al.*, 2015).

1.1.6 Economic and health burden

Flavivirus infections cause massive damage to human health and economies world-wide, often in areas that are least able to endure it.

For example, DENV is responsible for an estimated 390 million infections every year, causing significant morbidity (Bhatt *et al.*, 2013; Brady and Hay, 2020). While most DENV infections are asymptomatic, there are a significant amount of cases that manifest clinically, with symptoms ranging from a mild fever to potentially deadly manifestations like dengue haemorrhagic fever (now termed severe dengue) (Brady and Hay, 2020). While severe dengue is rare, the sheer volume of DENV cases represents a large economic and health burden on many health systems. In Brazil alone, DENV was thought to cost over $1200 million a year as measured in 2013 (Martelli *et al.*, 2015). Because of this, DENV has been the focus of intense efforts to develop a vaccine for many years, culminating with the licensing of a live-attenuated virus vaccine (termed Dengvaxia) in 20 countries (Thomas and Yoon, 2019). Despite conferring protection at the population level, it was observed that patients who were seronegative for DENV at the time of vaccination were at an increased risk for subsequently suffering from severe dengue (The Lancet Infectious Diseases, 2018). As such, people seronegative for DENV are not now administered Dengvaxia. An alternative live-attenuated vaccine, TAK-003, has recently reported promising protection levels, and has been shown to be safe to seronegative patients (López-Medina *et al.*, 2020).

WNV was first isolated in Uganda in 1937 and is now endemic in nearly every area of the world (Chancey *et al.*, 2015). The primary non-vector host for WNV is birds, and though both humans and horses can be infected and suffer disease they are regarded as dead-end hosts (Murray, Mertens and Desprès, 2010). Like ZIKV, WNV is a neurotropic virus (Murray *et al.*, 2006). Infection is usually asymptomatic or results in a mild, febrile illness, but can sometimes manifest with severe meningitis, encephalitis, and death. Recovery can be slow from both severe and mild diseases, with prolonged periods of weakness and fatigue potentially

resulting in either case (*Symptoms, Diagnosis, & Treatment | West Nile Virus | CDC*, 2018). Though the rate of severe neurological disease is thought to be low (around 1 in 150), as of yet there are no specific anti-viral therapies available and treatments must be supportive in nature (Kemmerly, 2003). As such there can be substantial costs associated with treating WNV infections. Though few studies have looked at the impact of WNV in the developing world, WNV cost around $800 million in North America from 1999-2012. This is likely a conservative estimate because the effect of mild disease on workplace productivity was not accounted for (Barrett, 2014; Shing *et al.*, 2019).

The distribution of YFV is largely localised to sub-Saharan Africa, although sylvatic cycles exist in Latin-America (Shearer *et al.*, 2018). Infection is usually symptomless or includes fever, nausea, and muscle pain, although a small proportion of patients suffer a second wave of more serious symptoms (jaundice, abdominal pain, and bleeding) after the initial recovery. Half of patients who suffer from the severe, second wave of symptoms subsequently die (*Yellow fever*, 2019). Unlike other flaviviruses, there is an effective vaccine for YFV which has aided in reducing both infections and deaths, although recent lapses in vaccination pipelines threaten to unwind past progress (Garske *et al.*, 2014). For example, in 2013 there was an estimated 78,000 deaths from YFV in Africa, though this was predicted to have been reduced by 27% by the use of vaccinations (Garske *et al.*, 2014).

1.1.7 Infection cycle

Flavivirus infection begins with E binding to cellular receptors and initiating clathrin-mediated endocytosis (Laureti *et al.*, 2018). Following this, the virus particle is trafficked through the endosomal pathway, where reduction in the pH of endosomes induces conformation changes in the virion and results in the formation of E homotrimers. The detection of endosomal pH changes may be facilitated through the protonation of conserved histidine residues in E, although observations in WNV suggest this may not be the case for all flaviviruses (Nelson *et al.*, 2009; Stiasny *et al.*, 2011). Regardless, the switch to E homotrimers facilitates the insertion of E into the endosomal membrane and subsequent fusion of the lipid bilayers, creating the fusion pore (Stiasny *et al.*, 2011). The RNA genome can then translocate into the cytoplasm through the fusion pore. It is thought that ubiquitination of C is required to allow uncoating of the viral RNP and facilitate release of the genome (Byk *et al.*, 2016). Cellular proteins such as vasolin-containing protein (VCP) have been shown to be involved in the disassembly of the viral RNPs (Ramanathan *et al.*, 2020) (Gestuveo *et al.*, 2021).

Incoming viral RNA initially engages cellular translational machinery to create the polyprotein, which is processed by host proteases and the viral NS2B/NS3^{pro} to liberate individual viral proteins. The viral RNA is used as a template for both further polyprotein translation and for RNA replication. To efficiently coordinate these processes and resources in space and time, flaviviruses induce large-scale re-arrangements of ER membranes to create replication factories (RF), a feature common to most positive-sense viruses, although the source of membranes can differ (Spuul *et al.*, 2011; Mazeaud, Freppel and Chatel-Chaix, 2018). Additionally, as viral RNA is highly immunogenic, sequestering RNA in RF can reduce detection by intracellular immune responses (Arakawa and Morita, 2019). As discussed, NS3 and NS5 cooperatively act to transcribe virus RNA from 3' to 5', generating negative-sense RNA that can be used as a template for positive-sense genome production. Together, NS3 (through its RTPase activity) and NS5 (through its guanylyltransferase/methyltransferase activities) can confer a 5' N^7 methylated

(me^7)-guanosine cap to nascent RNA to enable further translation and for packaging into the virion (Fajardo *et al.*, 2020).

Newly synthesised RNA is first exported from RF through a pore and can be used as a template for negative-strand replication or protein synthesis, be degraded to generate sfRNA, or is packaged into newly forming virions. C specifically encapsidates the full length genomic viral RNA, although if any specific packaging signals mediate this process or whether electrostatic interactions alone are sufficient is not yet fully understood (Pong *et al.*, 2011; Diosa-Toro *et al.*, 2020). A recent study using DENV has shown that specific residues in NS2A are able to specifically bind the 3' UTR of viral genomic RNA and is thought to do so immediately following RNA synthesis to shuttle the RNA to sites of assembly (Xie *et al.*, 2019). NS2A can also bind and recruit prM/E and NS2B/$NS3^{pro}$ to sites of assembly, and prM/E can form the viral envelope to package the readily available RNPs (Nicholls, Sevvana and Kuhn, 2020). These newly formed immature virions are exported through the Golgi network, where the declining pH induces reversible conformational changes which allows furin to proteolytically cleave prM, and so form a mature virion (Nicholls, Sevvana and Kuhn, 2020). Following this, a Golgi vesicle can fuse with the plasma membrane, releasing a fully matured virion into the extracellular milieu. Figure 1-6 depicts this cycle.

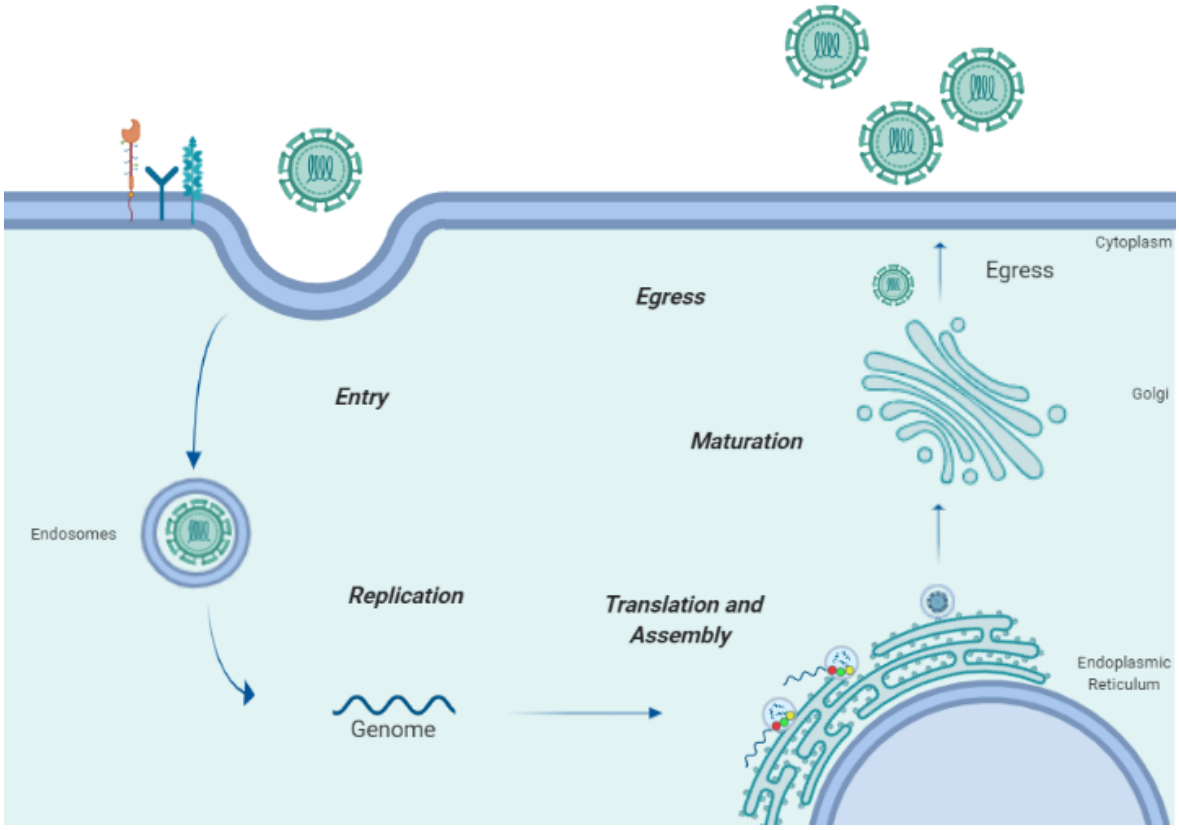

Figure 1-6: General lifecycle of flaviviruses

A schematic illustrating a simplified lifecycle of flaviviruses. Infection is initiated following engagement of cellular receptors, and trafficking through the endocytic pathway allows release of the viral genome into the cytoplasm. Translation of the genome produces a polyprotein which is processed into constituent parts by both cellular and viral proteases. Viral proteins induce structural rearrangements in the ER to form sites of viral replication. Following replication and further translation, progeny virions can assemble and bud into the ER and traffics to the Golgi apparatus. Flaviviruses undergoes proteolytic maturation in the Golgi and are subsequently exported from the cell. Created in Biorender.

1.2 ZIKV: historical perspective and properties

1.2.1 Discovery and spread

ZIKV was first discovered in 1947, when it was isolated from a rhesus macaque in Uganda's Zika forest, before being first identified in humans there in 1962/63 (Simpson, 1964; Haddow *et al.*, 2012). The WHO says that the first known human ZIKV infection was reported in 1952, likely based on a report from MacNamara, however it seems that this infection was rather the closely related Spondweni virus (Kucharski and Riley, 2016; 'WHO | The history of Zika virus', 2019). Following this discovery, serological studies revealed widespread exposure to ZIKV across equatorial Africa, and through the 60's to the 80's ZIKV spread to equatorial Asia (Duong, Dussart and Buchy, 2017). In 2007, the first outbreak of ZIKV disease was documented on the island of Yap in the federal states of Micronesia (Duffy *et al.*, 2009). While there were no deaths or cases of neurological complications in this outbreak, it was estimated that approximately 73% of the population were at one point infected with ZIKV. The reasons for such high prevalence is currently unknown, especially in the absence of any particular mutations that could explain the difference in pathogenicity, but the lack of natural immunity to ZIKV in an otherwise naïve population could explain the rapid circulation on Yap island (Duffy *et al.*, 2009). Previous similar outbreaks of ZIKV may have occurred but could have been masked by the similar clinical manifestations of similar diseases like DENV and the alphavirus chikungunya (CHIKV).

Following the Yap island outbreak, in late 2013-14 there were more outbreaks across several pacific islands including Easter Island, Cook Islands, New Caledonia and French Polynesia, where a high proportion of populations were reportedly infected (Delatorre, Fernández and Bello, 2018; Musso *et al.*, 2018). Among these outbreaks were the first signs of the clinical manifestations that would come to define future ZIKV outbreaks. Among these clinical manifestations were more serious symptoms with associated with ZIKV, primarily demonstrated by an increase in the reports of Guillain-Barré syndrome higher than what would be expected (Simon *et al.*, 2018). Concurrently, ZIKV was first associated with sexual

transmission, as ZIKV was found shedding in sperm of a man in Tahiti (Musso *et al.*, 2015). Additionally, in late 2013 there was some evidence for potential transplacental transmission (Besnard *et al.*, 2014). The biological mechanisms behind these defining clinical phenotypes will be discussed further below (Chapter 1.2.3). By the spring of 2015, Brazil first reported an unidentified illness which caused a rash, but phylogenetic and molecular clock analysis suggests that ZIKV arrived much early than this, possibly even as early as August of 2013 and was likely imported from the Pacific islands, possibly during the 2013 Confederations Cup (Costa *et al.*, 2020). As such it seems unlikely that the FIFA 2014 World Cup was responsible for the introduction as some have previously speculated.

Zika was formally identified in May of 2015 in Brazil, and other south American countries like Colombia report ZIKV-like illnesses circulating at this time (Tolosa *et al.*, 2017; Lowe *et al.*, 2018). By 2016, ZIKV had expanded into most of Brazil (excluding some of the more remote areas of the Amazon), and seroprevalence reached as high as 63% in some places. On the 1st February 2016, the WHO declared ZIKV a public health emergency (Netto *et al.*, 2017). As this might suggest, in 2016 there was a huge amount of ZIKV infections, with 200,000 suspected infections in Brazil alone as reported by the Pan American Health Organisation (PAHO) (*PAHO/WHO Data - ZIKA*, 2021). Since then however, the number of suspected ZIKV cases across the Americas has consistently fallen year-on-year from approximately 650,000 cases in 2016, to approximately 19,000 cases in 2020 (*PAHO/WHO Data - ZIKA*, 2021). While this is not an insignificant number of infections, it does demonstrate that as the world was ramping up a response to ZIKV, the virus was already disappearing. Since then, there has been some continued transmission in the Americas, as well as localised outbreaks in Asia. For example, Rajasthan state, India, first identified ZIKV cases in September 2018 and a total of 159 cases were reported during September and October of that year (Yadav *et al.*, 2019). These cases were focused in the capital city of Jaipur and seem to be caused by endemic Asian strains. Around the same time, the was also an outbreak in Madhya Pradesh state, where 130 cases were reported mainly

during November 2018 (Gupta *et al.*, 2019). Interestingly, neither outbreak seems to be associated with any neurological defects.

While the dynamics of ZIKV spread during the 2016 pandemic, and the symptoms associated with it, are well understood there are questions remaining as to the reasons underpinning the rapid propagation and subsequent sudden decline in infections. Seroprevalence studies in Brazil have shown there is a high positivity rate for ZIKV antibodies which may impart herd immunity on these populations (Netto *et al.*, 2017). Although there are many areas, such as India, that support *Aedes* mosquito populations they presumably contain a largely naïve population and yet have not suffered such a large outbreak. While recent serological data is missing for the Indian subcontinent, historical data suggests there is a low population seroprevalence for ZIKV antibodies (Khaiboullina *et al.*, 2018). So, what caused the outbreak in the Americas to be on a scale larger than anything seen previously? One answer could lie in weather patterns. El Niño is an irregular, complex weather event that occurs every few years and leads to unusually warm temperatures. This event was particularly strong in 2015, with areas several degrees warmer than usual. Studies have shown that there is a strong overlap between ZIKV incidence and extreme weather associated with El Niño, perhaps with the warmer weather creating ideal conditions for virus spread (Paz and Semenza, 2016; Rao *et al.*, 2019). Indeed, the 2015 El Niño event resulted in Uruguay and southern South America being colder than expected, and these are areas that did not experience as many cases. Therefore, the aforementioned lack of herd immunity, combined with the unusual and extreme weather, may have created the perfect storm for ZIKV to propagate rapidly. As discussed in 1.1.2, global temperatures are likely to influence the range and activity of the main vector of ZIKV transmission, *Aedes* mosquitoes.

1.2.2 Transmission

ZIKV is mainly spread to humans by the urban mosquito *Aedes aegypti*, though there have been many studies investigating the role of other vectors in the transmission of ZIKV (Ciota *et al.*, 2017; Du *et al.*, 2019; Gutiérrez-Bugallo *et al.*, 2019; Gomard *et al.*, 2020) **Error! Reference source not found.**. While *Aedes albopictus* can replicate ZIKV to high titres, there seems to be a barrier to transmission. Additionally, *Culex* species do not appear to replicate ZIKV or transmit it to high levels. This has been shown in several studies, including where mosquitos from Reunion island (2 species of *Culex quinquefasciatus*, *Aedes albopictus and, Aedes aegypti)*, were infected with African (Dak84) or Asian (PaRi_2015 and MAS66) ZIKV lineage. In this study, the *Culex* strains were not infected by any ZIKV strain, whereas both *Aedes* species were poorly infected, but *Aedes aegypti* had a higher transmission efficiency (Gomard *et al.*, 2020). Similarly, another study took ZIKV strains from the 2016 outbreak and a strain isolated in 2010 from Cambodia and tested the vector competence of *Aedes aegypti* and *albopictus*. As in the previous study while *Aedes albopictus* seemed to be infected to similar levels to *Aedes aegypti*, the latter was better able to transmit the virus (Ciota *et al.*, 2017). These reports suggest that while there are several candidate vectors for ZIKV transmission in urban areas, *Aedes aegypti* seems likely to be the primary vector.

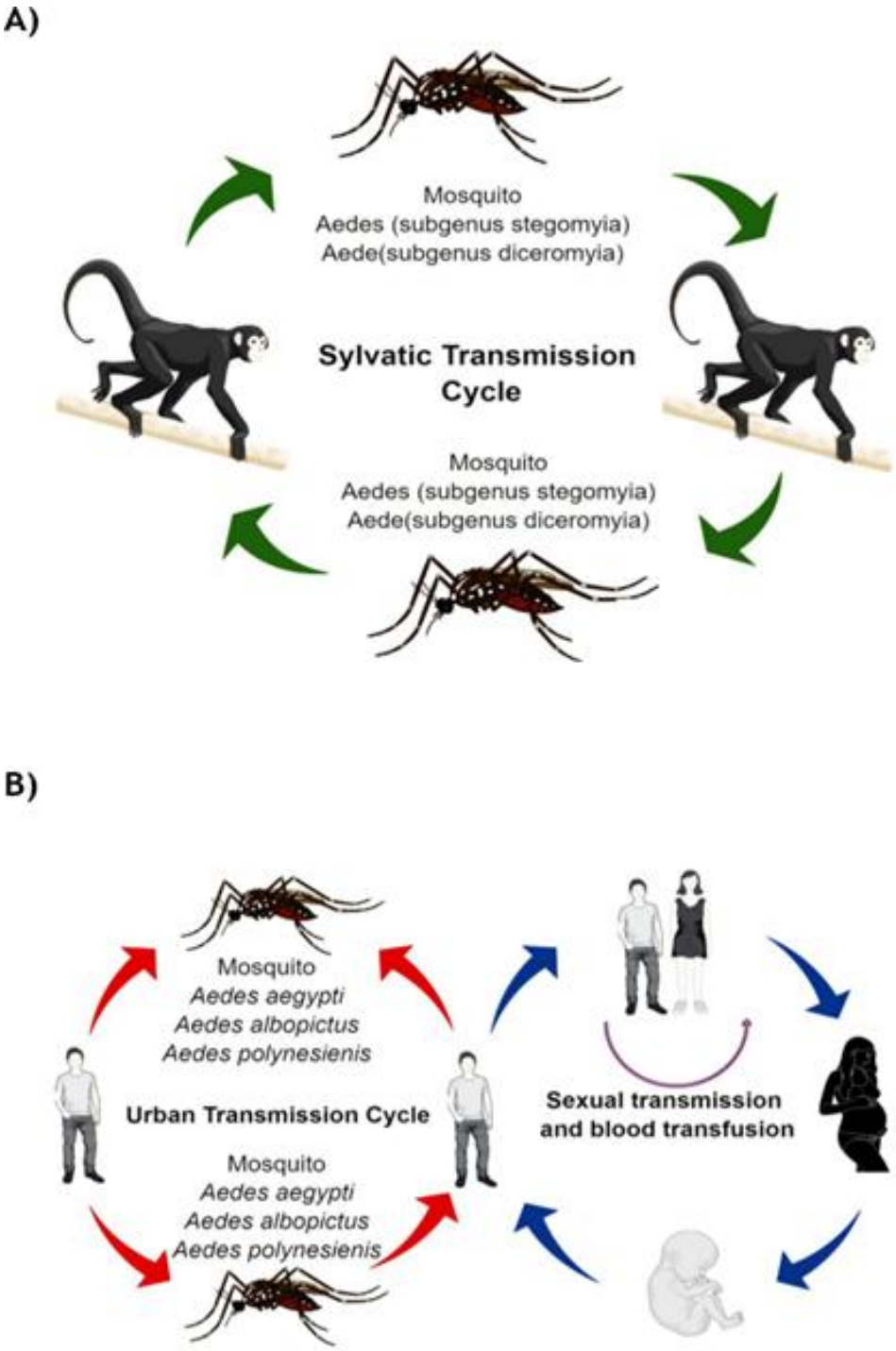

Figure 1-7: Zika transmission cycle.

There are two reported transmission cycles for ZIKV. A) A sylvatic cycle, whereby ZIKV is maintained through infections of non-human primates with arboreal Aedes mosquitoes. B) Amplification of ZIKV in humans following transmission by Aedes mosquitos, and a human-to-human cycle where ZIKV is sexually transmitted. Adapted from Rather et al (2017).

Additionally, *Aedes aegypti* displays several traits that are beneficial to human transmission; they can readily breed in standing-water found in urban environments, are generally day-biting while residing indoors, and can take multiple blood meals within a short period of time (Scott and Takken, 2012). Although *Aedes aegypti* is the primary human vector in urban centres, different *aedes* species, such as *Aedes africanus,* are responsible for the arboreal cycle which largely involves the infection of non-human primates (Berthet *et al.*, 2014). Large swathes of South America are at high risk for ZIKV transmission due to suitable environmental factors for the vector populations (Cunze *et al.*, 2019). As discussed earlier, the predicted habitable area for these vectors is likely to expand in the coming years and decades, exposing previously naïve populations to infection, potentially with similar effects to those as seen in Brazil in 2016.

In addition to mosquito transmission, it has become clear that ZIKV can be sexually transmitted (Moreira *et al.*, 2017). ZIKV RNA has been found in the semen of up to 50% of men infected with ZIKV, and for as long as 370 days following the onset of symptoms, although viral clearance from semen is estimated to be on average close to 25 and 38 days (Barzon *et al.*, 2018; Medina *et al.*, 2018). The occurrence of male-to-female sexual transmission is usually most commonly reported, though there have also been reports of female-to-male and male-to-male transmission (Mead, Hills and Brooks, 2018). While sexual transmission clearly represents an important transmission route for ZIKV, it is not clear what impact this may have had on the rapid spread seen in the Americas in 2016. Indeed, the incidence of sexual transmission in ZIKV has estimated to be around 3% of total viral spread, which is not thought to significantly increase the basic reproduction number (R_0) of the virus, but may have extended the duration of the epidemic (Gao *et al.*, 2016). As well as semen, the presence of ZIKV RNA and infectious particles have been detected in blood, breast milk and urine (Gourinat *et al.*, 2015; Sotelo *et al.*, 2017; Magnus *et al.*, 2018). A meta-analysis of the prevalence of ZIKV in donated blood has been conducted, which found that in collated studies, 1.02% of pooled, blood samples were positive for ZIKV RNA (Liu *et al.*, 2019). While several of the donors were symptomatic none of the blood recipients developed

symptoms, although some did develop anti-ZIKV IgG responses. It is not clear therefore, whether blood-transfusion contributes to the spread of ZIKV.

ZIKV has been shown to disseminate in breast milk, in one case for a month before and 9 days following birth of the child (Sotelo *et al.*, 2017). Here, breastfeeding was not commenced until after ZIKV was no longer detectable and at no point did the baby test positive for ZIKV. Additionally, a study of 4 other breastfeeding mothers with confirmed ZIKV infection revealed that while ZIKV RNA and infectious particles could be isolated from breast milk, there was no detectable transmission to children (Cavalcanti *et al.*, 2017). These results may tentatively suggest that transmission from breast milk is unlikely and may not represent a major route of transmission. ZIKV RNA is readily detectable in patient urine, often for longer and to higher levels than in serum and as such provides an easy way to test for the presence of ZIKV (Gourinat *et al.*, 2015). Additionally, in some cases infectious ZIKV particles have been extracted from patient urine, although it is doubtful whether this represents a major transmission pathway (F. C. Zhang *et al.*, 2016).

One of the hallmarks of the recent ZIKV outbreaks was the incidence of fetal abnormalities, and as such the mechanisms behind maternal-fetal vertical transmission have been thoroughly examined. It became apparent that maternal infection in earlier trimesters was associated with a higher risk to the fetus (Cao, Diamond and Mysorekar, 2017). Indeed, a recent report analysing 7 other prospective studies of ZIKV in pregnancy found that the estimated risk of vertical transmission fell from 47% in the first trimester to 25% in the third. This correlated with a decline in the estimated risk of developing congenital Zika syndrome (CZS) (Chapter 1.2.3) of 9% to 1% in the same trimesters (Ades *et al.*, 2020). Although this study used reports from diverse settings and sometimes incomplete data sets, it is in accordance with other reports (Pomar *et al.*, 2018; Teixeira *et al.*, 2020). While the exact mechanism behind vertical transmission has not yet been elucidated, the transplacental route of infection is possible because ZIKV displays tropisms for many placental cell types as shown through infections of primary

cultures or tissue explants, especially those that make up the placental in the first trimester (El Costa *et al.*, 2016). Additionally, primary human trophoblasts (PHTs) from full-term placentas release type-III IFN's that restrict ZIKV infection (Bayer *et al.*, 2016; Corry *et al.*, 2017). It may be possible that as the placenta develops, increasing PHTs can provide protection against infection resulting in the reduction of vertical transmission and CZS cases as pregnancy advances. While maternal-fetal vertical transmission in ZIKV infections may not be unique in flaviviruses (Platt *et al.*, 2018), it is clearly an important route of disease spread and the cause of severe fetal abnormalities termed CZS which is discussed, along with other symptoms of infection, described in detail in section 1.2.3, below.

1.2.3 Health implications

Most ZIKV infections are symptomless, with many publications suggesting that 80% of ZIKV patients are asymptomatic based on the analysis of the 2007 Yap Island outbreak (Duffy *et al.*, 2009). However, a large scale meta-analysis conducted in 2018 reported that the incidence of symptomless infection ranged from 29% to 82% in analysed studies, with discrepancies in sample sizes and study design frequently reported (Haby *et al.*, 2018). These inconsistencies could be due to the differences in study design or perhaps reveal variances in susceptibilities of different populations to ZIKV infection. Either way, a substantial number of ZIKV infections are asymptomatic. Patients with symptoms often present with a maculopapular rash, fever, conjunctivitis and arthralgia which usually appears after an incubation period of between 1-2 weeks (Duffy *et al.*, 2009). However, in more serious cases, patients can present with Guillain-Barré syndrome. Guillain-Barré syndrome is a rare (1 or 2 in 100,000), immune-related disease which usually follows an infection and is not due to direct damage caused by a pathogen. It causes inflammation of the peripheral nervous system (PNS) and patients present with progressive weakening of the arms, legs, and often cranial muscles, with severe disease leading to respiratory failure (Leonhard *et al.*, 2019). ZIKV-associated GBS occurs 5-12 days after symptom-onset and results in around 40% of patients being admitted to intensive care units (Leonhard *et al.*, 2020). While

some have suggested that ZIKV-associated GBS may be caused by a direct viral affect (Muñoz, Parra and Pardo, 2017), the delay in symptom onset does not necessarily support that. The symptoms of ZIKV-associated GBS are undoubtedly severe and is a major cause of ZIKV morbidity and an economic burden, though recent estimates suggest the incidence of GBS was relatively low at only 0.0061% (He *et al.*, 2020). Though this may be low, a meta-analysis suggests that the 2015/2016 ZIKV epidemic increased GBS incidence by up to 2.6 fold in the Americas (Capasso *et al.*, 2019).

As discussed in 1.2.2, ZIKV can be vertically transmitted from mother to fetus and abrogate fetal development. As such, ZIKV was added to the list of TORCH (**T**oxoplasmosis, **O**ther, **R**ubella, **C**ytomegalovirus and **H**erpes simplex virus) agents; these are pathogens that can cause debilitating congenital disease (Kovacs, 2020). ZIKV induces congenital defects such as microcephaly (where the head circumference is significantly smaller than expected for age and sex), collapsed skull, eye damage and decreased brain tissue (Moore *et al.*, 2017). While the list of symptoms is not exhaustive or descriptive of each case, together they represent a pattern of neurological and developmental defects that are commonly ascribed to neonates, and collectively are known as congenital Zika syndrome (CZS) (Pereira *et al.*, 2020). ZIKV infection has been shown to downregulate genes which regulate the cell-cycle and mitosis, as well as downregulate expression of genes associated with neural stem cells and neuronal cell development (N. Zhang *et al.*, 2016; Rombi *et al.*, 2020). Through these interactions, ZIKV may be able to generate the disease phenotypes seen in CZS. While microcephaly became the defining feature of CZS, it is not the default for clinical manifestations of neonatal ZIKV infection and severe neurological disease can be present without a reduced head circumference (Aragao *et al.*, 2017). While the full extent of the damage caused by CZS to infants is not yet known, it is clear that the socio-economic burden of ZIKV will continue into the future (Kuper *et al.*, 2019).

1.2.4 Replicative cycle

ZIKV entry to cells is primarily initiated through clathrin-mediated endocytosis following binding of ZIKV E to a cellular receptor. While the identity of the cellular receptor has been quite contentious, AXL has been proposed as a primary entry receptor in various cell types, along with other TAM and TIM kinases (Persaud *et al.*, 2018; Ghosh Roy, 2020). This has been disputed, as some studies have suggested that AXL instead inhibits an anti-ZIKV IFN response. Chen and colleagues found that AXL depletion did not inhibit entry but rather facilitated the activation of IFN responses which inhibited infection (Chen *et al.*, 2018). When this IFN response was also removed, even with AXL depletion infection was reinitiated. This suggests that in this system, AXL was either not an entry receptor or not the only one. Indeed, there have been several other suggested receptors that may act in concert or alone depending on cell/tissue type (Nowakowski *et al.*, 2016; F. Li *et al.*, 2017; Meertens *et al.*, 2017; Lee *et al.*, 2018). Despite the contention, AXL clearly plays an important role in ZIKV entry. It may not be the only, or indeed the primary receptor in every system as ZIKV seems capable of engaging multiple cellular receptors. For example, in human skin cells, which are first encountered by ZIKV following mosquito bites, AXL silencing significantly abrogated ZIKV infection (Hamel *et al.*, 2015). Additionally, although Sertoli cells (SC), which form an important part of the testes, can be infected with ZIKV, blockade of AXL binding reduces but does not eliminate ZIKV infection (Strange *et al.*, 2019). In this study, it was found other testicular cells such as Leydig cells (LC) are resistant to ZIKV infection. While LC express less surface AXL than SC, this difference does not seem to account for the differential phenotype. Interestingly, LC also display a higher basal expression of antiviral genes, such as IFIT1, compared to SC, which alone or in combination with the reduction of surface AXL makes them refractory to infection (Strange *et al.*, 2019). AXL has also been implicated in ZIKV entry in primary astrocytes (Ojha *et al.*, 2019). Additionally, this study found that ZIKV infection upregulated TLR3, depletion or inhibition of which reduced infection. ZIKV has also been shown to preferentially infect through the apical membrane of

polarised cell culture, and egress through the basolateral side. Polarised cells make up epithelial membranes that ZIKV would encounter in skin (Tamhankar and Patterson, 2019). Interestingly, ZIKV can potentially encounter such membrane barriers in the gut if transferred through breastfeeding, and there is some evidence that ZIKV can cross intestinal membranes (Hubert *et al.*, 2020). Though, as mentioned earlier, while ZIKV can be shed in breastmilk there is no evidence that this represents a viable route of transmission (Cavalcanti *et al.*, 2017).

Following internalisation, ZIKV traffics through the endosomal pathway whereby a drop in pH facilitates fusion with the late endosomal membrane. Inhibition of endosome acidification with bafilomycin A1 prevents fusion and thus leads to virus degradation, presumably in lysosomes (Owczarek *et al.*, 2019). Interesting NH_4CL treatment, which is thought to similarly inhibit endosomal acidification, results in ZIKV recycling out of the cell in recycling endosomes (Owczarek *et al.*, 2019). A drop in pH as encountered in the endosome is required to facilitate fusion between the ZIKV membrane and endosome. A study using DNA-linked lipids as a surrogate for virions found that a pH of 6 or below is sufficient to trigger fusion, although further decreases do not increase the rate of fusion as there is an unknown rate-limiting step (Rawle *et al.*, 2018). Endosomal proteins, such as Rab5C and Rab11A, have been shown to be important for ZIKV replication, and the interaction with Rab11A could suggest that ZIKV utilises recycling endosomes during entry (Takahashi *et al.*, 2012; Srivastava *et al.*, 2020). Following fusion and uncoating of the virion, the nucleocapsid disassociates releasing viral RNA into the cytoplasm. This disassociation probably happens following ubiquitination of C as is the case for DENV (Byk *et al.*, 2016) (Gestuveo *et al.*, *In press,* 2021).

Following nucleocapsid uncoating, the viral genome is used as a template for translation and progeny viral proteins can induce of rearrangements and invaginations of ER membranes, forming vesicle packets (VP) or RF (Cortese *et al.*, 2017; Rajah, Monel and Schwartz, 2020). These RFs allow spatial and temporal concentration of metabolites required for replication and to protect viral RNA from innate immune sensing. Pores in the RFs allow controlled export of RNA for

translation, or assembly in sites that appear to be juxtaposed to the sites of replication (Cortese *et al.*, 2017). The organisation of these structures seems to be aided by disruption to microtubule structures in ZIKV infected cells; microtubule stabilising drugs are antiviral against ZIKV and microtubule disrupting drugs enhance DENV replication (Chen *et al.*, 2008; Cortese *et al.*, 2017).

As mentioned, ZIKV assembly occurs in viral induced structures near RFs, implying that RNA encapsidation and assembly are coordinated as is the case for DENV (Welsch *et al.*, 2009). ZIKV prM and E alone are sufficient to produce empty virus-like particles (VLPs) which are exported from the cell (Garg *et al.*, 2017). How production of these empty particles is linked to nucleocapsid packaging is not clear, but studies have shown ZIKV NS2A can interact with and recruit viral RNA, NS2B/NS3 and C-prM-E, coordinating proteolytic cleavage of C and prM-E, allowing encapsidation of viral RNA (X. Zhang *et al.*, 2019). Following assembly, immature virions bud into the ER and are transported to the Golgi apparatus. Maturation occurs in the Golgi, when furin (or a furin-like protease) cleaves prM to M and allows structural changes to E which exposes the fusion loop. It is thought that maturation is delayed to prevent pre-emptive fusion and uncoating of the virion in cellular membranes (Sirohi *et al.*, 2016). The secretory pathway following assembly has not yet been fully defined. However, it appears that autophagosomes play an important role for ZIKV secretion as inhibition of autophagy in mice models reduced vertical transmission (Cao *et al.*, 2017; S. Zhang *et al.*, 2019). Additionally, Src-family kinases (SFKs), which are known to be important for regulating KDEL-dependent secretion pathways, also seem to be important for ZIKV egress. Indeed, some SFKs display increased activation following ZIKV infection, and pharmacological or genetic blockade of these SKFs reduces the egress of virions and VLPs (Li *et al.*, 2020).

1.2.5 Antivirals and vaccine development

While there are no currently licensed therapies or vaccines for the treatment of ZIKV, work is ongoing. According to the WHO pipeline tracker, there are currently (as of time of writing: Q1 2021) 16 ongoing trials for a ZIKV vaccine, of which only 2 have reached phase II ('WHO | WHO vaccine pipeline tracker', 2016). These vaccines include inactivated virus, DNA and peptides, with most immunogens being either the whole virus or prM/E. There are several characteristics to consider when designing a vaccine. Ideally one dose should provide long term immunity, administered regardless of age and pregnancy status, require no cold chain and long term storage, and provide protection for a fetus (Wilder-Smith *et al.*, 2018). There are several important issues that have hindered vaccine development so far. As a primary target for a potential vaccine is pregnant women, extra care must be taken to ensure safety to both mother and fetus, and there are ethical issues with including such a population in trials. Additionally, the current lack of infections and the large number of asymptomatic infections means there is a paucity of patients who can be recruited to demonstrate a vaccines efficacy (Abbink, Stephenson and Barouch, 2018). This means it is vital to develop good animal models for the study of ZIKV and the effect of infection on pregnancy (Caine, Jagger and Diamond, 2018).

In addition to a vaccine, therapeutics to treat ongoing cases are also needed. Several small molecules have been investigated for their anti-ZIKV efficacy. One such small-molecule inhibitor is Arbidol, which was originally designed to treat seasonal influenza infections but has been reported to inhibit a wide range of primarily enveloped viruses, including ZIKV (Fink *et al.*, 2018). The mechanism of action has not been fully explored but seems to be through the blocking of glycoprotein mediated attachment to host cells (Fink *et al.*, 2018). Another promising approach has been to modulate the host response at the site of a mosquito bite with a topical application of immune agonists (Bryden *et al.*, 2020). This activated skin-resident macrophages and protected local cellular targets from infection in mice models and explanted tissues and was found to be effective

against several different arboviruses. There have been several other promising small molecule inhibitors identified, some of which are reviewed by Baz and Boivin (Baz and Boivin, 2019). The mechanisms of action of these inhibitors vary and while some directly target viral proteins, some target the host cell. As such, it is vitally important to further our understanding of ZIKV and the pathways and proteins it interacts with during infection.

1.2.6 Interactions with the host cell

Investigating ZIKV interactions with a host cell is vitally important for elucidating important factors in the viral lifecycle. There are several ways to approach this, but large-scale, high-throughput methods are effective. In particular proteomic studies have been vital for investigating and revealing important pathways for ZIKV infection, including putative entry receptors and uncovering pathways of disease pathogenesis (Jiang *et al.*, 2018; Scaturro *et al.*, 2018; Scaturro, Kastner and Pichlmair, 2019; Srivastava *et al.*, 2020). While these studies have mainly focused on ZIKV NS proteins, there are some important ZIKV E interactors identified. For example, proteomic analysis of chemically labelled ZIKV E has been used to capture putative cellular-factors important in the early stages of infection and identified several hundred such proteins, including Neural Cell Adhesion Molecule 1 (NCAM-1) (Srivastava *et al.*, 2020). Further analysis revealed that NCAM1 is an important entry factor for ZIKV in Vero (African Green monkey kidney cells) and U-251 MG (human glioblastoma cells). Other studies have looked at the whole ZIKV interactome and identified cellular proteins important in cell signalling, as well as neural and neuronal development (Scaturro *et al.*, 2018). Notably, such studies have identified doublecortin (DCX) as a protein that was down-regulated by ZIKV infection (Jiang *et al.*, 2018). DCX is a protein involved in neural progenitor cells proliferation and defects in the *DCX* gene lead to malformation of the cerebral neocortex. Following identification of DCX by Jiang and colleagues, other groups have shown that ZIKV can reduce the number of DCX positive cells *in vivo* (W. Zhang *et al.*, 2019).

Additionally, the use of RNAi and CRISPR screening approaches have also been used to uncover important host factors in ZIKV infection (Savidis *et al.*, 2016). Here, depletion of proteins with diverse functions, such as ligand binding, endocytic trafficking and protein processing were identified. Other studies have used CRISPR to identify factors which protect cells from ZIKV infection, such as interferon alpha-inducible protein 6 (IFI6) and interferon lambda 2 (IFN-λ2) (Dukhovny *et al.*, 2019). These selected examples highlight how proteomics and RNAi screens can be a powerful discovery tool for identifying novel host-virus interactions.

1.3 GRP78

1.3.1 Zika virus E protein may interact with GRP78

As described, proteomic experiments can be important investigative tools for discovering host-virus interactions. A previous proteomic study carried out by Carolina Ramírez-Santana (Center for Autoimmune Diseases Research-CREA, School of Medicine and Health Sciences, Universidad del Rosario, 110010 Bogotá, Colombia. This experiment is described with her permission) in the Kohl lab, identified several putative interactors of ZIKV E (Royle *et al.*, 2020). One of these presumed interactors was the multi-faceted, ER-resident chaperone, glucose-regulated protein 78kDa (GRP78). GRP78 has been shown to be unable to bind maturing proteins with N-linked glycans within 38 aa of the N terminus, however mutation of these sites to prevent glycosylation results in GRP78 binding (Molinari and Helenius, 2000). As discussed in Chapter 1.1.3, ZIKV E contains a glycosylation site beyond the N terminus at residue 154. Therefore, GRP78 may be able to bind ZIKV E due to the absence of earlier glycosylation sites (Fontes-Garfias *et al.*, 2017). The interaction between GRP78 and ZIKV E is discussed in more detail in Chapter 5 and forms the basis for the investigation described there.

Here, I shall describe the normal function of GRP78, and its interactions with other viruses.

1.3.2 The structure and function of GRP78

GRP78, also known as heat-shock 70kDa protein A5 (HSPA5), or binding immunoglobulin protein (BiP) is an ER-resident chaperone protein responsible for both protein folding quality-control systems and activation of ER stress response signalling pathways (Foti *et al.*, 1999; Wang *et al.*, 2009; Ni, Zhang and Lee, 2011; Pfaffenbach and Lee, 2011). As a mainly ER resident protein, GRP78 contains a C-terminal lysine, aspartic acid, glutamic acid and leucine (KDEL) ER retention motif which is important for proper ER localisation (Munro and Pelham, 1986). GRP78 is a member of the heat-shock protein 70 (HSP70) family, a large family of cellular

chaperones with functions that are essential for many different pathways (Brocchieri, Conway De Macario and Macario, 2008). These proteins often have multiple designations and nomenclatures which can sometimes lead to confusion. For example, HSP70 (the prototype protein of the family GRP78 is a member of) has been found to mediate ZIKV entry and egress in mammalian cells (Pujhari *et al.*, 2019). This paper was incorrectly used as a basis for a study modelling the interaction between ZIKV E and GRP78, despite there being no mention of GRP78 in original study (Elfiky and Ibrahim, 2020). Therefore, to avoid confusion, I shall exclusively use GRP78 throughout.

GRP78 is a highly conserved protein that can be found in many orders of life (Ting and Lee, 1988). This homology is highlighted in Figure 9-1, which shows how GRP78 displays a high level of protein sequence identity in diverse organisms. Of note for this thesis, Figure 9-1 shows that GRP78 of *Homo sapiens* and *Aedes aegypti* share 81.40% protein sequence identity. In humans, the GRP78 gene is found on chromosome 9 and in humans codes for a 633 amino acid protein. Additionally there is a non-functional pseudogene which does not contribute to transcription (Hendershot *et al.*, 1994; Brocchieri, Conway De Macario and Macario, 2008). Transcription is largely regulated via the interaction of transcription factors such as ATF6-(N) and YY-1 with the ER stress element (ERSE) of the *grp78* promoter (Li *et al.*, 2000; Shi-Chen Ou *et al.*, 2011). *Grp78* transcription is increased in conditions of cell stress, as cell stress activates ATF6-(N) and allows recruitment of YY-1 to ERSE's (Baumeister *et al.*, 2005).

GRP78 is separated into 2 domains; the nucleotide-binding domain (NBD) between residues 25-408 where ATP binding and hydrolysis take place, and the substrate-binding domain (SBD) between resides 419-633 (Yang *et al.*, 2015; Sagara *et al.*, 2018). A short flexible linker sequence from 409 to 418 connects the two domains. This structure is illustrated in Figure 1-8. There are two different conformations: (1) The open conformation, when ATP is bound, and the NBD and SBD are tightly coupled. This state is characterised by accelerated protein binding and release kinetics but an overall low affinity for proteins. (2) The closed confirmation is

adopted in the presence of ADP, or the Apo (nucleotide-free) state. Here, the NBD and SBD have limited interaction and the SBD has a strong affinity for proteins, although the binding and release kinetics are slower (Yang *et al.*, 2015). In this manner, the disparate domains of GRP78 work in concert to orchestrate its vital cellular functions.

One such function of GRP78 is to act as a key sensor of the unfolded protein response (UPR), a pathway which is activated in response to conditions of stress in the ER (Hetz, 2012). Under stress conditions, accumulation and sensing of misfolded proteins by the SBD of GRP78 triggers ATP to ADP hydrolysis in the NBD, which induces a conformational switch to the closed conformation described previously (Sagara *et al.*, 2018). This switch allows both binding of misfolded proteins to the SBD and the release of UPR effector molecules. Under normal conditions GRP78 binds to and prevents the activation of 3 effector molecules; activating transcription factor 6α/ß (ATF6), inositol requiring enzyme 1α/ß (IRE1), and PKR-like ER kinase (PERK) (Harding *et al.*, 2000; Calfon *et al.*, 2002; Shen *et al.*, 2002; Chen and Brandizzi, 2013; Adams *et al.*, 2019). Following GRP78 disassociation, ATF6 translocates from the ER membrane to the Golgi (Shen *et al.*, 2002). In the Golgi, ATF6 is proteolytically processed and the liberated segment can relocate to the nucleus and where it acts to upregulated ER stress genes transcription, including *grp78* as mentioned earlier, and *CHOP*. When IRE1 disassociates from GRP78 it can splice X-box-binding protein 1 (*XBP-1*) into XBP-1s. In this spliced conformation, XBP1s acts as a transcription factor to upregulate production of UPR members (Calfon *et al.*, 2002; Chen and Brandizzi, 2013; Adams *et al.*, 2019). PERK can phosphorylate eukaryotic initiation factor 2 alpha (eIF2α) to halt translation (Harding *et al.*, 2000). Additionally, ATF4 transcription factor is preferentially transcribed following PERK activation and leads to upregulation of proapoptotic factors such as CHOP, and genes involved with amino acid metabolism and resistance to oxidative stress (Luhr *et al.*, 2019). Together, these factors act to positively upregulate stress pathways and to halt translation to prevent further cell damage, though if cellular homeostasis cannot be restored they can initiate controlled apoptosis (Sano and Reed, 2013).

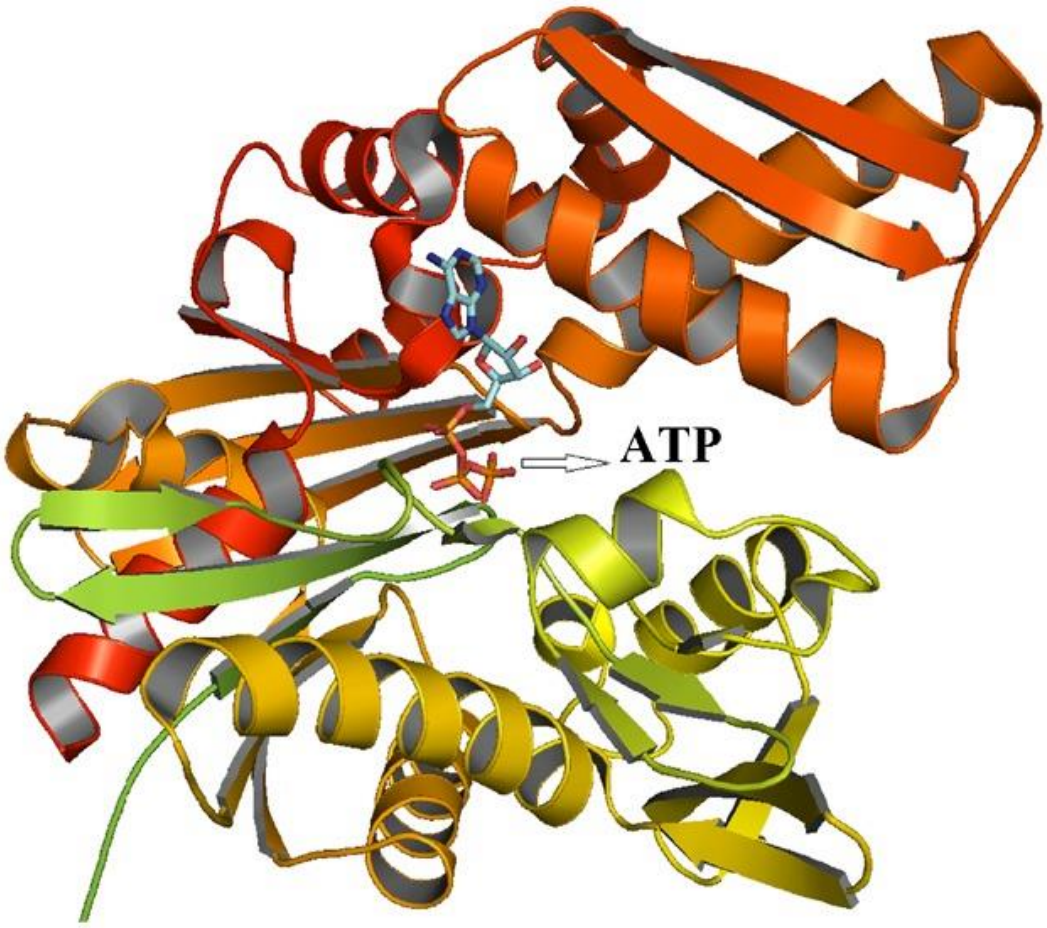

Figure 1-8: Resolved structure of human GRP78.

Schematic of GRP78 nucleotide (ATP) binding domain, with the red colour representing the N terminus and the transition to yellow following the C terminus. Figure taken from Avila et al (2013).

1.3.3 GRP78 and virus lifecycles

As GRP78 is such a ubiquitously expressed and vitally important protein for cell survival, it is perhaps unsurprising that it is implicated in many human diseases including cancer and Alzheimer's, and is an important co-factor for a wide array of other viruses at many different stages of infection (Booth *et al.*, 2015; Casas, 2017). GRP78 can localise to the surface of some cell types and as such has been shown to mediate the entry of several viruses (Quinones, de Ridder and Pizzo, 2008; Ni, Zhang and Lee, 2011; Conner *et al.*, 2020).

For example, GRP78 can localise to the plasma membrane of several neuronal cell types *in vitro* and facilitate the entry of JEV in these cells (Nain *et al.*, 2017). Similarly, another flavivirus, TMUV, requires GRP78 for efficient entry into BHK-21 cell culture (Zhao *et al.*, 2018). Flaviviruses are not the only ones to utilise GRP78 for entry. Several viruses in the *Betacoronavirus* genera of coronaviruses, including Middle-East respiratory syndrome (MERS) virus use GRP78 as an attachment factor through an interaction with the viral spike protein to enhance entry (Chu *et al.*, 2018). Following these discoveries, it has been proposed that GRP78 may also act as an attachment factor for severe-acute respiratory syndrome coronavirus 2 (SARS-CoV-2) via interactions with the viral spike protein, and while this interaction has been computationally modelled it has as of yet not been experimentally proven (Ibrahim *et al.*, 2020). There is some evidence to suggest that peptides that bind to the predicted GRP78 binding site on SARS-CoV-2 spike protein reduces infection (Allam *et al.*, 2020). However, this binding site overlaps with the binding site of other proposed receptors such as ACE2, so it is not yet clear what the mechanism of action behind these peptides are. Despite the lack of evidence, there have already been suggestions that this potential interaction could be a target for therapeutic intervention in SARS-CoV-2 infection or provide the basis for a vaccination scheme, though the feasibility or efficacy of such studies cannot be determined on the current evidence (Elfiky *et al.*, 2020; Palmeira *et al.*, 2020).

GRP78 is also important for the proper maturation and production of some viral proteins. For Sendai virus, the HN glycoprotein has been proposed to transiently associate with GRP78 to allow proper folding and disulfide bond formation during maturation (Roux, 1990). Additionally, variants of the respiratory syncytial virus (RSV) F glycoprotein which did not mature properly were found to bind to GRP78 for longer than those which matured, though whether the association with GRP78 resulted in differing maturation or whether GRP78 binds because of misprocessing is not known (Anderson, Stott and Wertz, 1992). Influenza neuraminidase (NA) protein also transiently associates with GRP78 during maturation (Hogue and Nayak, 1992). DENV has been shown to upregulate GRP78 during infection, and that toxin-mediated depletion of GRP78 reduced DENV viral antigen production (Wati *et al.*, 2009). Interestingly, there are conflicting reports on whether DENV utilises GRP78 as an entry co-factor, though these discrepancies could be due to differences in the cell-line used (Jindadamrongwech, Thepparit and Smith, 2004; Wati *et al.*, 2009).

Given that GRP78 is a major cellular chaperone it is perhaps unsurprising that GRP78 is involved in the folding and maturation of glycoproteins like those mentioned, but it does highlight the vital role it plays in the lifecycles of many viruses.

Virus	Stage of infection	Reference
DENV	Entry/translation/assembly	(Jindadamrongwech, Thepparit and Smith, 2004; Limjindaporn *et al.*, 2009; Wati *et al.*, 2009)
JEV	Entry	(Wu *et al.*, 2011)
TEMV	Entry	(Zhao *et al.*, 2018)
Influenza A	Egress	(Hogue and Nayak, 1992)
MERS	Entry	(Chu *et al.*, 2018)
SARS-CoV-2	Entry?	(Allam *et al.*, 2020)
Sendai virus	Assembly	(Roux, 1990)
HCMV	Assembly, Egress	(Buchkovich *et al.*, 2008; Shi-Chen Ou *et al.*, 2011)
RSV	Assembly/Maturation	(Anderson, Stott and Wertz, 1992)
Ebola	Transcription and translation	(Patrick Reid *et al.*, 2014)

Table 1-1: Selected known interactions between GRP78 and viruses.

A table listing some of the known interactions between viruses and GRP78 and listing the stage of infection that GRP78 is thought to be required for. Sources for information are listed in the table under references.

With that information in mind, GRP78 seemed like an ideal candidate to explore in the context of ZIKV infection.

- GRP78 has been implicated in the infection of related viruses, such as DENV and JEV, and so it seemed likely to be important for ZIKV.

- GRP78 is a highly conserved protein and so its function could be investigated in both mammalian and mosquito systems.

- As a highly studied protein, molecular tools (such as small-molecule inhibitors, siRNA and antibodies) are readily available and would facilitate any investigation.

Chapter 2. Aims

The molecular biology and host-cell interactors of ZIKV are not well understood. Proteomics and high-throughput RNAi experiments have been shown to be powerful tools to dissect host-virus interactions. While several studies have looked at the interaction of *flavivirus* non-structural protein with mammalian cells, not much is known about the interactome of E protein. Additionally, most molecular studies have focused on mammalian, rather than vector systems.

With this in mind, this project aimed to identify cellular factors that are important for ZIKV infection. To do this, diverse approaches were employed. The aims of this project were:

i. To perform a large-scale siRNA knockdown of host genes, including immune related, in the *Aedes aegypti* cell line, Aag2, and investigate the possible role of any hits in regulating ZIKV infection.

ii. To validate the putative interaction between ZIKV E and GRP78.

iii. To dissect the role that GRP78, and cellular interactors of GRP78, may play in the ZIKV lifecycle.

iv. Generate reverse genetics tools for ZIKV to facilitate future studies.

Chapter 3. Materials and Methods

3.1 Materials

3.1.1 Cell culture

A549 cells: Human alveolar carcinoma cells, A549 (ECACC, 86012804), were maintained in Dulbecco's Modified Eagle's Medium (DMEM, Thermo Fisher Scientific) supplemented with 10 % (v/v) fetal bovine serum (FBS) (Gibco). These cells were kept at 37 ^{o}C with 5 % CO_2. A549 cells expressing bovine viral diarrhea virus (BVDV) N-terminal protease (NPro), abbreviated A549-NPro cells (kindly provided by R. E. Randall, University of St Andrews), were maintained as described as above and with the addition of 2 µg/mL blasticidin to select BVDV NPro expressing cells. BVDV NPro inhibits IRF3 signalling and thereby reduces type 1 interferon induction (Hilton *et al.*, 2006).

Aag2 cells: Cells derived from homogenised embryos of *Aedes aegypti* (received from P. Eggleston, Keele University, UK) and were grown in L-15 (Life Technologies) and supplemented with 10% Tryptose Phosphate Broth (Life Technologies), 10% (v/v) FBS, and 100 units/mL of penicillin and 100 µg/mL of streptomycin. Cells were maintained at 28 ^{o}C with no CO_2.

HEK293T: Human embryonic kidney (HEK) cells that express a SV40 large T antigen (kindly provided by the Palmarini group, CVR). Cells were maintained in DMEM supplemented with 10 % (v/v) FBS, 0.1 mM non-essential amino acids (Thermo Fisher Scientific) and kept at 37 ^{o}C with 5 % CO_2.

Huh7: A hepatocyte-derived carcinoma cell line. Cells were maintained in DMEM supplemented with 10 % (v/v) FBS and kept at 37 ^{o}C with 5 % CO_2.

Vero E6 cells: African green monkey, Vero E6 (ATCC, CCL-81™), cells were maintained in DMEM supplemented with 10 % (v/v) FBS and kept at 37 ^{o}C with 5 % CO_2.

3.1.2 Cell culture reagents

Reagent utilised	Source
Avicel	FMC BioPolymer
Blasticidin	Sigma-Aldrich
Puromycin	Sigma-Aldrich
Tryptose Phosphate Broth (TPB)	Gibco
Non-essential amino acids (NEAA)	Thermo Fisher Scientific
Dulbecco Modified Eagle Medium (DMEM)	Gibco
Leibovitz's L-15	Gibco
Opti-Minimum Essential Medium (Opti-MEM)	Thermo Fisher Scientific
Phosphate buffered saline (PBS)	Sigma
Versene in PBS	E&O Laboratories
Trypsin	Thermo Fisher Scientific
Dimethyl sulphoxide (DMSO)	Sigma
DharmaFECT2	Horizon Discovery
Polyethyleneimine (PEI)	Kindly provided by Dr Margus Varjak (University of Tartu)
TransIT-LT1 transfection reagent	MirusBio
Formaldehyde (FA)	Sigma
Paraformaldehyde (PFA)	Sigma
Fetal bovine serum (FBS)	Gibco

Table 3-1: A list of cell culture reagents used and their suppliers.

3.1.3 Viruses

ZIKV PE243: ZIKV/H.sapiens/Brazil/PE243/2015. A ZIKV isolate obtained from a patient in Recife in Brazil, 2015. First described and characterised in the Kohl lab, this virus was amplified in C6/36 cells and Vero cells before use in this study (Donald *et al.*, 2016).

ZIKV Nanoluc: A chimeric ZIKV strain based upon the BeH819015 South American strain and encodes the 5' and 3' UTR's from PE243 (Mutso *et al.*, 2017). This virus has a Nanoluciferase (Nanoluc) molecule preceding a duplicated capsid and is followed by a foot and mouth disease virus (FMDV) 2A autoprotease. The full polyprotein then follows this construct.

WT ZIKV PE243: A reverse genetics version of ZIKV PE243. This contains no sequence differences from the aforementioned ZIKV PE243 and is encoded on 5 separate plasmids noted in Chapter 3.1.4.

HiBiT ZIKV PE243: A reverse genetics version of ZIKV PE243, containing a HiBiT moiety in the N terminus of NS1. This virus was tested in this study but was ultimately not viable.

3.1.4 Plasmids

Plasmid name	Description
pU57_Linker_CPER pU57_S1_CPER pU57_S2_CPER pU57_S2_HiBiT_CPER pU57_S3_CPER pU57_S4_CPER	Plasmids used to assemble the CPER generated WT and HiBiT ZIKV PE243 viruses. To generate HiBiT ZIKV PE243, S2_HiBiT_CPER was substituted for S2_CPER, and no other changes were made.
pCCI-SP6-Zika_Nanoluc	Plasmid encoding full ZIKV Nanoluc (kindly provided by Andres Merits, University of Tartu).
pCCI-SP6-ZikaReplicon_Nanoluc	Plasmid encoding the ZIKV Replicon Nanoluc polyprotein. This protein lacks all structural proteins except the last 30 aa of E (kindly provided by Andres Mertis, University of Tartu).

pGL4.13 FLuc	A firefly luciferase under control of a CMV promoter (Promega).
pVSV-G	Lentivirus helper vector that expresses the VSV envelope protein (kindly provided by Dr Sam Wilson, Centre for Virus Research, Glasgow)
pNLGP	Lentivirus helper vector that expresses Gag and Pol (kindly provided by Dr Sam Wilson, Centre for Virus Research, Glasgow)
LentiCRISPR v2	Backbone for guide RNA insertion. (Addgene plasmid # 52961)

Table 3-2: A list of Plasmids used.
A table documenting the plasmids used in this study and a short description of each.

3.1.5 Primers

Primer	Sequence
GRP78_Guide_1F	CACCGCAAGATGAAGCTCTCCCTGG
GRP78_Guide_1R	AAACCCAGGGAGAGCTTCATCTTGC
GRP78_Guide_2F	CACCGCAGCAGCATCGCGGCCACCA
GRP78_Guide_2R	AAACTGGTGGCCGCGATGCTGCTGC
GRP78_Guide_3F	CACCGGCTGAGCAGCAGCAGCATCG
GRP78_Guide_3R	AAACCGATGCTGCTGCTGCTCAGC C
GRP78_Guide_4F	CACCGGATGCTGCTGCTGCTCAGCG
GRP78_Guide_4R	AAACCGCTGAGCAGCAGCAGCATCC
GRP78_Guide_5F	CACCGTGGCAAGATGAAGCTCTCCC
GRP78_Guide_5R	AAACGGGAGAGCTTCATCTTGCCAC
U6_F	GAGGGCCTATTTCCCATGATTC
Post_Guide_R	CACTCCTTTCAAGACCTAGCTAGC
Linker_F	GCGGCGGCCGGTGTGGGGAAATCCATGGGTCTGGGTCGGCA TGGCATC

Linker_R	CGCAGTCTGATTCACACAGATCAACAACTCGGTTCACTAAACG AGCTCTGCTTATATAGACCTCCC
S1_F	AGTTGTTGATCTGTGTGAATCAGACTG
S1_R	GACATTCCTCCAAACAATGATTTGAAAGCTGC
S2_F	GCAGCTTTCAAATCATTGTTTGGAGGAATGTC
S2_R	CCTTTTTCCAGTCTTCACGTATACGTACCAC
S3_F	GTGGTACGTATACGTGAAGACTGGAAAAAGG
S3_R	ACGTCTCTTGACCAAGCCAGCGTTTCTTGT
S4_F	ACAAGAAACGCTGGCTTGGTCAAGAGACGT
S4_R	AGACCCATGGATTTCCCCACACCGGCCGCCGC
Ago2_F	GTAATACGACTCACTATAGGCAGTTCAAGCAGACGAACCA
Ago2_R	GTAATACGACTCACTATAGGTGATGTAGACGCGTCCTCTG
eGFP_F	GTAATACGACTCACTATAGGGGGCGTGCAGTGCTTCAGCCGC
eGFP_R	GTAATACGACTCACTATAGGGGTGGTTGTCGGGCAGCAGCAC
PIWI4_F	GTAATACGACTCACTATAGGGCCGTATATCCGAAAAAGTGCTG
PIWI4_R	GTAATACGACTCACTATAGGGAGAGTCCACTCGATGTGTTTCA
AAEL013045_T7F	GTAATACGACTCACTATAGGGGTGCAAATTGGGAGTTTTCAG C
AAEL013045_T7R	GTAATACGACTCACTATAGGGAGACGTACTCCTTCAAGCAGAT
AAEL011087_T7F	GTAATACGACTCACTATAGGGCATTTTCAGCCGCAGAATCAAC
AAEL011087_T7R	GTAATACGACTCACTATAGGGCAAAACAGTTATGCAGCTCAGC
AAEL007921_T7F	GTAATACGACTCACTATAGGGGAAGATATTGCCGAGGATGAC G
AAEL007921_T7R	GTAATACGACTCACTATAGGGCTGAGTTCGCAATGATCACACT
AAEL003245_T7F	GTAATACGACTCACTATAGGGGTCCCTGATGATGAACAAGGT G
AAEL003245_T7R	GTAATACGACTCACTATAGGGTGTACACCATTCGATCTCCCAT
AAEL004121_T7F	GTAATACGACTCACTATAGGGAGATGATGTGGCAGAAGAAAG C
AAEL004121_T7R	GTAATACGACTCACTATAGGGTCTCCTTCAGTAGCACCAGATC
AAEL012717_T7F	GTAATACGACTCACTATAGGGACATTTGTCACGTGTGTTCAGT

AAEL012717_T7R	GTAATACGACTCACTATAGGGCTCCAGAATGTTGTTCCTCGTC
AAEL005437_T7F	GTAATACGACTCACTATAGGGCTCCAGAATGTTGTTCCTCGTC
AAEL005437_T7R	GTAATACGACTCACTATAGGGGTCCAAACCATTCGATAGCCAA
AAEL014529_T7F	GTAATACGACTCACTATAGGGTTCCAGTTGAAATCGAGCATCC
AAEL014529_T7R	GTAATACGACTCACTATAGGGGATTTGTCCTCGTCCTTCTTCG
pCCI-SP6-Zika_F	CGATTAAGTTGGGTAACGCCAGGGT
pCCI-SP6-Zika_R	TAGACCCATGGATTTCCCCACACC
qPCR_GAPDH_F	TGCACCACCAACTGCTTAGC
qPCR_GAPDH_R	GGCATGGACTGTGGTCATGAG
qPCR_ZIKV_F	GTTGTCGCTGCTGAAATGGA
qPCR_ZIKV_R	GGGGACTCTGATTGGCTGTA

Table 3-3: A table of the names and sequences of all primers used in this study

3.1.6 siRNA

siRNA	Source (Thermo Fisher Scientific for all)
siN (Neg control siRNA 2)	4390846
siG	S6980
siG a	S6981
siDnaJB11	s28579
siDnaJC1	s34557
siDnaJC10	s28953
siHSP90B	s14373
siERN1	s200432
siKDELR1	s547
siKDELR2	s21689
siKDELR3	s21691

Table 3-4: A table of the siRNA used in this study and their source.

3.1.7 Antibodies

Antibody	Western blot	Immunofluorescence	Immunoprecipitation
Rabbit anti- GRP78 (Ab21685, Abcam)	1:2000	1:1000	1:100
Mouse anti-ZIKV E (AZ 1176, Aalto bio)	1:1000	1:1000	1:100
Rabbit anti-ß Actin (Ab8227, Abcam)	1:5000		
Anti-rabbit Alexa Fluor 488 (35552, Invitrogen)		1:1000	
Anti-rabbit Alexa Fluor 405 (A35551, Invitrogen)		1:1000	
Anti-mouse Alexa Fluor 568 (A11019, Invitrogen)		1:1000	
Anti-rabbit IgG (H and L) DyLight 680 (35568, Thermo Fisher Scientific)	1:5000		
Anti-mouse IgG (H and L) DyLight 800 (35521, Thermo Fisher Scientific).	1:5000		
Rabbit J2 anti-dsRNA IgG2a (Scicons)		1:2000	

Table 3-5: A table showing the antibodies used in this study.
The source of each antibody is shown alongside the working concentrations of each.

3.1.8 Commercial kits and general reagents

Name	Source
EndoFree Plasmid Maxi Kit	Qiagen
PureLink HiPure Plasmid Filter Maxiprep Kit	Invitrogen
QIAEX II® Gel Extraction Kit	Qiagen
QIAquick PCR Purification Kit	Qiagen
QIAprep Spin Miniprep Kit	Qiagen
Fast SYBR Green Master mix	Applied Biosystems
Nano-Glo Dual-Luciferase Reporter Assay System	Promega
Phosphate buffered saline	Sigma Aldrich
Passive Lysis Buffer	Promega
CellTitre-Glo Luminescent Cell Viability Assay	Promega
Nano-Glo Luciferase Assay System	Promega
MEGAScript RNAikit	Ambion
SeeBlue Plus2 Protein standard	Thermo Fisher Scientific
4X Bolt LDS Sample Buffer	Thermo Fisher Scientific
10× Bolt Sample Reducing Agent	Thermo Fisher Scientific
Toluidine blue	Sigma Aldrich
Amersham Protran 0.45 nitrocellulose membrane	GE Healthcare
Bolt 20x MES running buffer	Thermo Fisher Scientific
Semi-dry transfer buffer	Thermo Fisher Scientific
Dynabead Protein G	Thermo Fisher Scientific
GeneRuler 1kb Plus ladder	Thermo Fisher Scientific
6x DNA Loading Dye	Thermo Fisher Scientific
UltraPure agarose	Invitrogen

TAE buffer	Thermo Fisher Scientific
Ethidium bromide	Promega
Ampicillin sodium salt	Thermo Fisher Scientific
Kanamycin sulfate	Sigma Aldrich
LB broth	E&O Laboratories
LB agar	E&O Laboratories
Skimmed milk powder	Marvel
S.O.C. Media	Invitrogen
Halt protease inhibitor cocktail	Thermo Fisher Scientific
Prolong Diamond Antifade Mountant	Thermo Fisher Scientific
Vectorshield HardSet Antifade Mounting Medium	Vector Laboratories
DRAQ7	Abcam
Trizol	Thermo Fisher Scientific
Tween 20	Millipore
dNTP mix (10 mM)	Thermo Fisher Scientific
Random Primers	Promega
m7G cap analogue	Promega

Table 3-6: A table documenting commercial kits and reagents used.

3.1.9 Buffers

Several buffers were made in-house for this study. These were:

PBST: 0.1% (v/v) Tween 20 in PBS.

Western blot blocking buffer: 2% (w/v) skimmed milk powder in PBST.

Immunofluorescence blocking buffer: 5% (v/v) FBS in PBS.

Freeze/thaw buffer: 10% (v/v) FBS in PBS

Immunoprecipitation lysis buffer: 150 mM NaCl, 5 mM MgCl2, 20 mM HEPES (pH 7.4), 0.5% Triton X-100, 1:100 Halt protease inhibitor cocktail.

Immunoprecipitation wash buffer: 150 mM NaCl, 5 mM MgCl2, 20 mM HEPES (pH 7.4), 1:100 Halt protease inhibitor cocktail.

Protein sample buffer: 1x Bolt LDS Sample Buffer, 1x Bolt Sample Reducing Agent in H2O

3.1.10 Enzymes

Name	Source
GoTaq G2 Flexi DNA polymerase	Promega
Phusion® High-Fidelity DNA Polymerase	New England BioLabs
KOD Hot start DNA polymerase	Merck Millipore
SuperScript III reverse transcriptase	Thermo Fisher Scientific
SP6 RNA Polymerase	New England BioLabs
InFusion HD enzyme premix	Takara Bio

Table 3-7: A table listing the enzymes used in this study.

3.1.11 Bacteria

For general cloning techniques, DH5α competent cells (genotype; F - Φ80lacZΔM15 Δ(lacZYA-argF) U169 recA1 endA1 hsdR17 (rk-, mk+) phoA supE44 λthi1 gyrA96 relA1)(Thermo Fisher Scientific) were used.

Plasmids generated from In-Fusion reactions or use in the CPER reactions were amplified in Stellar Competent cells (genotype; F–, endA1, supE44, thi-1, recA1, relA1, gyrA96, phoA, Φ80d lacZΔ
M15, Δ (lacZYA - argF) U169, Δ (mrr - hsdRMS - mcrBC), ΔmcrA, λ–).

3.2 Methods

3.2.1 Cell culture maintenance

Mammalian cell lines were maintained in T75 vented, tissue-culture flasks in the appropriate media (Chapter 3.1.1) at 37 ^{o}C and in 5 % CO_2. To passage these cells, the media was removed, and cells were washed in 5 ml PBS Versene before addition of 3 ml Trypsin in PBS Versene for 5 mins. Detached cells were then re-suspended in a further 7 ml of the appropriate media, and a 1 ml aliquot of this was taken to seed new flasks. Aag2 cells were maintained in T25 non-vented, tissue-culture flasks in L-15 media at 28 ^{o}C with no CO_2. Once confluent, these cells were scraped into the media and were split 1:3.

For cell seeding, cells were counted with a TC20™ Automated Cell Counter (Bio-Rad). Cell seeding densities and media volumes are shown in Table 3-8. Unless stated otherwise, cells were seeding the day prior to experimentation.

Cell culture vessel	Cells seeded (mammalian)	Cells seeded (A549 for IF)	Cells seeded (Aag2)	Media (ml)
T25	1 x 10^6 cells/flask		2 x 10^6 cells/flask	5
6 well plate	4 x 10^5 cells/well		1 x 10^6 cells/well	3
12 well plate	2 x 10^5 cells/well	1 x 10^5 cells/well	5 x 10^5 cells/well	2
24 well plate	1 x 10^5 cells/well		2 x 10^5 cells/well	1
48 well plate	5 x 10^4 cells/well			0.5
96 well plate	2 x 10^4 cells/well		5 x 10^4 cells/well	0.1

Table 3-8: A table showing the seeding densities and medium volumes used in this study.

3.2.2 Cell culture transfection

In this study, several transfection methods were used. For the transfection of RNA (including siRNA and dsRNA) DharmaFECT2 was used, whereas LT1 or PEI were used for the transfection of DNA. Here, transfection reactions were assembled as follows.

RNA: siRNA/dsRNA

For transfection of a 24 well plate with siRNA or dsRNA:

- Reaction 1: 50 µl Opti-Mem + 2 µl DharmaFECT 2
- Reaction 2: 50 µl Opti-Mem + 1 µl siRNA (100 nM) / 300 ng dsRNA

For transfection of a 96 well plate with siRNA or dsRNA:

- Reaction 1: 12.5 µl Opti-Mem + 0.5 µl DharmaFECT 2
- Reaction 2: 12.5 µl Opti-Mem + 0.25 µl siRNA (100 nM)

RNA: *In vitro* transcribed RNA for virus rescue

For transfection of a T25 flask:

- Reaction 1: 500 µl Opti-Mem + 20 µl DharmaFECT 2
- Reaction 2: 500 µl Opti-Mem + 10 µl *in vitro* transcribed RNA

DNA: for the rescue of CPER constructs

For transfection of a T25 flask:

- Reaction 1: 500 µl Opti-Mem + 5 µl LT1
- Reaction 2: 500 µl Opti-Mem + 25 µl CPER product

DNA: transfection of non-CPER plasmids

For transfection of a T25 flask:

- Reaction 1: 500 µl Opti-Mem + 5 µl LT1
- Reaction 2: 500 µl Opti-Mem + 150ng plasmid

For transfection of a 24 well plate:

- Reaction 1: 50 µl Opti-Mem + 2 µl LT1
- Reaction 2: 50 µl Opti-Mem + 50 ng plasmid

DNA: for the generation of lentiviral vectors

For the transfection of a T25 flask:

- Reaction 1: 500 µl Opti-Mem + 44 µl PEI
- Reaction 2: 500 µl Opti-Mem + 5 µg LentiCRISPR v2 + 5 µg pNLGP + 1 µg VSV-G

Reaction 1 and 2 were incubated separately for 5 mins, before being added together for a further 25 mins. Meanwhile, cells previously seeded as described in Chapter 3.2.1 had the media replaced with the same volume of media containing 2% FBS. Finally, the reaction mix was added to cells. The following day, cell supernatant was again replaced with the same volume of media containing 2% FBS or as required for the specific experiment.

3.2.3 Lentivirus production and transduction of cells

HEK293T cells were seeded in T25 (Chapter 3.2.1) to 80% confluency and transfected with a transfer vector containing guide RNA and packaging vectors (Chapter 3.2.2). The following morning, cell media was replaced with 5 ml DMEM containing 10% (v/v) FBS and 1 µg/ml puromycin. Supernatant was harvested 72 hrs later and filtered to remove cellular debris before being aliquoted and stored at -80 ^{o}C.

To transduce cells, A549 were seeded in T25 flasks (Chapter 3.2.1) and 1 ml of filtered lentivirus was applied to cells for 48 hrs. Following, media was replaced with 5 ml DMEM containing 10 % (v/v) FBS and 1 µg/ml puromycin. Cells were then serially diluted in 6 well plates and left for 5 days, and individual cell colonies were ‘picked’ with sterile pipette tips and transferred into a 96 well plate for

expansion. Colonies were then assessed by immunofluorescence and Western blotting.

3.2.4 Virus rescue and amplification

ZIKV Nanoluc: *In vitro* transcription was performed on the pCCI-SP6-ZIKV_Nanoluc plasmid to generate RNA. The reaction was assembled on ice as follows: ATP/CTP/UTP/m^7G cap analogue (2 µl of each), GTP (0.5 µl), MEGAscript SP6 transfection buffer 10 x (2 µl), MEGAscript SP6 enzyme (2 µl), pCCI-SP6-ZIKV_Nanoluc (100 ng) and topped to 20 µl with ddH_2O. This reaction was then performed at 37 ^oC for 4 hrs before transfection into Vero E6 cells in T25 cells (Chapter 3.2.2).

7 days after transfection (or until CPE is observed, whichever was sooner), cell supernatant was harvested and aliquoted, and either stored at -80 ^oC or transferred onto A549 Npro cells for 1 hr (seeded at a density of $1x10^7$ cells in a T225 flask). Following, the supernatant was removed and replaced with DMEM containing 2 % (v/v) FBS for a further 7 days or until significant CPE is observed, whichever was sooner. Supernatant can then be clarified by centrifugation at 1000 x *g* and aliquoted for storage at -80 ^oC.

ZIKV PE243: An aliquot of virus (kindly provided by Dr Claire Donald) was adsorbed onto A549 NPro cells, seeded at a density of $1x10^7$ cells in a T225 flask, for 1 hr. Following, the supernatant was removed and replaced with DMEM containing 2 % (v/v) FBS for a further 7 days or until significant CPE is observed, whichever was sooner.

3.2.5 Circular polymerase extension reaction

To rescue the reverse genetics ZIKV PE243, 5 segments of the PE243 were commercially synthesised. These segments include:

- A linker (pU57_Linker_CPER), which contains a hepatitis D virus ribozyme (HDVR), SV40 poly(A) signal, junk DNA, a CMV promoter and shares an ~30 bp overlap with S1 and S5. This segment circularises the segments, and the junk DNA allows for de-coupling of RNA polymerase II and prevent a run-off into the 5' end of the genome.
- Segment 1 (pU57_S1_CPER), which covers the 5' UTR through to the just before the start of NS1, overlaps with the linker and S2.
- Segment 2 (pU57_S2_CPER), NS1 through to the start of NS3, overlaps with S1 and S3.
- Segment 3 (pU57_S3_CPER), NS3 through to the start of NS5, overlaps with S2 and S4.
- Segment 4 (pU57_S4_CPER), NS5 and the 3' UTR, overlaps with S3 and the linker.
- Segment 2 HiBiT (pU57_S2_HiBiT_CPER), a variant of S2, where the first 4 aa of NS1 are duplicated and followed by a HiBiT moiety, a 4GS linker, and the rest of NS1 as normal. This segment shares the same overlaps as S2.

Individual segments were amplified from these plasmids in a PCR reaction as follows: Plasmid template (1 µl), forward and reverse primer (1 µl each) (Chapter 3.1.5), dNTPs (1 µl), DMSO (1.5 µl), GC buffer (10 µl), Phusion polyermase (0.5 µl), topped up to 50 µl with water.

Conditions for the PCR:
Initial:

- 95 ^{o}C for 5 mins.

30 cycles:

- 95 ^{o}C for 30 s
- 55 ^{o}C for 30 s
- 72 ^{o}C for 3 mins

Final:

- 72 ^{o}C for 5 mins

Products were separate on a 1 % agarose gel at 90V for 1 hr, and bands of correct size were excised from the gel and purified using a QIAEX II® Gel Extraction Kit following the manufactures instructions. Purified bands were then used in a final circular polymerase extension reaction (CPER) as follows: Excised templates (0.1 pmol of each segment), forward and reverse primer for each segment (1 µl each) (Chapter 3.1.5), dNTPs (1 µl), DMSO (1.5 µl), GC buffer (10 µl), Phusion polymerase (0.5 µl), topped up to 50 µl with water.

Conditions for the CPER PCR:
Initial:

- 95 ^{o}C for 5 mins.

20 cycles:

- 95 ^{o}C for 30 s
- 55 ^{o}C for 30 s
- 72 ^{o}C for 10 mins

Final:

- 72 ^{o}C for 15 mins

Vero E6 cells seeded in a T25 were then transfected as described in Chapter 3.2.2.

3.2.6 Large scale siRNA screen

Aag2 cells were seeded in 96 well plates with 100 µl media (Chapter 3.1.1) and left to settle overnight. siRNA plates were provided by Ambion in a 96 well plate format, with 3 individual siRNAs against a specific target pooled in a single well, at a 1000 nM concentration of siRNA. From these master plates, working plates were created by taking 7.5 µl siRNA and supplemented with 17.5 µl of Opti-mem (siRNA concentration 300 nM). 25 µl Opti-mem and 2 µl DharmaFECT 2 per well was made up and added to the working plates to incubate for 30 mins (siRNA concentration 150 nM). The final 50 µl transfection mixture was added to the Aag2 for 24 hrs for a final siRNA concentration of 50 nM. Cells were then infected with ZIKV Nanoluc at an MOI 5 for 48 hrs, before media was removed and cells were lysed, and luciferase measured with Nano-Glo Luciferase Assay System as per the manufacturer's instructions.

3.2.7 Plaque assays

Harvested supernatants were serially diluted onto A549 NPro cells seeded in 12 well plates (Chapter 3.2.1) and overlaid with DMEM supplemented with 2% FBS and 1.2% Avicel for 5 days at 37 ^{o}C. 4% formaldehyde was used to fix cell monolayers for 20 min prior to staining with toluidine blue to visualise viral plaques.

3.2.8 Luciferase assays

Cell viability assay: To determine cell viability, a DMSO control, EGCG or HNK was serially diluted onto A549 cells seeded in a 24 well plate (Chapter 3.2.1) for 26 hrs. The media was removed, and CellTitre-Glo Luminescent Cell Viability Assay reagent was then added to cells following the manufacturer's instructions. A GloMax luciferase machine (Promega) was used to measure luminescence, and an integration time of 5 seconds was used.

Nanoluciferase assay: A549 cells were seeded in a 24 well plate (Chapter 3.2.1) and treated with DMSO or small-molecule inhibitors for 2 hrs prior to and/or (as specified) throughout a 24 hr infection with ZIKV Nanoluc at a MOI 0.1. For the virus pre-treatment assay, ZIKV Nanoluc was incubated with either 10 μM EGCG or DMSO for 2 hrs in DMEM plus 2% FBS prior to infection of cells. To the Nanoluc expressed by ZIKV Nanoluc, cells were first lysed in Passive Lysis Buffer before treatment with Nano-Glo Luciferase Assay System as per the manufacturer's instructions. Alternatively, A549 cells seeded in a 24 well plate were transfected with 10 or 25 μg of *in vitro* transcribed ZIKV replicon RNA for 24 hrs in the presence of 10 μM EGCG or DMSO. GloMax luciferase machine was used to measure luminescence, and an integration time of 5 seconds was used.

Dual luciferase assay: A549 cells, seeded in a 24 well plate (Chapter 3.2.1) were treated with siRNA (Chapter 3.2.2) for 72 hrs prior to infection with ZIKV Nanoluc at a MOI 5 for 48 hrs. 24 hrs into infection, 100 ng of pGL4.13 FLuc was transfected into cells (Chapter 3.2.2) for the remaining time of infection. The Firefly luciferase gene in pGL4.13, FLuc, is under the control of a CMV promoter. Cells were harvested and luciferase values were measured using the Nano-Glo Dual-Luciferase Reporter Assay System following the manufacturer's instructions. A GloMax luciferase machine was used to measure luminescence, and an integration time of 5 seconds was used.

3.2.9 Freeze/thaw assay

A549 cells were treated with siRNA (Chapter 3.2.1) and then infected with ZIKV PE243 at MOI 5 for 24 h. Supernatant was harvested from cells and split into two fractions. The first fraction was serially diluted and titrated on A549-NPro cells (Chapter 3.2.7). The second was subject to 3× freeze/thaw (f/t) cycles, whereby supernatants were cyclically frozen on dry ice for 5 min and thawed at 37 °C for 2 min and virus plaques counted on A549-NPros. Cell monolayers from corresponding cell supernatants were then washed with 1× trypsin and with 3× PBS washes to remove residual virus particles. These cells were scraped into 10 % (v/v)

FBS in PBS and subject to 3× f/t cycles, before cellular debris was pelleted at 4000 × *g* for 10 min. This clarified supernatant was serially diluted onto A549-NPros to calculate viral titre.

3.2.10 Western blot analysis

Proteins were harvested from cells in Passive Lysis Buffer with 0.1% Halt protease inhibitor cocktail and incubated on ice for 20 mins. Cell lysates were then clarified to remove cellular debris and were separated on Bolt 4–12% Bis-Tris Plus gels in MES running buffer at 100V for 1 hr 30 mins. These gels were then transferred to Protran 0.45 NC membranes using the Trans-Blot SD semi-dry transfer cell (Bio-Rad). The membrane was then blocked for 1 hr in 5% (w/v*)* milk in 0.1% PBST before incubated overnight at 4 °C in 5% (w/v) milk in 0.1% PBST containing the appropriate antibody (Chapter 3.1.73.1.7). Membranes were then washed for 3 x 10 mins 0.1% PBST before incubation with the appropriate fluorescent secondary antibody (Chapter 3.1.73.1.7). This again was followed by three 10 min washes with 0.1% PBST, a final 10 min wash in ddH_20, and fluorescently labelled antibodies were imaged on an Odyssey CLx (LI-COR Biosciences).

3.2.11 Immunofluorescence

A549 cells were seeded onto 13 mm coverslips (Chapter 3.2.1) and allowed to settle overnight. For infection, cells were infected with ZIKV PE243 an MOI 0.1 for 24 hrs and fixed with 4% formaldehyde for 20 min at room temperature. If no infection was performed, cells were fixed in the morning following. Cells were then permeabilised with 0.5% (v/v) Triton X-100 in PBS for 10 min and blocked with 5% (v/v) FBS in PBS for 1 hr. For any non-permeabilising conditions, cells were instead fixed in 8% (v/v) paraformaldehyde in PBS (as this is not stabilised with methanol) and no permeabilising buffer was used. Relevant antibodies (Chapter 3.1.7) were diluted in 5% (v/v) FBS in PBS and incubated with cells for 2 hrs at room temperature. Staining with secondary antibodies (Chapter 3.1.7) were also diluted in 5% (v/v) FBS in PBS was performed for 1 hr. Coverslips were mounted

onto glass microscope slides with HardSet Antifade Mounting Medium with 4′,6-diamidino-2-phenylindole (DAPI). Alternatively, where indicated, DRAQ7 nuclear stain was applied in the last FBS in PBS wash and coverslips were mounted using Prolong Diamond Antifade without DAPI. Images were taken on a Zeiss LSM 710 inverted confocal microscope (Carl Zeiss).

3.2.12 RNA extraction and RT-qPCR

A549 cells were seeded in a 24-well plate (Chapter 3.2.1) and RNA was harvested with 333 µl Trizol, with triplicate wells pooled to isolate total RNA. This RNA was purified with the addition of 200 µl chloroform/mL of Trizol, and the sample was vortexed for 15 seconds. Samples were centrifuged for 15 min at 12,000 x g at 4°C. 500 µl of isopropanol and 0.5 µl RNAse free glycogen (10 mg/ml) was added to the upper aqueous phase and this mix was incubated at room temperature for 10 min, before a further centrifugation for 15 min at 12,000 x g at 4°C. The RNA pellet was then washed with 70% (v/v) ethanol and centrifuged for a further 15 min at 12,000 x g.

To synthesise cDNA, 1 µg of purified RNA was used as template for Superscript III reverse transcriptase (RT) with random primers. Quantitative RT-PCR for ZIKV and the housekeeping gene GAPDH were detected with specific primers (Chapter 3.1.5). Amplification signal was detected using SYBR green Mastermix using an ABI7500 Fast qPCR machine according to manufacturer's protocol. Results were analysed using the ΔΔCt method (Livak and Schmittgen, 2001).

3.2.13 dsRNA synthesis

Cellular RNA was harvested and purified from Aag2 cells using Trizol as described in Chapter 3.2.12, and cDNA was created with Superscript III RT with random hexamer primers following the manufacturer's instructions. Genes of interest were amplified from cDNA in a PCR using primers that included a T7 gene sequence (Chapter 3.1.5). PCR products were purified using a QIAquick PCR Purification Kit,

and 1 µg of product was used as a template for dsRNA synthesis using a MEGAScript RNAi Kit following the manufacturer's instructions, and concentration of dsRNA was measured using a NanoDrop ND-1,000 spectrophotometer (Thermo Fisher Scientific).

3.2.14 Co-Immunoprecipitation

A549 or Aag2 cells were seeded (Chapter 3.2.1) and infected with ZIKV PE243 at an MOI 1 for 24 hrs or 48 hrs respectively. Supernatants were removed, cells were washed with PBS, and then cells were resuspended in IP lysis buffer (Chapter 3.1.9). After lysis, 1/50 of sample was taken for Western blot analysis (Chapter 3.1.10). Remaining immunoprecipitation samples were kept on ice for 20 min and centrifugated at 15,000 x *g* at 4 ^{o}C for 20 min. The supernatant was transferred into fresh tubes on ice and incubated with mouse anti-ZIKV E antibody or rabbit anti-GRP78 antibody for 2 hr at 4 ^{o}C. Following this, protein G magnetic beads were equilibrated in cold IP wash buffer (Chapter 3.1.9) and then added to supernatants for 1 hr at 4 ^{o}C, before 4 washes with cold washing buffer. Beads were re-suspended in protein sample buffer (Chapter 3.1.9) and subjected to proteomic analysis (as performed by Carolina Ramírez-Santana (Center for Autoimmune Diseases Research-CREA, School of Medicine and Health Sciences, Universidad del Rosario, 110010 Bogotá, Colombia) or boiled to elute proteins from beads prior to Western blot analysis (Chapter 3.2.10).

3.2.15 Mass spectrometry analysis

The mass spectrometry analysis described in Chapter 5 was performed by Carolina Ramírez-Santana (Center for Autoimmune Diseases Research-CREA, School of Medicine and Health Sciences, Universidad del Rosario, 110010 Bogotá, Colombia) and presented here with full permission. For completeness, the mass spectrometry analysis she undertook is described here.

Peptides were solubilised in 1% acetonitrile (ACN) (Rathburn Chemicals) with 0.05% formic acid (FoA) (Sigma-Aldrich) and were separated using an UltiMate 3000 RSLC nano liquid chromatography system (Thermo Fisher Scientific). This was conducted prior to analysis with electrospray ionisation (ESI) mass spectrometry on an LTQ-Orbitrap Elite mass spectrometer (Thermo Fisher Scientific). Peptide samples were desalted and concentrated on a C18 trap column (5 mM × 300 µM ID, 5 µM, 100 Å) (Thermo Fisher Scientific), for 4 min and washed for 7 min with 1% ACN with 0.05% FA at a flow rate of 25 µl/min. Subsequently, samples were separated through an Acclaim PepMap 100 C18 Column (150 mm × 75 µm ID, 3 µm, 100 Å) (Thermo Fisher Scientific) with a gradient flow rate of 300 nl/min, and was 4–40% of 80% ACN in 0.08% FA over 90 min, then 40–100% of 80% ACN in 0.08% FA over 14 min, held at 100% for 5 min, and then re-equilibrated to 4% of 80% ACN in 0.08% FA for a total of 125 min. Peptide ions were detected in the Orbitrap mass spectrometer with a precursor scan at 60,000 resolving power within the mass range of *m/z* 400–2000. Tandem mass spectrometry (MS/MS) was performed on the 20 most intense ions detected in the precursor scans. Singly-charged ions were excluded from selection. MS/MS by collision-induced dissociation (CID) was carried out and detected in the linear ion trap (LTQ). A dynamic exclusion of 180 s was used to prevent repeat analyses of high intensity ions.

3.2.16 Bacterial transformation

50 µl of either DH5α or Stellar competent cells were incubated with 1-2 µl of selected plasmid on ice for 20 mins prior to a 30 s heat shock at 42 °C. Cells were then incubated on ice for 2 minutes before they were added to 200 µl of S.O.C growth media. Bacterial cells were subsequently placed at 37 °C and rotated at 180 rpm for 1 hr. Cells were spread on LB agar plates containing either ampicillin or kanamycin, depending on the plasmid, (100 µg/mL) and incubated at 37 °C overnight.

3.2.17 Plasmid purification

Colonies were picked from LB agar plates generated in Chapter 3.2.17 and were used to create starter cultures by shaking at 37 ^{o}C at 180 rpm for 8 hrs in 10 ml of LB anti-biotic free medium. Subsequently, this starter culture was added to 100 ml of LB broth with 100 µg/mL of antibiotic, and shaken overnight at 37 ^{o}C at 180 rpm. Amplified bacterial cells were harvested via centrifugation at 1000 rpm for 20 mins. The cell pellet was lysed and purified by using either EndoFree Plasmid Maxi Kit or PureLink HiPure Plasmid Filter Maxiprep Kit, following the manufacturer's instructions in either case.

Chapter 4. Investigating *Aedes aegypti* immune factors that regulate ZIKV infection

4.1 Introduction

ZIKV persists in the environment through maintenance in competent mosquito species, and is spread to humans through transmission by different members of the *Aedes* mosquito genus, primarily *Aedes aegypti* (Musso and Gubler, 2016). Due to the lack of therapeutics or available vaccines against most arboviruses, the primary disease control mechanism has often been the use of insecticides to limit vector populations (Dos Santos *et al.*, 2020). However, vector populations are increasingly found to be resistant to the insecticides being deployed and therefore their further usefulness is questioned (Kupferschmidt, 2016). The release of genetically modified mosquitoes is also being considered and trialed, the most recent example being a large Oxitech pilot scheme, which plans to release many modified mosquitoes into the Florida Keys in 2021. In the past this system engineered male mosquitoes with a germline dependency on tetracycline, without which they and their progeny theoretically cannot survive (Phuc *et al.*, 2007). These releases are predicted to dramatically reduce the local mosquito populations, thereby reducing transmission of arboviruses such as ZIKV. Early reports from trial releases in Brazil however indicate that a subsection of the released *Aedes aegypti* mosquitoes were biologically fit enough to survive without tetracycline, and went on to reproduce with native mosquitoes (Evans *et al.*, 2019). If this phenomenon is observed with future releases of modified mosquitoes, the usefulness of these programs will likely be questioned.

Similarly, persistent infection of mosquito vectors with the endosymbiont bacteria *Wolbachia pipientis* has shown promise in reducing the transmission competence of these infected mosquitoes (Chouin-Carneiro *et al.*, 2020). Here, *Wolbachia* is maternally transmitted, and so released *Wolbachia* mosquitoes can integrate and introduce a chosen *Wolbachia* strain into native populations (Schultz *et al.*, 2017).

The mechanism of action of viral suppression is thought to be multifaceted and virus specific, though several studies have shown that *Wolbachia*-mediated reduction of lipid/cholesterol availability is important (Geoghegan *et al.*, 2017; Schultz *et al.*, 2018). Concerns surrounding efficacy, mosquito survival, resistance, and ethical issues have all been raised in response to the generation and release of these mosquitoes, and much work remains to be done (Meghani and Boëte, 2018).

Understanding the relationship between the mosquito immune response and infection is therefore vital to facilitate the development of new strategies to control arbovirus spread. The primary defense of arthropods against arbovirus infection is the RNA interference (RNAi) response (Lee *et al.*, 2019) and is shown in part in Figure 4-1. The 3 main types of small RNAs produced are exogenous small interfering RNA (exo-siRNA), PIWI-interacting RNA (piRNA) and microRNAs (miRNA), all of which have been implicated in regulating ZIKV infection. (Saldaña *et al.*, 2017; Varjak, Donald, *et al.*, 2017; Varjak, Maringer, *et al.*, 2017; Göertz *et al.*, 2019). Exo-siRNAs are traditionally considered to be the primary anti-viral pathway in *Aedes aegypti*. Exo-siRNAs are produced in the exo-siRNA pathway following the splicing of viral dsRNA intermediates by Dicer 2 (Drc2), which generates precise, 21 nucleotide (nt) long, double-stranded RNA (dsRNA) intermediates, which are then loaded onto the RNA-induced silencing complex (RISC) (Carthew and Sontheimer, 2009). The RISC is made up of proteins such as Argonaute 2 (Ago2) which process the 21 nt dsRNA into single stranded siRNA, which can target the complementary viral RNA and facilitate its degradation (Van Rij *et al.*, 2006). piRNAs, generated from the piRNA pathway, are longer than siRNA, being 25-29nt in length. They are produced via the 'ping-pong' amplification loop and show a bias for a characteristic uridine residue at position 1 in anti-sense sequences, and an adenine residue at position 10 in sense sequences (Varjak, Leggewie and Schnettler, 2018). miRNA, like siRNA, are non-coding RNA sequences of around 22 nt that are derived from dsRNA and can elicit gene silencing following processing by Dicer 1 and subsequent loading onto the RISC complex with Argonaute 1 (Lee *et al.*, 2019). Unlike siRNA, virus specific

miRNAs are unlikely to be produced in response to flavivirus infection because some of the machinery required for miRNA processing are located within the nucleus, where positive sense viral RNA is unlikely to reach. However, virus specific modulation of host miRNA has been shown to influence infection for several flaviviruses, including ZIKV (Saldaña *et al.*, 2017).

In ZIKV infected *Aedes aegypti* cells, virus specific siRNAs are produced and cells which lack Dcr2 support ZIKV replication to higher levels (Varjak, Donald, *et al.*, 2017). Conversely, silencing of Ago2 does not upregulate ZIKV infection in these cells as shown by Varjak and colleagues. Here, ZIKV differs from many other RNA viruses that see relief from restriction following Ago2 silencing (Sánchez-Vargas *et al.*, 2009; S. Chen *et al.*, 2011; Sasaki *et al.*, 2017; Varjak, Maringer, *et al.*, 2017). Additionally, Varjak *et al* found that while piRNAs are produced, they did not contain the specific signatures that are usually associated with them, and silencing of piRNA producing proteins such as Ago3, PIWI5 and PIWI 6 did not enhance ZIKV replication. PIWI 4, which is not associated with canonical piRNA pathways was, however, found to be antiviral, a finding that has been repeated for viruses other than ZIKV (Varjak, Maringer, *et al.*, 2017). While these findings are well established at the time of writing, upon commencement of the study they were not known.

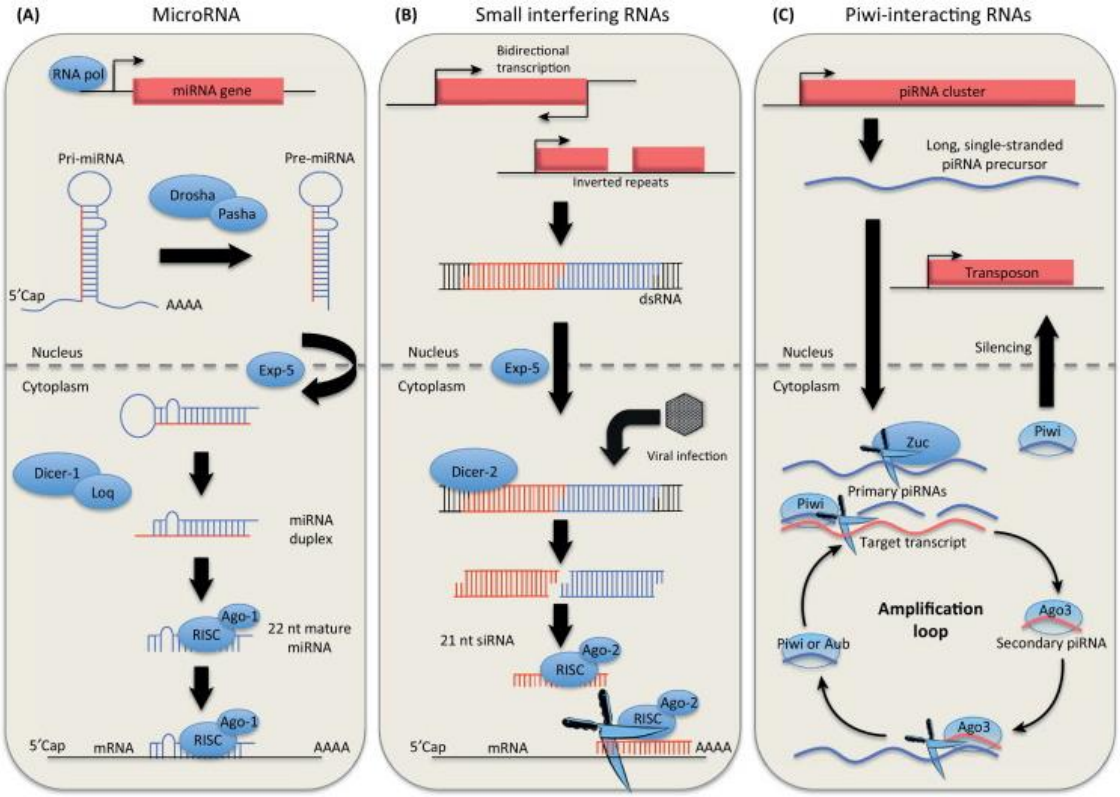

Figure 4-1: Mosquito anti-viral RNAi responses.

There are three different RNA interference (RNAi) pathways involved in response to virus infection: exogenous small interfering RNA (exo-siRNA), PIWI-interactiong RNA (piRNA) and microRNA (miRNA) pathways. Figure adapted from Lucas et al, 2013 (Lucas, Myles and Raikhel, 2013).

Other major factors involved in regulating the mosquito immune response to flaviviruses include the Toll and Janus kinase/signal transducer and activator of transcription (JAK/STAT) pathways (Angleró-Rodríguez *et al.*, 2017; Harsh and Eleftherianos, 2020). Activation of these pathways in response to infection can lead to expression of various antimicrobial peptides to protect against infection (Kumar *et al.*, 2018). There are flavivirus-specific differences in the response of Toll and JAK/STAT to infection, where activation of Toll signalling in *Aedes aegypti* seemed to be stronger in response to ZIKV infection, whereas JAK/STAT activation appears more pronounced in DENV infected mosquitoes (Souza-Neto, Sim and Dimopoulos, 2009; Angleró-Rodríguez *et al.*, 2017). Although some studies have investigated the wider mosquito immune response to ZIKV infection, most research has focused on DENV and therefore there is a broader base of knowledge (Mukherjee *et al.*, 2019).

As such there is a need to further investigate and identify key elements in the mosquito response, as well as other relevant host factors, to ZIKV infection. This knowledge could allow for targeted intervention in a key stage of ZIKV transmission.

4.1.1 Aims

The main aim of this study was:

- To investigate the wider mosquito immune response to ZIKV infection, and other host factors requited for infection, by performing a large-scale siRNA knockdown screen in Aag2 cells. This screen consists of pools of siRNAs targeting 998 host genes.

To facilitate this, there were several milestones to achieve first. These included:

- To rescue a ZIKV luciferase (ZIKV Nanoluc) reporter virus.
- To characterise the luciferase production kinetics of this reporter virus
- To test whether ZIKV Nanoluc can be used to assess the effect of siRNA-mediated knockdown of important cellular factors.

4.2 Results

4.2.1 Characterisation of a ZIKV reporter virus

The overall aim of the investigation described in Chapter 4 was to identify *Aedes aegypti* host factors which can regulate ZIKV infection using a previously established siRNA screen which targets 998 host genes. However, prior to commencement of the screen, several steps were taken to produce the reagents required and to establish experimental conditions. Firstly, I aimed to rescue a nanoluciferase (Nanoluc) tagged ZIKV virus (ZIKV Nanoluc) and characterise the virus to establish optimal conditions for future experiments. Nanoluc is a bioluminescent enzyme that produces light from chemical processing of a substrate. While Firefly or *Renilla* luciferases are often used, Nanoluc has several advantages which include a smaller size, increased stability and brighter luminescence (England, Ehlerding and Cai, 2016). When encoded in the viral polyprotein a Nanoluc reporter can provide a sensitive, high throughput readout for infection, with an increase in luciferase signal presumably correlating linearly with an increase in virus (Ramanathan *et al.*, 2020). The template DNA for the Nanoluc reporter virus (and subsequently described replicon) was generously provided by Prof Andres Merits (Institute of Technology, University of Tartu), and has previously been described (Mutso *et al.*, 2017). The structure of this reporter virus is based on a Brazilian isolate termed BeH819015. This virus did not have the 5' and 3' UTR sequence available at the time of assembly and so these sequences were taken from PE243, another Brazilian isolate which is also used extensively in the Kohl lab. The Nanoluc moiety is encoded in the polyprotein following a duplicated capsid, and precedes a foot-and-mouth disease virus (FMDV) 2A autoprotease, which is required for cleavage of the Nanoluc moiety from the subsequent complete ZIKV polypeptide (Donnelly *et al.*, 2001). This construct is displayed in Figure 4-2 alongside a ZIKV Nanoluc replicon which is used in subsequent studies described in this thesis (Chapter 5.2.3, Figure 5-8). This replicon encodes the same luciferase moiety, but full M and E proteins are lacking to prevent generation of infectious virions. The last 30 residues of E are retained to facilitate the insertion of NS1 and the subsequent polyprotein into the ER

membrane (Falgout, Chanock and Lai, 1989). A so called wild-type (WT) virus, lacking the Nanoluc and autoprotease moieties was also rescued.

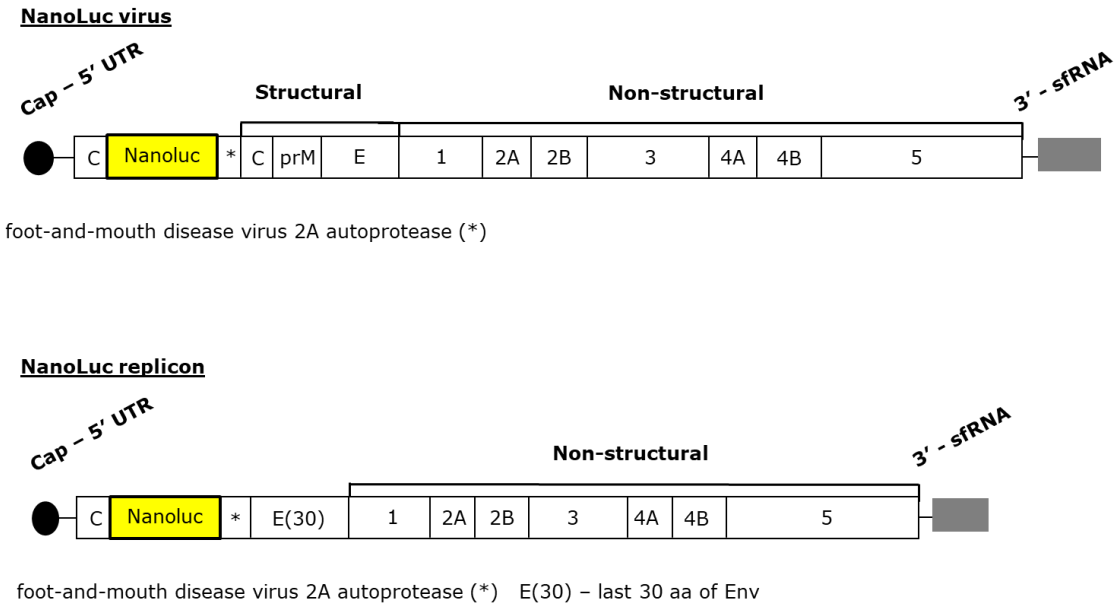

Figure 4-2: Diagram showing the structure of a ZIKV reporter virus.
(A) *The Brazilian ZIKV strain termed BeH819015 was used as a basis for constructing a reporter virus that was used in this study. The 5' and 3' untranslated regions (UTR) are taken from the PE243 Brazilian isolate. A duplicated capsid (C) precedes the Nanoluc moiety, which is cleaved from the polyprotein by a FMDV 2A autoprotease (*). The subsequent polyprotein is not modified.* ***(B)*** *A similarly constructed replicon is shown, where the structural proteins have been replaced with the last 30 residues of envelope.*

These constructs are cloned into a pCCI backbone with a SP6 promoter, and the genomic sequence can be linearised for RNA synthesis either by restriction enzyme or conducting PCR amplification on the backbone. This sequence is then used as a template for SP6 RNA polymerase-mediated *in vitro* production of mRNA, and the inclusion of a 7-methylguanosine cap in the reaction promotes the 5' capping of mRNA, which is essential for translation (Cowling, 2010). A successful *in vitro* reaction results in the formation of distinct bands on an agarose gel, shown in Figure 4-3. Following RNA purification, mRNA is then transfected into Vero E6 cells and amplified for up to 7 days or until significant cytopathic effects (CPE) are observed. Significant variations in the time taken for CPE to form were observed, which is likely due to variable efficiencies of both RNA transcription and transfection. As such flexibility was needed in determining when to harvest virus from these cells. Cell media was harvested and clarified before aliquots of this master stock were made. Plaque assays were performed to assess the titre of the master stock (Figure 4-3). A549 NPro cells were used to further amplify virus stocks for 5 days. The production of virus was confirmed following further plaque assays and the luciferase activity of WT and Nanoluc virus was measured in A549 NPro cells (Figure 4-3).

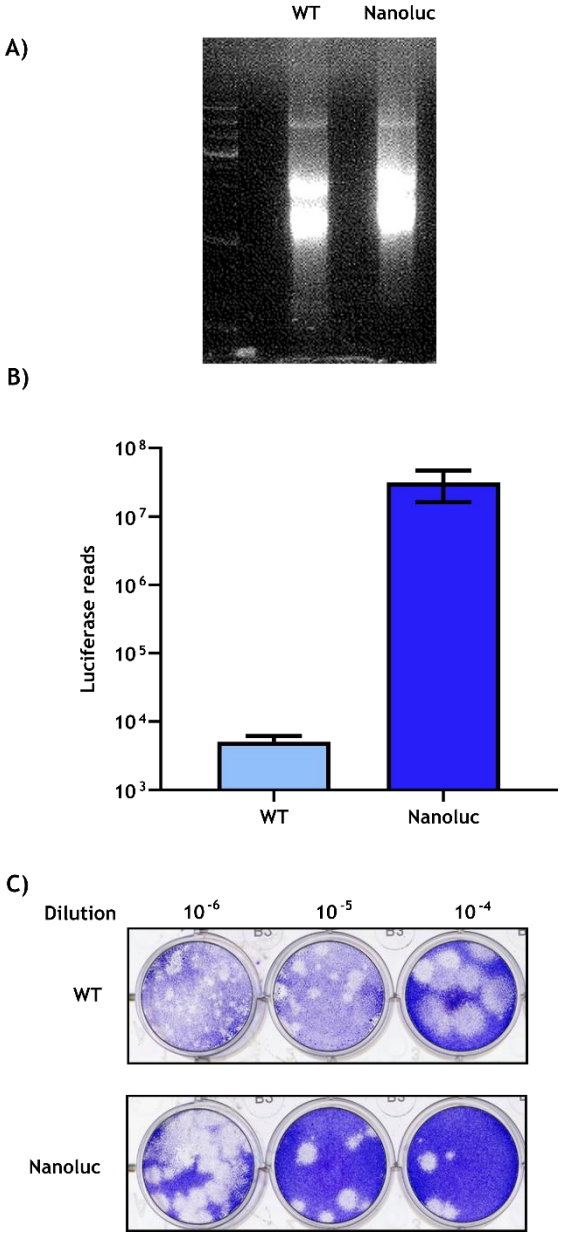

Figure 4-3: ZIKV Nanoluc virus can be rescued from plasmid DNA and amplified in cell culture.

(A) Agarose gel showing in vitro transcribed RNA encoding ZIKV WT (lane 1) and ZIKV Nanoluc (lane 2). ***(B)*** *A549 NPro cells were infected with ZIKV Nanoluc and ZIKV WT for 48 hrs at MOI 1. Cells were lysed at luciferase levels measured. Data represents triplicate independent experiments and errors bars are standard error of the mean.* ***(C)*** *Plaque assays showing successful rescue of ZIKV Nanoluc and ZIKV WT.*

As the viruses produced above would be used in both mammalian and mosquito systems it was important to establish the kinetics of their replication, especially with regards to luciferase production by the reporter virus, in cell lines that were to be utilised. To this end, A549 and Aag2 cells were infected with ZIKV Nanoluc for 24, 48 or 72 before cells were lysed and luciferase levels were measured (Figure 4-5). Luciferase levels increased steadily, though luciferase production was observed to be slower in Aag2 cells compared to the mammalian cells lines, though both displayed comparable readings. This is consistent with other studies which show ZIKV replication in mosquito cells is slower than mammalian cells (Moser *et al.*, 2018). From this it was established that a 24 hr infection was sufficient to get high levels (a least 1 $\log_{10}$ above background) of luciferase readings for infection in mammalian cells, though a 48 hr time point or later should be used as the minimum in Aag2 cells (Figure 4-5).

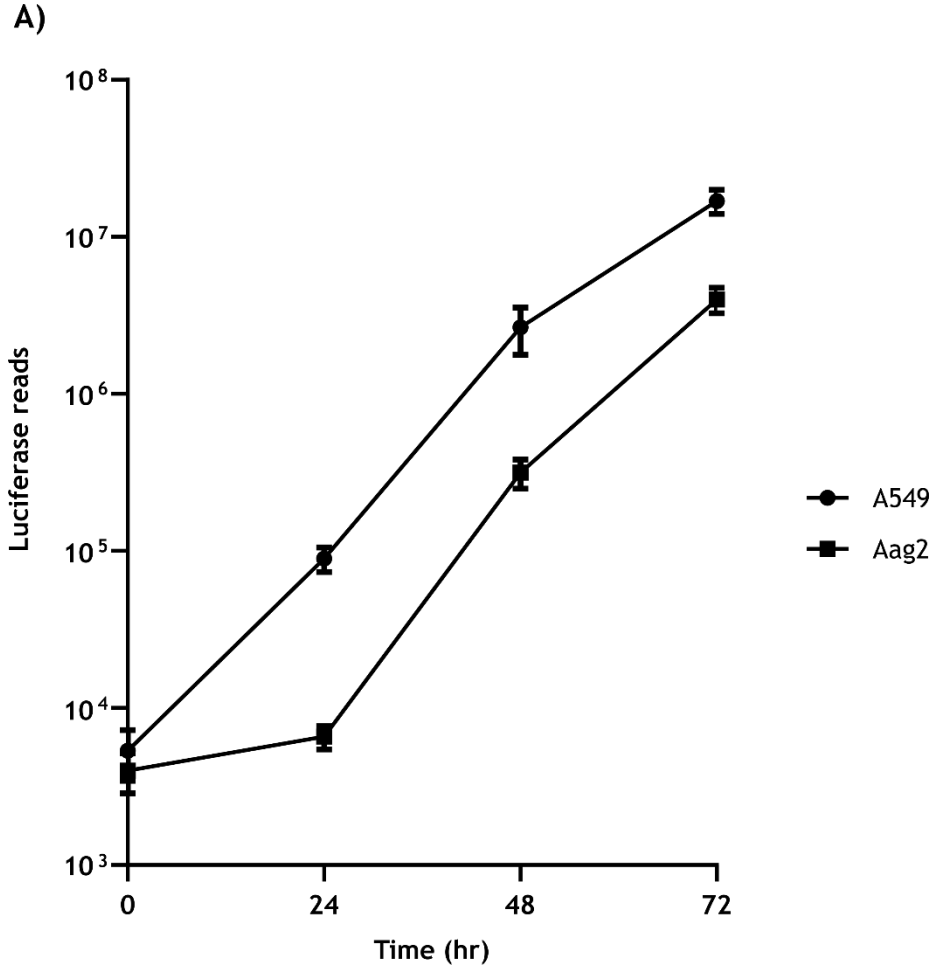

Figure 4-4: ZIKV Nanoluc replicates faster in mammalian cells than mosquito cells.

(A) *A549 and Aag2 cells were infected with ZIKV Nanoluc at an MOI 0.1 for indicated time periods. Results indicated data from triplicate, independent experiments, and error bars represent the standard error of the mean.*

4.2.2 Performing a large-scale siRNA screen

The siRNA screen described here had been previously designed and used in the Kohl lab to investigate the molecular interactors of SFV in Aag2 cells. This screen target 998 host factors involved in the *Aedes Aegypti* immune response, as well as other essential pathways. Targets included genes involved with ubiquitin/SUMO, Serpins, Rho, Rab/importins, DEAD-box helicases, Apoptosis, RNAi, IMD, JAK/STAT, Toll, WD-repeat proteins, Autophagy, and Prophenoloxidase pathways.

Before undertaking the siRNA screen, I endeavored to show that siRNA silencing of cellular factors can aid or restrict ZIKV infection, a change which can be quantified using luciferase levels as a readout. Although very little information was available with regards to important ZIKV cellular factors I could investigate as a positive control, two genes that are often vital for the antiviral RNAi response against related RNA viruses, Ago2 and PIWI4, were selected (Sánchez-Vargas *et al.*, 2009; Sasaki *et al.*, 2017; Tassetto *et al.*, 2019). siRNA against Ago2, PIWI4 and an eGFP control were transfected into Aag2 cells 24 hr prior to infection with ZIKV Nanoluc before cells were lysed and luciferase measured (Figure 4-5). Despite the vital role Ago2 plays in regulating infection of other flaviviruses, siRNA silencing had no effect on ZIKV luciferase activity when compared with the eGFP control. This phenotype had been confirmed in other studies (Varjak, Donald, *et al.*, 2017). Conversely, PIWI4 knockdown significantly increased ZIKV luciferase readings when compared with the eGFP control, indicating that it restricts ZIKV infection, although this effect was not very large. This finding has also been validated in another independent study (Varjak, Maringer, *et al.*, 2017). While the results of the Ago2 knockdown were initially surprising, the observed predicted effect of PIWI4 silencing indicated that the use of siRNA silencing in Aag2 cells could produce a measurable effect on ZIKV Nanoluc.

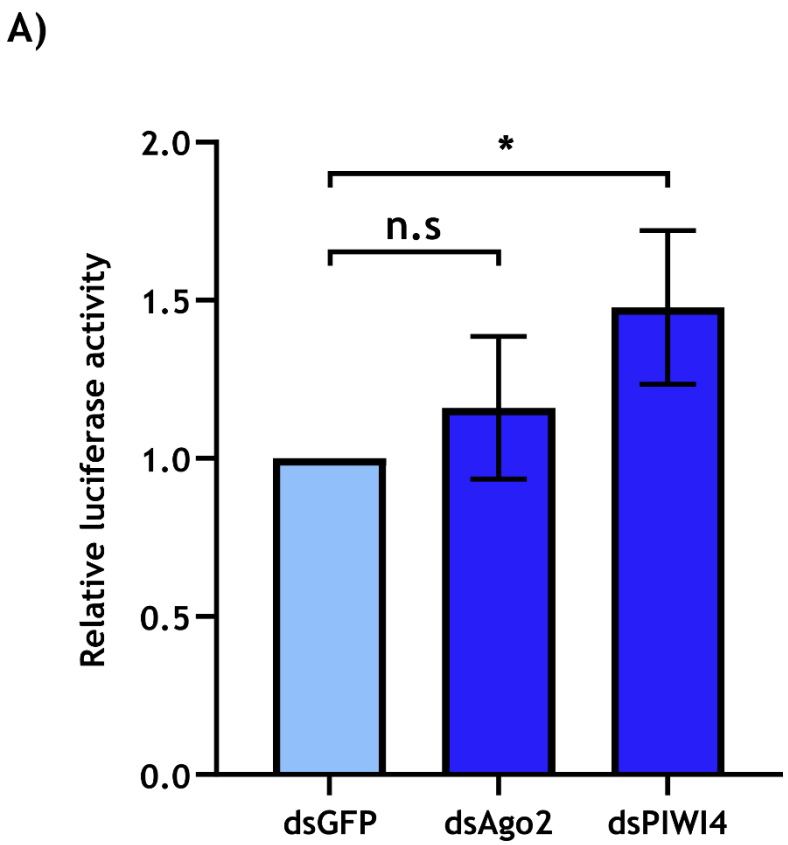

Figure 4-5: PIWI4 knockdown increases ZIKV replication

A) *Aag2 cells were transfected with siRNAs against Ago2, PIWI4 or eGFP as a control for 24 hrs. Cells were then infected with ZIKV Nanoluc at MOI 0.1 for 48 hrs before cells were lysed and luciferase levels measured, results given relative to the eGFP control. Results are compiled from triplicate independent repeats and error bars represent the standard error of the mean. An unpaired Student's t-test with Welch's correction was used to determine statistical significance where n.s = not significant, * p-value < 0.05.*

Using the infection and knockdown parameters previously established, I proceeded to carry out the siRNA screen. siRNAs were generated by Ambion (now part of Thermo Fisher Scientific) and were provided in a 96 well plate format, with each well containing a pool of 3 siRNA targeting a specific gene. Aliquots were made from these master plates and transfected into Aag2 cells seeded in 96 cells plates. Following infection, these cells were lysed, and luciferase readings were taken for every plate. This procedure was carried out 3 times and the results of each independent screen were later compiled. Due to the design of the plates and the absence of negative control siRNA wells, individual well luciferase readings were normalised against the plate average, under assumption that the majority of genes on the plate have neutral role in infection. While plate to plate variations might be anticipated, any outliers (those which are significantly anti- or pro-viral) were expected to be detected reliably. To be considered for further analysis, wells which had luciferase readings 2 standard deviations above or below the plate average were highlighted and compared to the comparable plate in each of the other repeats.

Using the above criteria, a total of 152 such hits were identified across the 3 repeats of the screen (by repeat: #1 – 43 hits, 2# – 58 hits, 3# – 41 hits). However, only 13 of these were common between any 2 screens, and there were 0 hits conserved across all 3 repeats of the screen. This is shown in the Venn diagram in Figure 4-6. There are several potential reasons for this observation, one being bias introduced through normalisation of values to plate averages, potentially hiding true effects if a given plate contains predominately pro-viral or anti-viral factors. Also, as seen in Figure 4-4, the effect of Piwi4 knockdown in a more controlled setting, while significant, was not very large and therefore the reporter virus used in the screen may not have been sensitive enough. Because of that, any potential hits could have been random outliers.

A)

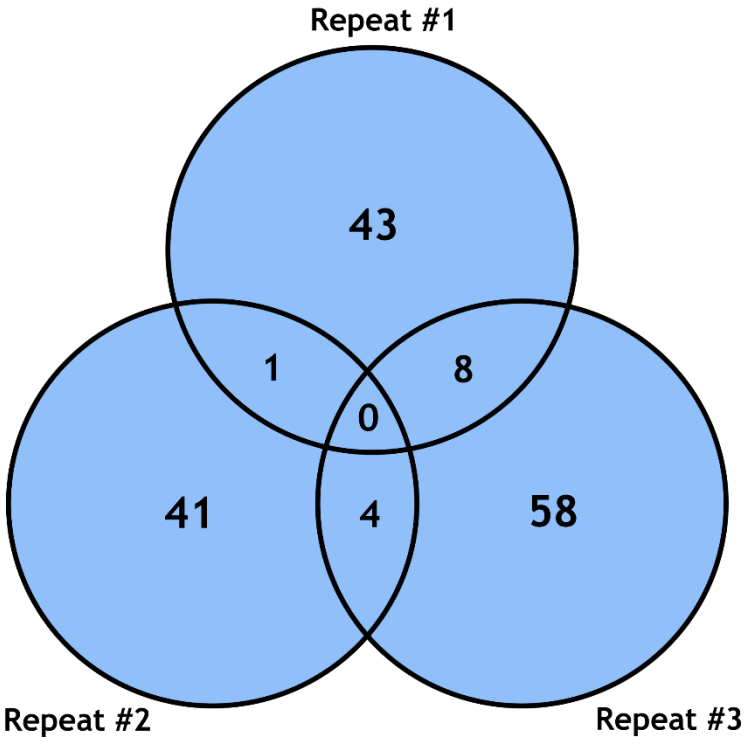

Figure 4-6: Venn diagram displaying the hits obtained from screen.

A) *Potential hits were identified if they were 2 standard deviations above or below the plate average when luciferase readings were measured. Using this criteria, 43 hits were found in repeat #1, 41 in repeat #2 and 58 in repeat #3. The number of hits overlapping between each repeat are indicated.*

Regardless, 8 of the 13 potential hits were taken forward for validation, and these factors are listed in Table 4-1. The hits listed here were identified as being 2 standard deviations above or below the plate average in 2 repeats of the screen and 'trended' in the same direction from the plate average in the third screen.

Accession No.	**Gene name**	**Average luciferase readings relative to plate averages (+/- SEM)**
AAEL013045	exosome complex exonuclease RRP41	1.327 (+/- 0.097)
AAEL011087	DNA-directed RNA polymerase II	1.349 (+/- 0.140)
AAEL003245	IMD pathway signalling I-Kappa-B Kinase 1	1.351 (+/- 0.065)
AAEL007921	Zinc finger protein 394	1.150 (+/- 0.094)
AAEL004121	ubiquitin-conjugating enzyme E2 q	1.217 (+/- 0.082)
AAEL012717	WD-repeat protein	1.520 (+/- 0.195)
AAEL005437	transient receptor potential channel	1.646 (+/- 0.379)
AAEL014529	Ran-binding protein	1.535 (+/- 0.171)

Table 4-1: A list of the hits identified from the siRNA screen.

Listed in the table are the Accession number (No.) and gene name of hits that were identified in the screen. Average luciferase readings normalised to individual plate averages are shown. The standard error of the mean (SEM) is also displayed.

4.2.3 Validation of potential regulators of ZIKV infection

To further investigate the potential of these hits of playing a role in ZIKV infection, dsRNA was synthesised against these targets and transfected into Aag2 cells along with a dseGFP negative control and dsPIWI4 as a positive control. Following, the Aag2 cells were infected with ZIKV Nanoluc before cells were lysed and luciferase levels measured and plotted relative to the controls (Figure 4-7). Additionally, RNA was harvested from control and knockdown samples and reverse transcription was performed. Following PCR amplification with gene specific primers, semi-quantitative agarose gel analysis showed that dsRNA effectively silenced the target, and an actin loading control is present for each sample (Figure 4-7). From this analysis, no significant difference was observed in viral luciferase levels between any of the hits, though PIWI4 knockdown did increase ZIKV luciferase. DNA-directed RNA polymerase II (hit – 2) displayed an elevated luciferase levels, though variability in independent repeats meant this did not achieve statistical significance as judged by an unpaired Student's t-test with Welch's correction (p value = 0.16).

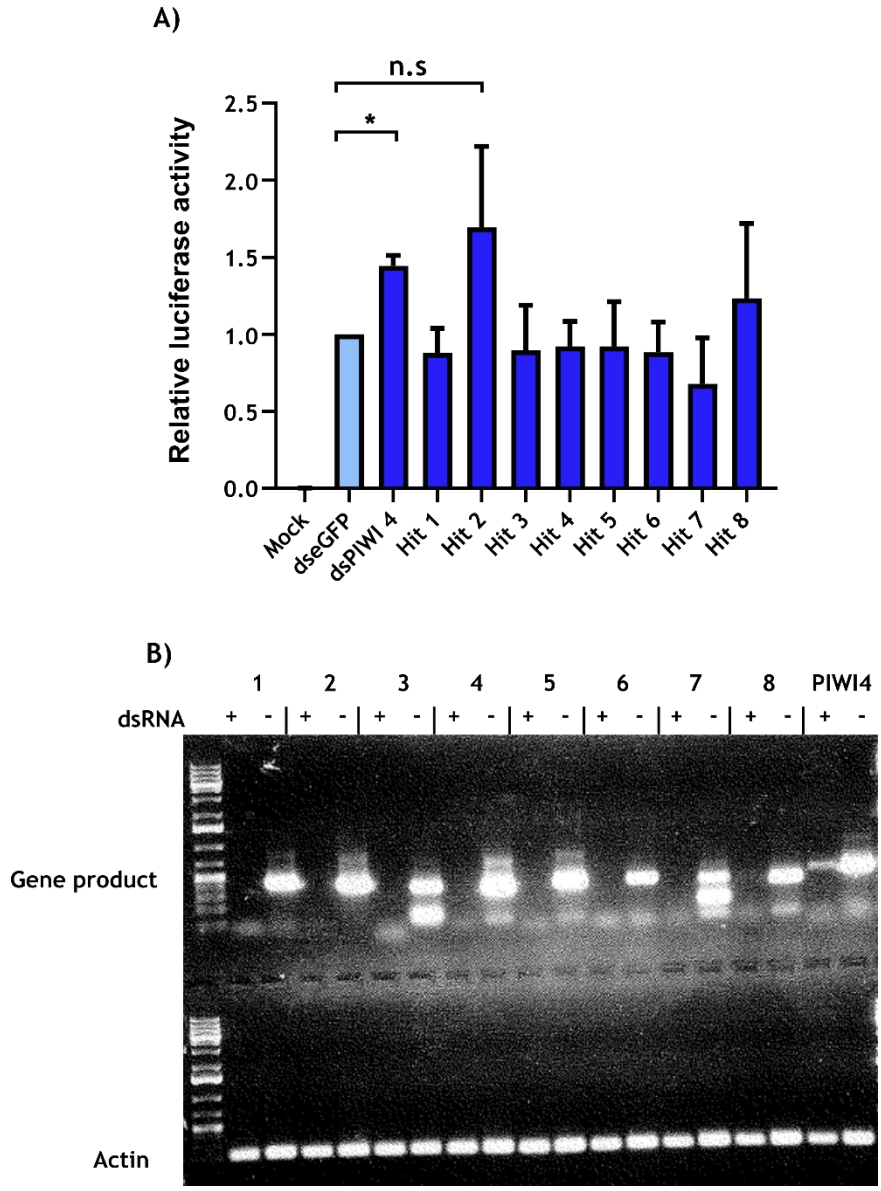

Figure 4-7: A validation screen using dsRNA found no significant difference in viral activity between hits and control.

A) *Aag2 cells were treated with dsRNA against hits identified in the screen and GFP and PIWI4 as a positive and negative control, respectively. Following, cells were infected with ZIKV Nanoluc for 48 hrs. An unpaired Student's t-test with Welch's correction was used to determine statistical significance, where n.s = not significant, * p-value < 0.05. B) RNA was extracted from cells following dsRNA treatment and infection, and a RT-PCR was performed to amplify specific gene products and an actin loading control. The samples were separated on an agarose gel.*

4.3 Discussion

The aim of this study was to rescue and characterise a ZIKV Nanoluc reporter virus for use in a large-scale siRNA screen to identify mosquito host-factors required for ZIKV infection. As an emerging arbovirus, it vital to understand the interactions between the virus and vector to aid development of control strategies. Here I show the successful rescue of the ZIKV reporter virus and its use in mosquito Aag2 cells, and that siRNA mediated knockdown of the known anti-viral agent PIWI4 was able to be measured using luciferase (Varjak, Maringer, *et al.*, 2017). However, no hits identified from the screen could be reliably verified as important for ZIKV infection following a validation screen.

The ZIKV Nanoluc reporter was rescued from plasmid DNA generously provided by Andres Merits, and its generation has been described by his group (Mutso *et al.*, 2017). Here I have shown that this virus can be propagated in Vero E6 cells prior to amplification in A549 NPro cells. A549 NPro cells contain BVDV NPro, which targets IRF-3 for proteasomal degradation resulting in a diminished innate immune response and can therefore supports ZIKV replication to a higher titre (Hilton *et al.*, 2006; Xia *et al.*, 2018). While being highly susceptible to infection, in my hands A549 NPro cells proved difficult to transfect with *in vitro* transcribed RNA or could not be used to rescue virus RNA, and so Vero E6 cells were chosen for initial rescue of the virus. Once harvested, the virus was propagated in A549 NPro cells.

Following amplification and establishing titre of the rescued virus, the replication and luciferase production kinetics of ZIKV Nanoluc were tested in both mammalian (A549) and mosquito (Aag2) cells. The replication of ZIKV in mammalian A549 cells was observed to be faster than Aag2 cells. My experiments established conditions for use in future experiments, where high levels of luciferase can be detected 24 hr after infection of mammalian cells, and 48 hrs or later for Aag2 cells. This reduction in virus replication kinetics in *Aedes aegypti* cell culture has been

observed for ZIKV in other studies, and is perhaps not surprising due to the propensity of these viruses to persistently infect their vector host (Salas-Benito and De Nova-Ocampo, 2015; Moser *et al.*, 2018), as well as robust RNAi responses. Persistent infection of vectors seems to be due to a mixture of viral and cellular factors, such as the production of defective interfering particles, and appears to be vital for viral transmission (Goic and Saleh, 2012).

When testing the siRNA knockdown protocol with ZIKV Nanoluc, very little information was available regarding factors that could influence ZIKV infection in mosquito cells. Initially two well-known anti-viral proteins were selected. Ago2 and PIWI4 have both been implicated in the anti-viral response for many diverse positive sense RNA viruses such as DENV, JEV, Semliki Forest virus (SFV) and Schmallenburg virus (Sánchez-Vargas *et al.*, 2009; Schnettler *et al.*, 2013; Dietrich *et al.*, 2017; Sasaki *et al.*, 2017; Varjak, Maringer, *et al.*, 2017). Here, cells treated with siRNA against Ago2 did not significantly increase ZIKV luciferase compared to control sieGFP cells. This was surprising and may suggest that the exo-siRNA pathway does not restrict ZIKV infection, or that ZIKV already encodes the ability to disarm this pathway. Although the mechanism behind this has not yet been uncovered, it has been independently confirmed in other experiments (Varjak, Donald, *et al.*, 2017). In contrast, PIWI4 knockdown did significantly increase ZIKV luciferase levels, a finding that has also been reported (Varjak, Donald, *et al.*, 2017). This demonstrated that the siRNA protocol used can successfully identify important host factors.

I then performed the large-scale siRNA screen. The targets for the screen had been designed prior to the commencement of this project to target genes that are potentially involved in *Aedes aegypti* immune responses as well as other host processes. Here, siRNAs were produced by a commercial vendor and were provided in a 96 well format, where each well contained a pool of 3 different siRNA targeted against a single gene. Aliquots were taken from the master plates to create daughter plates. From this, transfection mixes were assembled before siRNA was added to Aag2 cells. Following this, virus was applied to cells and nanoluciferase

readings taken. Nanoluciferase readings were normalised to plate averages and hits were characterised as being 2 standard deviations above or below the plate average. From this analysis protocol, no hits were conserved across all 3 repeats, and 13 repeats were identified in 2 separate screens. There are several potential reasons for the lack of conserved hits.

Firstly, it could be the case that none of the factors probed in the siRNA screen played a role in ZIKV infection. This seems highly unlikely considering the large number of targets (998 genes) and the fact that PIWI4, which I previously demonstrated to be anti-viral, was a target of the screen. In the test experiments, PIWI4 silencing significantly increased ZIKV luciferase readings by 47 %, which contrasts with the screen, where the average luciferase value was 0.2 % higher than the plate averages.

Secondly, a large amount of variability could have been introduced by the experimental and analysis protocol. From cell seeding to final luciferase readings a total of six pipetting actions were performed with multi-channel pipettes, often involving very small volumes. While great care was taken to perform the experiment diligently, there would still likely be a large amount of variation introduced by these pipetting actions. Additionally, due to the lack of negative control siRNA wells, analysis was performed by normalising individual well values to the plate average. This could potentially introduce bias, as plates containing several anti-viral (or pro-viral) factors could skew the average, disguising these effects. It seems likely a combination of these factors introduced a high level of variability that potential masked putative factors. Regardless, there were large variabilities between replicates.

Thirdly, the efficacy of each siRNA was not calculated. Though each well contained a pool of siRNAs against each target, the gene expression levels were untested, thus, it is possible that they were not effective in silencing the targeted gene. Similarly, while viral luciferase levels were measured 72 hrs after siRNA transfection (and 48 hrs after infection), it is possible that the expression of stable

proteins would not be affected in this timeframe, and so the contribution these may play in ZIKV infection would not be captured.

Lastly, another issue might be that ZIKV Nanoluc is not sensitive enough for the screen. As showed earlier, while silencing of PIWI4 in the test assay did result in 40% higher reads, knock down of PIWI4 has been shown to increase the number of released ZIKV particles by approximately 4-fold (Varjak, Donald, *et al.*, 2017). It may be the case that ZIKV-Nluc is not sensitive enough and cannot sufficiently capture the benefits/pitfalls of a specific gene silencing. While this is unlikely to be the sole shortcoming of this experiment, it may have contributed.

Of note, the screen previously performed for SFV did not detect hits that were conserved across all 3 repeats. In that screen, there were 84 hits conserved between any 2 repeats (Melanie Mcdonald, University of Glasgow. Personal communications). While this number is higher than the 13 detected in the study described here, the lack of repeatable hits suggests that there are flaws in the screen design independent of the virus under investigation, and that alternative designs should be used to conduct similar experiments in the future.

Despite these shortcomings, hits that were conserved across 2 screens (and trended in the same direction in the 3rd) were selected for further validation. Validation was conducted in a 12-well format to minimize the variations introduced by pipetting small volumes. Additionally, a negative control (dseGFP) and a positive control (PIWI4) were included so appropriate comparisons could be made. Analysis of triplicate independent repeats of the validation experiment revealed that silencing of the screen hits did not significantly impact ZIKV replication, though RNA expression of each target was indeed reduced by dsRNA transfection. Again, this experiment showed PIWI4 acts as an anti-viral factor in ZIKV infection.

In conclusion, this study established the replication kinetics of a ZIKV Nanoluc reporter virus in both mammalian and mosquito cell lines. This virus was used to

show that while Ago2 is not anti-viral for ZIKV, PIWI 4 is. Additionally, this reporter virus (along with the replicon that was also described) was used extensively in the subsequent chapters and as such is a vital tool. A large-scale siRNA screen was attempted, though it appears that ZIKV Nanoluc is not a viable option for a screen conducted in the format presented here.

4.4 Summary

- A ZIKV Nanoluc reporter virus can be reliably rescued from plasmid DNA and kinetics of luciferase production were investigated in mammalian and mosquito cell culture.

- ZIKV Nanoluc can be used as an investigative tool for uncovering host-virus interactions, though sensitivity of luciferase detection may be an issue.

- A large-scale siRNA screen was conducted, though no conclusive hits were identified.

- Ago2 is not an anti-viral factor in ZIKV infection in Aag2 cells, but PIWI4 is.

Chapter 5. GRP78 interacts with ZIKV E and is required for a productive infection

5.1 Introduction

The envelope (E) proteins of flaviviruses are vitally important structural proteins. E, along with matrix (M) protein, coat the surface of the virion. E protein engages with cellular receptors to initiate virus entry, and the fusion loop of E facilitates fusion with endosomal membranes, allowing nucleocapsid release into the cytoplasm. Additionally, as a structural protein, E is essential for virus assembly (Zhang *et al.*, 2017). Therefore, most research into the role of E in infection has focused on identifying entry receptors and elucidating the structure of E and the role it plays in facilitating entry and assembly, often with a view to designing therapeutic interventions (Perera-Lecoin *et al.*, 2013; Metz *et al.*, 2017; Shi *et al.*, 2018; Agrelli *et al.*, 2019; Qu *et al.*, 2020). Consequently, very little is known about the role E protein, especially ZIKV E, may play in the intermediate stages of infection. For example, recent reviews and interactome studies of ZIKV host-cell interactions contain little regarding ZIKV E interactions outside of the purview of entry, and focus predominantly on the non-structural proteins (Shah *et al.*, 2018; Lee and Shin, 2019; Scaturro, Kastner and Pichlmair, 2019; Golubeva *et al.*, 2020). There are some exceptions to this, as ZIKV E has been shown to co-localise with proteins involved in stress granule formation such as Ras-GTPase activating binding protein 1 (G3BP-1), though no direct interaction has yet been identified (Bonenfant *et al.*, 2019).

With that in mind, this investigation aimed to broaden the knowledge base related to ZIKV E in infection by focusing on investigating cellular interactors of E. A proteomic experiment previously undertaken in the Kohl lab by Carolina Ramírez-Santana (currently at the Center for Autoimmune Diseases Research-CREA, School of Medicine and Health Sciences, Universidad del Rosario, 110010 Bogotá, Colombia (Royle *et al.*, 2020)) uncovered a potential interaction between ZIKV E

and GRP78. In this study, E was immunoprecipitated from ZIKV PE243 infected A549 cells and analysed by electrospray ionization, mass spectrometry to identify cellular interactors. Results from this is listed in Table 5-1, where the presence or absence of each putative interactor in triplicate repeats (infected samples and mock control samples) are shown. ZIKV PE243 is a virus isolated from a patient in Recife, Brazil, and has been described previously (Donald *et al.*, 2016).

Protein	UniProt Accession	Infection 1	Infection 2	Infection 3	Control 4	Control 5	Control 6
LMNA	P02545	Yes	Yes	Yes	No	Yes	No
PGAM5	Q96HS1	Yes	Yes	No	Yes	No	No
GRP78	P11021	Yes	Yes	Yes	No	No	No
OASL	Q15646	Yes	Yes	No	No	No	No
TAO1	Q7L7X3	Yes	Yes	Yes	No	No	No

Table 5-1: Potential interactors of Zika (ZIKV) Envelope (E) as identified via proteomic analysis of infected A549 cells.

A549 cells were infected with ZIKV PE243 and E protein was immunoprecipitated to isolate cellular interactors. This was performed in triplicated alongside uninfected control cells, before electrospray ionization, mass spectrometry was used. The table lists the Protein acronym, UniProt Accession number, and whether, following analysis, these proteins were found in each of the infection or control samples.

As shown in Table 5-1, there were several hits identified as E interactors. Some of these, such as Oligoadenylate synthase-like (OASL), have previously been identified as virus interactors. OAS have been shown to be interferon stimulated gene (ISG), and OASL is a member of that family and has previously been implicated in WNV and HCV disease severity (Yakub *et al.*, 2005; Ishibashi, Wakita and Esumi, 2010). While this may appear a compelling candidate, it was not found in every infected sample. Another identified protein was a serine/threonine-protein kinase, encoded by the *TAOK1* gene, and is also known as thousand and one amino-acid protein 1 (TAO1). This protein is a mitogen-activated protein kinase kinase kinases (MAP3K) involved in DNA-damage repair and immune suppression (Zhang *et al.*, 2018). While this protein was found in all 3 infection samples (and absent in all the control samples), to the best of my knowledge there is no known implication of TAO1 with any virus infection though it is implicated in some cancers (Fang *et al.*, 2020).

The most interesting hit, however, was glucose-regulated protein 78kDa (GRP78). GRP78 is a multifaceted protein and a prominent ER-resident chaperone. It is a key mediator of the UPR, whereby in the presence of cellular stress, GRP78 and its effector molecules are activated to ensure the proper folding of proteins, the regulation and halt of translation, and the initiation of controlled cell-death if cellular stress is not resolved (Ibrahim, Abdelmalek and Elfiky, 2019). The molecular mechanisms of GRP78 are discussed in Chapter 1.3.2.

Of particular interest for this study, GRP78 has been implicated in the lifecycles of various viruses, including flaviviruses such as JEV, DENV and duck Tembusu virus (TMUV) (Wati *et al.*, 2009; Wu *et al.*, 2011; Zhao *et al.*, 2018). Interestingly, GRP78 seems to act at different stages of infection for even these related viruses, as is discussed in more detail in Chapter 1.3.3. Additionally, GRP78 is implicated in several types of cancers and there is substantial interest in developing therapeutics and small molecule inhibitors for use GRP78 mediated disease (Lu, Luo and Zhu, 2020). These small molecule inhibitors, such as Epigallocatechin gallate (EGCG) and Honokiol (HNK), function by inhibiting the GRP78-mediated

UPR response. EGCG and HNK compete with ATP for binding to the NBD of GRP78, thereby maintaining GPR78 in an open confirmation preventing the release of effector molecules and the binding of substrates. The use of these inhibitors in cell culture is well-documented (Martin *et al.*, 2013; Sagara *et al.*, 2018). These inhibitors, along with the availability of other molecular tools such as antibodies, meant fundamental research could be easily conducted.

For these reasons, GRP78 was selected for further study to uncover the role it plays in ZIKV infection.

5.1.1 Aims

I therefore had several aims for this study.

- Firstly, to verify the interaction between ZIKV E and GRP78 using immunoprecipitation experiments.

- Secondly, to use the available small-molecule inhibitors to block GRP78 function and assess the effect this has on ZIKV infection.

- Thirdly, deplete GRP78 expression with specific siRNA, and similarly investigate the effect on ZIKV infection.

- Lastly, to use evidence from the above experiments to propose a model for the role of GRP78 in ZIKV infection.

5.2 Results

5.2.1 GRP78 and ZIKV E interact and co-localise

Previous work (Table 5-1) identified several putative cellular interactors of ZIKV E, including GRP78. My first aim was to verify the interaction between ZIKV and GRP78, and to do this a co-immunoprecipitation (IP) experiment using ZIKV E as bait was performed. Here, ZIKV infected A549 cells were lysed and incubated with a specific anti-E antibody. E antibody-protein complexes were extracted with magnetic beads and eluted from beads by boiling in protein sample buffer. These eluted complexes were probed by western blot with GRP78 antibodies alongside cell lysates collected prior to IP (Figure 5-1). GRP78 was identified in the lysates of all samples but only in the infected cell IP experiment, and not in mock infected cells in IP samples. This confirmed the proteomic results which indicated the GRP78 could interact with ZIKV E. Further evidence may be provided by looking at the sub-cellular localisation of ZIKV E and GRP78 during by infection by visualising infected or mock infected A549 cells with immunofluorescence (IF) microscopy, as shown in Figure 5-1. This showed that while GRP78 normally displays diffuse, primarily cytoplasmic localisation, upon infection it re-localised to perinuclear sites coincident with ZIKV E staining. However, as both GRP78 and E may be expected to co-exist in the ER, the IF images do not provide proof of co-localisation between these proteins, especially as the resolution achieved is insufficient to provide conclusive evidence of a direct interaction.

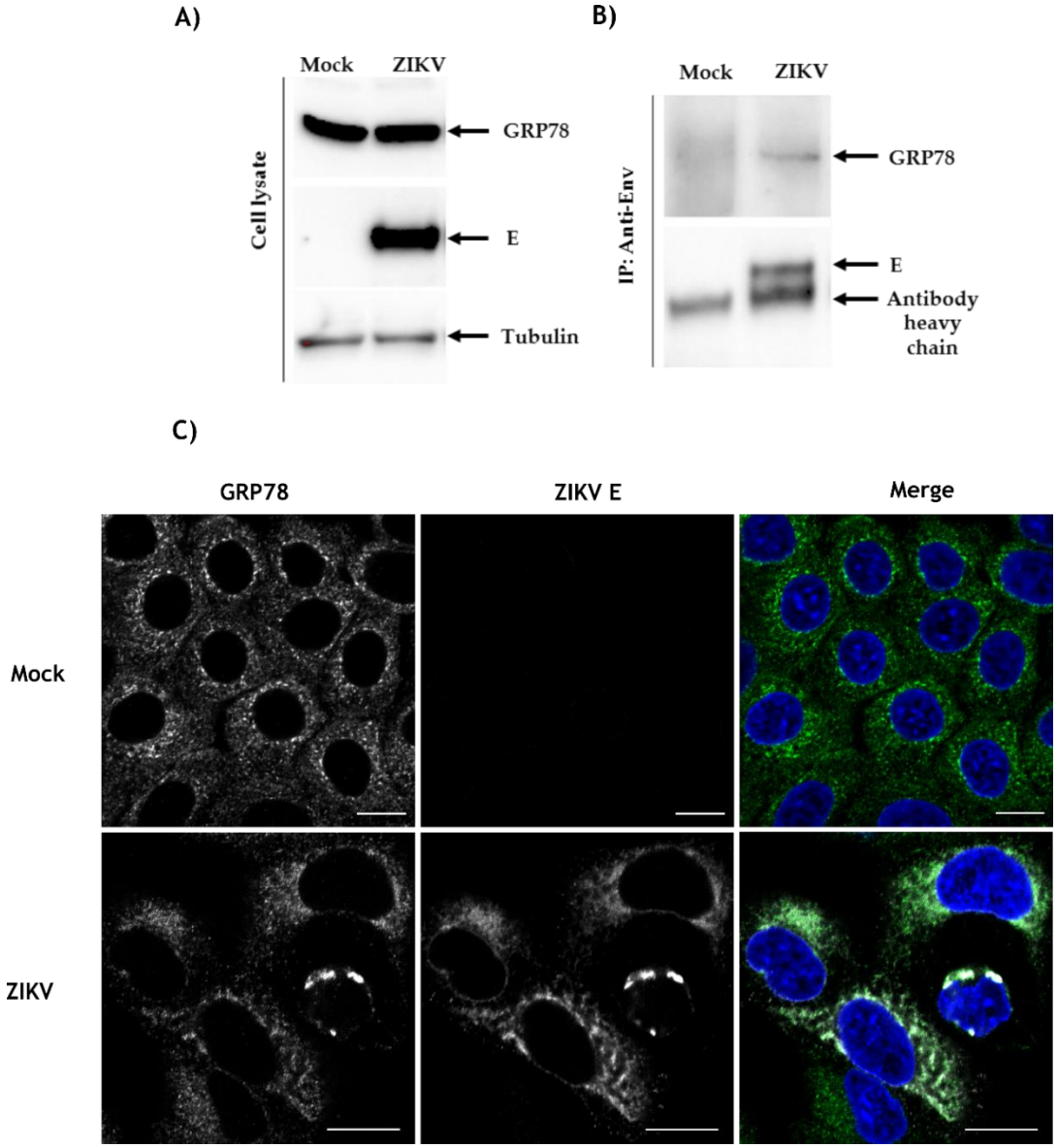

Figure 5-1: ZIKV E protein interacts with GPR78 in A549 cells.

A) *A549 cells were infected with ZIKV PE243 MOI 1 for 24 hrs and cell lysate samples were taken, and Western blot analysis was performed for GRP78, E and a tubulin loading control.* ***B)*** *An IP was performed on cell lysates with an E antibody, and this was probed for GRP78 and E staining by Western blot analysis. A549 cells were* ***C)*** *mock infected or cell infected with ZIKV PE243 MOI 0.1 for 24 hrs and stained with E (white) and GRP78 (green) antibodies and the nucleus was labelled with DAPI (blue). Images are representative of triplicate experiments and were taken on an LSM 710 confocal microscope.*

5.2.2 EGCG treatment inhibits ZIKV infection

As the interaction between GRP78 and ZIKV E had been confirmed, the next aim was to uncover the role GRP78 may play in infection.

Small molecule inhibitors, such as EGCG and HNK can competitively bind to the NBD, thereby maintaining GPR78 in an inactive confirmation preventing the release of effector molecules or the binding of substrates, and effectively inhibits activation of the ER stress response (Martin *et al.*, 2013; Sagara *et al.*, 2018). By using these inhibitors in the context of a ZIKV infection, I aimed to establish whether inhibition of the GRP78-mediated ER stress response impacted ZIKV replication. Initially, the viability of A549 or Huh7 cells treated with EGCG or HNK was assessed. This would allow a distinction between drug specific effects and cell health effects on virus replication to be made. The initial range of EGCG and HNK concentrations was determined following analysis of other relevant studies. Both EGCG and HNK have been commonly used in the μM range, and so the viability of cells were tested based on this (Zhou, Wang and Feng, 2014; Lv *et al.*, 2016). This data is shown in Figure 5-2, and provided a range of concentrations to use when testing the effect of these drugs on ZIKV. Using these concentrations, A549 and Huh7 cells were pretreated with EGCG and HNK for 2 hours before cells were infected with ZIKV Nanoluc. The drugs were maintained in media throughout the 24 hr infection period. As shown in Figure 5-3, EGCG treatment significantly reduced ZIKV luciferase readings at all the concentrations tested, however this effect was not seen for HNK treatment. The difference in results between the drug treatments was surprising and suggested that EGCG may be having an off-target effect, or that HNK was failing to inhibit GRP78 contrary to the literature reports. To investigate further, I planned to delineate the mechanism of action of EGCG. The specific concentration of EGCG selected for future experiments was the maximal concentration that maintained 90% cell viability, 10 μM.

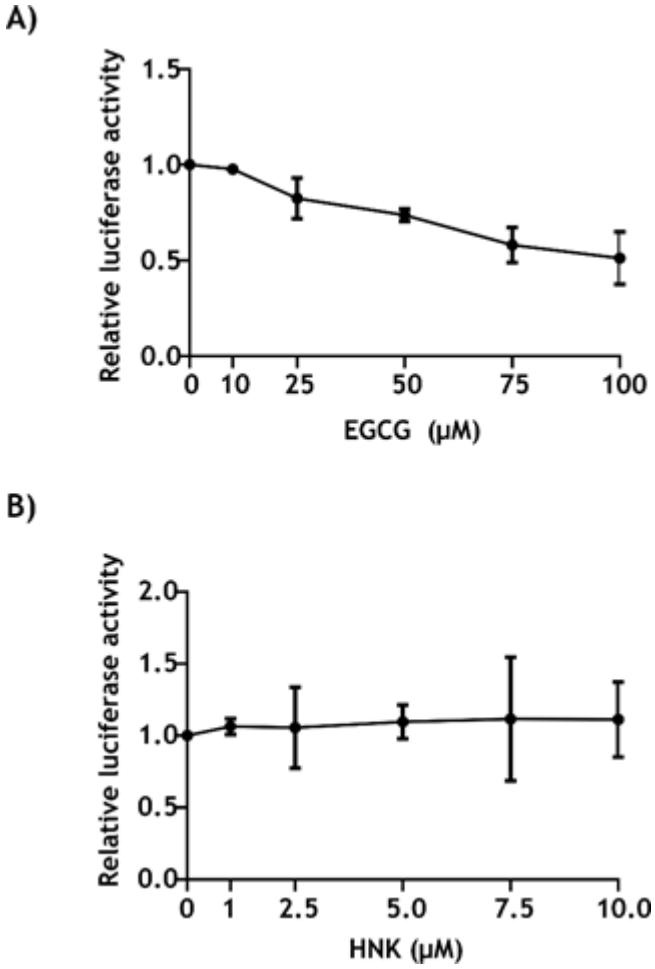

Figure 5-2: The cell viability of mammalian cells treated with EGCG or HNK

*A549 or Huh7 cells were treated with varying concentrations of either a DMSO control and either **A)** EGCG or **B)** HNK for 26 hrs. Following this, cells were lysed and cell viability measured using CellTitre glo assays. Luciferase readings are plotted relative to controls, and error bars represent the standard error of the mean from triplicate independent experiments.*

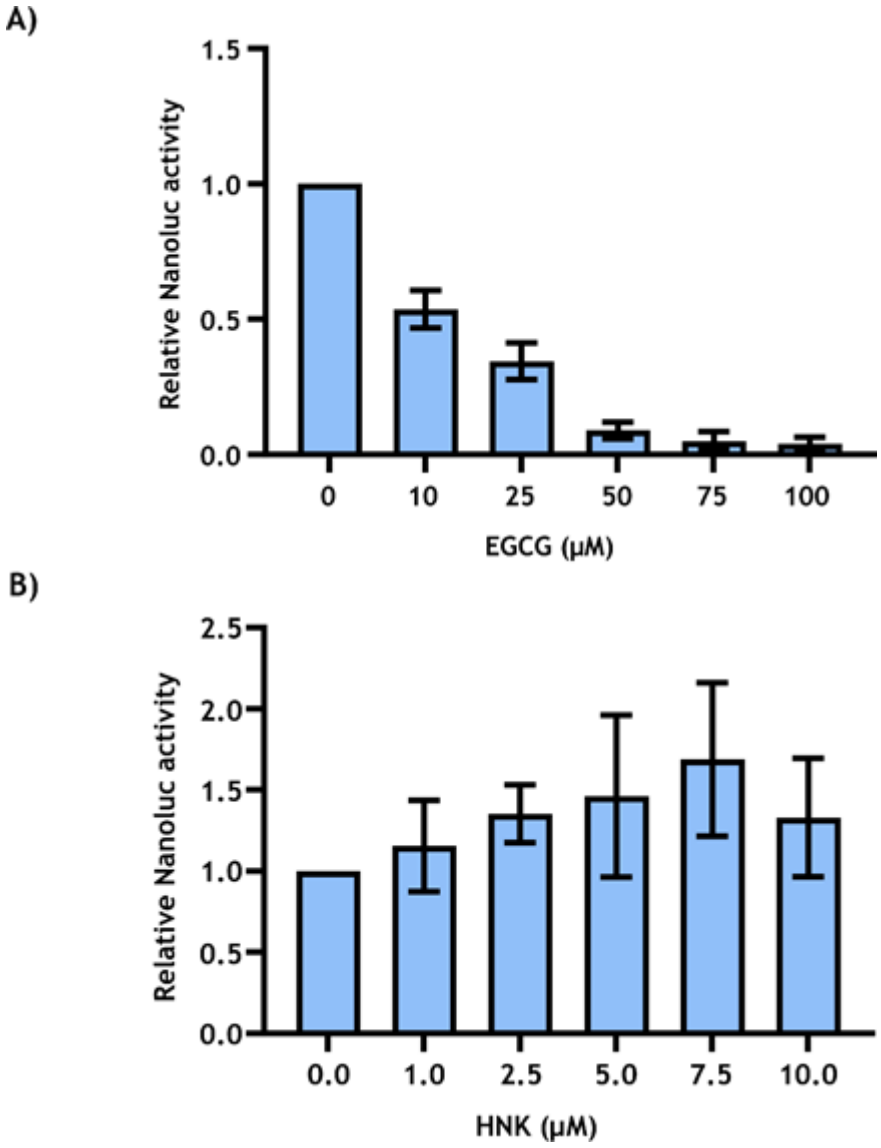

Figure 5-3: EGCG treatment reduces luciferase activity of a ZIKV Nanoluc reporter virus.

*A549 or Huh7 cells were pretreated with either **A)** EGCG or **B)** HNK for 2 hrs prior to infection with ZIKV Nanoluc at MOI 1 for 24 hrs. The drugs were maintained on the cells throughout. Following, cells were lysed and Nanoluc activity measured relative to untreated ZIKV infected cells. Error bars represent triplicate independent experiments and error bars represent the standard error of the mean. An unpaired Student's t-test with Welch's correction was used to determine statistical significance where n.s = not significant, * p-value < 0.05.*

5.2.3 EGCG treatment inhibits ZIKV infection independently of GRP78 inhibition

As demonstrated above, addition of EGCG throughout ZIKV infection significantly reduced viral luciferase readings. To dissect which step is affected, I performed ZIKV Nanoluc infections in A549 cells with EGCG added alongside the virus, or 1 hr or 4 hrs following removal of inoculum, before measuring luciferase at 24 hpi. Under these conditions, EGCG had no effect on viral luciferase readings if added even as early as 1 hpi (Figure 5-4). This again was surprising, as it suggested that EGCG was having an effect either directly on the virus in the early stages of infection, or that inhibition of GRP78-mediated stress responses in the first hour were rendering the cell refractory to infection.

To test the possibility that EGCG was acting directly on the virus, I pre-treated both A549 cells and ZIKV Nanoluc particles with either EGCG or DMSO vehicle control for 2 hrs, before applying EGCG or DMSO treated viral inoculum to both EGCG or DMSO treated cells for 1 hr. Cells were thoroughly washed before and after addition of the virus, and the media was replaced with DMSO or EGCG containing medium (depending on which they were treated with initially) for the remainder of infection (Figure 5-4). Strikingly, ZIKV Nanoluc treated with EGCG before infection displayed reduced luciferase regardless of the treatment state of the cells. Conversely, ZIKV Nanoluc treated with DMSO did not show a reduction in infection, even in cells which were pre-treated with, and subsequently maintained in, media containing EGCG. This strongly indicated that EGCG acted directly on the virion and was probably not inhibiting viral replication following cellular entry or inhibiting entry via effects on the cell.

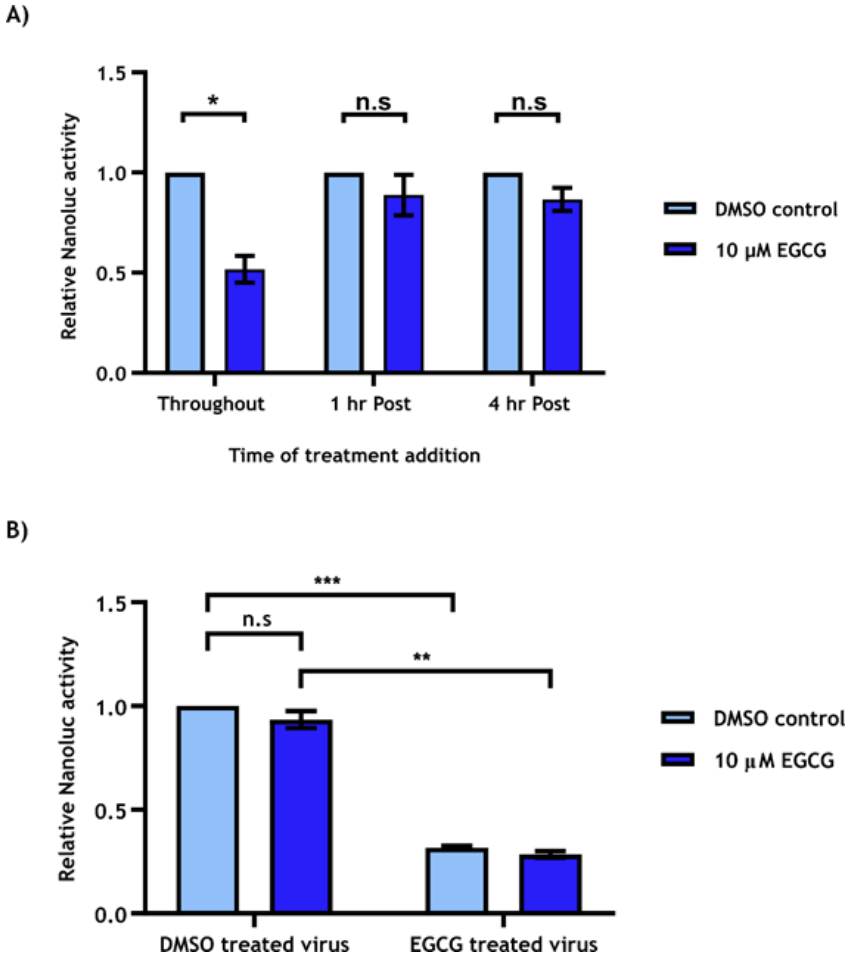

Figure 5-4: EGCG inhibits ZIKV independent of GRP78.

A) A549 cells infected with ZIKV Nanoluc at MOI 0.1 for 24 hrs and were treated with EGCG either during inoculation and throughout infection (indicated as "Throughout"), or 1 hr or 4 hrs following inoculum removal. Cells were lysed and luciferase levels were measured relative to a DMSO control for each timepoint. Bars represent results from triplicate independent experiments and error bars represent the standard error of the mean. ***B)*** *ZIKV and A549 cells were separately incubated with either EGCG or a DMSO vehicle control for 2 hrs. Following, DMSO or EGCG treated A549 cells were infected with either DMSO treated or EGCG treated virus at MOI 0.1 for 24 hrs before cell lysis and luciferase levels were measured and plotted relative to the DMSO treated virus, DMSO treated cell control. Bars represent results from triplicated independent experiments and error bars represent the standard error of the mean. An unpaired Student's t-test with Welch's correction was used to determine statistical significance where n.s = not significant, * p-value < 0.05, ** p-value < 0.01 and *** p-value < 0.001.*

To further verify the finding that EGCG was acting independent of viral replication, I transfected cells with a ZIKV Nanoluc replicon (a construct missing the flavivirus structural proteins but with all non-structural proteins necessary for replication, as outlined in Chapter 4.2.1) and treated these cells with EGCG. Compared to a DMSO control, there was no significant change in luciferase readings generated by the replicon, further indicating that EGCG treatment has no effect on ZIKV replication (Figure 5-5). When transfecting higher levels (25 µg) of the ZIKV Nanoluc replicon, some cell death was also observed. These results suggest that inhibition of ER-stress responses do not affect ZIKV infection in A549 cell culture.

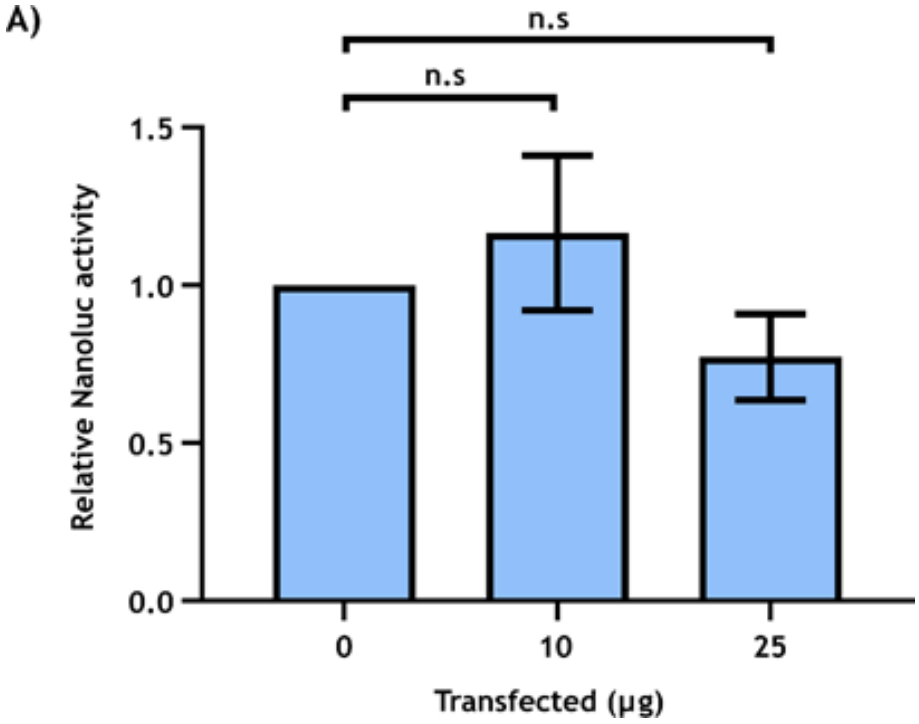

Figure 5-5: EGCG treatment does not affect replication of a ZIKV replicon

A549 cells were transfected with a ZIKV Nanoluc replicon for 24 hrs. EGCG was added to the cells 4 hpt for the remainder. Cells were lysed and luciferase levels were measured and plotted relative to a DMSO treated control. Bars represent results from triplicated independent experiments and error bars represent the standard error of the mean. An unpaired Student's t-test with Welch's correction was used to determine statistical significance where n.s = not significant.

5.2.4 GRP78 silencing impairs ZIKV infection

While inhibition of GRP78 mediated stress responses with small-molecule inhibitors did not impact viral replication, I next sought to investigate the potential of GRP78 to directly influence ZIKV infection. Indeed, knockdown of GRP78 had been shown to impact infection of related flaviviruses such as DENV, JEV and TMUV (Wati *et al.*, 2009; Nain *et al.*, 2017; Zhao *et al.*, 2018). To this end, specific siRNAs (siG and siGa) were used to knockdown GRP78 expression, and protein levels were determined with Western blot analysis (Figure 5-6). This knockdown effect was quantified with densitometry relative to an actin loading control and plotted relative to a scrambled siRNA (siN) control (Figure 5-6). Both siRNA's significantly reduced GRP78 expression, and siG was selected for further experiments.

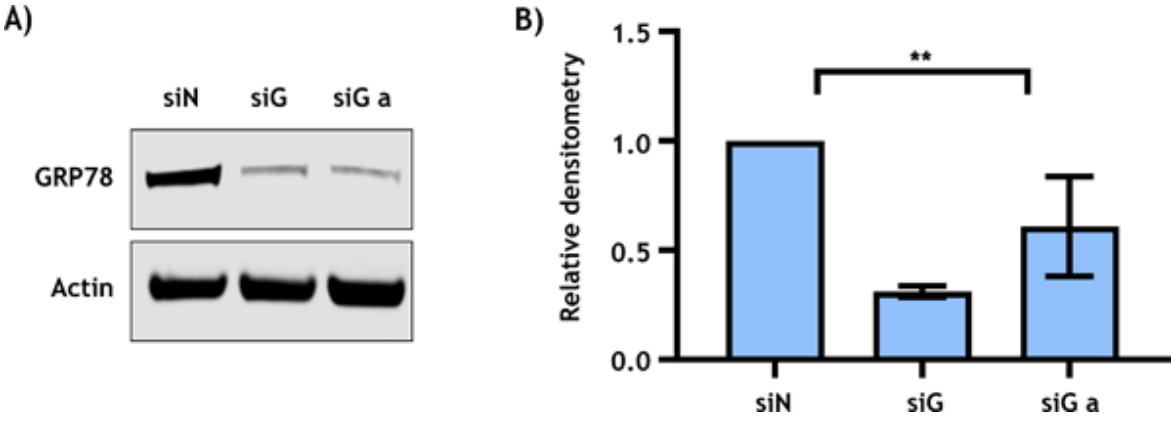

Figure 5-6: GRP78 can be depleted with specific siRNA.

A) *A549 cells were treated with scrambled siRNA (siN), or two different GRP78 siRNA (siG and siGa) for 72 hrs prior to harvesting of cell lysates. Lysates were analysed by Western blot for GRP78 and an actin loading control.* ***B)*** *Densitometry analysis was performed on triplicate independent blots where values were plotted relative to loading controls and normalised to siN, and error bars represent the standard error of the mean. An unpaired Student's t-test with Welch's correction was used to determine statistical significance where n.s = not significant, * p-value < 0.05, ** p-value < 0.01.*

Next, I aimed to assess the effect of this siRNA on ZIKV during infection of A549 cells. Following a 48 hr infection, cell supernatant was harvested from ZIKV PE243 infected siG or control cells, and plaque assays were performed to calculate virus titer (Figure 5-7). This experiment showed there was a significant reduction in virus titer following GRP78 knockdown, indicating that it plays an important role in ZIKV infection. Additionally, siN or siG treated cells were also infected with ZIKV Nanoluc (Figure 5-7). Similarly, Nanoluc readings were significantly reduced following GRP78 silencing, further indicating that GRP78 is important for ZIKV infection. While the above results confirmed the importance of GRP78 for ZIKV infection, they provide little indication of how and why this may be the case. I therefore endeavored to identify the stage(s) at which ZIKV requires GRP78 for infection by probing entry, replication, protein expression and assembly, and egress in turn.

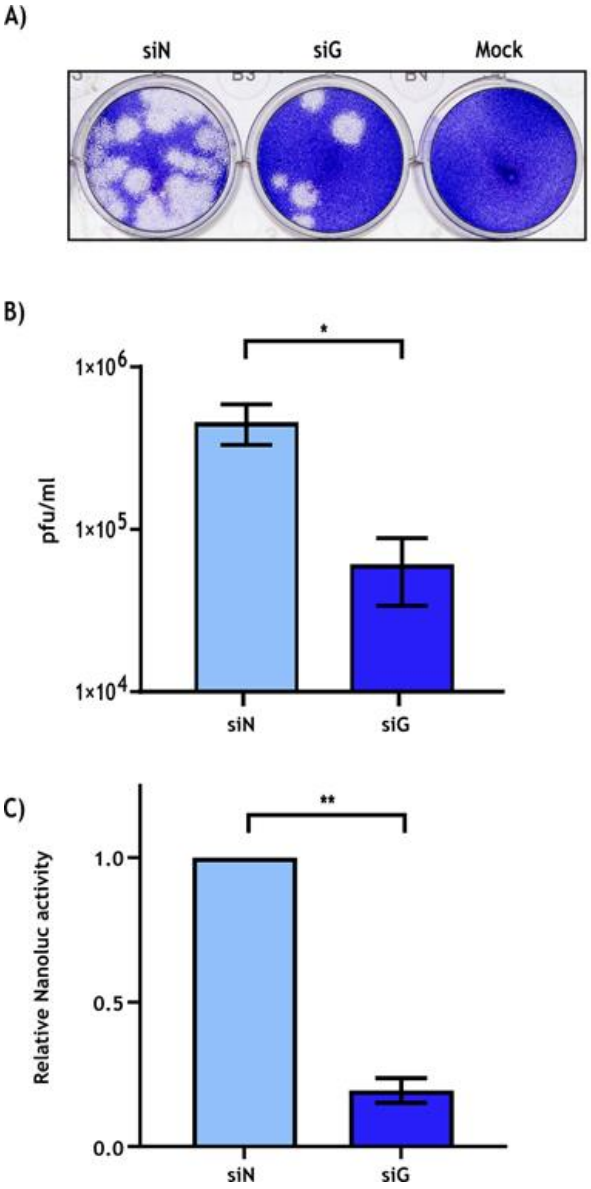

Figure 5-7: GRP78 depletion reduces ZIKV luciferase and viral titres

A) *A549 cells were treated with siRNA for 72 hrs prior to a 24 hr infection with ZIKV PE243 at MOI 0.1. Following infection, cell supernatant was harvested, and virus titre calculated from plaque assay on A549 Npro cells.* ***B)*** *Titres from triplicate independent experiments were analysed and plotted relative to siN control cells.* ***C)*** *Additionally, A549 cells treated with siRNA (as described for* ***A****) were infected with ZIKV Nanoluc for 24 hrs at MOI 0.1. Results from triplicate independent repeats are shown and error bars represent the standard error of the mean. An unpaired Student's t-test with Welch's correction was used to determine statistical significance where n.s = not significant, * p-value < 0.05*

The impact of GRP78 on ZIKV entry to host cells was examined first. While GRP78 is classically regarded as a ER resident chaperone, it has also been found to be present in mitochondria, the nucleus, the cytoplasm, excreted from cells, and importantly, localise to the cell surface of some cell-types (Jindadamrongwech, Thepparit and Smith, 2004; Sun *et al.*, 2006; Ni, Zhang and Lee, 2011). Indeed, as mentioned earlier GRP78 has also been implicated as an attachment/entry factor for some viruses (Nain *et al.*, 2017; Chu *et al.*, 2018). Therefore, I stained A549 cells with a GRP78 specific antibody under non-permeabilising conditions to detect cell surface GRP78 (Figure 5-8). This staining confirmed the presence of surface GRP78 in A549 cells as has been previously described (Kang *et al.*, 2016). Next, A549 cells were treated with siG or siN prior to a high MOI ZIKV PE243 infection, and RNA was harvested after 2 hrs. This is before viral replication has been initiated and, in this way, only incoming viral genomes would be detected. RT-qPCR analysis showed there was no difference in the amount of incoming ZIKV RNA between siN or siG cells, suggesting that GRP78 does not play a role in ZIKV entry in A549 cells (Figure 5-9). To verify this finding, GRP78 antibodies and an unrelated antibody (actin) were incubated with A549 cells prior to infection with ZIKV Nanoluc. While this method was used to show that GRP78 is an important entry factor for JEV, antibody mediated blockade of GRP78 did not reduce ZIKV entry as there was no significant difference in luciferase readings following infection, supporting the RT-qPCR analysis (Figure 5-9) (Nain *et al.*, 2017). Together this data suggests that GRP78 is not important for ZIKV entry.

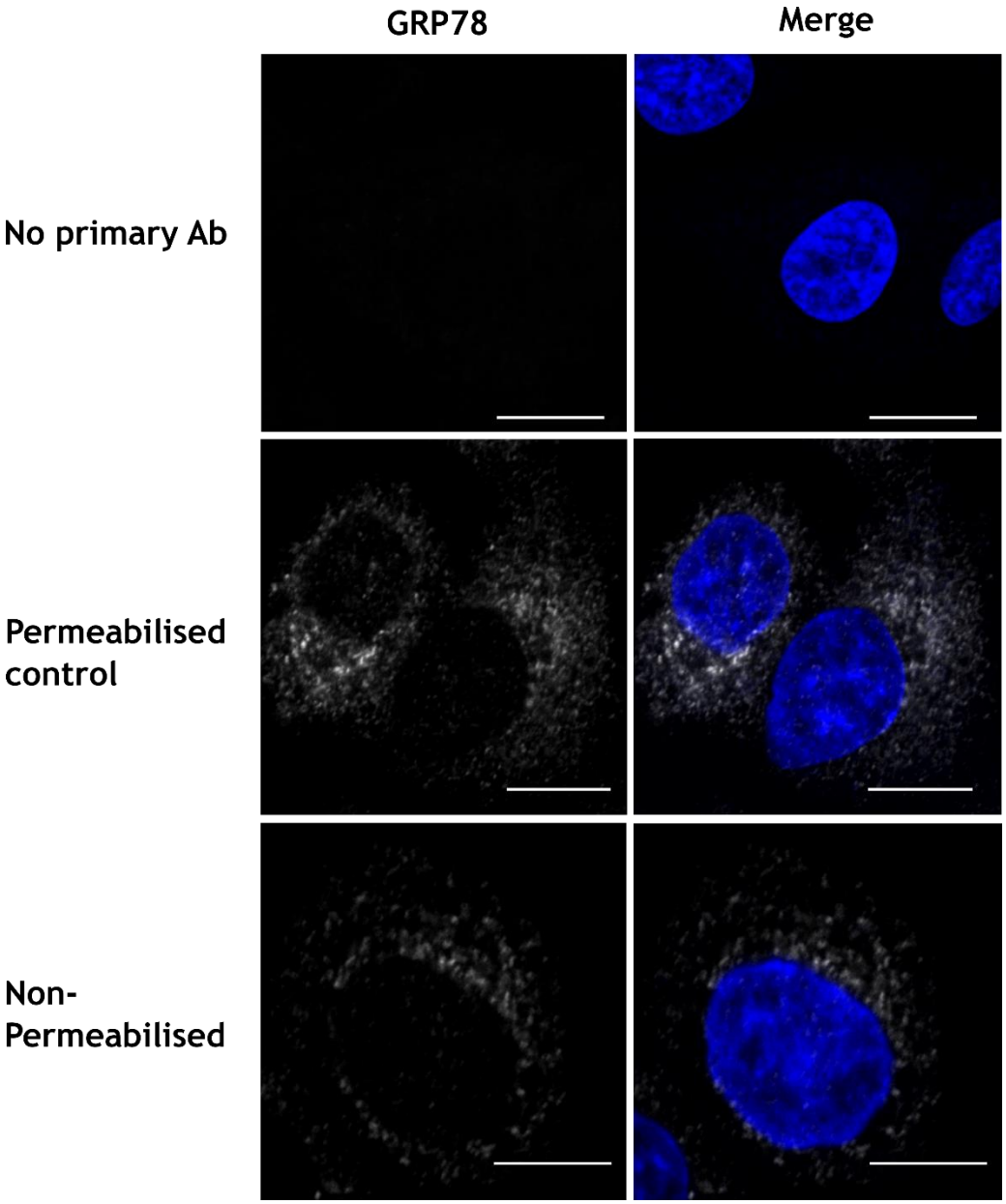

Figure 5-8: GRP78 localises to the plasma membrane of A549 cells.
A549 cells were seeded onto coverslips and left to adhere overnight. Subsequently cells were stained with the live-cell nuclear stain Hoechst 33342 (blue) and fixed with formaldehyde under non-permeabilising, or permeabilising conditions as indicated. Where indicated, a GRP78 antibody was used to visualise surface GRP78, and all cells were stained with a secondary antibody regardless. Images were taken on an LSM 710 confocal microscope and are representative of duplicate experiments. Scale bars represent 10 μm.

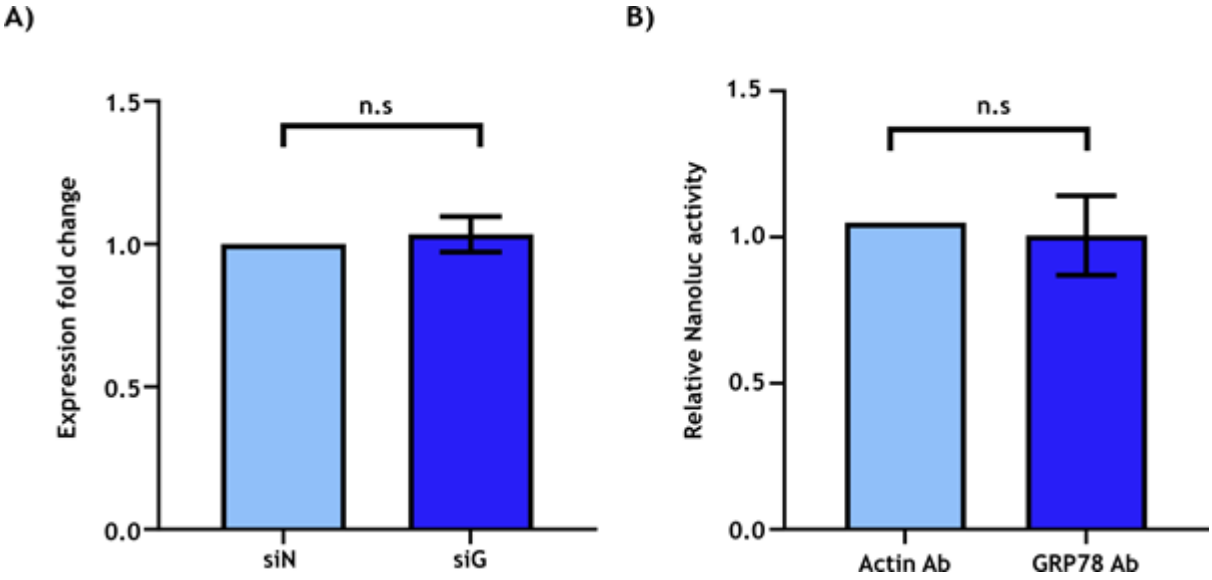

Figure 5-9: GRP78 is not required for ZIKV entry.

A) A549 cells were treated with siRNA for 72 hrs prior to infection with ZIKV PE243 at MOI 5 for 2 hrs. Following infection, RNA was harvested from cells and RT-qPCR analysis was performed. Results represent the expression fold change of RNA relative to a GAPDH control and is normalised to the siN treated control sample. Data from triplicate independent repeats are shown and error bars represent the standard error of the mean. ***B)*** *A549 cells were incubated with a GRP78 antibody or an unrelated actin antibody for 2 hrs prior to infection with ZIKV Nanoluc at MOI 0.1 for 24 hrs. Cells were lysed and luciferase readings were taken and plotted relative to cells treated with an actin antibody. Data from triplicate independent repeats are shown and error bars represent the standard error of the mean. An unpaired Student's t-test with Welch's correction was used to determine statistical significance where n.s = not significant.*

The next step in the viral lifecycle I examined was the role GRP78 may play in replication of the viral genome. Following uncoating of the genome and initial translation, ZIKV replication occurs in sites juxtaposed to the ER in so called 'vesicle packets' that are presumably derived from the ER membrane early in infection (Cortese *et al.*, 2017). A549 cells were treated with siN or siG before infection with ZIKV PE243. RNA was extracted from these cells at several timepoints following infection, and the relative fold-increase in viral RNA was plotted (Figure 5-10). This analysis showed there was no significant decrease in viral RNA levels over infection in cells treated with siN or siG, indicating that GRP78 may not be important for ZIKV replication. This also indirectly supports the entry data, as any defect in viral entry would presumably result in reduced RNA levels.

A)

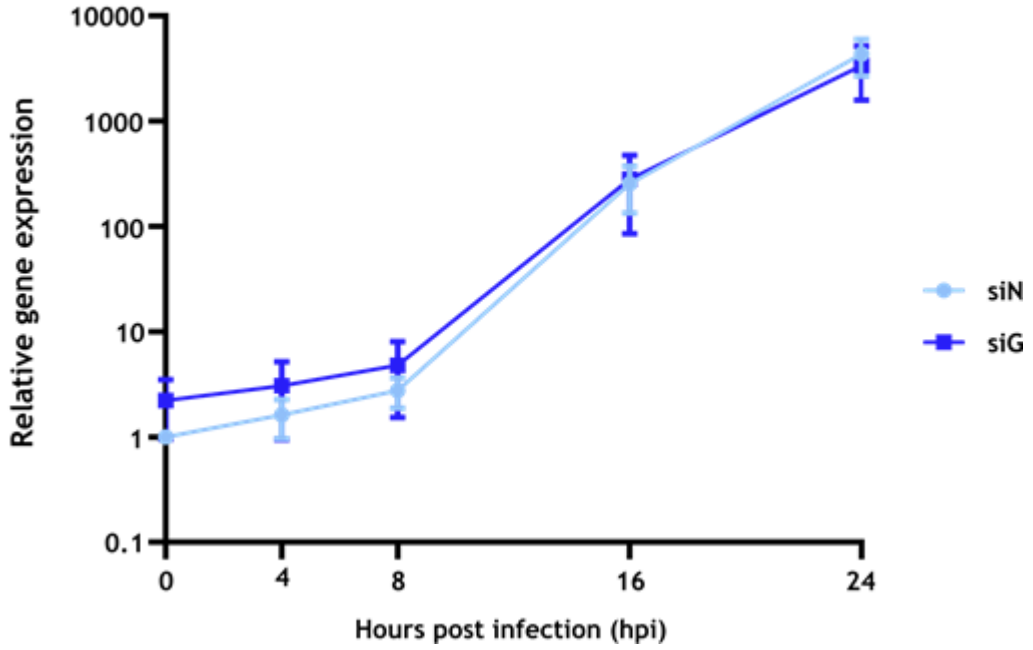

Figure 5-10: GRP78 depletion does not affect ZIKV RNA production.

A) *A549 cells were treated with siN or siG for 72 hrs prior to infection with ZIKV PE243 at MOI 0.1. RNA samples were harvested at 4, 8, 16 and 24 hpi and qPCR analysis was performed. Viral RNA copy number was measured by RT-qPCR relative to a GAPDH control and was normalised to viral RNA detected at 0 hr in the control. Results are plotted from triplicate independent experiments and error bars represent the standard error of the mean.*

Subsequently, I probed the potential for GRP78 to be involved in viral protein production. As a protein chaperone, it is plausible that ZIKV could co-opt GRP78 to facilitate viral protein folding or translation. Indeed as mentioned previously, it is thought that GRP78 is required by DENV to facilitate viral translation (Wati *et al.*, 2009). To test this, A549 cells were transfected with siN or siG and infected with ZIKV PE243. Cell lysates were harvested, and Western blot analysis was performed to visualise levels of ZIKV E and NS5 protein, both of which were observed to be lower in GRP78 depleted cells (Figure 5-11). This suggests that GRP78 depletion reduced the translation of the viral polyprotein. Additionally, when siN or siG treated A549 cells were infected with ZIKV Nanoluc for 16 hrs (a time point prior to ZIKV egress from a549 cells in my hands), luciferase levels were observed to be reduced (Figure 5-12). This indicated that the reduction in luciferase readings was not due to reduced secondary infections and must have occurred during a single cycle.

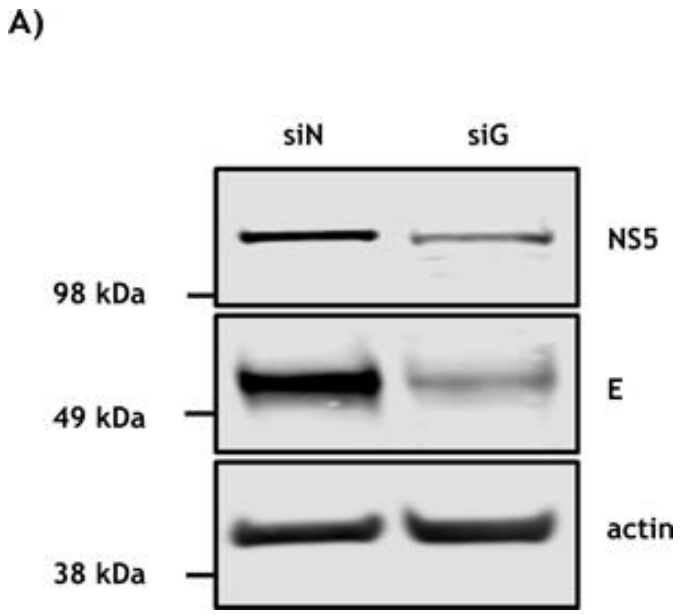

Figure 5-11: GRP78 depletion reduces viral protein expression.

A) *A549 cells were treated with siN or siG for 72 hrs prior to infection with ZIKV PE243 at MOI 0.1 for 48 hrs. Cell lysates were harvested and Western blot analysis was performed for NS5, E and an actin loading control. Image is representative of triplicate experiments.*

A)

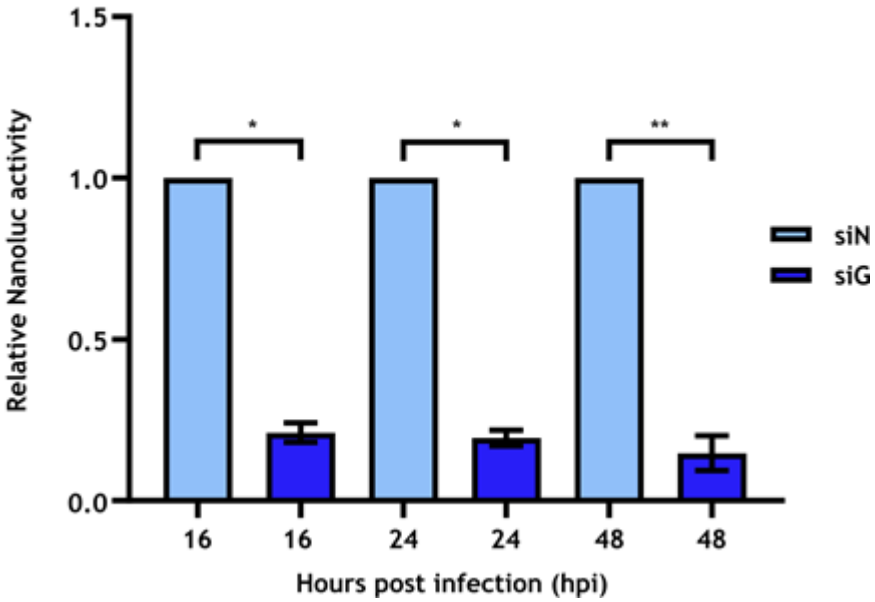

Figure 5-12: GRP78 depletion reduces ZIKV Nanoluc levels during a single round of infection.

A) *A549 cells were treated with siN or siG for 72 hrs before infection with ZIKV Nanoluc at MOI 0.1 for 16, 24 or 48 hrs. Cells were lysed, and luciferase levels were plotted relative to siN values at the comparable timepoints. Values represent results from triplicate individual experiments and error bars represent the standard error of the mean. An unpaired Student's t-test with Welch's correction was used to determine statistical significance where n.s = not significant, * p-value < 0.05, ** p-value < 0.01.*

Although I observed that viral translation was perturbed following GRP78 depletion, it was also conceivable that GRP78 could also play a role in virion transport and egress. GRP78 has been shown to aid the assembly and egress of Human cytomegalovirus (Buchkovich *et al.*, 2008). Additionally, studies have shown that JEV infection utilises GRP78 and its interaction with the KDEL receptor (KDELR) to assist virion trafficking through the ER-Golgi apparatus (Wang *et al.*, 2016). The KDELR shuttles between the ER and Golgi and recognises proteins with a KDEL motif to trigger retrograde transport to the ER, and JEV through an interaction with GRP78 can hijack this system (Capitani and Sallese, 2009). While a similar mechanism might be possible for ZIKV, DENV interacts with KDELR through a direct interaction with prM, and WNV does not require KDELR for egress at all (M. Y. Li *et al.*, 2015). This again highlights important differences between related flaviviruses. To investigate the potential for a block in egress following GRP78 depletion, A549 cells were treated with siN or siG and infected with ZIKV PE243. Following removal of the inoculum, cells were thoroughly washed and replaced with fresh medium. After infection, supernatant samples were taken from both siN and siG cells (labelled siN S and siG S respectively) and plaque assays were performed. Additionally, remaining cells were scraped into PBS and 3 freeze/thaw cycles were performed to release intracellular virions. These samples were clarified, and plaque assays performed (labelled siN C and siG C). The titre of these samples is plotted on Figure 5-13. This shows that there was a significant reduction in supernatant viral titre following GRP78 depletion (as was observed earlier in Figure 5-7) and that there was a similar reduction in intracellular virus levels. The fold reduction of viral titre between siN and siG (from both supernatant and cytoplasm) is also plotted, and there was no significant difference in this fold reduction between supernatant and cytoplasm samples (Figure 5-13). This indicates that there was no block in the egress of infectious virus particles following GPR78 knockdown; if there was you might expect an increase of intracellular virus in the siG relative to the intracellular siN sample. Additionally, I investigated the possibility that KDELR may be important for ZIKV egress due to the joint role they play in JEV egress along with GRP78. Here, A549 cells were treated with siRNA specific against 3 isoforms of KDELR (KDELR1, 2 and 3) and

cells were infected with ZIKV Nanoluc (Figure 5-14). No significant difference was seen in a multicycle infection, suggesting that KDELRs are not important during ZIKV infection as is the case for WNV. Together, these data show that GRP78 is not important for ZIKV egress and highlight vital differences in the egress mechanism of ZIKV from mammalian cells.

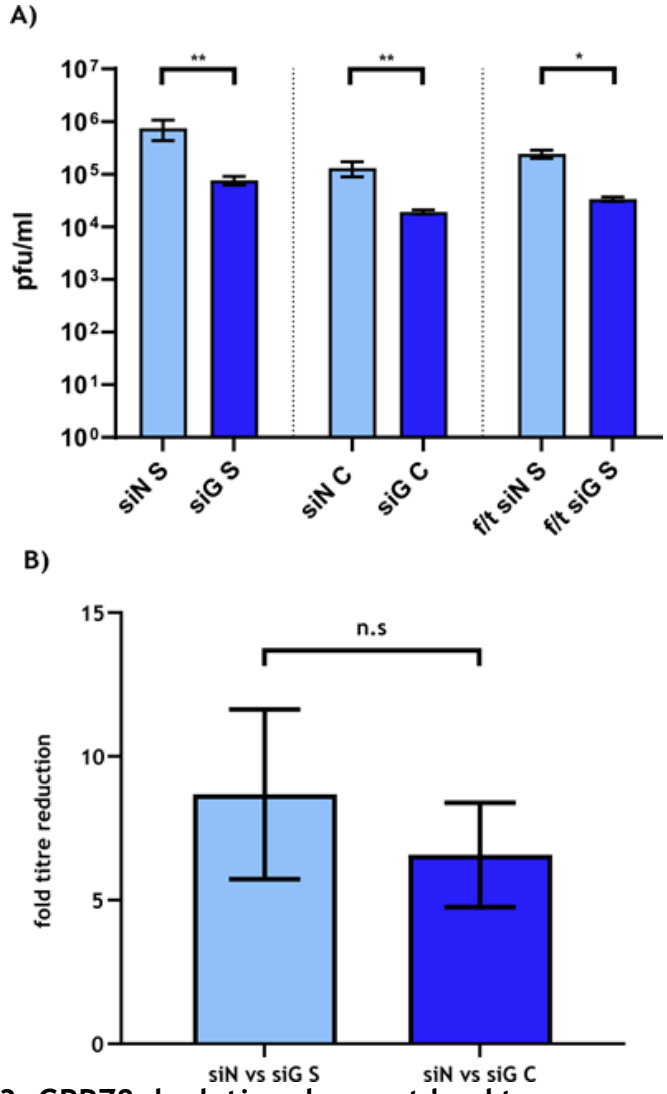

Figure 5-13: GRP78 depletion does not lead to an accumulation of intracellular ZIKV particles.

A) *A549 cells were treated with siN or siG for 72 hrs prior to ZIKV PE243 infection at MOI 0.1 for 24 hrs. Supernatant was harvested from cells are plaque assays were performed (siN S and siG S). Cells were thoroughly washed before cells were scraped into PBS and subject to 3 sequential freeze/thaw cycles. These cells were then clarified, and plaque assays were performed on these samples (siN C and siG C). The effect of freeze/thaw cycles on virus titre was also assessed, where supernatant virus samples were subjected to same conditions as siN C and siG C (f/t siN S and f/t siG S).* ***B)*** *The fold reduction in titre between siN and siG samples were calculated and plotted. Results were collated from triplicate independent experiments and error bars represent the standard error of the mean. An unpaired Student's t-test with Welch's correction was used to determine statistical significance where n.s = not significant, * p-value < 0.05, ** p-value < 0.01.*

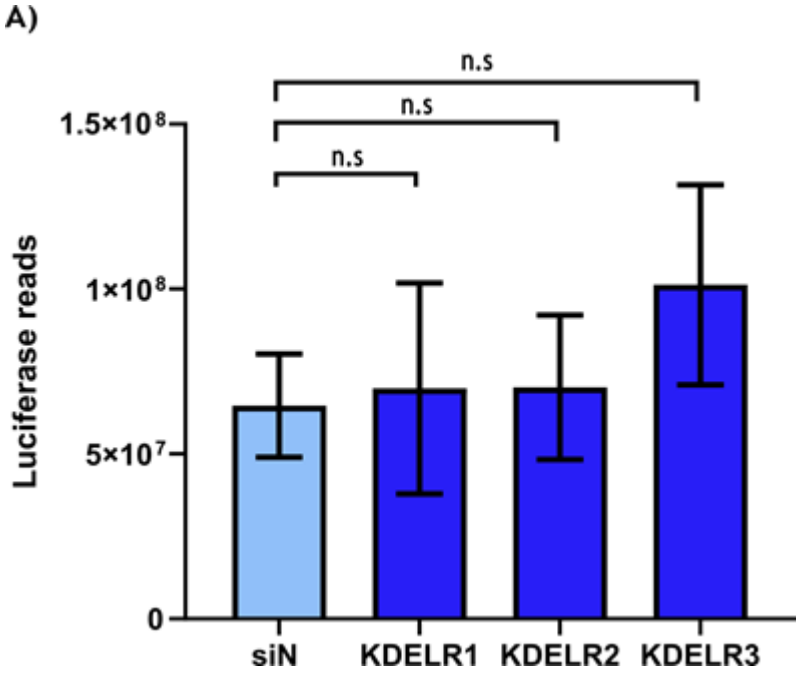

Figure 5-14: KDELR depletion does not significantly reduce ZIKV infection.
A) *A549 cells were treated with siRNA against KDELR 1,2 and 3 for 72 hrs before infection with ZIKV Nanoluc at MOI 0.1 for 48 hrs. Cell lysates were harvested and viral luciferase was measured relative to a siN control. Results represent results from triplicate independent experiments and error bars represent the standard error of the mean. An unpaired Student's t-test with Welch's correction was used to determine statistical significance where n.s = not significant.*

5.2.5 GRP78 depletion may induce a specific reduction in viral translation

The previous experiments suggested that GRP78 may be involved with ZIKV protein translation and/or assembly as suggested by the reduction of viral protein levels. Additionally, GRP78 depletion had no significant impact on other parts of the virus replication cycle. Initially, I proceeded to investigate whether GRP78 was involved in translation. The results in Figure 5-11/Figure 5-12 suggest that viral protein production was reduced following GRP78 depletion, and while there was no noticeable difference in the cellular actin loading control, this experiment did not rule out the possibility that GRP78 silencing was causing a cell wide translation shut-off, rather than a virus specific effect. It could also be the case that GRP78 depletion reduces the stability of viral proteins, resulting in the observed reduction in protein levels. To investigate this further, siN and siG treated A549 cells were either transfected with a firefly luciferase plasmid under control of a CMV promoter (T), infected with ZIKV Nanoluc (I), or both (T+I). Following infection, cell lysates were harvested and firefly and/or nanoluciferase readings were recorded (Figure 5-15). These data reveal several aspects of GRP78 involvement in ZIKV infection.

- Firstly, this confirms that GRP78 depletion reduces viral nanoluciferase readings (Nanoluc: siN I vs siG I).

- Secondly, this data suggests that in control cells ZIKV infection reduces host translation as shown by a significant reduction of firefly readings (Firefly: siN T vs siN T+I).

This is perhaps unsurprising as several viruses are known to induce host shut-off, including famously Influenza A virus (Levene and Gaglia, 2018). Additionally, DENV and ZIKV have both been shown to block host translation, though the mechanism behind this was not discovered in the study by Roth and colleagues (Roth *et al.*, 2017). This experiment is not a perfect proxy for investigating host translation

shut-off, however. A transfected firefly reporter plasmid must first be transcribed, and RNA exported from the nucleus. It could be that ZIKV infection is interfering with the transcription or nuclear export process. This possibility should be considered when interpreting the results shown here.

- Thirdly, GRP78 depletion did not significantly affect host-cell specific protein levels (Firefly: siN T vs siG T) which suggests that the reduction of viral translation observed here is a specific effect.

- Fourthly, and perhaps most interesting, was the observation that GRP78 depletion apparently relieved the blockade of host-cell translation which was previously observed in the control cells (Firefly: siN T+I vs siG T+I). As mentioned, ZIKV infection could be reducing transcription or export of the Firefly transcripts, and it could be that GRP78 depletion reducing viral protein levels via another mechanism, results in the relief in that restriction.

This perhaps indicates that GRP78 is required by ZIKV to re-direct host translation machinery or resources to viral protein production. Simply, in infected cells, GRP78 depletion reduced viral protein production and may have restored host translation, although other experiments are required to investigate the possibility of other mechanisms underpinning the reduction in Firefly production.

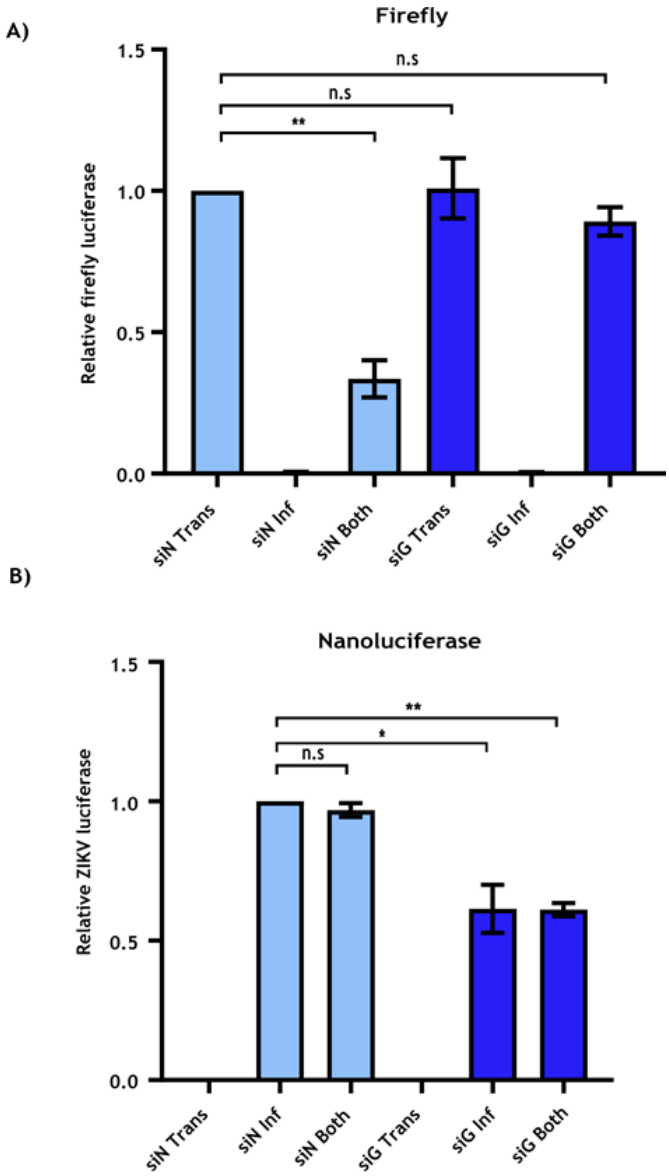

Figure 5-15: GRP78 depletion does not reduce host-cell translation but ZIKV infection does.

A549 cells were treated with siN or siG for 72 hrs. Cells were then either transfected with pGL4.13 FLuc expressing plasmid (labelled 'Trans'), infected with Nanoluc at MOI 5 (labelled 'Inf') or both (labelled 'Both'). Following, cells were lysed and ***A)*** *Nanoluc readings or* ***B)*** *FLuc readings were measured. ZIKV-Nanoluc readings were plotted relative to siN 'Inf', while FLuc readings are plotted relative to siN 'Trans'. Results are representative of triplicate independent experiments and error bars show the standard error of the mean. An unpaired Student's t-test with Welch's correction was used to determine statistical significance where n.s = not significant, * p-value < 0.05, ** p-value < 0.01.*

Due to the observation that GRP78 is important for ZIKV protein levels, and the fact that GRP78 re-localises to a perinuclear location which could be consistent with viral replication factories, I investigated the state of ZIKV dsRNA, a replication intermediate which is known to reside inside these compartments. A549 cells were seeded on coverslips and transfected with either siN or siG prior to infection. These cells were then immunostained for GRP78 and dsRNA, and then labelled with DAPI (Figure 5-16). In siN cells, dsRNA is seen to tightly localise in a perinuclear location which correlates with GRP78 staining. However, in siG cells dsRNA localisation is altered and is seen to be diffuse throughout the cytoplasm. This may indicate that GRP78 is required for the proper localisation of dsRNA, and therefore replication factory localisation, in infected cells.

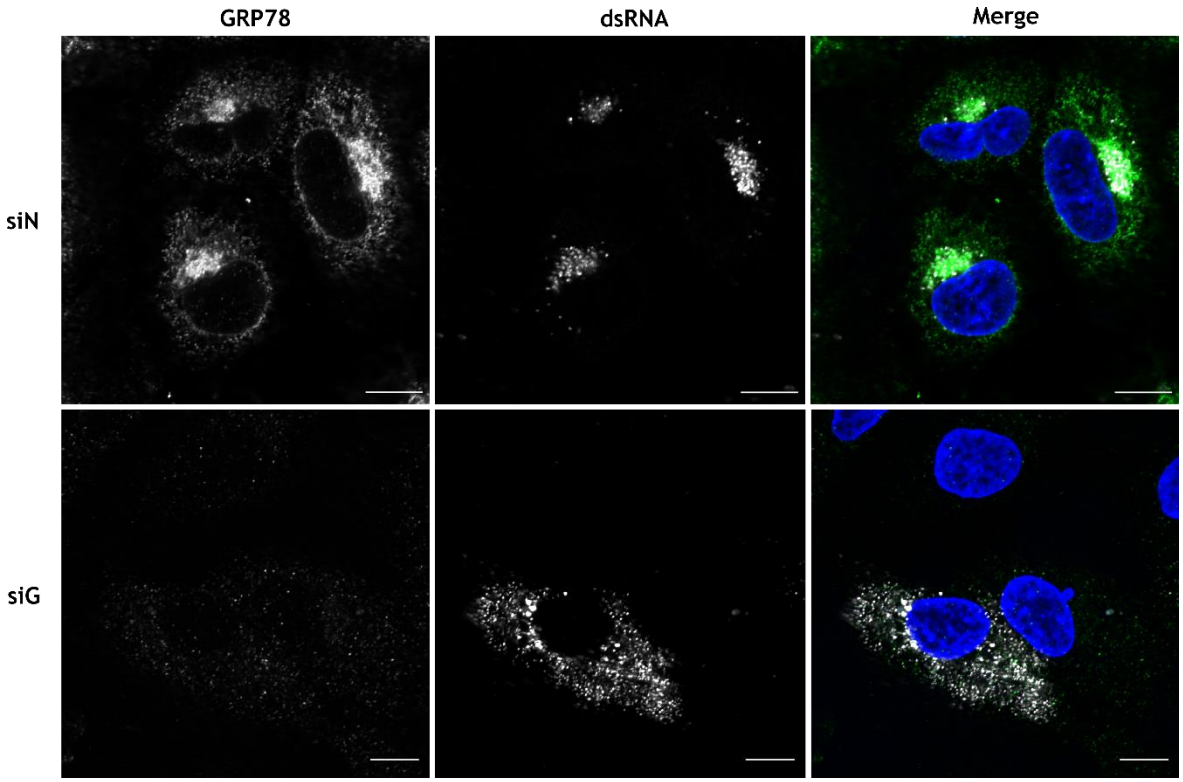

Figure 5-16: GRP78 depletion results in re-localisation of viral dsRNA.
A549 cells were seeded onto coverslips and left to adhere overnight. Cells were then treated with either siN or siG for 72 hrs prior to infection with ZIKV PE243. GRP78 (green) and dsRNA (white) were labelled with specific antibodies and nuclear DNA was stained with DAPI. Images were taken on an LSM 710 confocal microscope and are representative of triplicate experiments. Scale bars represent 10 μm.

5.2.6 GRP78 interacts with ZIKV E in mosquito cell culture and is required for infection

As an arbovirus, ZIKV is transmitted to humans primarily by *Aedes aegypti* mosquitos, as previously discussed (Chapter 1.2.2). It is therefore important to investigate the cellular partners of ZIKV in *Aedes aegypti* systems, similar to the investigation performed in Chapter 4. Of importance, GPR78 is a remarkably conserved protein and there is an 82.7% sequence identity between human and *Aedes aegypti* GRP78. It seems likely that ZIKV would seek to target proteins which are conserved between the vector and mammalian host to make efficient use of its limited coding capacity. Therefore, I decided to investigate whether GRP78 may also facilitate ZIKV infection in *Aedes aegypti* cell culture.

To test whether ZIKV E interacts with GRP78 in this system, Aag2 (and A549) cells were infected with ZIKV PE243 before cell lysates were harvested. Lysates were co-immunoprecipitated with a GRP78 antibody and probed for E and GRP78 expression by Western blot analysis. In infected cells, GRP78 pull-down samples immunoprecipitate with ZIKV E, suggesting that *Aedes aegypti* GRP78 can also interact with E (Figure 5-17). Silencing of GRP78 with specific dsRNA reduced luciferase readings of Aag2 cells infected with ZIKV Nanoluc compared with control cells, confirming that the GRP78 is important for ZIKV in both vector and host (Figure 5-17).

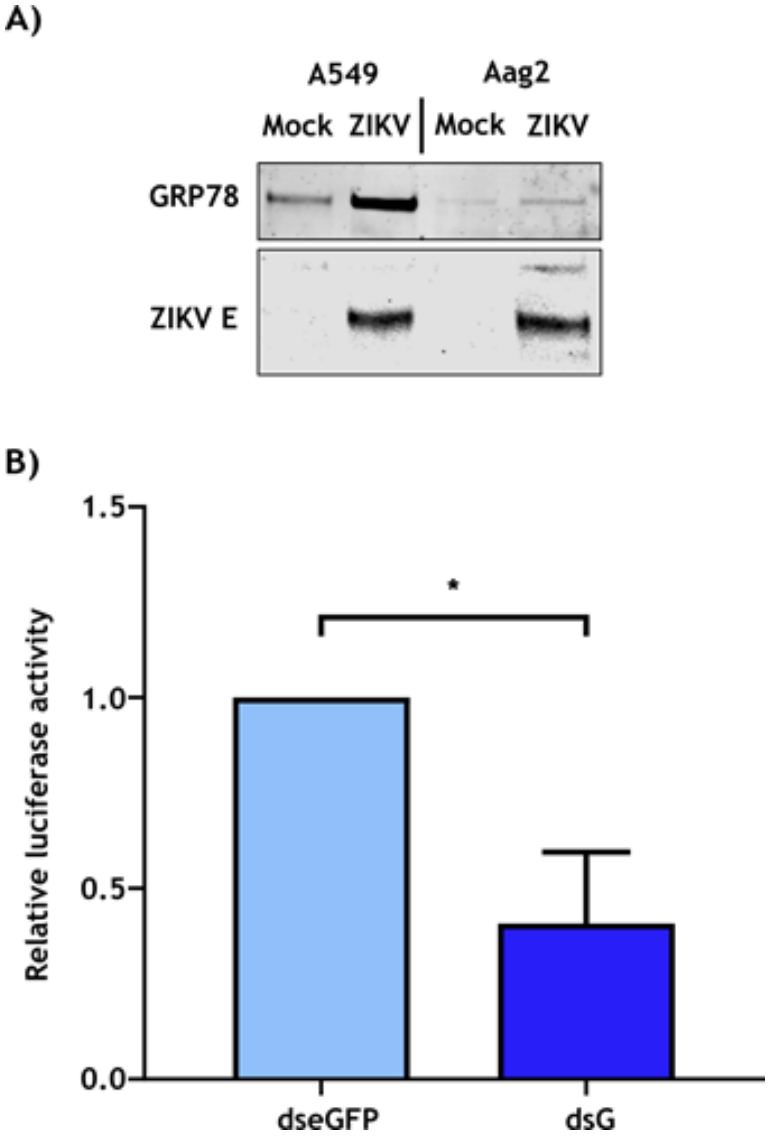

Figure 5-17: Mosquito GRP78 interacts with ZIKV E and is a pro-viral factor

A) *A549 or Aag2 cells were infected with ZIKV PE243 at MOI 5 for 72 hrs. Cells were harvested and co-immunoprecipitation with an GRP78 antibody was performed. Western blot analysis was performed on samples for E and GRP78. Images are representative of triplicate experiments.* ***B)*** *Aag2 cells were treated with dsRNA against GRP78 (dsG) or eGFP (dseGFP) as a control. Cells were then infected with ZIKV Nanoluc for 48 hrs before cells were lysed and luciferase levels were measured. Luciferase is plotted relative to dsGFP and results are from triplicate independent experiments, where error bars represent the standard error of the mean. An unpaired Student's t-test with Welch's correction was used to determine statistical significance where n.s = not significant, * p-value < 0.05.*

5.3 Discussion

This study aimed to verify and characterise the interaction between GRP78 and ZIKV E. To do this, small molecule inhibitors of GRP78-mediated stress responses, and siRNA directed against GRP78, were employed to elucidate the role this protein plays in ZIKV infection. Classically, E protein has mainly been considered as a structural protein that facilitates entry and virion assembly. Here, it was shown that ZIKV E interacts with GRP78, and that GRP78 contributes to ZIKV protein translation and replication factory localisation.

The proteomics results were verified with co-immunoprecipitation and immunofluorescence experiments. While I did not investigate the mechanics underpinning this interaction, EDIII of DENV is known to interact with GRP78 and this mechanism could conceivably be conserved in ZIKV E (Limjindaporn *et al.*, 2009). Indeed, computational modelling has predicted that residues located in ZIKV EDIII can potentially dock with GRP78 (Elfiky and Ibrahim, 2020). More recently, this has been confirmed in a yeast-2-hybrid screen where GRP78 was identified as an interactor ZIKV EDIII (Khongwichit *et al.*, 2021). While these results were published too late to inform the direction of this study, they do serve to confirm the observed interaction described here. I will further discuss the study by *Khongwichit et al, 2021* in more detail where appropriate, as this work has subsequently replicated several of the findings described here, though with some notable differences.

I went on to investigate whether GRP78 was important for ZIKV infection. I initially looked at the impact of two small-molecule inhibitors (EGCG and HNK) that are known to bind to and prevent GRP78 ATPase functions, and therefore prevent GRP78 coordination of the UPR (Sagara *et al.*, 2018). EGCG has previously been shown to inhibit the infection of viruses including Ebola (Patrick Reid *et al.*, 2014). Here, EGCG was found to inhibit ZIKV infection in A549 cells, though HNK did not, and EGCG was found to act before the first hour of infection. One possibility was

that EGCG was exerting its antiviral effect on cell surface GRP78, and thereby maintaining GRP78 in an open confirmation and thereby reducing ZIKV binding efficiency. Indeed, EGCG binding to GRP78 at the cell surface has also been postulated as the mechanism of action behind EGCG-mediated SARS-CoV-2 inhibition (Sagara *et al.*, 2018; Allam *et al.*, 2020). If this were the case however, HNK may have been expected to produce the same phenotype as the mechanisms of action are conserved between both molecules (Martin *et al.*, 2013). Another possibility was that EGCG was having an off-target effect, either on another cellular protein or perhaps even 'off-target' directly on the virus. Indeed, by incubating ZIKV with EGCG and infecting cells which had not been exposed to EGCG, I could recapitulate the inhibition of ZIKV infection. Conversely, DMSO treated ZIKV was not inhibited upon infection of cells pre-treated with EGCG. Concurrent with these observations, a separate study was published by Carneiro and colleagues documenting a similar phenotype (Carneiro *et al.*, 2016). Carneiro *et al* showed that pre-treating Vero cells with EGCG did not protect cells from ZIKV infection, however pretreatment of ZIKV did significantly reduce infection. This study used a $\log_{10}$ higher concentration of EGCG than described here (100 μM vs 10 μM) and a different cell line (Vero E6 vs A549) and no mechanism was provided. Subsequently, another study showed that EGCG was able to directly bind to ZIKV E protein, potentially inhibiting cell attachment (Sharma *et al.*, 2017). Together these data suggest that EGCG and HNK inhibition of GRP78-mediated cell stress responses do not impact ZIKV infection. While the activation of cell-stress pathways, including those associated with GRP78 (IRE1 and ATF6), is well documented in ZIKV infections, it is not clear whether these pathways were activated in the systems I tested (Gladwyn-Ng *et al.*, 2018; Tan *et al.*, 2018; Alfano *et al.*, 2019). Khongwichit *et al, 2021* documented an increase in UPR in A549 cells infected with ZIKV, though the functional relevance of this finding in relation to infection was not investigated further (Khongwichit *et al.*, 2021). While my data may suggest that UPR inhibition does not affect ZIKV infection in A549 cells, there is always the possibility of cell-type and/or model specific differences.

Following the observation that GRP78 ATPase inhibition had no effect on ZIKV infection, I investigated the possibility that GRP78 could influence infection via other means. Using siRNA, GRP78 was specifically depleted from A549 cells. During ZIKV infection of these cells I observed that virus titre and the activity of a Nanoluciferase reporter virus were significantly reduced. This showed that GRP78 was important for ZIKV infection, and to further investigate how this may be the case I examined each stage of the virus lifecycle in turn.

Initially, I focused on the role GRP78 may play in ZIKV entry. GRP78 has been implicated in the entry of several diverse viruses, such as JEV, TMUV and MERS (Nain *et al.*, 2017; Chu *et al.*, 2018; Zhao *et al.*, 2018). This is perhaps partly as a consequence of high levels of GRP78 surface expression in cell-lines that are commonly used for these studies, including A549 cells, but it nevertheless clear that GRP78 can also re-localise to cell surfaces in stress conditions (Zhang *et al.*, 2010; Kang *et al.*, 2016; Tseng, Zhang and Lee, 2019). Indeed, here I affirm that A549 cells express GRP78 at the plasma membrane. Despite this, in ZIKV-infected, GRP78 depleted cells, there was no significant difference in the quantities of internalised viral RNA shortly after infection compared to control cells. Additionally, incubating GRP78 antibodies with A549 cells prior to infection had no effect on ZIKV replication in my hands. This contrasts with findings reported by *Khongwichit et al, 2021*, where treatment of A549 cells with antibodies directed against the N-terminus of GRP78 marginally, but statistically significantly, reduced ZIKV infection. Antibodies directed against the C-terminus of GRP78 had no such effect in this study. The experimental design here was similar, though Khongwichit and colleagues used a 10x fold higher concentration of GRP78 antibody (Khongwichit *et al.*, 2021). There is a potential that the incomplete silencing of GRP78 with siRNA still left enough GRP78 to facilitate entry, or that the amount of GRP78 antibody I used was insufficient to block viral attachment. However, on balance, I believe these observations suggest that GRP78 is not a major route of entry for ZIKV in A549 cells.

Subsequent experiments performed here established that GRP78 was important for ZIKV protein expression, a phenotype that has been reported for a related flavivirus, DENV, and again more recently for ZIKV (Wati *et al.*, 2009; Khongwichit *et al.*, 2021). Additionally, I showed that this reduction of viral protein levels was virus specific, as GRP78 depletion potentially did not reduce cellular translation in uninfected cells. Interestingly, in infected cells there was a significant reduction in a Firefly reporter expression, a phenotype possibly indicative of viral hijacking of host translational machinery and one that has been described previously for ZIKV (Roth *et al.*, 2017). Despite this, GRP78 expression was not only maintained but increased in ZIKV cells, though the mechanism behind this remains elusive. This finding was also reported by *Khongwichit et al*, 2021, where they observed an increase in GRP78 mRNA and protein levels as infection progressed, implying there is a specific upregulation of GRP78 expression rather than maintenance of existing GRP78.

One of the most interesting findings was that GRP78 depletion in virus infected cells restored Firefly reporter expression to control levels. This is particularly fascinating as it potentially suggests ZIKV requires GRP78 to hijack cellular translational machinery. Without GRP78, viral protein expression dropped, and cellular translation increased relative to an infected cell. To further investigate this phenotype, I looked at the localisation of viral replication factories as visualised by dsRNA. dsRNA is a replication intermediatory produced during replication of *flavivirus* genomes (Cortese *et al.*, 2017). No dsRNA can be seen in uninfected A549 cells, and in infected cells dsRNA tightly localises to a perinuclear location consistent with the predicted location of ZIKV replication factories (Cortese *et al.*, 2017). In these infected cells, GRP78 can be seen to cluster to these locations coincident with dsRNA and ZIKV E. Following GRP78 depletion, dsRNA staining loses the clustered organisation and instead displays a diffuse phenotype. While the mechanism behind this change is not entirely clear, it is tempting to speculate that GRP78 is required to coordinate the localisation of replication factories in space and time to facilitate efficient translation. Without GRP78, the amount of viral RNA does not change as measured by qPCR, and indeed

the total staining of dsRNA does not appear to change. While speculative, it is possible that the initial rounds of viral translation (before replication factory formation) in GRP78 depleted cells are still sufficient to produce sufficient NS3 and NS5 to facilitate viral replicase formation and explain the lack of reduction in viral RNA levels (Sanford *et al.*, 2019). Therefore, one explanation could be that in cells without GRP78, if the viral replication factories are not coordinated near the ER it is possible that viral transcripts cannot efficiently access translational machinery. This could explain both the reduction in viral protein expression and the apparent rescue of host-cell protein production following GRP78 depletion. However, it is also possible that GRP78 depletion reduces the stability of viral proteins, lowering protein levels. Another possibility is that without the spatial-temporal organisation of replication factories in GRP78 depleted cells, viral RNA is more exposed to cellular innate immune responses (Arakawa and Morita, 2019). This explanation does not necessarily reconcile with the lack of difference between viral RNA levels in siN and siG cells, although further experimentation is required to investigate this.

While the effect of GRP78 on viral protein levels was clear, it was also possible that GRP78 could play an additional role in facilitating the egress of ZIKV. GRP78 has been shown to be important for the egress of Influenza A virus and helps traffic HMCV (Hogue and Nayak, 1992; Buchkovich *et al.*, 2008; Shi-Chen Ou *et al.*, 2011). Therefore, I investigated whether GRP78 depletion resulted in an intracellular accumulation of infectious virus, which may explain the reduction in virus titre. To do this, control cells and GRP78 depleted cells were infected and subjected to multiple freeze/thaw cycles before these samples were assessed by plaque assay. The titre of these samples was compared to the titre of virus in the extracellular medium prior to freeze/thaw. Here, I observed that the relative fold difference in excreted virus between control and siGRP78 cells was not significantly different to the comparable intracellular samples. This indicated that there was no accumulation of intracellular virus.

In addition to the experiments in mammalian cell-culture, I also investigated the role that the GRP78 may play in *Aedes aegypti* cells infected with ZIKV. GRP78 is highly conserved between species as shown in Chapter 9, I therefore hypothesised and went on to show that ZIKV E interacts with *Aedes aegypti* GRP78 and is a pro-viral factor. As a virus that infects diverse hosts, it could be expected that ZIKV may have evolved to target cellular factors that are conserved between targets organisms. This seems to hold true for GRP78, and future discovery studies could look towards other highly conserved proteins for inspiration.

In conclusion, this study expands the knowledge surrounding ZIKV E cellular interactors and hints at a potential role for GRP78 in ZIKV replication factory formation.

5.4 Summary

- A previously conducted proteomic study was used as a basis to identify potential ZIKV E interactors.

- GRP78 was found to interact with ZIKV E and co-localise in mammalian cells.

- EGCG, an GRP78 ATPase inhibitor, impaired ZIKV infection by acting directly on the virus and so independent of GRP78 inhibition. Another drug, HNK, had no effect.

- Silencing of GRP78 reduced ZIKV infection via reduced ZIKV protein expression, as measured by Western blot and the luciferase activity of a reporter virus. Parameters associated with viral entry, RNA production and egress were also measured following GRP78 depletion, and no effect on the virus was observed.

- The reduction in ZIKV translation was virus specific, and host translation was not affected. However, GRP78 expression was seen to be upregulated in infected cells.

- Viral replication factories, as visualised by proxy (dsRNA immunostaining), were seen to co-localise with GRP78 during infection and clustered in a perinuclear location.

Chapter 6. Developing tools to further investigate the role of GRP78 in ZIKV infection

6.1 Introduction

6.1.1 ZIKV reverse-genetic systems

There are limited tools available for the study of emerging viruses such as ZIKV. An important requirement for such research is a supply of virus of known genetic heritage. The primary virus used in the study described in Chapter 5 was an ZIKV isolate termed PE243, which as previously noted was isolated from a patient in Recife, Brazil during the 2015/16 epidemic (Donald *et al.*, 2016). As described by Donald *et al*, this virus was initially amplified in C6/36 *Aedes albopictus* cells and followed by further amplification in Vero cells to generate a master stock of virus for research. Generation of more virus requires further amplification in cell culture, and given that a low number of passages through cell culture can introduce mutations and phenotypic differences into ZIKV, there is a finite amount of patient-isolate virus available (Duggal *et al.*, 2019). As such, there is a need to develop a reverse-genetics (RG) system for ZIKV PE243 to allow reliable recapitulation of the original virus isolate and could also allow for generation of a patient isolate from scratch, avoiding the need for multiple passages for propagation. RG systems have been created for ZIKV Nanoluc, as described in Chapter 4.2.1, as well as several other ZIKV viruses, though to the best of my knowledge no such system exists for ZIKV PE243 (Widman *et al.*, 2017; Ávila-Pérez *et al.*, 2018; Münster *et al.*, 2018).

While useful, ZIKV Nanoluc has limitations. Primarily, as a recombinant virus consisting of sequences from both PE243 and BeH819015, ZIKV Nanoluc does not truly represent a virus found naturally (Mutso *et al.*, 2017). Therefore, one aim of this study was to generate an RG system for ZIKV PE243. To do this I aimed to

employ a bacterium-free circular polymerase extension reaction (CPER) method to generate a circularised ZIKV DNA backbone from multiple linear fragments. CPER was first described by Quan *et al*, and has since been used to rescue viruses such as WNV, YFV and another ZIKV strain (Quan and Tian, 2009; Edmonds *et al.*, 2013; Setoh *et al.*, 2017; Sanchez-Velazquez *et al.*, 2020).

Additionally, as described in Chapter 4.3, ZIKV Nanoluc was not as useful as first imagined when used in the siRNA screen as this virus struggled to capture differences in virus infection kinetics. The proposed ZIKV PE243 RG virus would be capable of being modified with other luciferase tags, which might better reflect a WT virus and perform more favourably in screens. Nanoluc, while significantly smaller than other luciferase molecules such as Firefly luciferase, is still ~ 19 kDa (England, Ehlerding and Cai, 2016). A NanoBiT binary tag is a split-tag based on Nanoluc and consists of a large subunit (LgBiT) and a 11 aa peptide tag (HiBiT) (Liang *et al.*, 2020). An 11 aa tag might be expected to incur a smaller fitness cost for ZIKV than a Nanoluc tag and could create a more suitable reporter virus. This tag has been successfully incorporated into a YFV reporter virus, and so I aimed to employ this same strategy for ZIKV (Sanchez-Velazquez *et al.*, 2020). These RG viruses would not only be important for this current study but could be useful for future ZIKV work.

6.1.2 GRP78 knockout cell line

Another tool I was interested in generating to further investigate the role of GRP78 in ZIKV infection was a *grp78* knockout (K/O) cell line. In Chapter 5.2.4, siRNA was employed to reduce GRP78 expression. This treatment reduced GRP78 expression by approximately 70% but did not abrogate it completely and the remaining GRP78 could potentially still provide some of the functionality that ZIKV requires. For this reason, I aimed to generate a *grp78* K/O cell line.

Additionally, production of this cell line could facilitate the generation and use of *grp*78 mutants (Tsai *et al.*, 2015). There are several conceivable ways to employ such mutants. For example, the inability to bind nucleotides or substrates could be engineered which would enable further mechanistic studies into the role of GRP78 in ZIKV infection. For example, a T229A mutation has been shown to significantly reduce ATPase activity, preventing the switch from an open to closed confirmation and thus reduces the peptide binding affinity of GRP78 (Yang *et al.*, 2015). Other mutations in the NBD, such as at R197, also impair the ability of GRP78 to bind interactors, such as DnaJ co-chaperones (Awad *et al.*, 2008). To the best of my knowledge, no *grp78* K/O cell line currently exists, although there are several inducible *grp78* K/O mice genotypes that have been generated (Luo *et al.*, 2006; Wey *et al.*, 2012; Zhu *et al.*, 2013).

6.1.3 Cellular partners of GRP78

While Chapter 5 indicated that GRP78 interacted with ZIKV E and was important for infection, questions remained about the mechanisms behind GRP78's role in infection. GRP78 is known to be a prolific chaperone and interacts with many cellular proteins; some of these interactions were previously outlined in Chapter 1.3.2. I hypothesised that cellular partners of GRP78 may also play a role in facilitating ZIKV infection. I aimed to perform a Search Tool for Retrieval of Interacting Genes/Proteins (STRING) analysis to identify potential GRP78 cellular interactors, and investigate the role, if any, these proteins may play in ZIKV infection (Szklarczyk *et al.*, 2019). To do this, I aimed to use the ZIKV PE243 RG viruses introduced in Chapter 6.1.1 to perform a targeted screen of GRP78 partners. Additionally, the role of these interactors could be further explored in the absence of GRP78 by using the *grp78* K/O cell-line proposed in Chapter 6.1.2, analysing whether there is cooperativity between these host-factors in facilitating ZIKV infection.

6.1.4 Aims

- To generate a RG system for ZIKV PE243, ideally for both, a WT and a reporter virus, variant.

- To create a *grp78* K/O cell-line using CRISPR/Cas9 technology.

- Finally, to use these tools cooperatively to conduct further studies into the interaction between GRP78 and ZIKV.

6.2 Results

6.2.1 Generating a ZIKV PE243 reverse genetics system

The initial aim of this study was to generate a ZIKV PE243 RG system. The design of the RG system was based on the CPER system, and this has previously been used to recreate a different ZIKV strain (Setoh *et al.*, 2017). As shown in Figure 6-1, PE243 was separated 5 segments of roughly equal size. Plasmids containing these fragments were synthesized by GeneArt (Thermo Fisher Scientific), and PCR amplification of these fragments generated linear DNA moieties for use in the final CPER reaction. To enable the linking and circularisation of the complete PE243 genome, DNA fragments share a short overlap with neighbouring fragments. Different versions of segment 2 were produced; one encoding the WT virus sequence (to create the WT ZIKV PE243), and one with a HiBiT (to create a HiBiT ZIKV PE243, Chapter 6.1.1) moiety incorporated into the N-terminus of NS1. The first 4 aa of NS1 were duplicated before the insertion of HiBiT, and this is followed by a 4GS linker, and subsequently the full length NS1. This design was chosen as it has previously been used to generate a HiBiT YFV reporter virus (Sanchez-

Velazquez *et al.*, 2020). Therefore, 2 CPER reactions were performed to generate a WT and a HiBiT ZIKV PE243 sequence. Vero E6 cells were transfected with these circularised constructs. Five days post-transfection, cell lysates were harvested and titrated on A549 NPro cells to confirm the presence of infectious virus. While the WT ZIKV PE243 samples formed plaques on A549 NPro cells, there were no plaques formed by HiBiT ZIKV PE243 (Figure 6-2). This experiment was repeated in triplicate, and no plaques were formed following HiBiT ZIKV PE243 CPER transfection in any repeat. Luciferase readings and RNA were also taken from HiBiT ZIKV PE243 and WT ZIKV PE243 and are shown in Figure 6-2. Here, no luciferase readings above background levels were detected, and only cDNA for the WT virus was generated. Additionally, no cDNA was detected in the samples where no reverse transcriptase step was performed, showing that input transfection DNA was not being detected. This indicated that while the rescue of WT ZIKV PE243 using CPER was successful, no HiBiT ZIKV PE243 was recovered.

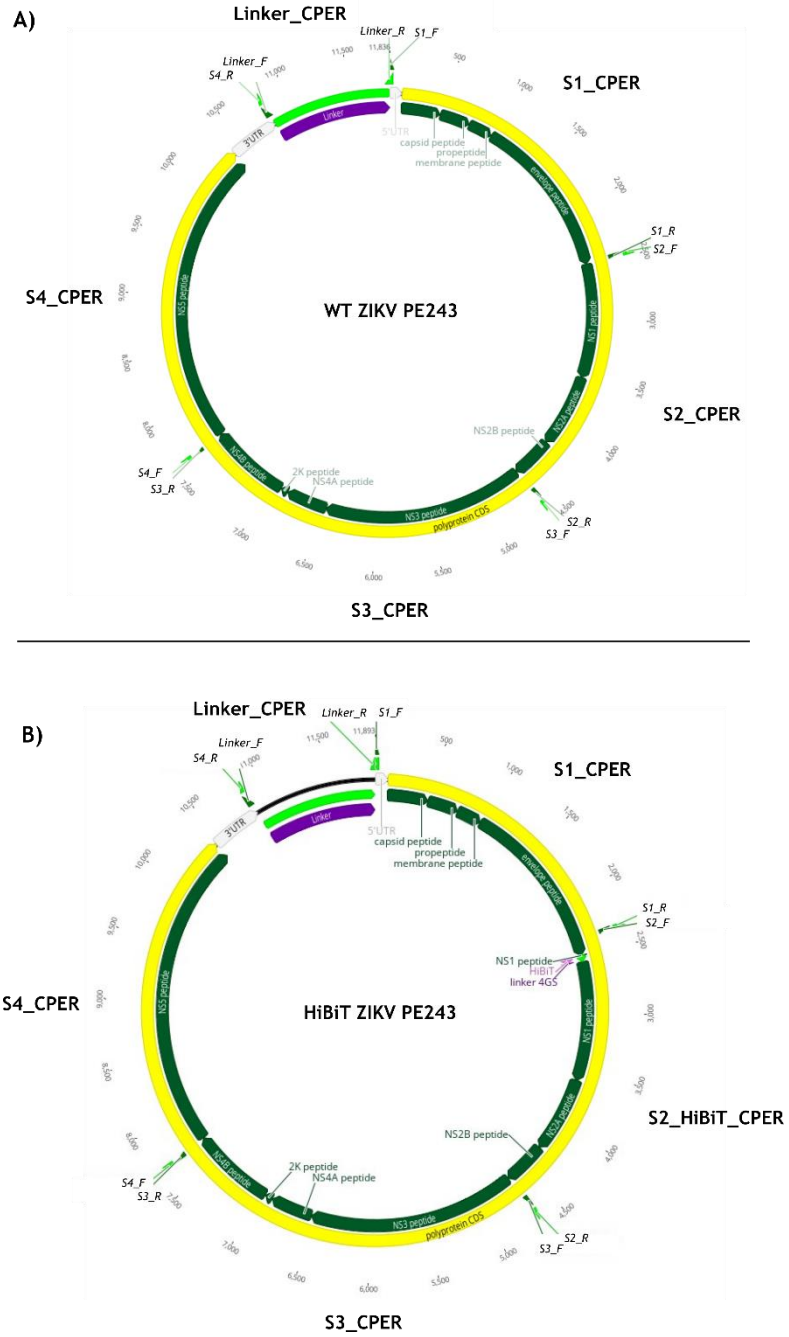

Figure 6-1: Design of a ZIKV reverse genetics system.

A) *Schematic showing the structure of the ZIKV reverse genetic system. ZIKV PE243 genome was separated into 5 segments, the lengths of each are shown here.* ***B)*** *An additional variant of segment 2 is included, which contains a HiBiT fragment and was substituted for WT segment 2 for generation of HiBiT ZIKV PE243.*

A)

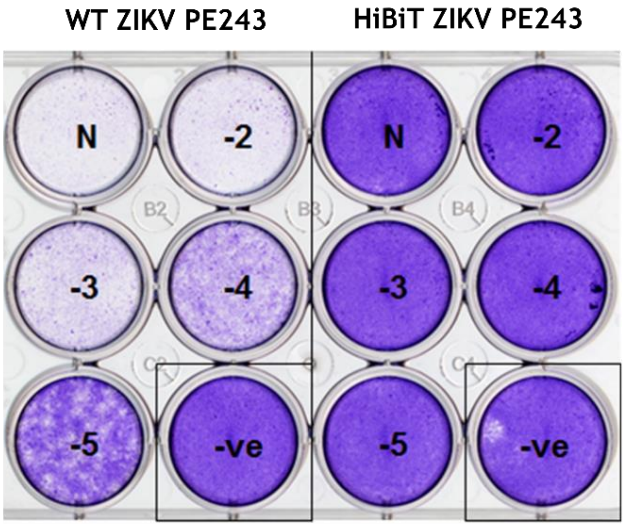
WT ZIKV PE243
HiBiT ZIKV PE243
N
-2
-3
-4
-5
-ve
N
-2
-3
-4
-5
-ve

B)

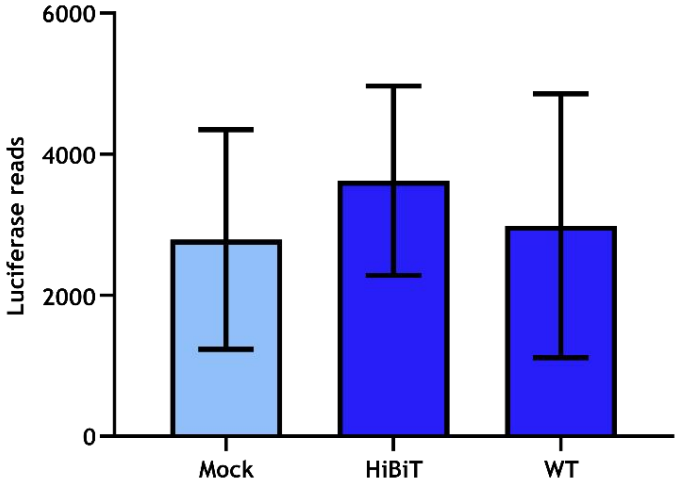
Luciferase reads
6000
4000
2000
0
Mock
HiBiT
WT

C)

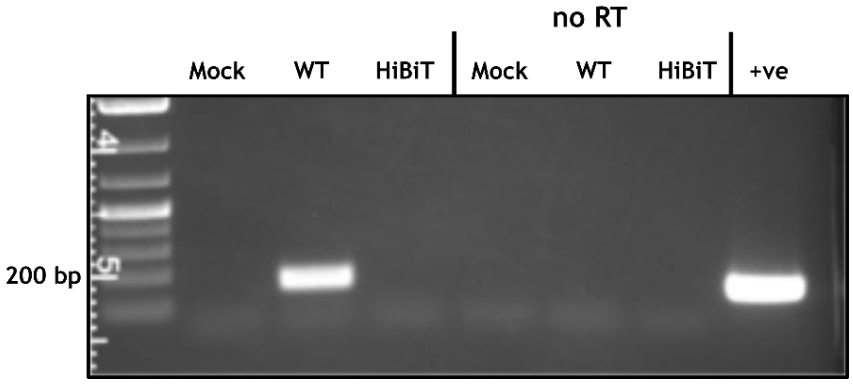
no RT
Mock
WT
HiBiT
Mock
WT
HiBiT
+ve
200 bp

Figure 6-2: WT ZIKV PE243 can be rescued from a CPER reverse genetics system.

A) *CPER reactions were performed to produce annealed WT ZIKV PE243 and HiBiT ZIKV PE243. These constructs were transfected into Vero E6 cells for 5 days and the supernatant was subsequently harvested. The supernatant was serially diluted onto A549 NPro cells and plaque assays were performed, and fold dilutions are indicated.* ***B)*** *5 days after transfection of WT ZIKV PE243 and HiBiT ZIKV PE243 constructs into Vero E6 cells, lysates were harvested, and luciferase levels were measured and plotted relative to values of cells transfected with unannealed segments as a control. Cell lysates were harvested, and luciferase levels measured relative to the siN control.* ***C)*** *RNA was extracted from transfected cells and cDNA was either generated or no reverse transcriptase (RT) step was performed as a control to detect input DNA. cDNA was separated on an agarose gel. A sample of known ZIKV heritage (+ve) was included as a positive control. Error bars represent the standard error the mean.*

Next, I compared the growth kinetics of the rescued WT ZIKV PE243 with the patient isolated PE243. Any discrepancies here might indicate the RG rescued virus would not be suitable for further studies. A549 cells were infected with both viruses at low MOI, and RNA was harvested from cells at regular time intervals before RT-qPCR was performed. These growth curves are shown in Figure 6-3 and show there was no significant difference in the kinetics of viral RNA production. This reverse genetic generated WT ZIKV PE243 virus was therefore suitable for use in future experiments and for future ZIKV studies.

A)

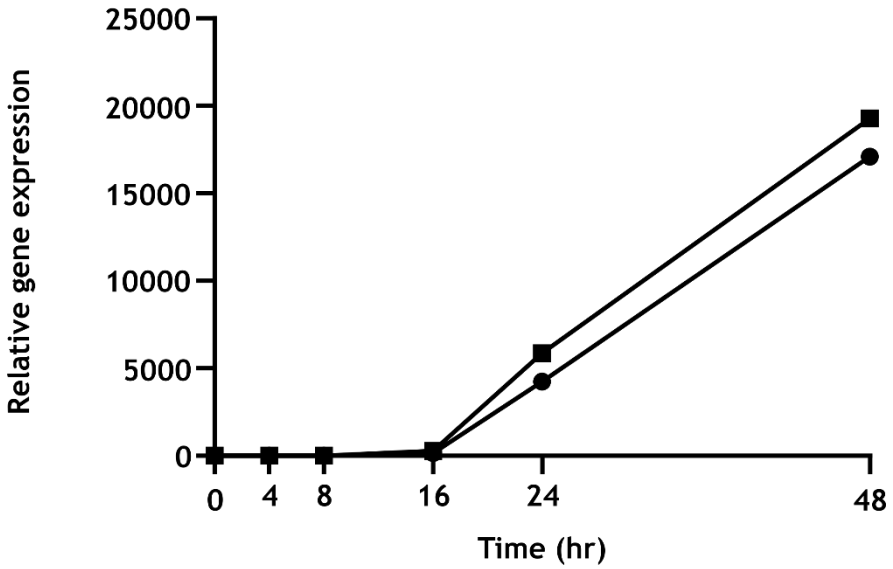

Figure 6-3: ZIKV PE243 from patient isolates or from CPER reverse genetics have similar replication kinetics.

A) *A549 cells were mock-infected or infected with ZIKV PE243 or WT ZIKV PE243 at MOI 0.1 for 48 hrs. RNA was harvested and RT-qPCR was performed. RNA levels were normalised to 0 hr ZIKV PE243 samples and displayed relative to a GAPDH internal control. The experiment was independently repeated in duplicate, and while error bars which represent the standard error the mean were plotted, they are too small to be displayed.*

6.2.2 Generating a GRP78 knockout cell line

A useful tool for further investigating the role of GRP78 in ZIKV infection would be the generation of a GRP78 K/O cell line. This would allow recapitulation of A549 cells with *grp78* mutants, which could lack ATPase activity, lack the ability to bind its partners, or be unable to bind ZIKV E. Therefore, I used a lentivirus to deliver CRISPR/Cas9 constructs to K/O GRP78 in A549 cells (Shalem *et al.*, 2014). Constructs for lentivirus production were kindly provided by Dr Sam Wilson (Centre for Virus Research, Glasgow). Five separate guide strand oligomers (gsRNA) targeting exon 1 of GRP78 were synthesized and ligated into a lentivirus CRISPRv2 plasmid containing a puromycin resistance marker. This plasmid was transfected into HEK293T cells alongside packaging vectors pVSV-G (encoding VSV-G) and pNLGP (Gag and Pol) to produce lentivirus. Lentivirus was harvested and aliquoted from HEK293T cells. A549 cells were seeded and transduced with lentivirus containing the gsRNA against GRP78 (GRP78 1 – 5), as well as an empty control plasmid. Cells were subsequently treated with a puromycin to select for transduced cells before they were serially diluted, and single-cell colonies were selected and amplified. Surviving colonies were assessed for GRP78 expression by immunofluorescence, as shown in Figure 6-4. While the immunofluorescence analysis was inconclusive, promising colonies were further expanded and GRP78 expression was probed by Western blotting (Figure 6-4). From this analysis, no surviving colonies showed a reduction in GRP78 expression when compared to control cells.

A)

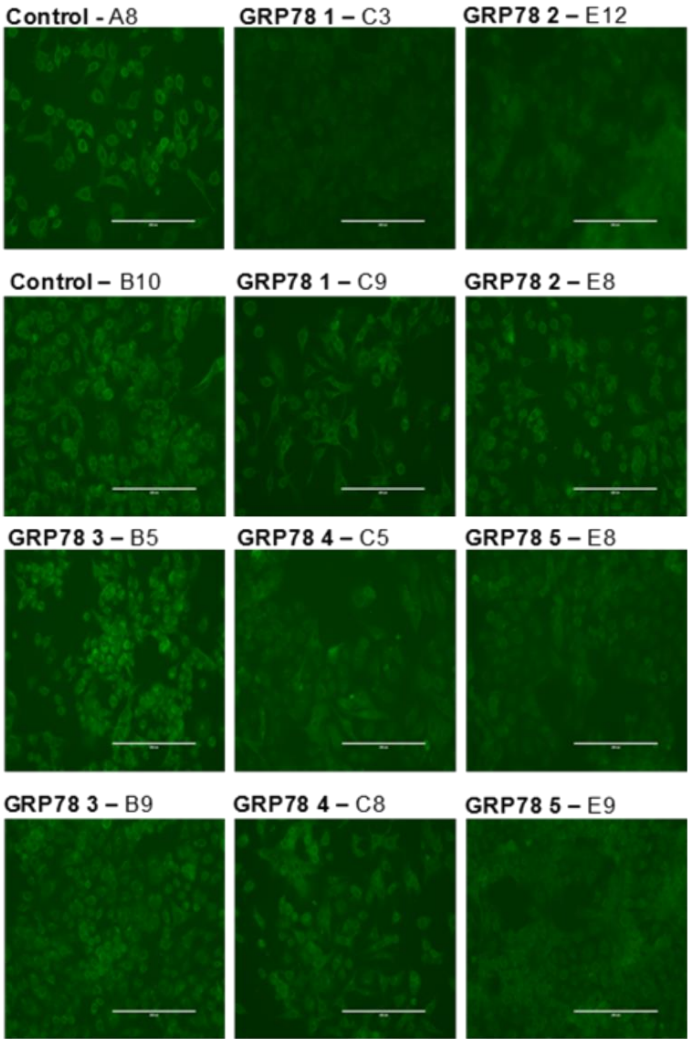
Control - A8
GRP78 1 – C3
GRP78 2 – E12
Control – B10
GRP78 1 – C9
GRP78 2 – E8
GRP78 3 – B5
GRP78 4 – C5
GRP78 5 – E8
GRP78 3 – B9
GRP78 4 – C8
GRP78 5 – E9

B)

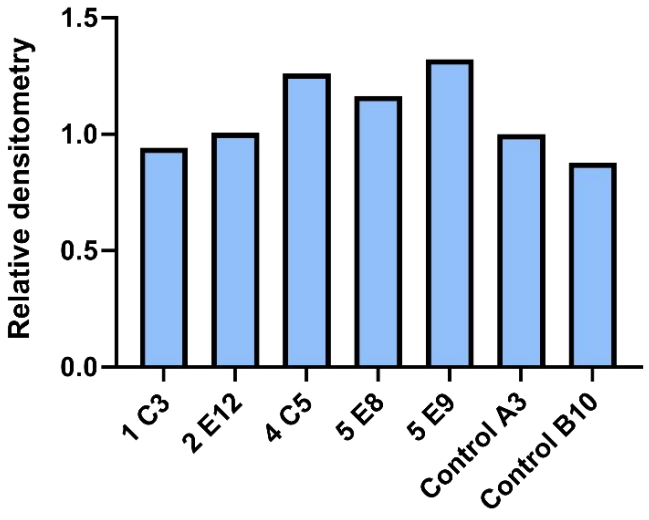
Relative densitometry
1.5
1.0
0.5
0.0
1 C3
2 E12
4 C5
5 E8
5 E9
Control A3
Control B10

Figure 6-4: Lentiviral CRISPR/Cas9 generation of a GRP78 K/O cell line.
A549 cells were transduced with lentivirus containing CRISPR/Cas9 gsRNA against GRP78 or an empty vector control. Following puromycin selection, cells were serially diluted, and single cell colonies were expanded. ***A)*** *Surviving colonies were labelled with GRP78 antibodies.* ***B)*** *Surviving colony cell lysates were harvested and probed for GRP78 expression via Western blot analysis, densitometry of which is shown.*

6.2.3 DnaJC1 is an important factor for ZIKV infection

To further understand the role that GRP78 plays in ZIKV infection, I aimed to investigate whether any of the functional cellular partners of GRP78 were also important using the rescued WT ZIKV PE243 from Chapter 6.2.1. To do this, I first performed a STRING analysis of GRP78 interactor partners, which is shown in Figure 6-5. A subsection of these candidates, which are listed in Figure 6-5, were selected for further analysis by performing a targeted siRNA screen.

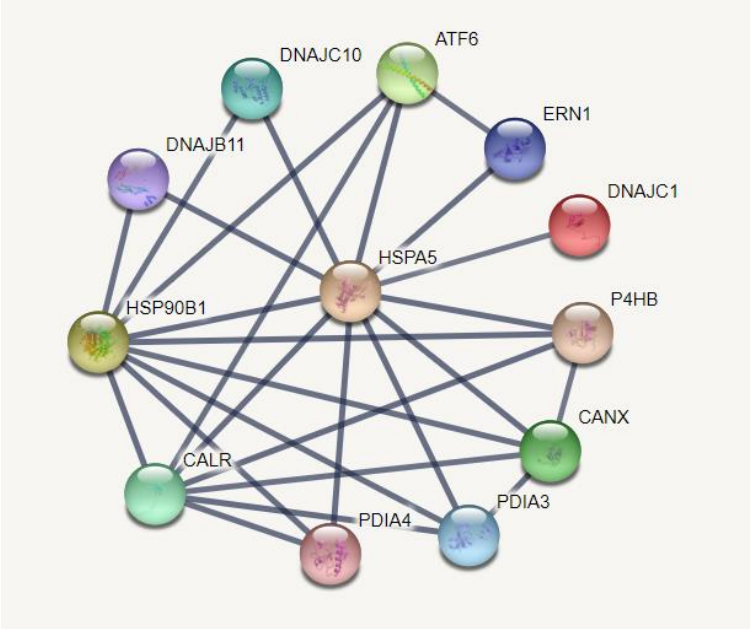

Protein	Function	References
DnaJB11	Cooperates with GRP78 to aid protein folding.	(Shen, Meunier and Hendershot, 2002)
DnaJC1	Coordinates GRP78 to the cell surface and ribosomal exit tunnel. Can halt translation in the absence of GRP78.	(Dudek *et al.*, 2005; Misra *et al.*, 2005; Benedix *et al.*, 2010)
DnaJC10	Works with GRP78 to enhance the ER-associated degradation pathway.	(Hagiwara *et al.*, 2011)
HSP90B1	Shares some function with GRP78 and participates in protein folding, often more selective than GRP78.	(Zhu and Lee, 2015)
ERN1 (IRE1)	Binds GRP78 in inactive state, when released acts to upregulate transcription of UPR members.	(Adams *et al.*, 2019)

Figure 6-5: STRING analysis of GRP78 interactors.

A) *STRING analysis of GRP78 (HSPA5) interactors. Highest confidence (0.900) interactors demonstrated from text-mining and experiments were listed, with edge thickness representing the confidence of an interaction and vertices representing the nodes of the network.* ***B)*** *Selected proteins from the STRING interaction web are listed, with the name and function of these proteins.*

Of the potential GRP78 interactors identified in the STRING analysis, DnaJ heat shock protein family (Hsp40) proteins were heavily represented, and were chosen for further analysis because of the association with both HSP70-mediated protein folding, and a role in some virus infections (Xu, 2018). For example, DnaJB6 interacts with JEV NS3 protein and is inhibitory to infection (Cao *et al.*, 2019). Additionally, both GRP78 and DnaJB11 (which was selected for further analysis in this study) are important for Simian Virus 40 (SV40) infection (Goodwin *et al.*, 2011). Goodwin and colleagues showed that GRP78 binds to SV40 capsid to facilitate exit from the ER, and that this binding was dependent on DnaJB11. In addition to DnaJ proteins, heat-shock protein 90 B1 (HSP90B1) was also selected. HSP90B1, together with GRP78, has been shown to be upregulated in caprine-parainfluenza virus type 3 (CPIV3) infections (Zhong *et al.*, 2019). Finally, endoplasmic reticulum to nucleus signaling 1 (ERN1), also known as IRE1, was selected. IRE1 has previously been shown to be upregulated during ZIKV infection of neural cells, and the UPR generally has been shown to be activated as a result of ZIKV infection (Tan *et al.*, 2018). Despite this, in Chapter 5.2.2 I described how small-molecule inhibitors of the GRP78-mediated UPR had no effect on ZIKV infection in A549 cells, and so I aimed to investigate the role of IRE1 further. To explore the role of the candidates listed in Figure 6-5, I performed an siRNA screen.

A549 cells were transfected with siRNA against the candidate interactors, with siN and siG present as a negative and positive control, respectively. Following, A549 cells were infected at a low MOI for 48 hrs with WT ZIKV PE243 before RNA was harvested from the cells. RT-qPCR was performed on these samples and viral RNA was measured relative to the siN sample and normalised to GAPDH levels (Figure 6-6). This analysis showed that silencing of DnaJC1 significantly reduced viral RNA production in a multi-cycle, low MOI infection. Aside from silencing of DnaJC1 (and the GRP78 control) no other significant effects were observed. This screen was also conducted with ZIKV Nanoluc infection, and DnaJC1 silencing was found to significantly reduce viral luciferase readings relative to the siN control sample. Similar to the results described in Chapter 4, ZIKV Nanoluc was not as sensitive to

changes in viral replication as a WT virus is. In this case, WT ZIKV PE2434 RNA levels were reduced by ~65% in siDnaJC1 compared to the siN control, whereas nanoluciferase readings reduced by ~50% when making the same comparison.

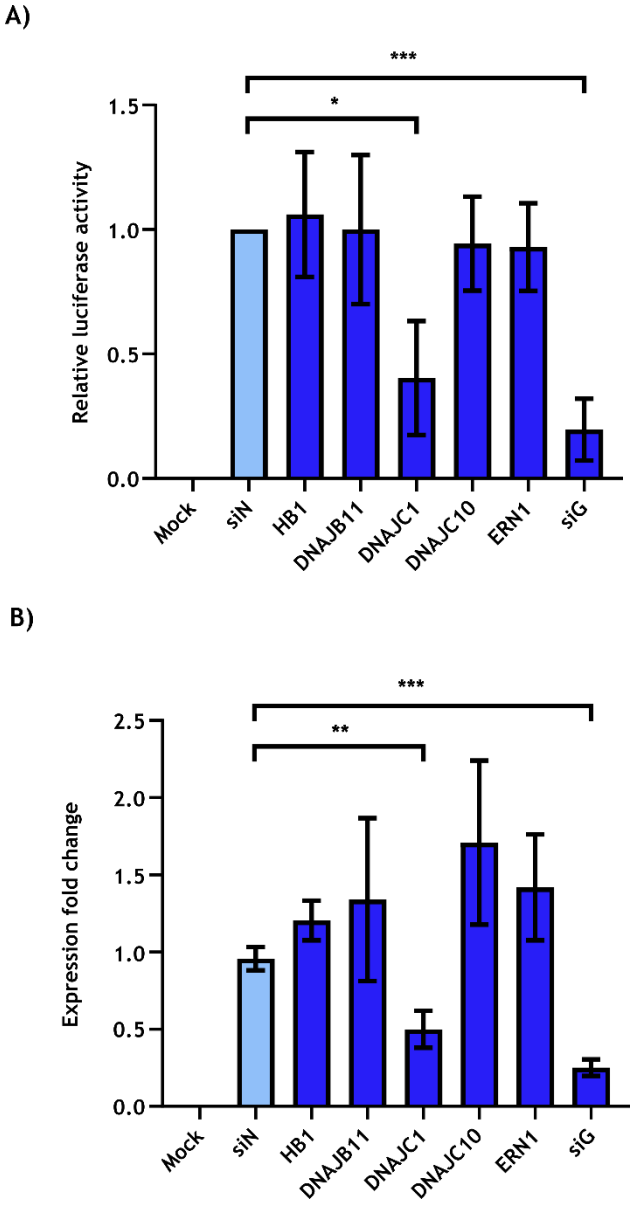

Figure 6-6: siRNA screen of GRP78 interactors reveals DnaJC1 is a pro-ZIKV factor.

A549 cells were treated with siRNA against identified GRP78 interactors. Following, cells were infected with either WT ZIKV PE243 or ZIKV Nanoluc at MOI 0.1 for 48 hrs. ***A)*** *RNA was harvested, and RT-qPCR was performed to measure viral RNA. Viral RNA levels are displayed relative to the siN control and are normalised to GAPDH levels.* ***B)*** *Cell lysates were harvested, and luciferase levels measured relative to the siN control. Triplicate independent repeats were performed. Error bars represent the standard error the mean. An unpaired Student's t-test with Welch's correction was used to determine statistical significance where n.s = not significant, * p-value < 0.05, ** p-value < 0.01.*

These results indicated that DnaJC1 was a pro-viral factor. DnaJC1, also known as human tumour cell DnaJ-like protein 1 (HTJ1) or ER j domain protein 1 (ERdj1) is an accessory protein and co-chaperone for GRP78. The mouse homolog of DnaJC1, murine tumour cell DnaJ-like protein 1 (MTJ1) has been shown to interact with GRP78 and facilitate the migration of GRP78 to the plasma membrane (Misra *et al.*, 2005). Additionally, DnaJC1 has been shown to recruit GRP78 to the ribosome exit tunnel. Of note, in the absence of GRP78, DnaJC1 can bind to the ribosome and inhibit translation (Dudek *et al.*, 2005; Benedix *et al.*, 2010). Therefore, DnaJC1 is implicated in the localisation of GRP78 and the regulation of translation. As such, and because GRP78 seems to play an important role in viral translation and relocalised during infection (Chapter 5.2.5, Chapter 5.2.1), DnaJC1 presented an attractive target for further study.

I therefore investigated whether siRNA mediated knockdown of DnaJC1 could produce a similar phenotype as seen following GRP78 depletion. Of interest was the effect of DnaJC1 on the localisation of viral dsRNA. With that in mind, A549 cells seeded on coverslips were treated with siN or siRNA against DnaJC1 (siDnaJC1) and infected with WT ZIKV PE243. These cells were then labelled for DnaJC1 or dsRNA and stained with DAPI (Figure 6-7). This showed that following DnaJC1 depletion there was no change in dsRNA localisation, implying that DnaJC1 may have a mechanism of action in ZIKV independent of GRP78. Further work would be needed to dissect this phenotype further.

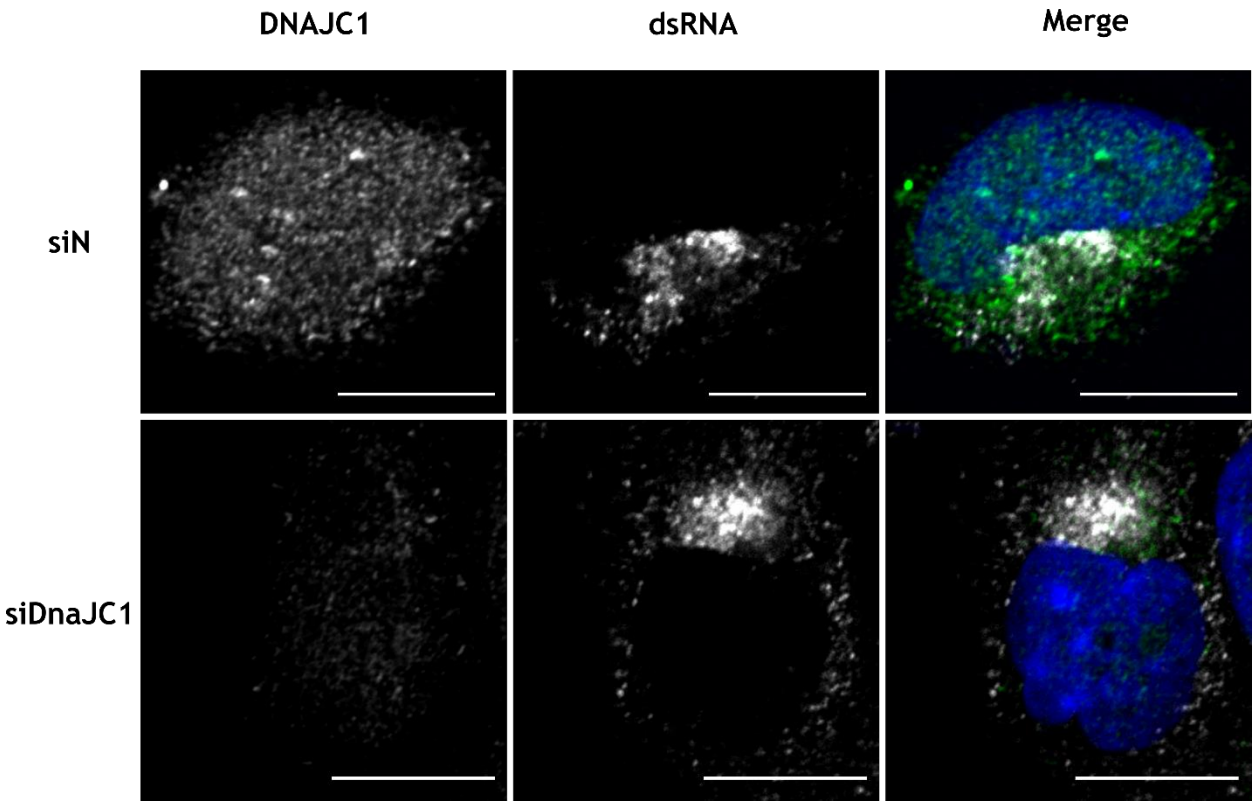

Figure 6-7: DnaJC1 depletion does not affect dsRNA localisation.

Cells were treated with siN or siDnaJC1 and infected with WT ZIKV PE243. Cells were labelled for DnaJC1 (green), dsRNA (white), and stained with DAPI (blue). Error bars represent 10 µm, and images were taken on a ZEISS LSM 710 confocal microscope and represent duplicate repeats.

6.3 Discussion

One aim of this study was to produce a ZIKV PE243 RG system to provide a sensitive virus for experimental screens and to ensure the longevity of a genetically stable PE243 virus. To the best of my knowledge such a system for this strain of ZIKV does not exist. To do this, I employed a CPER system to anneal overlapping segments in a single reaction, a technique that has previously been used for another ZIKV strain (Setoh *et al.*, 2017). Here, I attempted to create both a WT virus and a virus containing a HiBiT moiety in the N-terminus of NS1. The first 29 aa of the N terminus of flavivirus NS1 forms what is known as a ß-roll, a hydrophobic stretch of residues that is needed for viral membrane insertion (Akey *et al.*, 2014; Rastogi, Sharma and Singh, 2016). While clearly important, this region of NS1 has been shown to be able to tolerate the addition of reporter moieties in several flaviviruses. Notably, Sanchez-Velazquez *et al* and Tamura *et al* generated a YFV HiBiT-NS1 virus, and a JEV HiBiT-NS1 virus, respectively. (Sanchez-Velazquez *et al.*, 2020; Syzdykova *et al.*, 2021). Both the YFV and JEV HiBiT-NS1 reporter viruses were produced using the same cloning strategy I employed as described in Chapter 6.2.1. While I successfully rescued and characterised WT ZIKV PE243 using the CPER system, I was unable to rescue the HiBiT virus, which produced neither plaques nor luciferase readings. There could be several potential reasons for this. While similarity exists between *flavivirus* NS1 (full length: ZIKV PE243 and JEV, strain Jaoars982 = 56.82% identity), this increases when looking only at the ß-roll domain (ß-roll domain: ZIKV PE243 and JEV, strain Jaoars982 = 60.71% identity). Chapter 9, Figure 9-2 shows the alignment of several flavivirus NS1 sequences, highlighting that sequence conservation is shared across the *flavivirus* family. Despite this, the ß-roll domain of DENV NS1 has been shown to be intolerant to insertions in a genome-wide mutagenesis study, suggesting that the cloning strategy employed for YFV and JEV may not work with DENV (Eyre *et al.*, 2017). Furthermore, a similar study conducted by Fulton and colleagues, whereby 15 nt insertions were introduced across the ZIKV genome, revealed that while the C-terminal ß-ladder domain of

NS1 could tolerate insertions, the ß-roll domain could not (Fulton *et al.*, 2017). This analysis also revealed that ZIKV E was highly tolerant of insertions, all of which occurred in the ectodomain of E and the majority of which were found in the highly variable region of EDII. Therefore, further attempts to create a ZIKV HiBiT virus should utilise information from studies such as that conducted by Fulton *et al*, and target regions of high plasticity such as EDII or the ß-ladder domain of NS1.

Although I did not manage to rescue a ZIKV HiBiT reporter virus, I did rescue a WT ZIKV PE243. This virus displayed similar replication kinetics to the ZIKV PE243 amplified from a patient isolate and so provides a genetically stable source of virus for future research.

To further aid the investigation into GRP78 and potential interaction partners, I attempted to create a K/O cell line using a CRISPR/Cas9 lentivirus delivery system. 5 different gsRNA were generated, all of which targeted exon 1, to maximise the chances that a functional silencing of *grp78* was achieved. Following transduction of A549 cells with the lentiviruses and subsequent puromycin selection, cells were serially diluted, and 96 colonies were selected and expanded for each gsRNA. While these colonies had survived the initial transduction and puromycin treatment, very few colonies survived further expansion. This suggested that, while cells could survive the transient loss of *grp*78, a persistent loss was ultimately fatal; these cells had not yet been assessed for GRP78 expression at this point and so this suggestion is speculative. The cells that did survive colony expansion were assessed for GRP78 expression via Western blot analysis and immunofluorescence. While immunofluorescent analysis was inconclusive for some colonies, Western blot analysis revealed there was no K/O cell line generated. Surviving colonies therefore most likely had gsRNA integration in sites that provided puromycin resistance but were unable to exert their silencing effect. While data from the first attempt is shown in Chapter 6.2.2, this process was repeated for a second time with similar results.

To the best of my knowledge there is no *grp78* K/O cell line available. There are several mice models, but these are either inducible and not constitutive models, or heterozygous models where only one allele of *grp78* has been silenced (Wang *et al.*, 2010; Ji *et al.*, 2011; Zhu *et al.*, 2013). Indeed, it has been reported that homozygous *grp78* K/O is lethal to embryos (Luo *et al.*, 2006). Therefore, it seems likely that GRP78 function is absolutely essential to the long-term survival of cell culture or developing embryos, and this could explain the lack of cell culture K/O model available. Future attempts to create a *grp78* cell culture model should aim to use a inducible K/O system, such as some recently developed inducible CRISPR/Cas9 based methods (Nishimura and Fukagawa, 2017).

Despite the lack of K/O cell-line, I proceeded in the investigation of GRP78 interactors in the context of a ZIKV infection. I therefore used the WT ZIKV PE243 in a targeted screen of GRP78 interactors to investigate the potential for these to also influence ZIKV infection. A STRING analysis of GRP78 interactors was performed and identified several promising candidates, including a number of DnaJ co-chaperones and members of the UPR response. Silencing of these interactors with specific siRNA revealed that DnaJC1 is a pro-ZIKV factor. In a low MOI ZIKV PE243 multi-cycle infection, DnaJC1 silencing significantly reduced viral RNA production. Also, DnaJC1 silencing reduced luciferase production of a ZIKV Nanoluc reporter virus, though similar to the results seen in Chapter 4.2.2, luciferase measurements from the Nanoluc virus seemed to be less sensitive to effects on viral replication than other metrics. Nevertheless, these experiments show that DnaJC1 is a pro-viral factor.

DnaJC1 has been shown to be able to interact with GRP78 and facilitate the localisation of GRP78 to both the plasma membrane and the ribosomal exit tunnel (Dudek *et al.*, 2005; Misra *et al.*, 2005; Benedix *et al.*, 2010). The observation that DnaJC1 is important in GRP78 localisation is therefore intriguing, especially considering the observation that GRP78 relocalises to presumed ZIKV replication factories in infected cells as shown in Chapter 5.2.1 and Chapter 5.2.5. Thus, I thought it was conceivable that DnaJC1 may impart its pro-viral effect in concert

with GRP78. If this were the case, I expected that DnaJC1 silencing may produce a similar phenotype to GRP78 silencing, and that ZIKV dsRNA perinuclear localisation would be disrupted. When I explored this hypothesis, I found that DnaJC1 silencing did not produce the same phenotype as seen for GRP78, suggesting that it may exert its pro-viral effect independent of GRP78 or via another mechanism. Thus, it would be interesting in the future to carry out further experiments on GRP78 interaction partners and on their roles in flavivirus infection.

6.4 Summary

- A CPER-based RG system was used to create a WT PE243 virus.

- A STRING analysis of GRP78 interactors revealed potential targets for a targeted siRNA screen using the RG virus.

- DnaJC1 was identified as a pro-ZIKV factor. The mechanism behind this effect is currently unknown.

Chapter 7. Summary

7.1 General discussion and project outcomes

During this project, I aimed to inform on novel ZIKV-host interactions. As an arbovirus, it is important to investigate ZIKV in both a mammalian and mosquito setting. To do this I planned to use discovery platforms, such as siRNA screens, and data obtained from mass-spec based proteomic approaches, to maximise the chances of success.

The first major aim was to investigate immune and other host factors than can regulate ZIKV infection in *Aedes aegypti* cell culture by utilising a pre-existing siRNA screen (Chapter 4). This siRNA screen consisted of 998 targets potentially involved in the *Aedes aegypti* immune response and other host processes and had previously been designed in the lab. Initially, I characterised a ZIKV Nanoluc virus rescued by use of reverse genetics, with an aim to use it in the siRNA screen (Chapter 4.2.1). From this, I showed that Ago2 silencing did not impact ZIKV replication. This was surprising, as Ago2 has been considered a classical restriction factor for positive sense RNA viruses in arthropod vectors. Additionally, I also showed that PIWI4 silencing did significantly increase luciferase readings of the ZIKV Nanoluc virus, though this was a relatively marginal increase. Both of these findings expand knowledge surrounding the RNAi response of *Aedes aegypti* to ZIKV infection, and have been verified in another study by Varjak *et al* (Varjak, Donald, *et al.*, 2017). In the study by Varjak et al, PIWI4 depletion was seen to reduce ZIKV infectious particle release by ~4 fold, substantially higher than I observed when using the Nanoluc expressing reporter. Retrospectively, this was perhaps the first indication that ZIKV Nanoluc did not provide enough sensitivity for use in a screen.

Nevertheless, following the characterisation of ZIKV Nanoluc and the establishment of a positive control, I conducted the siRNA screen (Chapter 4.2.2). Here, I identified several potential hits that were conserved across 2 repeats of the screen, though none of which were conserved in all 3. I therefore selected all hits which were found in 2 screens, and trended in the same direction in the third, for further analysis. These genes were depleted with specific dsRNA, and semi-quantitative analysis of cellular RNA levels revealed that these successfully depleted the targets. Despite this, only knockdown of PIWI4, which was included as a positive control and was not identified in the screen despite its inclusion, significantly changed ZIKV Nanoluc levels. This indicated that none of the hits from the screen regulate ZIKV infection to a significant degree.

Concurrent with this investigation, I attempted to uncover the nature of the interaction between GRP78 and ZIKV E. A previous mass-spec based proteomic study conducted by Carolina Ramírez-Santana (Center for Autoimmune Diseases Research-CREA, School of Medicine and Health Sciences, Universidad del Rosario, 110010 Bogotá, Colombia) had identified this potential interaction in A549 cells (Chapter 5). I initially verified this interaction by co-immunoprecipitating ZIKV E and probing for GRP78 in mock-infected and infected cells. Additionally, I showed that GRP78 relocalises to sites co-incident with ZIKV E staining during infection (Chapter 5.2.1). Of importance to a study which takes the viral vector and host into account, GRP78 was found to similarly interact with ZIKV E in mosquito cells (Chapter 5.2.6).

The next step I took was to investigate the functional role of GRP78 during ZIKV infection. Small-molecule inhibitors of GRP78-mediated stress response did not inhibit ZIKV infection, although EGCG was seen to inhibit ZIKV infection most likely through direct action on the virion (Chapter 5.2.2 and Chapter 5.2.3). This finding has been independently verified in other studies and may present an opportunity for devising a therapeutic intervention for ZIKV infection (Carneiro *et al.*, 2016; Sharma *et al.*, 2017).

While inhibition of the GRP78-mediated stress responses did not impact ZIKV infection, siRNA mediated depletion of GRP78 significantly reduced ZIKV replication. The mechanism behind the pro-viral function of GRP78 was thoroughly dissected by taking each stage of infection in turn. Entry, RNA replication, and egress of ZIKV was not affected by GRP78 depletion, but there was a significant reduction in viral protein levels (Chapter 5.2.4). These results are largely in agreement with a study subsequently published by Khongwichit *et al* (Khongwichit *et al.*, 2021). The reduction in viral protein expression was shown to be specific to ZIKV, as production of a firefly luciferase reporter under a CMV promoter was unaffected by GRP78 knockdown (Chapter 5.2.5).

A particularly interesting observation was that GRP78 depletion may relieve the restriction of host translation as seen in ZIKV infected cells, implying that GRP78 is required by ZIKV to co-opt cellular translational machinery. However, the reduction in Firefly levels could be due to a reduction in mRNA transcription or export, and an alternative method of measuring protein production should be used to confirm this. Further , I observed that viral dsRNA (which is thought to localise to viral replication factories) tightly clustered to a perinuclear site in infected cells, and that this localisation is disrupted following GRP78 depletion (Chapter 5.2.5). Both findings suggest that GRP78 is instrumental in organising viral translation and sheds light on the replication factory formation process, though the exact mechanisms underpinning these data needs to be elucidated.

To further explore the role of GRP78 in ZIKV infection, I decided to perform a screen of known GRP78 interactors identified in a STRING analysis. Prior to this, as ZIKV Nanoluc had proven to be less than ideal for sensitive screen experiments, and to guarantee a genetically stable supply of ZIKV, I endeavored to create a PE243 reverse genetic system. I successfully used a CPER-based system to recreate WT ZIKV PE243 (Chapter 6.2.1). This is an important asset for future ZIKV research, and I used this virus to identify DnaJC1 as important pro-ZIKV factor (Chapter 6.2.3). Whether DnaJC1 acts cooperatively with GRP78 to influence ZIKV infection, or whether it is independent of GRP78 remains to be discovered.

Nevertheless, to the best of my knowledge this is the first evidence that links DnaJC1 to a viral infection.

7.2 Future Studies

Despite the decline of the South American ZIKV epidemic over the last few years, the threat posed by a re-occurrence of ZIKV disease has not been eliminated. The expansion of competent mosquito vectors to naïve host populations, as well as the lack of therapeutic interventions to prevent or treat ZIKV disease means it is imperative to further delineate vital virus-host interactions.

To that end, this study uncovered vital ZIKV host factors, namely GRP78 and DnaJC1, developed a reverse genetic system to facilitate ZIKV research, and shed light on the mosquito RNAi response to ZIKV infection. While important findings, there are several ways in which these discoveries could be expanded on.

My work here validated the interaction of ZIKV E and GRP78 and uncovered a mechanistic relationship between them. Importantly, several other putative interactors of ZIKV E were discovered in the initial proteomics experiment (Table 5-1). Some of these interactors, such as OAS, have been implicated in other virus infections and are therefore ideal candidates for further study (Yakub *et al.*, 2005). For these studies, a similar experimental flow as has been described in Chapter 5 could be utilised.

With regards to GRP78, there are still several unanswered questions. These include:

- How is the interaction between GRP78 and ZIKV E functionally important?

While GRP78 is clearly important for ZIKV infection, whether this is dependent on a physical interaction with E was not fully assessed. It is entirely possible that mutations in either GRP78 or E which abrogate their interaction could replicate

the phenotype seen after siG treatment. Conversely, the interaction between them could be coincidental and not important in the context of infection. The predicted binding site between E and GRP78 has been computationally modelled by Elfiky *et al*, and mutations to implicated residues in ZIKV E could be introduced using the WT ZIKV PE243 RG system described in Chapter 6.2.1 (Elfiky and Ibrahim, 2020). Alternatively, mutations in the relevant residues in GRP78 could be made and these constructs could be introduced to a (conditionally) GRP78 K/O cell line if one can be successfully produced.

- How does GRP78 hijack host translational machinery and coordinate viral replication factory localisation?

As shown in Chapter 5.2.5, GRP78 depletion may relieve a restriction in host translation that usually occurs following ZIKV infection. This result implied that GRP78 is required to facilitate viral requisitioning of host translational machinery. Additionally, I showed that GRP78 depletion resulted in the dispersion of viral dsRNA (stained as a proxy for replication factories), implying that GRP78 could organise or impact their localisation. Whether these phenotypes are linked was not discovered in this investigation. One possibility could be that GRP78 is required to coordinate replication factory localisation, without which ZIKV does not have efficient access to host translational machinery, reducing the restriction to host translation. Further work should look to investigate this prospect. Through the use of electron microscopy, the structure of these replication factories could be examined in more detail as has been previously described earlier (Cortese *et al.*, 2017).

- Does DnaJC1 work cooperatively with GRP78 to regulate ZIKV infection?

While DnaJC1 was shown to be important for ZIKV infection, I did not establish whether it coordinated with GRP78 to achieve this phenotype. Considering the clear link between GRP78 and ZIKV translation regulation, and considering the regulation of GRP78 localisation to ribosomes by DnaJC1, it seems plausible that

some aspect of this relationship is important for ZIKV translation (Dudek *et al.*, 2005). Despite this possibility, DnaJC1 silencing was not seen to disrupt viral replication factory localisation as GRP78 silencing did (Chapter 6.2.3). Nevertheless, DnaJC1 certainly represents a promising target for further study, and together with more research into GRP78, could inform on the regulation of ZIKV translation.

- Could a GRP78 knockout cell line be produced?

In Chapter 6.2.2, I attempted to create a GRP78 K/O A549 cell line using a lentivirus delivered CRISPR/Cas9 system. Despite several attempts and the rescue of puromycin resistant colonies, no GRP78 K/O cells were produced. This may not be entirely surprising, as to the best of my knowledge there is no K/O cell line available and only inducible or heterozygous K/O animal models exist (Zhu *et al.*, 2013). Therefore, future attempts to create such a cell line should focus on using conditional K/O systems (Nishimura and Fukagawa, 2017).

One of the key outcomes of this study was the production of a ZIKV PE243 reverse genetics system. I also attempted to create a reporter virus variant encoding a HiBit moiety, however the choice of insertion position, while viable for related viruses like YFV, did not support ZIKV replication (Sanchez-Velazquez *et al.*, 2020). Studies have highlighted regions in the ZIKV genome that are more tolerant to insertions, and these should be utilised for the creation of a HiBiT ZIKV which may be more suitable for use in sensitive screens. With this virus, a modified siRNA screen (like the one described in Chapter 4.2.2) with the inclusion of siN and positive controls on each plate could be performed.

7.3 Key outcomes

ZIKV still poses a significant threat to human health, and as a newly emerging virus, fundamental research is still required to elucidate vital host interactions and generate research tools. This study achieved several key outcomes:

- Ago2 does not regulate ZIKV infection, but PIWI4 does.
- ZIKV entry can be inhibited with the small-molecule inhibitor, EGCG.
- GRP78 is an important host interactor for ZIKV and may be required to hijack host translational machinery.
- DnaJC1, a GRP78 interaction partner, is also important for ZIKV infection.
- An easy-to-handle reverse genetics system was adopted to facilitate future ZIKV research.

Chapter 8. References

Abbink, P., Stephenson, K. E. and Barouch, D. H. (2018) 'Zika virus vaccines', *Nature Reviews Microbiology*. Nature Publishing Group, pp. 594–600. doi: 10.1038/s41579-018-0039-7.

Adams, A. P. *et al.* (2013) 'Pathogenesis of modoc virus (Flaviviridae; Flavivirus) in persistently infected hamsters', *American Journal of Tropical Medicine and Hygiene*. The American Society of Tropical Medicine and Hygiene, 88(3), pp. 455–460. doi: 10.4269/ajtmh.12-0110.

Adams, C. J. *et al.* (2019) 'Structure and molecular mechanism of ER stress signaling by the unfolded protein response signal activator IRE1', *Frontiers in Molecular Biosciences*. Frontiers Media S.A., p. 11. doi: 10.3389/fmolb.2019.00011.

Ades, A. E. *et al.* (2020) 'Vertical transmission of Zika virus and its outcomes: a Bayesian synthesis of prospective studies', *The Lancet Infectious Diseases*. Lancet Publishing Group, 0(0). doi: 10.1016/S1473-3099(20)30432-1.

Agrelli, A. *et al.* (2019) 'ZIKA virus entry mechanisms in human cells', *Infection, Genetics and Evolution*. Elsevier B.V., pp. 22–29. doi: 10.1016/j.meegid.2019.01.018.

Akey, D. L. *et al.* (2014) 'Flavivirus NS1 structures reveal surfaces for associations with membranes and the immune system', *Science*. American Association for the Advancement of Science, 343(6173), pp. 881–885. doi: 10.1126/science.1247749.

Akey, D. L. *et al.* (2015) 'Structure-guided insights on the role of NS1 in flavivirus infection', *BioEssays*. John Wiley and Sons Inc., 37(5), pp. 489–494. doi:

10.1002/bies.201400182.

Alfano, C. *et al.* (2019) 'The unfolded protein response: A key player in zika virus-associated congenital microcephaly', *Frontiers in Cellular Neuroscience*. Frontiers Media S.A., 13. doi: 10.3389/fncel.2019.00094.

Allam, L. *et al.* (2020) 'Targeting the GRP78-Dependant SARS-CoV-2 Cell Entry by Peptides and Small Molecules', *Bioinformatics and Biology Insights*. SAGE Publications Inc., 14, p. 117793222096550. doi: 10.1177/1177932220965505.

Alvarez, D. E. *et al.* (2005) 'Long-Range RNA-RNA Interactions Circularize the Dengue Virus Genome', *Journal of Virology*. American Society for Microbiology, 79(11), pp. 6631–6643. doi: 10.1128/jvi.79.11.6631-6643.2005.

Anderson, K., Stott, E. J. and Wertz, G. W. (1992) 'Intracellular processing of the human respiratory syncytial virus fusion glycoprotein: Amino acid substitutions affecting folding, transport and cleavage', *Journal of General Virology*, 73(5), pp. 1177–1188. doi: 10.1099/0022-1317-73-5-1177.

Angleró-Rodríguez, Y. I. *et al.* (2017) 'Aedes aegypti molecular responses to Zika Virus: Modulation of infection by the toll and Jak/Stat immune pathways and virus host factors', *Frontiers in Microbiology*. Frontiers Media S.A., 8(OCT). doi: 10.3389/fmicb.2017.02050.

Apte-Sengupta, S., Sirohi, D. and Kuhn, R. J. (2014) 'Coupling of replication and assembly in flaviviruses', *Current Opinion in Virology*. Elsevier B.V., pp. 134–142. doi: 10.1016/j.coviro.2014.09.020.

Aragao, M. F. V. V. *et al.* (2017) 'Nonmicrocephalic infants with congenital zika syndrome suspected only after neuroimaging evaluation compared with those with microcephaly at birth and postnatally: How large is the Zika virus "iceberg"?',

American Journal of Neuroradiology. American Society of Neuroradiology, 38(7), pp. 1427–1434. doi: 10.3174/ajnr.A5216.

Arakawa, M. and Morita, E. (2019) 'Flavivirus replication organelle biogenesis in the endoplasmic reticulum: Comparison with other single-stranded positive-sense RNA viruses', *International Journal of Molecular Sciences*. MDPI AG, 20(9). doi: 10.3390/ijms20092336.

Assenberg, R. *et al*. (2009) 'Crystal Structure of a Novel Conformational State of the Flavivirus NS3 Protein: Implications for Polyprotein Processing and Viral Replication', *Journal of Virology*. American Society for Microbiology, 83(24), pp. 12895–12906. doi: 10.1128/jvi.00942-09.

Ávila-Pérez, G. *et al*. (2018) 'Reverse genetic approaches for the generation of recombinant Zika virus', *Viruses*. MDPI AG. doi: 10.3390/v10110597.

Ávila-Pérez, G. *et al*. (2019) 'A natural polymorphism in Zika virus NS2A protein responsible of virulence in mice', *Scientific Reports*. Nature Research, 9(1), pp. 1–17. doi: 10.1038/s41598-019-56291-4.

Awad, W. *et al*. (2008) 'BiP mutants that are unable to interact with endoplasmic reticulum DnaJ proteins provide insights into interdomain interactions in BiP', *Proceedings of the National Academy of Sciences of the United States of America*. National Academy of Sciences, 105(4), pp. 1164–1169. doi: 10.1073/pnas.0702132105.

Barba-Spaeth, G. *et al*. (2016) 'Structural basis of potent Zika-dengue virus antibody cross-neutralization', *Nature*. Nature Publishing Group, 536(7614), pp. 48–53. doi: 10.1038/nature18938.

Barnard, T. R. *et al*. (2020) 'Molecular Determinants of Flavivirus Virion Assembly'.

doi: 10.1016/j.tibs.2020.12.007.

Barrett, A. D. T. (2014) ‘Economic burden of West Nile virus in the United States’, *American Journal of Tropical Medicine and Hygiene*. American Society of Tropical Medicine and Hygiene, pp. 389–390. doi: 10.4269/ajtmh.14-0009.

Barzon, L. *et al.* (2018) ‘Virus and Antibody Dynamics in Travelers With Acute Zika Virus Infection’, *Clinical Infectious Diseases*. Oxford University Press, 66(8), pp. 1173–1180. doi: 10.1093/cid/cix967.

Baumeister, P. *et al.* (2005) ‘Endoplasmic Reticulum Stress Induction of the Grp78/BiP Promoter: Activating Mechanisms Mediated by YY1 and Its Interactive Chromatin Modifiers’, *Molecular and Cellular Biology*. American Society for Microbiology, 25(11), pp. 4529–4540. doi: 10.1128/mcb.25.11.4529-4540.2005.

Bayer, A. *et al.* (2016) ‘Type III Interferons Produced by Human Placental Trophoblasts Confer Protection against Zika Virus Infection’, *Cell Host and Microbe*. Cell Press, 19(5), pp. 705–712. doi: 10.1016/j.chom.2016.03.008.

Baz, M. and Boivin, G. (2019) ‘Antiviral agents in development for zika virus infections’, *Pharmaceuticals*. MDPI AG, 12(3), p. 101. doi: 10.3390/ph12030101.

Benedix, J. *et al.* (2010) ‘BiP modulates the affinity of its co-chaperone ERj1 for ribosomes’, *Journal of Biological Chemistry*. Elsevier, 285(47), pp. 36427–36433. doi: 10.1074/jbc.M110.143263.

Berg, M. G. *et al.* (2015) ‘Discovery of a Novel Human Pegivirus in Blood Associated with Hepatitis C Virus Co-Infection’, *PLOS Pathogens*. Edited by C. Drosten. Public Library of Science, 11(12), p. e1005325. doi: 10.1371/journal.ppat.1005325.

Berthet, N. *et al.* (2014) ‘Molecular characterization of three zika flaviviruses

obtained from sylvatic mosquitoes in the Central African Republic', *Vector-Borne and Zoonotic Diseases*. Mary Ann Liebert Inc., 14(12), pp. 862–865. doi: 10.1089/vbz.2014.1607.

Besnard, M. *et al*. (2014) 'Evidence of perinatal transmission of Zika virus, French Polynesia, December 2013 and February 2014', *Eurosurveillance*. European Centre for Disease Prevention and Control (ECDC), 19(13), p. 20751. doi: 10.2807/1560-7917.ES2014.19.13.20751.

Best, S. M. (2017) 'The Many Faces of the Flavivirus NS5 Protein in Antagonism of Type I Interferon Signaling', *Journal of Virology*. American Society for Microbiology, 91(3). doi: 10.1128/jvi.01970-16.

Bhatt, S. *et al*. (2013) 'The global distribution and burden of dengue', *Nature*. Nature Publishing Group, 496(7446), pp. 504–507. doi: 10.1038/nature12060.

Blitvich, B. J. and Firth, A. E. (2015) 'Insect-specific flaviviruses: A systematic review of their discovery, host range, mode of transmission, superinfection exclusion potential and genomic organization', *Viruses*. MDPI AG, pp. 1927–1959. doi: 10.3390/v7041927.

Bonenfant, G. *et al*. (2019) 'Zika Virus Subverts Stress Granules To Promote and Restrict Viral Gene Expression', *Journal of Virology*. American Society for Microbiology, 93(12). doi: 10.1128/jvi.00520-19.

Booth, L. *et al*. (2015) 'GRP78/BiP/HSPA5/Dna K is a universal therapeutic target for human disease', *Journal of Cellular Physiology*. Wiley-Liss Inc., 230(7), pp. 1661–1676. doi: 10.1002/jcp.24919.

Brady, O. J. and Hay, S. I. (2020) 'The global expansion of dengue: How aedes aegypti mosquitoes enabled the first pandemic arbovirus', *Annual Review of*

Entomology. Annual Reviews Inc., pp. 191–208. doi: 10.1146/annurev-ento-011019-024918.

Brecher, M. *et al*. (2017) 'A conformational switch high-throughput screening assay and allosteric inhibition of the flavivirus NS2B-NS3 protease', *PLOS Pathogens*. Edited by T. C. Pierson. Public Library of Science, 13(5), p. e1006411. doi: 10.1371/journal.ppat.1006411.

Brocchieri, L., Conway De Macario, E. and Macario, A. J. L. (2008) 'Hsp70 genes in the human genome: Conservation and differentiation patterns predict a wide array of overlapping and specialized functions', *BMC Evolutionary Biology*. BioMed Central, 8(1), p. 19. doi: 10.1186/1471-2148-8-19.

Bryden, S. R. *et al*. (2020) 'Pan-viral protection against arboviruses by activating skin macrophages at the inoculation site', *Science Translational Medicine*. American Association for the Advancement of Science, 12(527), p. 2421. doi: 10.1126/scitranslmed.aax2421.

Buchkovich, N. J. *et al*. (2008) 'Human Cytomegalovirus Specifically Controls the Levels of the Endoplasmic Reticulum Chaperone BiP/GRP78, Which Is Required for Virion Assembly', *Journal of Virology*. American Society for Microbiology, 82(1), pp. 31–39. doi: 10.1128/jvi.01881-07.

Byk, L. A. *et al*. (2016) 'Dengue virus genome uncoating requires ubiquitination', *mBio*. American Society for Microbiology, 7(3), pp. 804–820. doi: 10.1128/mBio.00804-16.

Caine, E. A., Jagger, B. W. and Diamond, M. S. (2018) 'Animal models of zika virus infection during pregnancy', *Viruses*. MDPI AG. doi: 10.3390/v10110598.

Calfon, M. *et al*. (2002) 'IRE1 couples endoplasmic reticulum load to secretory

capacity by processing the XBP-1 mRNA', *Nature*. Nature, 415(6867), pp. 92–96. doi: 10.1038/415092a.

Cao, B. *et al*. (2017) 'Inhibition of autophagy limits vertical transmission of Zika virus in pregnant mice', *Journal of Experimental Medicine*. Rockefeller University Press, 214(8), pp. 2303–2313. doi: 10.1084/jem.20170957.

Cao, B., Diamond, M. S. and Mysorekar, I. U. (2017) 'Maternal-fetal transmission of zika virus: Routes and signals for infection', *Journal of Interferon and Cytokine Research*. Mary Ann Liebert Inc., pp. 287–294. doi: 10.1089/jir.2017.0011.

Cao, Y.-Q. *et al*. (2019) 'Hsp40 Protein DNAJB6 Interacts with Viral NS3 and Inhibits the Replication of the Japanese Encephalitis Virus', *International Journal of Molecular Sciences*. MDPI AG, 20(22), p. 5719. doi: 10.3390/ijms20225719.

Capasso, A. *et al*. (2019) 'Incidence of Guillain-Barré Syndrome (GBS) in Latin America and the Caribbean before and during the 2015–2016 Zika virus epidemic: A systematic review and meta-analysis', *PLOS Neglected Tropical Diseases*. Edited by D. Harley. Public Library of Science, 13(8), p. e0007622. doi: 10.1371/journal.pntd.0007622.

Capitani, M. and Sallese, M. (2009) 'The KDEL receptor: New functions for an old protein', *FEBS Letters*. No longer published by Elsevier, pp. 3863–3871. doi: 10.1016/j.febslet.2009.10.053.

Carbaugh, D. L. and Lazear, H. M. (2020) 'Flavivirus Envelope Protein Glycosylation: Impacts on Viral Infection and Pathogenesis', *Journal of Virology*. American Society for Microbiology, 94(11). doi: 10.1128/jvi.00104-20.

Carneiro, B. M. *et al*. (2016) 'The green tea molecule EGCG inhibits Zika virus entry', *Virology*, 496, pp. 215–218. doi: 10.1016/j.virol.2016.06.012.

Carthew, R. W. and Sontheimer, E. J. (2009) ‘Origins and Mechanisms of miRNAs and siRNAs’, *Cell*. NIH Public Access, pp. 642–655. doi: 10.1016/j.cell.2009.01.035.

Casas, C. (2017) ‘GRP78 at the centre of the stage in cancer and neuroprotection’, *Frontiers in Neuroscience*. Frontiers Research Foundation, p. 177. doi: 10.3389/fnins.2017.00177.

Cavalcanti, M. G. *et al.* (2017) ‘Zika virus shedding in human milk during lactation: an unlikely source of infection?’, *International Journal of Infectious Diseases*. Elsevier B.V., 57, pp. 70–72. doi: 10.1016/j.ijid.2017.01.042.

Chambers, T. J. *et al.* (1990) ‘Flavivirus Genome Organization, Expression, and Replication’, *Annual Review of Microbiology*. Annual Reviews, 44(1), pp. 649–688. doi: 10.1146/annurev.mi.44.100190.003245.

Chambers, T. J. *et al.* (1993) ‘Mutagenesis of the yellow fever virus NS2B protein: effects on proteolytic processing, NS2B-NS3 complex formation, and viral replication.’, *Journal of Virology*, 67(11).

Chancey, C. *et al.* (2015) ‘The global ecology and epidemiology of west nile virus’, *BioMed Research International*. Hindawi Limited. doi: 10.1155/2015/376230.

Chang, R. Y. *et al.* (2013) ‘Japanese encephalitis virus non-coding RNA inhibits activation of interferon by blocking nuclear translocation of interferon regulatory factor 3’, *Veterinary Microbiology*. Vet Microbiol, 166(1–2), pp. 11–21. doi: 10.1016/j.vetmic.2013.04.026.

Chen, Jian *et al.* (2018) ‘AXL promotes Zika virus infection in astrocytes by antagonizing type i interferon signalling’, *Nature Microbiology*. Nature Publishing Group, 3(3), pp. 302–309. doi: 10.1038/s41564-017-0092-4.

Chen, S. *et al*. (2011) 'Ago-2-Mediated Slicer Activity Is Essential for Anti-Flaviviral Efficacy of RNAi', *PLoS ONE*. Edited by K. T. Jeang. Public Library of Science, 6(11), p. e27551. doi: 10.1371/journal.pone.0027551.

Chen, S. *et al*. (2017) 'Innate immune evasion mediated by flaviviridae non-structural proteins', *Viruses*. MDPI AG. doi: 10.3390/v9100291.

Chen, S. T. *et al*. (2011) 'Targeting C-type lectin for the treatment of flavivirus infections', in *Advances in Experimental Medicine and Biology*. Springer, Boston, MA, pp. 769–776. doi: 10.1007/978-1-4419-7877-6_40.

Chen, W. *et al*. (2008) 'Vimentin is required for dengue virus serotype 2 infection but microtubules are not necessary for this process', *Archives of Virology*. Arch Virol, 153(9), pp. 1777–1781. doi: 10.1007/s00705-008-0183-x.

Chen, Y. and Brandizzi, F. (2013) 'IRE1: ER stress sensor and cell fate executor', *Trends in Cell Biology*. NIH Public Access, pp. 547–555. doi: 10.1016/j.tcb.2013.06.005.

Chouin-Carneiro, T. *et al*. (2020) 'Wolbachia strain wAlbA blocks Zika virus transmission in Aedes aegypti', *Medical and Veterinary Entomology*. Blackwell Publishing Ltd, 34(1), pp. 116–119. doi: 10.1111/mve.12384.

Chu, H. *et al*. (2018) 'Middle East respiratory syndrome coronavirus and bat coronavirus HKU9 both can utilize GRP78 for attachment onto host cells.', *The Journal of biological chemistry*. American Society for Biochemistry and Molecular Biology, 293(30), pp. 11709–11726. doi: 10.1074/jbc.RA118.001897.

Chu, J. J. H. and Ng, M. L. (2004) 'Interaction of West Nile virus with αvβ3 integrin mediates virus entry into cells', *Journal of Biological Chemistry*. JBC Papers in Press, 279(52), pp. 54533–54541. doi: 10.1074/jbc.M410208200.

Ci, Y. *et al*. (2020) 'Zika NS1-induced ER remodeling is essential for viral replication', *Journal of Cell Biology*. Rockefeller University Press, 219(2). doi: 10.1083/jcb.201903062.

Ciota, A. T. *et al*. (2017) 'Effects of Zika virus strain and Aedes mosquito species on vector competence', *Emerging Infectious Diseases*. Centers for Disease Control and Prevention (CDC), 23(7), pp. 1110–1117. doi: 10.3201/eid2307.161633.

Clements, A. N. and Harbach, R. E. (2017) 'History of the discovery of the mode of transmission of yellow fever virus', *Journal of Vector Ecology*. Wiley-Blackwell, 42(2), pp. 208–222. doi: 10.1111/jvec.12261.

Conner, C. *et al*. (2020) 'Cell surface GRP78 promotes stemness in normal and neoplastic cells', *Scientific Reports*. Nature Research, 10(1), p. 3474. doi: 10.1038/s41598-020-60269-y.

Corry, J. *et al*. (2017) 'Organotypic models of type III interferon-mediated protection from Zika virus infections at the maternal–fetal interface', *Proceedings of the National Academy of Sciences of the United States of America*. National Academy of Sciences, 114(35), pp. 9433–9438. doi: 10.1073/pnas.1707513114.

Cortese, M. *et al*. (2017) 'Ultrastructural Characterization of Zika Virus Replication Factories.', *Cell reports*. Elsevier, 18(9), pp. 2113–2123. doi: 10.1016/j.celrep.2017.02.014.

El Costa, H. *et al*. (2016) 'ZIKA virus reveals broad tissue and cell tropism during the first trimester of pregnancy', *Scientific Reports*. Nature Publishing Group, 6(1), pp. 1–9. doi: 10.1038/srep35296.

Costa, L. C. *et al*. (2020) 'New Insights on the Zika Virus Arrival in the Americas and Spatiotemporal Reconstruction of the Epidemic Dynamics in Brazil', *Viruses*.

MDPI AG, 13(1), p. 12. doi: 10.3390/v13010012.

Cowling, V. H. (2010) ‘Regulation of mRNA cap methylation’, *Biochemical Journal*. Portland Press Ltd, pp. 295–302. doi: 10.1042/BJ20091352.

Cox, B. D., Stanton, R. A. and Schinazi, R. F. (2015) ‘Predicting Zika virus structural biology: Challenges and opportunities for intervention’. doi: 10.1177/2040206616653873.

Cunze, S. *et al*. (2019) ‘Vector distribution and transmission risk of the Zika virus in South and Central America’, *PeerJ*. PeerJ Inc., 2019(11). doi: 10.7717/peerj.7920.

Dejnirattisai, W. *et al*. (2016) ‘Dengue virus sero-cross-reactivity drives antibody-dependent enhancement of infection with zika virus’, *Nature Immunology*. Nature Publishing Group, 17(9), pp. 1102–1108. doi: 10.1038/ni.3515.

Delatorre, E., Fernández, J. and Bello, G. (2018) ‘Investigating the role of easter island in migration of Zika virus from south pacific to Americas’, *Emerging Infectious Diseases*. Centers for Disease Control and Prevention (CDC), pp. 2119–2121. doi: 10.3201/eid2411.180586.

Dietrich, I. *et al*. (2017) ‘The Antiviral RNAi Response in Vector and Non-vector Cells against Orthobunyaviruses’, *PLOS Neglected Tropical Diseases*. Edited by D. G. Bausch. Public Library of Science, 11(1), p. e0005272. doi: 10.1371/journal.pntd.0005272.

Diosa-Toro, M. *et al*. (2020) ‘Role of RNA-binding proteins during the late stages of Flavivirus replication cycle’, *Virology Journal*. BioMed Central Ltd., 17(1), pp. 1–14. doi: 10.1186/s12985-020-01329-7.

Dokland, T. *et al*. (2004) 'West Nile virus core protein: Tetramer structure and ribbon formation', *Structure*. Elsevier, 12(7), pp. 1157–1163. doi: 10.1016/j.str.2004.04.024.

Donald, C. L. *et al*. (2016) 'Full Genome Sequence and sfRNA Interferon Antagonist Activity of Zika Virus from Recife, Brazil', *PLOS Neglected Tropical Diseases*. Edited by A. C. Morrison. Lippincott Williams and W, 10(10), p. e0005048. doi: 10.1371/journal.pntd.0005048.

Donnelly, M. L. L. *et al*. (2001) *Printed in Great Britain The ' cleavage ' activities of foot-and-mouth disease virus 2A site-directed mutants and naturally occurring ' 2A-like ' sequences*, *Journal of General Virology*.

Douam, F. and Ploss, A. (2018) 'Yellow Fever Virus: Knowledge Gaps Impeding the Fight Against an Old Foe', *Trends in Microbiology*. Elsevier Ltd, pp. 913–928. doi: 10.1016/j.tim.2018.05.012.

Du, S. *et al*. (2019) 'Aedes mosquitoes acquire and transmit Zika virus by breeding in contaminated aquatic environments', *Nature Communications*. Nature Publishing Group, 10(1). doi: 10.1038/s41467-019-09256-0.

Dudek, J. *et al*. (2005) 'ERj1p has a basic role in protein biogenesis at the endoplasmic reticulum', *Nature Structural and Molecular Biology*. Nature Publishing Group, 12(11), pp. 1008–1014. doi: 10.1038/nsmb1007.

Duffy, M. R. *et al*. (2009) 'Zika Virus Outbreak on Yap Island, Federated States of Micronesia', *New England Journal of Medicine*. Massachusetts Medical Society, 360(24), pp. 2536–2543. doi: 10.1056/nejmoa0805715.

Duggal, N. K. *et al*. (2019) 'Mutations present in a low-passage Zika virus isolate result in attenuated pathogenesis in mice', *Virology*. Academic Press Inc., 530,

pp. 19–26. doi: 10.1016/j.virol.2019.02.004.

Dukhovny, A. *et al*. (2019) 'A CRISPR Activation Screen Identifies Genes That Protect against Zika Virus Infection', *Journal of Virology*. American Society for Microbiology, 93(16). doi: 10.1128/jvi.00211-19.

Duong, V., Dussart, P. and Buchy, P. (2017) 'Zika virus in Asia', *International Journal of Infectious Diseases*. Elsevier B.V., pp. 121–128. doi: 10.1016/j.ijid.2016.11.420.

Edmonds, J. *et al*. (2013) 'A Novel Bacterium-Free Method for Generation of Flavivirus Infectious DNA by Circular Polymerase Extension Reaction Allows Accurate Recapitulation of Viral Heterogeneity', *Journal of Virology*. American Society for Microbiology, 87(4), pp. 2367–2372. doi: 10.1128/jvi.03162-12.

Elfiky, A. A. *et al*. (2020) 'A possible role for GRP78 in cross vaccination against COVID-19'. doi: 10.1016/j.jinf.2020.09.004.

Elfiky, A. A. and Ibrahim, I. M. (2020) 'Zika virus envelope – heat shock protein A5 (GRP78) binding site prediction', *Journal of Biomolecular Structure and Dynamics*. J Biomol Struct Dyn, pp. 1–13. doi: 10.1080/07391102.2020.1784794.

England, C. G., Ehlerding, E. B. and Cai, W. (2016) 'NanoLuc: A Small Luciferase Is Brightening Up the Field of Bioluminescence', *Bioconjugate Chemistry*. American Chemical Society, pp. 1175–1187. doi: 10.1021/acs.bioconjchem.6b00112.

Esswein, S. R. *et al*. (2020) 'Structural basis for Zika envelope domain III recognition by a germline version of a recurrent neutralizing antibody', *Proceedings of the National Academy of Sciences of the United States of America*. National Academy of Sciences, 117(18), pp. 9865–9875. doi:

10.1073/pnas.1919269117.

Evans, B. R. *et al.* (2019) 'Transgenic Aedes aegypti Mosquitoes Transfer Genes into a Natural Population', *Scientific Reports*. Nature Publishing Group, 9(1), pp. 1–6. doi: 10.1038/s41598-019-49660-6.

Eyre, N. S. *et al.* (2017) 'Genome-Wide Mutagenesis of Dengue Virus Reveals Plasticity of the NS1 Protein and Enables Generation of Infectious Tagged Reporter Viruses', *Journal of Virology*. American Society for Microbiology, 91(23). doi: 10.1128/jvi.01455-17.

Fajardo, T. *et al.* (2020) 'The flavivirus polymerase NS5 regulates translation of viral genomic RNA', *Nucleic acids research*. NLM (Medline), 48(9), pp. 5081–5093. doi: 10.1093/nar/gkaa242.

Falgout, B., Chanock, R. and Lai, C. J. (1989) 'Proper processing of dengue virus nonstructural glycoprotein NS1 requires the N-terminal hydrophobic signal sequence and the downstream nonstructural protein NS2a.', *Journal of Virology*. American Society for Microbiology, 63(5), pp. 1852–1860. doi: 10.1128/jvi.63.5.1852-1860.1989.

Falgout, B. and Markoff, L. (1995) 'Evidence that flavivirus NS1-NS2A cleavage is mediated by a membrane-bound host protease in the endoplasmic reticulum.', *Journal of virology*. American Society for Microbiology, 69(11), pp. 7232–7243. doi: 10.1128/jvi.69.11.7232-7243.1995.

Fan, W. *et al.* (2017) 'Integrin αvß3 promotes infection by Japanese encephalitis virus', *Research in Veterinary Science*. Elsevier B.V., 111, pp. 67–74. doi: 10.1016/j.rvsc.2016.12.007.

Fang, C.-Y. *et al.* (2020) 'The Diverse Roles of TAO Kinases in Health and Diseases',

International Journal of Molecular Sciences. MDPI AG, 21(20), p. 7463. doi: 10.3390/ijms21207463.

Fernandez, E. *et al*. (2017) 'Human antibodies to the dengue virus E-dimer epitope have therapeutic activity against Zika virus infection', *Nature Immunology*. Nature Publishing Group, 18(11), pp. 1261–1269. doi: 10.1038/ni.3849.

Ferreira-De-Lima, V. H. and Lima-Camara, T. N. (2018) 'Natural vertical transmission of dengue virus in Aedes aegypti and Aedes albopictus: A systematic review', *Parasites and Vectors*. BioMed Central, p. 77. doi: 10.1186/s13071-018-2643-9.

Fink, S. L. *et al*. (2018) 'The Antiviral Drug Arbidol Inhibits Zika Virus', *Scientific Reports*. Nature Publishing Group, 8(1), pp. 1–9. doi: 10.1038/s41598-018-27224-4.

Fontes-Garfias, C. R. *et al*. (2017) 'Functional Analysis of Glycosylation of Zika Virus Envelope Protein.', *Cell reports*. NIH Public Access, 21(5), pp. 1180–1190. doi: 10.1016/j.celrep.2017.10.016.

Foti, D. M. *et al*. (1999) 'Conservation and divergence of the yeast and mammalian unfolded protein response. Activation of specific mammalian endoplasmic reticulum stress element of the grp78/BiP promoter by yeast Hac1.', *The Journal of biological chemistry*, 274(43), pp. 30402–9. Available at: http://www.ncbi.nlm.nih.gov/pubmed/10521417 (Accessed: 29 June 2018).

Fulton, B. O. *et al*. (2017) 'Transposon Mutagenesis of the Zika Virus Genome Highlights Regions Essential for RNA Replication and Restricted for Immune Evasion', *Journal of Virology*. American Society for Microbiology, 91(15). doi: 10.1128/jvi.00698-17.

Gao, D. *et al*. (2016) 'Prevention and Control of Zika as a Mosquito-Borne and Sexually Transmitted Disease: A Mathematical Modeling Analysis', *Scientific Reports*. Nature Publishing Group, 6. doi: 10.1038/srep28070.

Garg, H. *et al*. (2017) 'Development of Virus-Like-Particle Vaccine and Reporter Assay for Zika Virus', *Journal of Virology*. American Society for Microbiology, 91(20). doi: 10.1128/jvi.00834-17.

Garske, T. *et al*. (2014) 'Yellow Fever in Africa: Estimating the Burden of Disease and Impact of Mass Vaccination from Outbreak and Serological Data', *PLoS Medicine*. Public Library of Science, 11(5). doi: 10.1371/journal.pmed.1001638.

Geoghegan, V. *et al*. (2017) 'Perturbed cholesterol and vesicular trafficking associated with dengue blocking in Wolbachia-infected Aedes aegypti cells', *Nature Communications*. Nature Publishing Group, 8(1), pp. 1–10. doi: 10.1038/s41467-017-00610-8.

Gestuveo, R. J. *et al*. (2021) 'Analysis of Zika virus capsid-Aedes aegypti mosquito interactome reveals pro-viral host factors critical for establishing infection', *Nature Communications*. Nature Research, 12(1), pp. 1–16. doi: 10.1038/s41467-021-22966-8.

Ghosh Roy, S. (2020) 'TAM receptors: A phosphatidylserine receptor family and its implications in viral infections', in *International Review of Cell and Molecular Biology*. Elsevier Inc., pp. 81–122. doi: 10.1016/bs.ircmb.2020.09.003.

Gladwyn-Ng, I. *et al*. (2018) 'Stress-induced unfolded protein response contributes to Zika virus–associated microcephaly', *Nature Neuroscience*. Nature Publishing Group, 21(1), pp. 63–71. doi: 10.1038/s41593-017-0038-4.

Göertz, G. P. *et al*. (2016) 'Noncoding Subgenomic Flavivirus RNA Is Processed by

the Mosquito RNA Interference Machinery and Determines West Nile Virus Transmission by Culex pipiens Mosquitoes', *Journal of Virology*. American Society for Microbiology, 90(22), pp. 10145–10159. doi: 10.1128/jvi.00930-16.

Göertz, G. P. *et al*. (2018) 'Functional RNA during Zika virus infection', *Virus Research*. Elsevier B.V., pp. 41–53. doi: 10.1016/j.virusres.2017.08.015.

Göertz, G. P. *et al*. (2019) 'Subgenomic flavivirus RNA binds the mosquito DEAD/H-box helicase ME31B and determines Zika virus transmission by Aedes aegypti', *Proceedings of the National Academy of Sciences of the United States of America*. National Academy of Sciences, 116(38), pp. 19136–19144. doi: 10.1073/pnas.1905617116.

Goic, B. and Saleh, M. C. (2012) 'Living with the enemy: Viral persistent infections from a friendly viewpoint', *Current Opinion in Microbiology*. Curr Opin Microbiol, pp. 531–537. doi: 10.1016/j.mib.2012.06.002.

Golubeva, V. A. *et al*. (2020) 'Network of Interactions between ZIKA Virus Non-Structural Proteins and Human Host Proteins', *Cells*. MDPI AG, 9(1), p. 153. doi: 10.3390/cells9010153.

Gomard, Y. *et al*. (2020) 'Contrasted transmission efficiency of Zika virus strains by mosquito species Aedes aegypti, Aedes albopictus and Culex quinquefasciatus from Reunion Island', *Parasites and Vectors*. BioMed Central, 13(1), p. 398. doi: 10.1186/s13071-020-04267-z.

Goo, L. *et al*. (2017) 'A single mutation in the envelope protein modulates flavivirus antigenicity, stability, and pathogenesis', *PLoS Pathogens*. Public Library of Science, 13(2), p. e1006178. doi: 10.1371/journal.ppat.1006178.

Goodwin, E. C. *et al*. (2011) 'BiP and multiple DNAJ molecular chaperones in the

endoplasmic reticulum are required for efficient simian virus 40 infection', *mBio*. American Society for Microbiology, 2(3). doi: 10.1128/mBio.00101-11.

Gould, E. A. *et al*. (2003) 'Origins, evolution, and vector/host coadaptations within the Genus Flavivirus', in *Advances in Virus Research*, pp. 277–314. doi: 10.1016/S0065-3527(03)59008-X.

Gourinat, A. C. *et al*. (2015) 'Detection of zika virus in urine', *Emerging Infectious Diseases*. Centers for Disease Control and Prevention (CDC), 21(1), pp. 84–86. doi: 10.3201/eid2101.140894.

Gray, T. J. *et al*. (2011) 'Case report: West nile virus (Kunjin subtype) disease in the Northern Territory of Australia - A case of encephalitis and review of all reported cases', *American Journal of Tropical Medicine and Hygiene*. The American Society of Tropical Medicine and Hygiene, 85(5), pp. 952–956. doi: 10.4269/ajtmh.2011.11-0165.

Gregory, C. J. *et al*. (2017) 'Modes of Transmission of Zika Virus', *Journal of Infectious Diseases*. Oxford University Press, pp. S875–S883. doi: 10.1093/infdis/jix396.

Gupta, N. *et al*. (2019) 'Zika virus in India: past, present and future', *QJM: An International Journal of Medicine*. Oxford University Press (OUP). doi: 10.1093/qjmed/hcz273.

Gutiérrez-Bugallo, G. *et al*. (2019) 'Vector-borne transmission and evolution of Zika virus', *Nature Ecology and Evolution*. Nature Publishing Group, pp. 561–569. doi: 10.1038/s41559-019-0836-z.

Guzman, M. G. *et al*. (2010) 'Dengue: a continuing global threat', *Nature Reviews Microbiology*. Nature Publishing Group, 8(12), pp. S7–S16. doi:

10.1038/nrmicro2460.

Haby, M. M. *et al*. (2018) 'Prevalence of asymptomatic Zika virus infection: A systematic review', *Bulletin of the World Health Organization*. World Health Organization, pp. 402-413D. doi: 10.2471/BLT.17.201541.

Haddow, A. D. *et al*. (2012) 'Genetic Characterization of Zika Virus Strains: Geographic Expansion of the Asian Lineage', *PLoS Neglected Tropical Diseases*. Edited by K. E. Olson, 6(2), p. e1477. doi: 10.1371/journal.pntd.0001477.

Hagiwara, M. *et al*. (2011) 'Structural Basis of an ERAD Pathway Mediated by the ER-Resident Protein Disulfide Reductase ERdj5', *Molecular Cell*. Elsevier, 41(4), pp. 432–444. doi: 10.1016/j.molcel.2011.01.021.

Hamel, R. *et al*. (2015) 'Biology of Zika Virus Infection in Human Skin Cells', *Journal of Virology*. American Society for Microbiology, 89(17), pp. 8880–8896. doi: 10.1128/jvi.00354-15.

Harding, H. P. *et al*. (2000) 'Perk is essential for translational regulation and cell survival during the unfolded protein response', *Molecular Cell*. Cell Press, 5(5), pp. 897–904. doi: 10.1016/S1097-2765(00)80330-5.

Harsh, S. and Eleftherianos, I. (2020) 'Flavivirus Infection and Regulation of Host Immune and Tissue Homeostasis in Insects', *Frontiers in Immunology*. Frontiers Media S.A., 11. doi: 10.3389/fimmu.2020.618801.

Hartlage, A. S., Cullen, J. M. and Kapoor, A. (2016) 'The Strange, Expanding World of Animal Hepaciviruses', *Annual Review of Virology*. Annual Reviews, 3(1), pp. 53–75. doi: 10.1146/annurev-virology-100114-055104.

He, D. *et al*. (2020) 'New estimates of the zika virus epidemic attack rate in

northeastern Brazil from 2015 to 2016: A modelling analysis based on Guillain-Barré syndrome (GBS) surveillance data', *PLoS Neglected Tropical Diseases*. Public Library of Science, 14(4), pp. 1–23. doi: 10.1371/journal.pntd.0007502.

Hendershot, L. M. *et al.* (1994) 'Localization of the gene encoding human bip/grp78, the endoplasmic reticulum cognate of the hsp70 family, to chromosome 9q34', *Genomics*. Genomics, 20(2), pp. 281–284. doi: 10.1006/geno.1994.1166.

Hetz, C. (2012) 'The unfolded protein response: Controlling cell fate decisions under ER stress and beyond', *Nature Reviews Molecular Cell Biology*. Nature Publishing Group, pp. 89–102. doi: 10.1038/nrm3270.

Hilton, L. *et al.* (2006) 'The NPro product of bovine viral diarrhea virus inhibits DNA binding by interferon regulatory factor 3 and targets it for proteasomal degradation.', *Journal of virology*. American Society for Microbiology (ASM), 80(23), pp. 11723–32. doi: 10.1128/JVI.01145-06.

Hogue, B. G. and Nayak, D. P. (1992) 'Synthesis and processing of the influenza virus neuraminidase, a type II transmembrane glycoprotein.', *Virology*, 188(2), pp. 510–7. doi: 10.1016/0042-6822(92)90505-j.

Houe, H. (1995) 'Epidemiology of bovine viral diarrhea virus.', *The Veterinary clinics of North America. Food animal practice*. Elsevier, 11(3), pp. 521–547. doi: 10.1016/S0749-0720(15)30465-5.

Huang, Y. J. S. *et al.* (2014) 'Flavivirus-Mosquito interactions', *Viruses*. MDPI AG, pp. 4703–4730. doi: 10.3390/v6114703.

Huang, Y. J. S., Higgs, S. and Vanlandingham, D. L. (2019) 'Arbovirus-mosquito vector-host interactions and the impact on transmission and disease pathogenesis

of arboviruses', *Frontiers in Microbiology*. Frontiers Media S.A. doi: 10.3389/fmicb.2019.00022.

Hubert, M. *et al*. (2020) 'Evidence That Zika Virus Is Transmitted by Breastfeeding to Newborn A129 (Ifnar1 Knock-Out) Mice and Is Able to Infect and Cross a Tight Monolayer of Human Intestinal Epithelial Cells', *Frontiers in Microbiology*. Frontiers Media S.A., 11, p. 2630. doi: 10.3389/fmicb.2020.524678.

Hung, Y. F. *et al*. (2015) 'Amino terminal region of dengue virus NS4A cytosolic domain binds to highly curved liposomes', *Viruses*. MDPI AG, 7(7), pp. 4119–4130. doi: 10.3390/v7072812.

Ibrahim, I. M. *et al*. (2020) 'COVID-19 spike-host cell receptor GRP78 binding site prediction', *Journal of Infection*. W.B. Saunders Ltd, 80(5), pp. 554–562. doi: 10.1016/j.jinf.2020.02.026.

Ibrahim, I. M., Abdelmalek, D. H. and Elfiky, A. A. (2019) 'GRP78: A cell's response to stress', *Life Sciences*. Elsevier Inc., pp. 156–163. doi: 10.1016/j.lfs.2019.04.022.

Ishibashi, M., Wakita, T. and Esumi, M. (2010) '2′,5′-Oligoadenylate synthetase-like gene highly induced by hepatitis C virus infection in human liver is inhibitory to viral replication in vitro', *Biochemical and Biophysical Research Communications*, 392(3), pp. 397–402. doi: 10.1016/j.bbrc.2010.01.034.

Ji, C. *et al*. (2011) 'Liver-specific loss of glucose-regulated protein 78 perturbs the unfolded protein response and exacerbates a spectrum of liver diseases in mice', *Hepatology*. John Wiley & Sons, Ltd, 54(1), pp. 229–239. doi: 10.1002/hep.24368.

Jiang, X. *et al*. (2018) 'Proteomic Analysis of Zika Virus Infected Primary Human Fetal Neural Progenitors Suggests a Role for Doublecortin in the Pathological

Consequences of Infection in the Cortex', *Frontiers in Microbiology*. Frontiers Media S.A., 9(JUN), p. 1067. doi: 10.3389/fmicb.2018.01067.

Jindadamrongwech, S., Thepparit, C. and Smith, D. R. (2004) 'Identification of GRP 78 (BiP) as a liver cell expressed receptor element for dengue virus serotype 2', *Archives of Virology*, 149(5), pp. 915–927. doi: 10.1007/s00705-003-0263-x.

Kang, B. R. *et al.* (2016) 'Cell surface GRP78 as a biomarker and target for suppressing glioma cells', *Scientific Reports*. Nature Publishing Group, 6(1), pp. 1–7. doi: 10.1038/srep34922.

Kemmerly, S. A. (2003) 'Diagnosis and treatment of west nile infections.', *The Ochsner journal*. Ochsner Clinic, L.L.C. and Alton Ochsner Medical Foundation, 5(3), pp. 16–7. Available at: http://www.ncbi.nlm.nih.gov/pubmed/21765764 (Accessed: 15 January 2021).

Khaiboullina, S. *et al.* (2018) 'History of ZIKV Infections in India and Management of Disease Outbreaks', *Frontiers in Microbiology*. Frontiers Media S.A., 9(SEP), p. 2126. doi: 10.3389/fmicb.2018.02126.

Khongwichit, S. *et al.* (2021) 'A functional interaction between GRP78 and Zika virus E protein', *Scientific Reports*. Nature Publishing Group, 11(1), p. 393. doi: 10.1038/s41598-020-79803-z.

Khromykh, A. A. *et al.* (2001) 'Essential Role of Cyclization Sequences in Flavivirus RNA Replication', *Journal of Virology*. American Society for Microbiology, 75(14), pp. 6719–6728. doi: 10.1128/jvi.75.14.6719-6728.2001.

Kovacs, A. A. Z. (2020) 'Zika, the Newest TORCH Infectious Disease in the Americas', *Clinical Infectious Diseases*. Oxford University Press, 70(12), pp. 2673–2674. doi: 10.1093/cid/ciz709.

Kraemer, M. U. G. *et al.* (2015) 'The global distribution of the arbovirus vectors Aedes aegypti and Ae. Albopictus', *eLife*. eLife Sciences Publications Ltd, 4(JUNE2015). doi: 10.7554/eLife.08347.

Kucharski, A. and Riley, S. (2016) 'First published report of Zika virus infection in people: Simpson, not MacNamara', *The Lancet Infectious Diseases*, 17, pp. 15–17. doi: 10.1126/science.

Kuhn, R. J. *et al.* (2002) 'Structure of dengue virus: Implications for flavivirus organization, maturation, and fusion', *Cell*. Cell Press, 108(5), pp. 717–725. doi: 10.1016/S0092-8674(02)00660-8.

Kumar, A. *et al.* (2018) 'Mosquito innate immunity', *Insects*. MDPI AG, p. 1000097. doi: 10.3390/insects9030095.

Kümmerer, B. M. and Rice, C. M. (2002) 'Mutations in the Yellow Fever Virus Nonstructural Protein NS2A Selectively Block Production of Infectious Particles', *Journal of Virology*. American Society for Microbiology, 76(10), pp. 4773–4784. doi: 10.1128/jvi.76.10.4773-4784.2002.

Kuper, H. *et al.* (2019) 'Social and economic impacts of congenital Zika syndrome in Brazil: Study protocol and rationale for a mixed-methods study', *Wellcome Open Research*. F1000 Research Ltd, 3, p. 127. doi: 10.12688/wellcomeopenres.14838.2.

Kupferschmidt, K. (2016) 'After 40 years, the most important weapon against mosquitoes may be failing', *Science*. American Association for the Advancement of Science (AAAS). doi: 10.1126/science.aal0254.

Laureti, M. *et al.* (2018) 'Flavivirus Receptors: Diversity, Identity, and Cell Entry', *Frontiers in immunology*. NLM (Medline), p. 2180. doi:

10.3389/fimmu.2018.02180.

Lee, C. M. *et al*. (2015) 'Determinants of Dengue Virus NS4A Protein Oligomerization', *Journal of Virology*. American Society for Microbiology, 89(12), pp. 6171–6183. doi: 10.1128/jvi.00546-15.

Lee, E. *et al*. (2010) 'Both E Protein Glycans Adversely Affect Dengue Virus Infectivity but Are Beneficial for Virion Release', *Journal of Virology*. American Society for Microbiology, 84(10), pp. 5171–5180. doi: 10.1128/jvi.01900-09.

Lee, H. *et al*. (2017) 'Identification of novel small molecule inhibitors against NS2B/NS3 serine protease from Zika virus', *Antiviral Research*. Elsevier B.V., 139, pp. 49–58. doi: 10.1016/j.antiviral.2016.12.016.

Lee, I. *et al*. (2018) 'Probing molecular insights into Zika virus–host interactions', *Viruses*. MDPI AG. doi: 10.3390/v10050233.

Lee, J. K. and Shin, O. S. (2019) 'Advances in zika virus–host cell interaction: Current knowledge and future perspectives', *International Journal of Molecular Sciences*. MDPI AG. doi: 10.3390/ijms20051101.

Lee, W. S. *et al*. (2019) 'Mosquito antiviral defense mechanisms: A delicate balance between innate immunity and persistent viral infection', *Parasites and Vectors*. BioMed Central Ltd., 12(1), pp. 1–12. doi: 10.1186/s13071-019-3433-8.

Leonhard, S. E. *et al*. (2019) 'Diagnosis and management of Guillain–Barré syndrome in ten steps', *Nature Reviews Neurology*. Nature Publishing Group, 15(11), pp. 671–683. doi: 10.1038/s41582-019-0250-9.

Leonhard, S. E. *et al*. (2020) 'Guillain-barré syndrome related to zika virus infection: A systematic review and meta-analysis of the clinical and

electrophysiological phenotype', *PLoS Neglected Tropical Diseases*. Public Library of Science, 14(4), pp. 1–24. doi: 10.1371/journal.pntd.0008264.

Lequime, S. and Lambrechts, L. (2014) 'Vertical transmission of arboviruses in mosquitoes: A historical perspective', *Infection, Genetics and Evolution*. Elsevier, 28, pp. 681–690. doi: 10.1016/j.meegid.2014.07.025.

Lequime, S., Paul, R. E. and Lambrechts, L. (2016) 'Determinants of Arbovirus Vertical Transmission in Mosquitoes', *PLoS Pathogens*. Public Library of Science. doi: 10.1371/journal.ppat.1005548.

Leung, J. Y. *et al*. (2008) 'Role of Nonstructural Protein NS2A in Flavivirus Assembly', *Journal of Virology*. American Society for Microbiology, 82(10), pp. 4731–4741. doi: 10.1128/jvi.00002-08.

Levene, R. E. and Gaglia, M. M. (2018) 'Host shutoff in influenza A virus: Many means to an end', *Viruses*. MDPI AG. doi: 10.3390/v10090475.

Li, F. *et al*. (2017) 'AXL is not essential for Zika virus infection in the mouse brain', *Emerging Microbes & Infections*. Nature Publishing Group, 6(3), p. e16. doi: 10.1038/emi.2017.10.

Li, G. *et al*. (2019) 'An attenuated Zika virus NS4B protein mutant is a potent inducer of antiviral immune responses', *npj Vaccines*. Nature Research, 4(1), pp. 1–10. doi: 10.1038/s41541-019-0143-3.

Li, M. *et al*. (2000) 'ATF6 as a Transcription Activator of the Endoplasmic Reticulum Stress Element: Thapsigargin Stress-Induced Changes and Synergistic Interactions with NF-Y and YY1', *Molecular and Cellular Biology*. American Society for Microbiology, 20(14), pp. 5096–5106. doi: 10.1128/mcb.20.14.5096-5106.2000.

Li, M. Y. *et al.* (2015) 'KDEL receptors assist dengue virus exit from the endoplasmic reticulum', *Cell Reports*. Elsevier, 10(9), pp. 1496–1507. doi: 10.1016/j.celrep.2015.02.021.

Li, M. Y. *et al.* (2020) 'Lyn kinase regulates egress of flaviviruses in autophagosome-derived organelles', *Nature Communications*. Nature Research, 11(1), pp. 1–16. doi: 10.1038/s41467-020-19028-w.

Li, X.-D. *et al.* (2016) 'Transmembrane Domains of NS2B Contribute to both Viral RNA Replication and Particle Formation in Japanese Encephalitis Virus', *Journal of Virology*. American Society for Microbiology, 90(12), pp. 5735–5749. doi: 10.1128/jvi.00340-16.

Li, Y. *et al.* (2015) 'Membrane topology of NS2B of dengue virus revealed by NMR spectroscopy', *Biochimica et Biophysica Acta - Biomembranes*. Elsevier, 1848(10), pp. 2244–2252. doi: 10.1016/j.bbamem.2015.06.010.

Li, Z. *et al.* (2017) 'Existing drugs as broad-spectrum and potent inhibitors for Zika virus by targeting NS2B-NS3 interaction', *Cell Research*. Nature Publishing Group, 27(8), pp. 1046–1064. doi: 10.1038/cr.2017.88.

Li, Z., Zhang, J. and Li, H. (2017) 'Flavivirus NS2B/NS3 protease: Structure, function, and inhibition', in *Viral Proteases and Their Inhibitors*. Elsevier, pp. 163–188. doi: 10.1016/B978-0-12-809712-0.00007-1.

Liang, X. Y. *et al.* (2020) 'Development of HiBiT-Tagged Recombinant Infectious Bronchitis Coronavirus for Efficient in vitro and in vivo Viral Quantification', *Frontiers in Microbiology*. Frontiers Media S.A., 11, p. 2100. doi: 10.3389/fmicb.2020.02100.

Limjindaporn, T. *et al.* (2009) 'Interaction of dengue virus envelope protein with

endoplasmic reticulum-resident chaperones facilitates dengue virus production', *Biochemical and Biophysical Research Communications*, 379(2), pp. 196–200. doi: 10.1016/j.bbrc.2008.12.070.

Lin, C. *et al.* (1993) *Cleavage at a Novel Site in the NS4A Region by the Yellow Fever Virus NS2B-3 Proteinase Is a Prerequisite for Processing at the Downstream 4A/4B Signalase Site*, *JOURNAL OF VIROLOGY*.

Lin, C. W. *et al.* (2008) 'Interferon antagonist function of Japanese encephalitis virus NS4A and its interaction with DEAD-box RNA helicase DDX42', *Virus Research*. Elsevier, 137(1), pp. 49–55. doi: 10.1016/j.virusres.2008.05.015.

Lindenbach, B. D. and Rice, C. M. (2003) 'Molecular biology of flaviviruses.', *Advances in virus research*, 59, pp. 23–61. Available at: http://www.ncbi.nlm.nih.gov/pubmed/14696326 (Accessed: 29 June 2018).

Liu, R. *et al.* (2019) 'Prevalence of Zika virus in blood donations: A systematic review and meta-analysis', *BMC Infectious Diseases*. BioMed Central Ltd., p. 590. doi: 10.1186/s12879-019-4226-6.

Liu, W. J. *et al.* (2002) 'Complementation Analysis of the Flavivirus Kunjin NS3 and NS5 Proteins Defines the Minimal Regions Essential for Formation of a Replication Complex and Shows a Requirement of NS3 in cis for Virus Assembly', *Journal of Virology*. American Society for Microbiology, 76(21), pp. 10766–10775. doi: 10.1128/jvi.76.21.10766-10775.2002.

López-Medina, E. *et al.* (2020) 'Efficacy of a Dengue Vaccine Candidate (TAK-003) in Healthy Children and Adolescents 2 Years after Vaccination', *The Journal of Infectious Diseases*. Oxford University Press (OUP), XX, pp. 1–12. doi: 10.1093/infdis/jiaa761.

Lowe, R. *et al.* (2018) 'The zika virus epidemic in brazil: From discovery to future implications', *International Journal of Environmental Research and Public Health*. MDPI AG, 15(1), p. 96. doi: 10.3390/ijerph15010096.

Lu, G., Luo, H. and Zhu, X. (2020) 'Targeting the GRP78 Pathway for Cancer Therapy', *Frontiers in Medicine*. Frontiers Media S.A., 7, p. 351. doi: 10.3389/fmed.2020.00351.

Lucas, K. J., Myles, K. M. and Raikhel, A. S. (2013) 'Small RNAs: A new frontier in mosquito biology', *Trends in Parasitology*. Elsevier, pp. 295–303. doi: 10.1016/j.pt.2013.04.003.

Luhr, M. *et al.* (2019) 'The kinase PERK and the transcription factor ATF4 play distinct and essential roles in autophagy resulting from tunicamycin-induced ER stress', *Journal of Biological Chemistry*. American Society for Biochemistry and Molecular Biology Inc., 294(20), pp. 8197–8217. doi: 10.1074/jbc.RA118.002829.

Luo, D. *et al.* (2008) 'Crystal Structure of the NS3 Protease-Helicase from Dengue Virus', *Journal of Virology*. American Society for Microbiology, 82(1), pp. 173–183. doi: 10.1128/jvi.01788-07.

Luo, S. *et al.* (2006) 'GRP78/BiP Is Required for Cell Proliferation and Protecting the Inner Cell Mass from Apoptosis during Early Mouse Embryonic Development', *Molecular and Cellular Biology*. American Society for Microbiology, 26(15), pp. 5688–5697. doi: 10.1128/mcb.00779-06.

Lv, X. Q. *et al.* (2016) 'Honokiol inhibits EMT-mediated motility and migration of human non-small cell lung cancer cells in vitro by targeting c-FLIP', *Acta Pharmacologica Sinica*. Nature Publishing Group, 37(12), pp. 1574–1586. doi: 10.1038/aps.2016.81.

Ma, J. *et al*. (2018) 'Zika Virus Non-structural Protein 4A Blocks the RLR-MAVS Signaling', *Frontiers in Microbiology*. Frontiers Media S.A., 9(JUN), p. 1350. doi: 10.3389/fmicb.2018.01350.

Magnus, M. M. *et al*. (2018) 'Risk of Zika virus transmission by blood donations in Brazil', *Hematology, Transfusion and Cell Therapy*. Elsevier Editora Ltda, 40(3), pp. 250–254. doi: 10.1016/j.htct.2018.01.011.

Manokaran, G. *et al*. (2015) 'Dengue subgenomic RNA binds TRIM25 to inhibit interferon expression for epidemiological fitness', *Science*. American Association for the Advancement of Science, 350(6257), pp. 217–221. doi: 10.1126/science.aab3369.

Manzano, M. *et al*. (2011) 'Identification of cis-acting elements in the 3′-untranslated region of the dengue virus type 2 RNA that modulate translation and replication', *Journal of Biological Chemistry*. American Society for Biochemistry and Molecular Biology, 286(25), pp. 22521–22534. doi: 10.1074/jbc.M111.234302.

Márquez-Jurado, S. *et al*. (2018) 'An Alanine-to-Valine Substitution in the Residue 175 of Zika Virus NS2A Protein Affects Viral RNA Synthesis and Attenuates the Virus In Vivo', *Viruses*. MDPI AG, 10(10), p. 547. doi: 10.3390/v10100547.

Martelli, C. M. T. *et al*. (2015) 'Economic Impact of Dengue: Multicenter Study across Four Brazilian Regions', *PLOS Neglected Tropical Diseases*. Edited by M. S. Carvalho. Public Library of Science, 9(9), p. e0004042. doi: 10.1371/journal.pntd.0004042.

Martin, S. *et al*. (2013) 'Inducing apoptosis of cancer cells using small-molecule plant compounds that bind to GRP78', *British Journal of Cancer*, 109(2), pp. 433–443. doi: 10.1038/bjc.2013.325.

Mazeaud, C., Freppel, W. and Chatel-Chaix, L. (2018) 'The Multiples Fates of the Flavivirus RNA Genome During Pathogenesis', *Frontiers in Genetics*. Frontiers Media SA, 9, p. 595. doi: 10.3389/fgene.2018.00595.

McLean, J. E. *et al*. (2011) 'Flavivirus NS4A-induced autophagy protects cells against death and enhances virus replication', *Journal of Biological Chemistry*. American Society for Biochemistry and Molecular Biology, 286(25), pp. 22147–22159. doi: 10.1074/jbc.M110.192500.

Mead, P. S., Hills, S. L. and Brooks, J. T. (2018) 'Zika virus as a sexually transmitted pathogen', *Current Opinion in Infectious Diseases*. Lippincott Williams and Wilkins, pp. 39–44. doi: 10.1097/QCO.0000000000000414.

Medina, F. A. *et al*. (2018) 'Duration of the Presence of Infectious Zika Virus in Semen and Serum', *The Journal of Infectious Diseases*. Oxford University Press, 219(1), pp. 31–40. doi: 10.1093/infdis/jiy462.

Meertens, L. *et al*. (2012) 'The TIM and TAM families of phosphatidylserine receptors mediate dengue virus entry', *Cell Host and Microbe*. NIH Public Access, 12(4), pp. 544–557. doi: 10.1016/j.chom.2012.08.009.

Meertens, L. *et al*. (2017) 'Axl Mediates ZIKA Virus Entry in Human Glial Cells and Modulates Innate Immune Responses', *Cell Reports*, 18(2), pp. 324–333. doi: 10.1016/j.celrep.2016.12.045.

Meghani, Z. and Boëte, C. (2018) 'Genetically engineered mosquitoes, Zika and other arboviruses, community engagement, costs, and patents: Ethical issues', *PLoS Neglected Tropical Diseases*. Public Library of Science, 12(7). doi: 10.1371/journal.pntd.0006501.

Messina, J. P. *et al*. (2019) 'The current and future global distribution and

population at risk of dengue', *Nature Microbiology*. Nature Publishing Group, 4(9), pp. 1508–1515. doi: 10.1038/s41564-019-0476-8.

Metz, S. W. *et al.* (2017) 'In Vitro Assembly and Stabilization of Dengue and Zika Virus Envelope Protein Homo-Dimers', *Scientific Reports*. Nature Publishing Group, 7(1). doi: 10.1038/s41598-017-04767-6.

Miao, Z. *et al.* (2017) 'Prevalence and clinical impact of human pegivirus-1 infection in HIV-1-infected individuals in Yunnan, China', *Viruses*. MDPI AG, 9(2). doi: 10.3390/v9020028.

Miller, S. *et al.* (2007) 'The non-structural protein 4A of dengue virus is an integral membrane protein inducing membrane alterations in a 2K-regulated manner', *Journal of Biological Chemistry*. J Biol Chem, 282(12), pp. 8873–8882. doi: 10.1074/jbc.M609919200.

Misra, U. K. *et al.* (2005) 'The Role of MTJ-1 in Cell Surface Translocation of GRP78, a Receptor for α_2 -Macroglobulin-Dependent Signaling', *The Journal of Immunology*, 174(4), pp. 2092–2097. doi: 10.4049/jimmunol.174.4.2092.

Modis, Y. *et al.* (2004) 'Structure of the dengue virus envelope protein after membrane fusion', *Nature*. Nature, 427(6972), pp. 313–319. doi: 10.1038/nature02165.

Molinari, M. and Helenius, A. (2000) 'Chaperone selection during glycoprotein translocation into the endoplasmic reticulum', *Science*. American Association for the Advancement of Science, 288(5464), pp. 331–333. doi: 10.1126/science.288.5464.331.

Moon, S. L. *et al.* (2015) 'Flavivirus sfRNA suppresses antiviral RNA interference in cultured cells and mosquitoes and directly interacts with the RNAi machinery.',

Virology. NIH Public Access, 485, pp. 322–9. doi: 10.1016/j.virol.2015.08.009.

Moore, C. A. *et al.* (2017) 'Characterizing the pattern of anomalies in congenital zika syndrome for pediatric clinicians', *JAMA Pediatrics*. American Medical Association, pp. 288–295. doi: 10.1001/jamapediatrics.2016.3982.

Moreira, J. *et al.* (2017) 'Sexually acquired Zika virus: a systematic review', *Clinical Microbiology and Infection*. Elsevier B.V., pp. 296–305. doi: 10.1016/j.cmi.2016.12.027.

Moser, L. A. *et al.* (2018) 'Growth and adaptation of Zika virus in mammalian and mosquito cells', *PLOS Neglected Tropical Diseases*. Edited by L. A. Moreira. Public Library of Science, 12(11), p. e0006880. doi: 10.1371/journal.pntd.0006880.

Mukherjee, D. *et al.* (2019) 'The mosquito immune system and the life of dengue virus: What we know and do not know', *Pathogens*. MDPI AG. doi: 10.3390/pathogens8020077.

Muller, D. A. and Young, P. R. (2013) 'The flavivirus NS1 protein: Molecular and structural biology, immunology, role inpathogenesis and application asadiagnostic biomarker.', *Antiviral Research*. Elsevier B.V., pp. 192–208. doi: 10.1016/j.antiviral.2013.03.008.

Muñoz-Jordán, J. L. *et al.* (2005) 'Inhibition of Alpha/Beta Interferon Signaling by the NS4B Protein of Flaviviruses', *Journal of Virology*. American Society for Microbiology, 79(13), pp. 8004–8013. doi: 10.1128/jvi.79.13.8004-8013.2005.

Muñoz, L. S., Parra, B. and Pardo, C. A. (2017) 'Neurological Implications of Zika Virus Infection in Adults', *Journal of Infectious Diseases*. Oxford University Press, pp. S897–S905. doi: 10.1093/infdis/jix511.

Munro, S. and Pelham, H. R. B. (1986) ‘An hsp70-like protein in the ER: Identity with the 78 kd glucose-regulated protein and immunoglobulin heavy chain binding protein’, *Cell*. Cell, 46(2), pp. 291–300. doi: 10.1016/0092-8674(86)90746-4.

Münster, M. *et al*. (2018) ‘A reverse genetics system for Zika virus based on a simple molecular cloning strategy’, *Viruses*. MDPI AG, 10(7). doi: 10.3390/v10070368.

Murray, K. O. *et al*. (2006) ‘Risk factors for encephalitis and death from West Nile virus infection’, *Epidemiology and Infection*. Cambridge University Press, 134(6), pp. 1325–1332. doi: 10.1017/S0950268806006339.

Murray, K. O., Mertens, E. and Desprès, P. (2010) ‘West Nile virus and its emergence in the United States of America’, *Veterinary Research*. BioMed Central. doi: 10.1051/vetres/2010039.

Musso, D. *et al*. (2015) ‘Potential sexual transmission of zika virus’, *Emerging Infectious Diseases*. Centers for Disease Control and Prevention (CDC), 21(2), pp. 359–361. doi: 10.3201/eid2102.141363.

Musso, D. *et al*. (2018) ‘Zika virus in French Polynesia 2013–14: anatomy of a completed outbreak’, *The Lancet Infectious Diseases*. Lancet Publishing Group, pp. e172–e182. doi: 10.1016/S1473-3099(17)30446-2.

Musso, D. and Gubler, D. J. (2016) ‘Zika virus’, *Clinical Microbiology Reviews*. American Society for Microbiology, 29(3), pp. 487–524. doi: 10.1128/CMR.00072-15.

Mutso, M. *et al*. (2017) ‘Reverse genetic system, genetically stable reporter viruses and packaged subgenomic replicon based on a Brazilian zika virus isolate’, *Journal of General Virology*. Microbiology Society, 98(11), pp. 2712–2724. doi:

10.1099/jgv.0.000938.

Nain, M. *et al*. (2017) 'GRP78 Is an Important Host Factor for Japanese Encephalitis Virus Entry and Replication in Mammalian Cells.', *Journal of virology*. American Society for Microbiology, 91(6), pp. e02274-16. doi: 10.1128/JVI.02274-16.

Nelson, S. *et al*. (2009) 'Protonation of Individual Histidine Residues Is Not Required for the pH-Dependent Entry of West Nile Virus: Evaluation of the "Histidine Switch" Hypothesis', *Journal of Virology*. American Society for Microbiology, 83(23), pp. 12631–12635. doi: 10.1128/jvi.01072-09.

Netto, E. M. *et al*. (2017) 'High Zika virus seroprevalence in Salvador, northeastern Brazil limits the potential for further outbreaks', *mBio*. American Society for Microbiology, 8(6). doi: 10.1128/mBio.01390-17.

Neufeldt, C. J. *et al*. (2018) 'Rewiring cellular networks by members of the Flaviviridae family', *Nature Reviews Microbiology*. Nature Publishing Group, pp. 125–142. doi: 10.1038/nrmicro.2017.170.

Ng, W. C. *et al*. (2017) 'The 5' and 3' untranslated regions of the flaviviral genome', *Viruses*. MDPI AG. doi: 10.3390/v9060137.

Ngan, N. T. T. *et al*. (2019) 'Zika virus proteins NS2A and NS4A are major antagonists that reduce IFN-β promoter activity induced by the MDA5/RIG-I signaling pathway', *Journal of Microbiology and Biotechnology*. Korean Society for Microbiology and Biotechnology, 29(10), pp. 1665–1674. doi: 10.4014/jmb.1909.09017.

Ni, M., Zhang, Y. and Lee, A. S. (2011) 'Beyond the endoplasmic reticulum: atypical GRP78 in cell viability, signalling and therapeutic targeting.', *The Biochemical journal*. NIH Public Access, 434(2), pp. 181–8. doi:

10.1042/BJ20101569.

Nicholls, C. M. R., Sevvana, M. and Kuhn, R. J. (2020) 'Structure-guided paradigm shifts in flavivirus assembly and maturation mechanisms', in *Advances in Virus Research*. Academic Press Inc., pp. 33–83. doi: 10.1016/bs.aivir.2020.08.003.

Nishimura, K. and Fukagawa, T. (2017) 'An efficient method to generate conditional knockout cell lines for essential genes by combination of auxin-inducible degron tag and CRISPR/Cas9', *Chromosome Research*. Springer Netherlands, 25(3–4), pp. 253–260. doi: 10.1007/s10577-017-9559-7.

Niu, J. *et al.* (2018) 'TIM-1 promotes Japanese encephalitis virus entry and infection', *Viruses*. MDPI AG, 10(11). doi: 10.3390/v10110630.

Nowakowski, T. J. *et al.* (2016) 'Expression Analysis Highlights AXL as a Candidate Zika Virus Entry Receptor in Neural Stem Cells', *Cell Stem Cell*, 18(5), pp. 591–596. doi: 10.1016/j.stem.2016.03.012.

Ojha, C. R. *et al.* (2019) 'Toll-like receptor 3 regulates Zika virus infection and associated host inflammatory response in primary human astrocytes', *PLOS ONE*. Edited by D.-Y. Jin. Public Library of Science, 14(2), p. e0208543. doi: 10.1371/journal.pone.0208543.

Oliveira, E. R. A. *et al.* (2017) 'The flavivirus capsid protein: Structure, function and perspectives towards drug design', *Virus Research*. Elsevier B.V., pp. 115–123. doi: 10.1016/j.virusres.2016.10.005.

Oliveira, L. G. and Peron, J. P. S. (2019) 'Viral receptors for flaviviruses: Not only gatekeepers', *Journal of Leukocyte Biology*. John Wiley and Sons Inc., 106(3), pp. 695–701. doi: 10.1002/JLB.MR1118-460R.

Owczarek, K. *et al*. (2019) 'Zika virus: Mapping and reprogramming the entry', *Cell Communication and Signaling*. BioMed Central Ltd., 17(1). doi: 10.1186/s12964-019-0349-z.

PAHO/WHO Data - ZIKA (2021). Available at: https://www.paho.org/data/index.php/en/mnu-topics/zika.html (Accessed: 15 January 2021).

Palmeira, A. *et al*. (2020) 'Preliminary virtual screening studies to identify grp78 inhibitors which may interfere with sars-cov-2 infection', *Pharmaceuticals*. MDPI AG, 13(6), pp. 1–13. doi: 10.3390/ph13060132.

Papageorgiou, L. *et al*. (2016) 'An updated evolutionary study of Flaviviridae NS3 helicase and NS5 RNA-dependent RNA polymerase reveals novel invariable motifs as potential pharmacological targets', *Molecular BioSystems*. Royal Society of Chemistry, 12(7), pp. 2080–2093. doi: 10.1039/c5mb00706b.

Patkar, C. G. and Kuhn, R. J. (2008) 'Yellow Fever Virus NS3 Plays an Essential Role in Virus Assembly Independent of Its Known Enzymatic Functions', *Journal of Virology*. American Society for Microbiology, 82(7), pp. 3342–3352. doi: 10.1128/jvi.02447-07.

Patrick Reid, S. *et al*. (2014) 'HSPA5 is an essential host factor for Ebola virus infection', *Antiviral Research*. Elsevier B.V., 109(1), pp. 171–174. doi: 10.1016/j.antiviral.2014.07.004.

Paz, S. and Semenza, J. C. (2016) 'El Niño and climate change - Contributing factors in the dispersal of Zika virus in the Americas?', *The Lancet*. Lancet Publishing Group, p. 745. doi: 10.1016/S0140-6736(16)00256-7.

Pereira, H. V. F. S. *et al*. (2020) 'Neurological outcomes of congenital Zika

syndrome in toddlers and preschoolers: a case series', *The Lancet Child and Adolescent Health*. Elsevier B.V., 4(5), pp. 378–387. doi: 10.1016/S2352-4642(20)30041-9.

Perera-Lecoin, M. *et al*. (2013) 'Flavivirus entry receptors: An update', *Viruses*. Multidisciplinary Digital Publishing Institute (MDPI), pp. 69–88. doi: 10.3390/v6010069.

Persaud, M. *et al*. (2018) 'Infection by Zika viruses requires the transmembrane protein AXL, endocytosis and low pH', *Virology*. Academic Press Inc., 518, pp. 301–312. doi: 10.1016/j.virol.2018.03.009.

Petersen, L. R. *et al*. (2016) 'Zika Virus', *New England Journal of Medicine*. Edited by L. R. Baden. Massachusetts Medical Society, 374(16), pp. 1552–1563. doi: 10.1056/NEJMra1602113.

Petersen, L. R., Brault, A. C. and Nasci, R. S. (2013) 'West Nile virus: review of the literature.', *JAMA*. NIH Public Access, 310(3), pp. 308–15. doi: 10.1001/jama.2013.8042.

Pfaffenbach, K. T. and Lee, A. S. (2011) 'The critical role of GRP78 in physiologic and pathologic stress', *Current Opinion in Cell Biology*, pp. 150–156. doi: 10.1016/j.ceb.2010.09.007.

Phuc, H. *et al*. (2007) 'Late-acting dominant lethal genetic systems and mosquito control', *BMC Biology*. BioMed Central, 5, p. 11. doi: 10.1186/1741-7007-5-11.

Pierson, T. C. and Diamond, M. S. (2020) 'The continued threat of emerging flaviviruses', *Nature Microbiology*. Nature Research, pp. 796–812. doi: 10.1038/s41564-020-0714-0.

Pijlman, G. P. *et al*. (2008) 'A Highly Structured, Nuclease-Resistant, Noncoding RNA Produced by Flaviviruses Is Required for Pathogenicity', *Cell Host and Microbe*. Elsevier, 4(6), pp. 579–591. doi: 10.1016/j.chom.2008.10.007.

Płaszczyca, A. *et al*. (2019) 'A novel interaction between dengue virus nonstructural protein 1 and the NS4A-2K-4B precursor is required for viral RNA replication but not for formation of the membranous replication organelle', *PLOS Pathogens*. Edited by G. Randall. Public Library of Science, 15(5), p. e1007736. doi: 10.1371/journal.ppat.1007736.

Platt, D. J. *et al*. (2018) 'Zika virus-related neurotropic flaviviruses infect human placental explants and cause fetal demise in mice', *Science Translational Medicine*. American Association for the Advancement of Science, 10(426). doi: 10.1126/scitranslmed.aao7090.

Pomar, L. *et al*. (2018) 'Maternal-fetal transmission and adverse perinatal outcomes in pregnant women infected with Zika virus: Prospective cohort study in French Guiana', *BMJ (Online)*. BMJ Publishing Group, 363, p. 4431. doi: 10.1136/bmj.k4431.

Pong, W. L. *et al*. (2011) 'RNA binding property and RNA chaperone activity of dengue virus core protein and other viral RNA-interacting proteins', *FEBS Letters*. FEBS Lett, 585(16), pp. 2575–2581. doi: 10.1016/j.febslet.2011.06.038.

Prasad, V. M. *et al*. (2017) 'Structure of the immature Zika virus at 9 A resolution', *Nature Structural and Molecular Biology*. Nature Publishing Group, 24(2), pp. 184–186. doi: 10.1038/nsmb.3352.

Puerta-Guardo, H. *et al*. (2019) 'Flavivirus NS1 Triggers Tissue-Specific Vascular Endothelial Dysfunction Reflecting Disease Tropism', *Cell Reports*. Elsevier B.V.,

26(6), pp. 1598-1613.e8. doi: 10.1016/j.celrep.2019.01.036.

Pujhari, S. *et al*. (2019) 'Heat shock protein 70 (Hsp70) mediates Zika virus entry, replication, and egress from host cells', *Emerging Microbes & Infections*. Taylor and Francis Ltd., 8(1), pp. 8–16. doi: 10.1080/22221751.2018.1557988.

Pulkkinen, L. I. A., Butcher, S. J. and Anastasina, M. (2018) 'Tick-borne encephalitis virus: A structural view', *Viruses*. MDPI AG. doi: 10.3390/v10070350.

Qu, P. *et al*. (2020) 'A new class of broadly neutralizing antibodies that target the glycan loop of Zika virus envelope protein', *Cell Discovery*. Springer Nature, 6(1), p. 5. doi: 10.1038/s41421-019-0140-8.

Quan, J. and Tian, J. (2009) 'Circular polymerase extension cloning of complex gene libraries and pathways', *PLoS ONE*. Public Library of Science, 4(7), p. 6441. doi: 10.1371/journal.pone.0006441.

Quinones, Q. J., de Ridder, G. G. and Pizzo, S. V (2008) 'GRP78: a chaperone with diverse roles beyond the endoplasmic reticulum.', *Histology and histopathology*, 23(11), pp. 1409–16. doi: 10.14670/HH-23.1409.

Rajah, M. M., Monel, B. and Schwartz, O. (2020) 'The entanglement between flaviviruses and ER-shaping proteins', *PLOS Pathogens*. Edited by M. J. Evans. Public Library of Science, 16(4), p. e1008389. doi: 10.1371/journal.ppat.1008389.

Ramanathan, H. N. *et al*. (2020) 'A sensitive yellow fever virus entry reporter identifies valosin-containing protein (VCP/P97) as an essential host factor for flavivirus uncoating', *mBio*. American Society for Microbiology, 11(2). doi: 10.1128/mBio.00467-20.

Rana, J. *et al*. (2018) 'Role of Capsid Anchor in the Morphogenesis of Zika Virus',

Journal of Virology. American Society for Microbiology, 92(22). doi: 10.1128/jvi.01174-18.

Randolph, V. B., Winkler, G. and Stollar, V. (1990) 'Acidotropic amines inhibit proteolytic processing of flavivirus prM protein', *Virology*. Academic Press, 174(2), pp. 450–458. doi: 10.1016/0042-6822(90)90099-D.

Rao, V. B. *et al*. (2019) 'Future increase in extreme El Nino events under greenhouse warming increases Zika virus incidence in South America', *npj Climate and Atmospheric Science*. Nature Research, 2(1), pp. 1–7. doi: 10.1038/s41612-019-0061-0.

Rastogi, M., Sharma, N. and Singh, S. K. (2016) 'Flavivirus NS1: A multifaceted enigmatic viral protein', *Virology Journal*. BioMed Central Ltd. doi: 10.1186/s12985-016-0590-7.

Rathore, A. P. S. and St. John, A. L. (2020) 'Cross-Reactive Immunity Among Flaviviruses', *Frontiers in Immunology*. Frontiers Media S.A., p. 334. doi: 10.3389/fimmu.2020.00334.

Rawle, R. J. *et al*. (2018) 'PH Dependence of Zika Membrane Fusion Kinetics Reveals an Off-Pathway State', *ACS Central Science*. American Chemical Society, 4(11), pp. 1503–1510. doi: 10.1021/acscentsci.8b00494.

Ricciardi-Jorge, T. *et al*. (2017) 'Development of a quantitative NS1-capture enzyme-linked immunosorbent assay for early detection of yellow fever virus infection', *Scientific Reports*. Nature Publishing Group, 7(1), pp. 1–9. doi: 10.1038/s41598-017-16231-6.

Van Rij, R. P. *et al*. (2006) 'The RNA silencing endonuclease Argonaute 2 mediates specific antiviral immunity in Drosophila melanogaster', *Genes and Development*.

Cold Spring Harbor Laboratory Press, 20(21), pp. 2985–2995. doi: 10.1101/gad.1482006.

Roby, J. A. *et al*. (2015) 'Post-translational regulation and modifications of flavivirus structural proteins', *Journal of General Virology*. Society for General Microbiology, pp. 1551–1569. doi: 10.1099/vir.0.000097.

Rodenhuis-Zybert, I. A. *et al*. (2010) 'Immature dengue virus: A veiled pathogen?', *PLoS Pathogens*. Public Library of Science, 6(1). doi: 10.1371/journal.ppat.1000718.

Rombi, F. *et al*. (2020) 'The journey of Zika to the developing brain', *Molecular Biology Reports*. Springer, pp. 3097–3115. doi: 10.1007/s11033-020-05349-y.

Rosales Ramirez, R. and Ludert, J. E. (2018) 'The Dengue Virus Nonstructural Protein 1 (NS1) Is Secreted from Mosquito Cells in Association with the Intracellular Cholesterol Transporter Chaperone Caveolin Complex', *Journal of Virology*. American Society for Microbiology, 93(4). doi: 10.1128/jvi.01985-18.

Rosen, L. (1988) 'Further observations on the mechanism of vertical transmission of flaviviruses by Aedes mosquitoes', *American Journal of Tropical Medicine and Hygiene*. Am J Trop Med Hyg, 39(1), pp. 123–126. doi: 10.4269/ajtmh.1988.39.123.

Roth, H. *et al*. (2017) 'Flavivirus infection uncouples translation suppression from cellular stress responses', *mBio*. American Society for Microbiology, 8(1). doi: 10.1128/mBio.02150-16.

Roux, L. (1990) 'Selective and transient association of sendai virus HN glycoprotein with BiP', *Virology*, 175(1), pp. 161–166. doi: 10.1016/0042-6822(90)90196-X.

Royle, J. *et al*. (2020) 'Glucose-Regulated Protein 78 Interacts with Zika Virus Envelope Protein and Contributes to a Productive Infection', *Viruses*, 12(5), p. 524. doi: 10.3390/v12050524.

Saeedi, B. J. and Geiss, B. J. (2013) 'Regulation of flavivirus RNA synthesis and capping', *Wiley Interdisciplinary Reviews: RNA*. NIH Public Access, pp. 723–735. doi: 10.1002/wrna.1191.

Sagara, K. R. D. *et al*. (2018) 'Glucose-regulated protein 78 substrate-binding domain alters its conformation upon EGCG inhibitor binding to nucleotide-binding domain: Molecular dynamics studies OPEN', *SCIeNTIfIC REpoRtS* |, 8, p. 5487. doi: 10.1038/s41598-018-22905-6.

Salas-Benito, J. S. and De Nova-Ocampo, M. (2015) 'Viral interference and persistence in mosquito-borne flaviviruses', *Journal of Immunology Research*. Hindawi Publishing Corporation. doi: 10.1155/2015/873404.

Saldaña, M. A. *et al*. (2017) 'Zika virus alters the microRNA expression profile and elicits an RNAi response in Aedes aegypti mosquitoes', *PLOS Neglected Tropical Diseases*. Edited by P. M. Armstrong. Public Library of Science, 11(7), p. e0005760. doi: 10.1371/journal.pntd.0005760.

Sánchez-Vargas, I. *et al*. (2009) 'Dengue virus type 2 infections of Aedes aegypti are modulated by the mosquito's RNA interference pathway', *PLoS Pathogens*. Public Library of Science, 5(2). doi: 10.1371/journal.ppat.1000299.

Sanchez-Velazquez, R. *et al*. (2020) 'Generation of a reporter yellow fever virus for high throughput antiviral assays', *Antiviral Research*. Elsevier B.V., 183, p. 104939. doi: 10.1016/j.antiviral.2020.104939.

Sanford, T. J. *et al*. (2019) 'Circularization of flavivirus genomic RNA inhibits de

novo translation initiation', *Nucleic acids research*. NLM (Medline), 47(18), pp. 9789–9802. doi: 10.1093/nar/gkz686.

Sano, R. and Reed, J. C. (2013) 'ER stress-induced cell death mechanisms', *Biochimica et Biophysica Acta - Molecular Cell Research*. Elsevier, pp. 3460–3470. doi: 10.1016/j.bbamcr.2013.06.028.

Dos Santos, C. R. *et al*. (2020) 'Insecticide resistance, fitness and susceptibility to Zika infection of an interbred Aedes aegypti population from Rio de Janeiro, Brazil', *Parasites and Vectors*. BioMed Central Ltd., 13(1), p. 293. doi: 10.1186/s13071-020-04166-3.

Sasaki, T. *et al*. (2017) 'Argonaute 2 suppresses Japanese encephalitis virus infection in Aedes aegypti', *Japanese Journal of Infectious Diseases*. National Institute of Health, 70(1), pp. 38–44. doi: 10.7883/yoken.JJID.2015.671.

Savidis, G. *et al*. (2016) 'Identification of Zika Virus and Dengue Virus Dependency Factors using Functional Genomics', *CellReports*, 16, pp. 232–246. doi: 10.1016/j.celrep.2016.06.028.

Scaturro, P. *et al*. (2018) 'An orthogonal proteomic survey uncovers novel Zika virus host factors', *Nature*. Nature Publishing Group, pp. 253–257. doi: 10.1038/s41586-018-0484-5.

Scaturro, P., Kastner, A. L. and Pichlmair, A. (2019) 'Chasing intracellular Zika virus using proteomics', *Viruses*. MDPI AG, 11(9). doi: 10.3390/v11090878.

Schnettler, E. *et al*. (2013) 'Knockdown of piRNA pathway proteins results in enhanced semliki forest virus production in mosquito cells', *Journal of General Virology*. Microbiology Society, 94(PART7), pp. 1680–1689. doi: 10.1099/vir.0.053850-0.

Schuessler, A. *et al.* (2012) 'West Nile Virus Noncoding Subgenomic RNA Contributes to Viral Evasion of the Type I Interferon-Mediated Antiviral Response', *Journal of Virology*. American Society for Microbiology, 86(10), pp. 5708–5718. doi: 10.1128/jvi.00207-12.

Schultz, M. J. *et al.* (2017) 'Variable Inhibition of Zika Virus Replication by Different Wolbachia Strains in Mosquito Cell Cultures', *Journal of Virology*. American Society for Microbiology, 91(14), pp. 339–356. doi: 10.1128/jvi.00339-17.

Schultz, M. J. *et al.* (2018) 'Wolbachia wStri blocks Zika virus growth at two independent stages of viral replication', *mBio*. American Society for Microbiology, 9(3), pp. 738–756. doi: 10.1128/mBio.00738-18.

Scott, T. W. and Takken, W. (2012) 'Feeding strategies of anthropophilic mosquitoes result in increased risk of pathogen transmission', *Trends in Parasitology*. Elsevier Current Trends, pp. 114–121. doi: 10.1016/j.pt.2012.01.001.

Setoh, Y. X. *et al.* (2017) 'De Novo Generation and Characterization of New Zika Virus Isolate Using Sequence Data from a Microcephaly Case'. doi: 10.1128/mSphereDirect.00190-17.

Shah, P. S. *et al.* (2018) 'Comparative Flavivirus-Host Protein Interaction Mapping Reveals Mechanisms of Dengue and Zika Virus Pathogenesis', *Cell*. Cell Press, 175(7), pp. 1931-1945.e18. doi: 10.1016/J.CELL.2018.11.028.

Shalem, O. *et al.* (2014) 'Genome-scale CRISPR-Cas9 knockout screening in human cells', *Science*. American Association for the Advancement of Science, 343(6166), pp. 84–87. doi: 10.1126/science.1247005.

Shang, Z. *et al*. (2018) 'Crystal Structure of the Capsid Protein from Zika Virus', *Journal of Molecular Biology*. Academic Press, 430(7), pp. 948–962. doi: 10.1016/j.jmb.2018.02.006.

Sharma, N. *et al*. (2017) 'Epigallocatechin gallate, an active green tea compound inhibits the Zika virus entry into host cells via binding the envelope protein', *International Journal of Biological Macromolecules*. Elsevier B.V., 104, pp. 1046–1054. doi: 10.1016/j.ijbiomac.2017.06.105.

Shearer, F. M. *et al*. (2018) 'Existing and potential infection risk zones of yellow fever worldwide: a modelling analysis', *The Lancet Global Health*. Elsevier Ltd, 6(3), pp. e270–e278. doi: 10.1016/S2214-109X(18)30024-X.

Shen, J. *et al*. (2002) 'ER stress regulation of ATF6 localization by dissociation of BiP/GRP78 binding and unmasking of golgi localization signals', *Developmental Cell*. Cell Press, 3(1), pp. 99–111. doi: 10.1016/S1534-5807(02)00203-4.

Shen, Y., Meunier, L. and Hendershot, L. M. (2002) 'Identification and characterization of a novel endoplasmic reticulum (ER) DnaJ homologue, which stimulates ATPase activity of BiP in vitro and is induced by ER stress', *Journal of Biological Chemistry*. Elsevier, 277(18), pp. 15947–15956. doi: 10.1074/jbc.M112214200.

Shi-Chen Ou, D. *et al*. (2011) 'Transcriptional activation of endoplasmic reticulum chaperone GRP78 by HCMV IE1-72 protein', *Cell Research*. Nature Publishing Group, 21(4), pp. 642–653. doi: 10.1038/cr.2011.10.

Shi, Y. *et al*. (2018) 'Structures of zika virus E & NS1: Relations with virus infection and host immune responses', in *Advances in Experimental Medicine and Biology*. Springer New York LLC, pp. 77–87. doi: 10.1007/978-981-10-8727-1_6.

Shing, E. *et al.* (2019) 'The direct healthcare costs attributable to West Nile virus illness in Ontario, Canada: A population-based cohort study using laboratory and health administrative data', *BMC Infectious Diseases*. BioMed Central Ltd., 19(1), p. 1059. doi: 10.1186/s12879-019-4596-9.

Simmonds, P. *et al.* (2017) 'ICTV virus taxonomy profile: Flaviviridae', *Journal of General Virology*. Microbiology Society, 98(1), pp. 2–3. doi: 10.1099/jgv.0.000672.

Simon, O. *et al.* (2018) 'Zika virus outbreak in New Caledonia and Guillain-Barré syndrome: a case-control study', *Journal of NeuroVirology*. Springer, 24(3), pp. 362–368. doi: 10.1007/s13365-018-0621-9.

Simpson, D. I. H. (1964) 'Zika virus infection in man', *Transactions of the Royal Society of Tropical Medicine and Hygiene*, 58(4), pp. 335–338. doi: 10.1016/0035-9203(64)90201-9.

Sirohi, D. *et al.* (2016) 'The 3.8 Å resolution cryo-EM structure of Zika virus.', *Science (New York, N.Y.)*. American Association for the Advancement of Science, 352(6284), pp. 467–70. doi: 10.1126/science.aaf5316.

Sirohi, D. and Kuhn, R. J. (2017) 'Zika Virus Structure, Maturation, and Receptors', *The Journal of Infectious Diseases*. Narnia, 216(suppl_10), pp. S935–S944. doi: 10.1093/infdis/jix515.

Slonchak, A. *et al.* (2020) 'Zika virus noncoding RNA suppresses apoptosis and is required for virus transmission by mosquitoes', *Nature Communications*. Nature Research, 11(1). doi: 10.1038/s41467-020-16086-y.

Smit, J. M. *et al.* (2011) 'Flavivirus cell entry and membrane fusion', *Viruses*. Multidisciplinary Digital Publishing Institute (MDPI), 3(2), pp. 160–171. doi: 10.3390/v3020160.

Smith, D. B. *et al.* (2014) 'Expanded classification of hepatitis C virus into 7 genotypes and 67 subtypes: Updated criteria and genotype assignment web resource', *Hepatology*. John Wiley and Sons Inc., 59(1), pp. 318–327. doi: 10.1002/hep.26744.

Smith, D. B. *et al.* (2017) 'Proposed revision to the taxonomy of the genus Pestivirus, family Flaviviridae', *Journal of General Virology*. Microbiology Society, 98(8), pp. 2106–2112. doi: 10.1099/jgv.0.000873.

Sotelo, J. R. *et al.* (2017) 'Persistence of Zika Virus in Breast Milk after Infection in Late Stage of Pregnancy', *Emerging infectious diseases*. Centers for Disease Control and Prevention, 23(5), pp. 856–857. doi: 10.3201/eid2305.161538.

Souza-Neto, J. A., Sim, S. and Dimopoulos, G. (2009) 'An evolutionary conserved function of the JAK-STAT pathway in anti-dengue defense', *Proceedings of the National Academy of Sciences of the United States of America*. National Academy of Sciences, 106(42), pp. 17841–17846. doi: 10.1073/pnas.0905006106.

Spuul, P. *et al.* (2011) 'Assembly of Alphavirus Replication Complexes from RNA and Protein Components in a Novel trans-Replication System in Mammalian Cells', *Journal of Virology*. American Society for Microbiology, 85(10), pp. 4739–4751. doi: 10.1128/jvi.00085-11.

Srivastava, M. *et al.* (2020) 'Chemical proteomics tracks virus entry and uncovers NCAM1 as Zika virus receptor', *Nature Communications*. Nature Research, 11(1), pp. 1–10. doi: 10.1038/s41467-020-17638-y.

Stiasny, K. *et al.* (2011) 'Molecular mechanisms of flavivirus membrane fusion', *Amino Acids*. Springer, pp. 1159–1163. doi: 10.1007/s00726-009-0370-4.

Strange, D. P. *et al.* (2019) 'Axl promotes zika virus entry and modulates the

antiviral state of human sertoli cells', *mBio*. American Society for Microbiology, 10(4). doi: 10.1128/mBio.01372-19.

Sun, F.-C. *et al*. (2006) 'Localization of GRP78 to mitochondria under the unfolded protein response.', *The Biochemical journal*. Portland Press Ltd, 396(1), pp. 31–9. doi: 10.1042/BJ20051916.

Sun, H., Chen, Q. and Lai, H. (2018) 'Development of antibody therapeutics against flaviviruses', *International Journal of Molecular Sciences*. MDPI AG. doi: 10.3390/ijms19010054.

Swarbrick, C. M. D. *et al*. (2017) 'NS3 helicase from dengue virus specifically recognizes viral RNA sequence to ensure optimal replication', *Nucleic Acids Research*. Oxford University Press, 45(22), pp. 12904–12920. doi: 10.1093/nar/gkx1127.

Symptoms, Diagnosis, & Treatment | West Nile Virus | CDC (2018). Available at: https://www.cdc.gov/westnile/symptoms/index.html (Accessed: 15 January 2021).

Syzdykova, L. R. *et al*. (2021) 'Fluorescent tagging the NS1 protein in yellow fever virus: Replication-capable viruses which produce the secretory GFP-NS1 fusion protein', *Virus Research*. Elsevier B.V., 294, p. 198291. doi: 10.1016/j.virusres.2020.198291.

Szklarczyk, D. *et al*. (2019) 'STRING v11: Protein-protein association networks with increased coverage, supporting functional discovery in genome-wide experimental datasets', *Nucleic Acids Research*. Oxford University Press, 47(D1), pp. D607–D613. doi: 10.1093/nar/gky1131.

Tajima, S. *et al*. (2005) 'Genetic characterization of Yokose virus, a flavivirus

isolated from the bat in Japan', *Virology*. Virology, 332(1), pp. 38–44. doi: 10.1016/j.virol.2004.06.052.

Takahashi, S. *et al*. (2012) 'Rab11 regulates exocytosis of recycling vesicles at the plasma membrane', *Journal of Cell Science*. The Company of Biologists Ltd, 125(17), pp. 4049–4057. doi: 10.1242/jcs.102913.

Tamhankar, M. and Patterson, J. L. (2019) 'Directional entry and release of Zika virus from polarized epithelial cells', *Virology Journal*. BioMed Central Ltd., 16(1), p. 99. doi: 10.1186/s12985-019-1200-2.

Tan, L. K. *et al*. (2019) 'Flavivirus Cross-Reactivity to Dengue Nonstructural Protein 1 Antigen Detection Assays', *Diagnostics*. MDPI AG, 10(1), p. 11. doi: 10.3390/diagnostics10010011.

Tan, T. Y. *et al*. (2020) 'Capsid protein structure in Zika virus reveals the flavivirus assembly process', *Nature Communications*. Nature Research, 11(1). doi: 10.1038/s41467-020-14647-9.

Tan, T. Y., Fibriansah, G. and Lok, S.-M. (2020) 'Capsid protein is central to the birth of flavivirus particles', *PLOS Pathogens*. Edited by M. J. Evans. Public Library of Science, 16(5), p. e1008542. doi: 10.1371/journal.ppat.1008542.

Tan, Z. *et al*. (2018) 'ZIKV infection activates the IRE1-XBP1 and ATF6 pathways of unfolded protein response in neural cells', *Journal of Neuroinflammation*. BioMed Central Ltd., 15(1), p. 275. doi: 10.1186/s12974-018-1311-5.

Tassetto, M. *et al*. (2019) 'Control of RNA viruses in mosquito cells through the acquisition of vDNA and endogenous viral elements', *eLife*. eLife Sciences Publications Ltd, 8. doi: 10.7554/eLife.41244.

Teixeira, F. M. E. *et al*. (2020) 'Maternal-Fetal Interplay in Zika Virus Infection and Adverse Perinatal Outcomes', *Frontiers in Immunology*. Frontiers Media S.A., p. 175. doi: 10.3389/fimmu.2020.00175.

The Lancet Infectious Diseases (2018) 'The dengue vaccine dilemma', *The Lancet Infectious Diseases*. Lancet Publishing Group, p. 123. doi: 10.1016/S1473-3099(18)30023-9.

Thomas, S. J. and Yoon, I. K. (2019) 'A review of Dengvaxia®: development to deployment', *Human Vaccines and Immunotherapeutics*. Taylor and Francis Inc., 15(10), pp. 2295–2314. doi: 10.1080/21645515.2019.1658503.

Ting, J. and Lee, A. S. (1988) 'Human Gene Encoding the 78,000-Dalton Glucose-Regulated Protein and Its Pseudogene: Structure, Conservation, and Regulation', *DNA*. DNA, 7(4), pp. 275–286. doi: 10.1089/dna.1988.7.275.

Tolosa, N. *et al*. (2017) 'Zika Virus Disease in Children in Colombia, August 2015 to May 2016', *Paediatric and Perinatal Epidemiology*. Blackwell Publishing Ltd, 31(6), pp. 537–545. doi: 10.1111/ppe.12391.

Tsai, Y. L. *et al*. (2015) 'Characterization and mechanism of stress-induced translocation of 78-kilodalton glucose-regulated protein (GRP78) to the cell surface', *Journal of Biological Chemistry*. American Society for Biochemistry and Molecular Biology Inc., 290(13), pp. 8049–8064. doi: 10.1074/jbc.M114.618736.

Tseng, C. C., Zhang, P. and Lee, A. S. (2019) 'The COOH-Terminal Proline-Rich Region of GRP78 Is a Key Regulator of Its Cell Surface Expression and Viability of Tamoxifen-Resistant Breast Cancer Cells', *Neoplasia (United States)*. Neoplasia Press, Inc., 21(8), pp. 837–848. doi: 10.1016/j.neo.2019.05.008.

Varjak, M., Maringer, K., *et al*. (2017) 'Aedes aegypti Piwi4 Is a Noncanonical PIWI

Protein Involved in Antiviral Responses.', *mSphere*. American Society for Microbiology (ASM), 2(3). doi: 10.1128/mSphere.00144-17.

Varjak, M., Donald, C. L., *et al*. (2017) 'Characterization of the Zika virus induced small RNA response in Aedes aegypti cells', *PLOS Neglected Tropical Diseases*. Edited by K. E. Olson. Public Library of Science, 11(10), p. e0006010. doi: 10.1371/journal.pntd.0006010.

Varjak, M., Leggewie, M. and Schnettler, E. (2018) 'The antiviral piRNA response in mosquitoes?' doi: 10.1099/jgv.0.001157.

Villordo, S. M., Alvarez, D. E. and Gamarnik, A. V. (2010) 'A balance between circular and linear forms of the dengue virus genome is crucial for viral replication', *RNA*. Cold Spring Harbor Laboratory Press, 16(12), pp. 2325–2335. doi: 10.1261/rna.2120410.

Volk, D. E. *et al*. (2007) 'Solution structure of the envelope protein domain III of dengue-4 virus', *Virology*. NIH Public Access, 364(1), pp. 147–154. doi: 10.1016/j.virol.2007.02.023.

Wang, B. *et al*. (2020) 'Structural basis for STAT2 suppression by flavivirus NS5', *Nature Structural and Molecular Biology*. Nature Research, 27(10), pp. 875–885. doi: 10.1038/s41594-020-0472-y.

Wang, M. *et al*. (2009) 'Role of the unfolded protein response regulator GRP78/BiP in development, cancer, and neurological disorders.', *Antioxidants & redox signaling*. Mary Ann Liebert, Inc., 11(9), pp. 2307–16. doi: 10.1089/ars.2009.2485.

Wang, M. *et al*. (2010) 'Essential role of the unfolded protein response regulator GRP78/BiP in protection from neuronal apoptosis', *Cell Death and Differentiation*. Nature Publishing Group, 17(3), pp. 488–498. doi: 10.1038/cdd.2009.144.

Wang, R. Y. L. *et al*. (2016) 'A KDEL retrieval system for ER-golgi transport of Japanese encephalitis viral particles', *Viruses*. MDPI AG, 8(2). doi: 10.3390/v8020044.

Wati, S. *et al*. (2009) 'Dengue virus infection induces upregulation of GRP78, which acts to chaperone viral antigen production.', *Journal of virology*. American Society for Microbiology Journals, 83(24), pp. 12871–80. doi: 10.1128/JVI.01419-09.

Weaver, S. C. and Reisen, W. K. (2010) 'Present and future arboviral threats', *Antiviral Research*. NIH Public Access, pp. 328–345. doi: 10.1016/j.antiviral.2009.10.008.

Welsch, S. *et al*. (2009) 'Composition and Three-Dimensional Architecture of the Dengue Virus Replication and Assembly Sites', *Cell Host and Microbe*, 5(4), pp. 365–375. doi: 10.1016/j.chom.2009.03.007.

Wey, S. *et al*. (2012) 'Inducible knockout of GRP78/BiP in the hematopoietic system suppresses Pten-null leukemogenesis andAKT oncogenic signaling', *Blood*. American Society of Hematology, 119(3), pp. 817–825. doi: 10.1182/blood-2011-06-357384.

White, J. M. *et al*. (2008) 'Structures and mechanisms of viral membrane fusion proteins: Multiple variations on a common theme', *Critical Reviews in Biochemistry and Molecular Biology*. Taylor and Francis Inc., pp. 189–219. doi: 10.1080/10409230802058320.

'WHO | The history of Zika virus' (2019) *WHO*. World Health Organization. Available at: http://www.who.int/emergencies/zika-virus/timeline/en/ (Accessed: 22 June 2020).

'WHO | WHO vaccine pipeline tracker' (2016) *WHO*. World Health Organization. Available at: http://www.who.int/immunization/research/vaccine_pipeline_tracker_spreadsheet/en/ (Accessed: 18 January 2021).

Widman, D. G. *et al*. (2017) 'A reverse genetics platform that spans the Zika virus family tree', *mBio*. American Society for Microbiology, 8(2). doi: 10.1128/mBio.02014-16.

Wilder-Smith, A. *et al*. (2018) 'Zika vaccines and therapeutics: Landscape analysis and challenges ahead', *BMC Medicine*. BioMed Central Ltd., 16(1), p. 84. doi: 10.1186/s12916-018-1067-x.

Williams, S. H. *et al*. (2020) 'Discovery of Jogalong virus, a novel hepacivirus identified in a Culex annulirostris (Skuse) mosquito from the Kimberley region of Western Australia', *PLOS ONE*. Edited by N. Forrester. Public Library of Science, 15(1), p. e0227114. doi: 10.1371/journal.pone.0227114.

Wu, Y. P. *et al*. (2011) 'Japanese encephalitis virus co-opts the ER-stress response protein GRP78 for viral infectivity', *Virology Journal*. BioMed Central, 8, p. 128. doi: 10.1186/1743-422X-8-128.

Xia, H. *et al*. (2018) 'An evolutionary NS1 mutation enhances Zika virus evasion of host interferon induction.', *Nature communications*. Nature Publishing Group, 9(1), p. 414. doi: 10.1038/s41467-017-02816-2.

Xie, X. *et al*. (2013) 'Membrane Topology and Function of Dengue Virus NS2A Protein', *Journal of Virology*. American Society for Microbiology, 87(8), pp. 4609–4622. doi: 10.1128/jvi.02424-12.

Xie, X. *et al*. (2019) 'Dengue NS2A Protein Orchestrates Virus Assembly', *Cell Host*

and Microbe. Cell Press, 26(5), pp. 606-622.e8. doi: 10.1016/j.chom.2019.09.015.

Xu, H. (2018) 'Cochaperones enable Hsp70 to use ATP energy to stabilize native proteins out of the folding equilibrium', *Scientific Reports*. Nature Publishing Group, 8(1), p. 13213. doi: 10.1038/s41598-018-31641-w.

Yadav, P. D. *et al.* (2019) 'Zika virus outbreak in Rajasthan, India in 2018 was caused by a virus endemic to Asia', *Infection, Genetics and Evolution*. Elsevier B.V., 69, pp. 199–202. doi: 10.1016/j.meegid.2019.01.026.

Yakub, I. *et al.* (2005) 'Single nucleotide polymorphisms in genes for 2′-5′-oligoadenylate synthetase and RNase L in patients hospitalized with West Nile virus infection', *Journal of Infectious Diseases*. J Infect Dis, 192(10), pp. 1741–1748. doi: 10.1086/497340.

Yang, J. *et al.* (2015) 'Close and Allosteric Opening of the Polypeptide-Binding Site in a Human Hsp70 Chaperone BiP', *Structure*. Cell Press, 23(12), pp. 2191–2203. doi: 10.1016/j.str.2015.10.012.

Yao, Y. *et al.* (2019) 'Discovery, X-ray Crystallography and Antiviral Activity of Allosteric Inhibitors of Flavivirus NS2B-NS3 Protease', *Journal of the American Chemical Society*. American Chemical Society, 141(17), pp. 6832–6836. doi: 10.1021/jacs.9b02505.

Yap, S. S. L. *et al.* (2017) 'Dengue virus glycosylation: What do we know?', *Frontiers in Microbiology*. Frontiers Media S.A., p. 1415. doi: 10.3389/fmicb.2017.01415.

Yellow fever (2019). Available at: https://www.who.int/news-room/fact-sheets/detail/yellow-fever (Accessed: 24 March 2021).

Yuan, L. *et al*. (2017) 'A single mutation in the prM protein of Zika virus contributes to fetal microcephaly', *Science*. American Association for the Advancement of Science, 358(6365), pp. 933–936. doi: 10.1126/science.aam7120.

Zaitsev, B. N. *et al*. (2014) 'Force-induced globule-coil transition in laminin binding protein and its role for viral-cell membrane fusion', *Journal of Molecular Recognition*. John Wiley and Sons Ltd, 27(12), pp. 727–738. doi: 10.1002/jmr.2399.

Zhang, F. C. *et al*. (2016) 'Excretion of infectious Zika virus in urine', *The Lancet Infectious Diseases*. Lancet Publishing Group, pp. 641–642. doi: 10.1016/S1473-3099(16)30070-6.

Zhang, N. *et al*. (2016) 'Zika Virus Disrupts Neural Progenitor Development and Leads to Microcephaly in Mice', *Cell Stem Cell*. Cell Press, 19(1), pp. 120–126. doi: 10.1016/j.stem.2016.04.017.

Zhang, S. *et al*. (2019) 'Chloroquine inhibits endosomal viral RNA release and autophagy-dependent viral replication and effectively prevents maternal to fetal transmission of Zika virus', *Antiviral Research*. Elsevier B.V., 169. doi: 10.1016/j.antiviral.2019.104547.

Zhang, W. *et al*. (2019) 'In utero infection of Zika virus leads to abnormal central nervous system development in mice', *Scientific Reports*. Nature Publishing Group, 9(1). doi: 10.1038/s41598-019-43303-6.

Zhang, X. *et al*. (2017) 'Structures and functions of the envelope glycoprotein in flavivirus infections', *Viruses*. MDPI AG. doi: 10.3390/v9110338.

Zhang, X. *et al*. (2019) 'Zika virus NS2A-mediated virion assembly', *mBio*. American Society for Microbiology, 10(5), pp. 2375–2394. doi:

10.1128/mBio.02375-19.

Zhang, Y. *et al*. (2003) 'Structures of immature flavivirus particles', *EMBO Journal*. European Molecular Biology Organization, 22(11), pp. 2604–2613. doi: 10.1093/emboj/cdg270.

Zhang, Y. *et al*. (2010) 'Cell surface relocalization of the endoplasmic reticulum chaperone and unfolded protein response regulator GRP78/BiP.', *The Journal of biological chemistry*. American Society for Biochemistry and Molecular Biology, 285(20), pp. 15065–75. doi: 10.1074/jbc.M109.087445.

Zhang, Z. *et al*. (2018) 'TAOK1 negatively regulates IL-17-mediated signaling and inflammation', *Cellular and Molecular Immunology*. Chinese Soc Immunology, 15(8), pp. 794–802. doi: 10.1038/cmi.2017.158.

Zhao, B. *et al*. (2017) 'Structure and function of the Zika virus full-length NS5 protein', *Nature Communications*. Nature Publishing Group, 8(1), pp. 1–9. doi: 10.1038/ncomms14762.

Zhao, D. *et al*. (2018) 'Identification of Glucose-Regulated Protein 78 (GRP78) as a Receptor in BHK-21 Cells for Duck Tembusu Virus Infection.', *Frontiers in microbiology*. Frontiers Media SA, 9, p. 694. doi: 10.3389/fmicb.2018.00694.

Zhong, C. *et al*. (2019) 'Proteomics analysis reveals heat shock proteins involved in caprine parainfluenza virus type 3 infection', *BMC Veterinary Research*. BioMed Central Ltd., 15(1), p. 151. doi: 10.1186/s12917-019-1897-6.

Zhou, D. H., Wang, X. and Feng, Q. (2014) 'EGCG enhances the efficacy of cisplatin by downregulating hsa-miR-98-5p in NSCLC A549 cells', *Nutrition and Cancer*. Routledge, 66(4), pp. 636–644. doi: 10.1080/01635581.2014.894101.

Zhou, Y. *et al*. (2007) 'Structure and Function of Flavivirus NS5 Methyltransferase', *Journal of Virology*. American Society for Microbiology, 81(8), pp. 3891–3903. doi: 10.1128/jvi.02704-06.

Zhu, G. *et al*. (2013) 'GRP78 plays an essential role in adipogenesis and postnatal growth in mice', *FASEB Journal*. The Federation of American Societies for Experimental Biology, 27(3), pp. 955–964. doi: 10.1096/fj.12-213330.

Zhu, G. and Lee, A. S. (2015) 'Role of the unfolded protein response, GRP78 and GRP94 in organ homeostasis', *Journal of Cellular Physiology*. Wiley-Liss Inc., 230(7), pp. 1413–1420. doi: 10.1002/jcp.24923.

Zhu, L. *et al*. (2015) 'Conformational change study of dengue virus NS2B-NS3 protease using 19F NMR spectroscopy', *Biochemical and Biophysical Research Communications*. Academic Press Inc., 461(4), pp. 677–680. doi: 10.1016/j.bbrc.2015.04.090.

Zmurko, J., Neyts, J. and Dallmeier, K. (2015) 'Flaviviral NS4b, chameleon and jack-in-the-box roles in viral replication and pathogenesis, and a molecular target for antiviral intervention', *Reviews in Medical Virology*. John Wiley and Sons Ltd, pp. 205–223. doi: 10.1002/rmv.1835.

Zou, J. *et al*. (2014) 'Dimerization of Flavivirus NS4B Protein', *Journal of Virology*. American Society for Microbiology, 88(6), pp. 3379–3391. doi: 10.1128/jvi.02782-13.

Chapter 9. Appendices

9.1 Sequence alignments

```
Aedes_aegypti        MKLLVPLALVAAVAVL----TCTAEEKKEQDYGTVVGIDLGTTYSCVGVYKNGRVEIIAN 56
Aedes_albopictus     MKLLVPLALVAALAVL----SCTAEEKKEQDYGTVVGIDLGTTYSCVGVYKNGRVEIIAN 56
Bovine               ----MKLSLVAAVLLLLLGTARAEEEDKKEDVGTVVGIDLGTTYSCVGVFKNGRVEIIAN 56
Human                ----MKLSLVAA-MLLLLSAARAEEEDKKEDVGTVVGIDLGTTYSCVGVFKNGRVEIIAN 55
Mouse                ---MMKFTVVAA-ALLLLGAVRAEEEDKKEDVGTVVGIDLGTTYSCVGVFKNGRVEIIAN 56
                        : :::***  :*      : **.*::* *****************:**********

Aedes_aegypti        DQGNRITPSYVAFTADGERLIGDAAKNQLTTNPENTVFDAKRLIGREFTDSTVQHDAKLL 116
Aedes_albopictus     DQGNRITPSYVAFTADGERLIGDAAKNQLTTNPENTVFDAKRLIGREFTDSTVQHDAKLL 116
Bovine               DQGNRITPSYVAFTPEGERLIGDAAKNQLTSNPENTVFDAKRLIGRTWNDPSVQQDIKFL  116
Human                DQGNRITPSYVAFTPEGERLIGDAAKNQLTSNPENTVFDAKRLIGRTWNDPSVQQDIKFL  115
Mouse                DQGNRITPSYVAFTPEGERLIGDAAKNQLTSNPENTVFDAKRLIGRTWNDPSVQQDIKFL  116
                     ************** :***************:*************** :.* :**:* *:*

Aedes_aegypti        PFKVIEKNSKPHIKVSTSQG-DKVFAPEEISAMVLGKMKETAEAYLGKKVTHAVVTVPAY 175
Aedes_albopictus     PFKVIEKNSKPHIKVSTSQG-DKVFAPEEISAMVLGKMKETAEAYLGKKVTHAVVTVPAY 175
Bovine               PFKVVEKKTKPYIQVDVGGGQTKTFAPEEISAMVLTKMKETAEAYLGKKVTHAVVTVPAY  176
Human                PFKVVEKKTKPYIQVDIGGGQTKTFAPEEISAMVLTKMKETAEAYLGKKVTHAVVTVPAY  175
Mouse                PFKVVEKKTKPYIQVDIGGGQTKTFAPEEISAMVLTKMKETAEAYLGKKVTHAVVTVPAY  176
                     ****:**::**:*:*. . *  *.*********** ************************

Aedes_aegypti        FNDAQRQATKDAGVIAGLNVMRIINEPTAAAIAYGLDKKDGEKNVLVFDLGGGTFDVSLL 235
Aedes_albopictus     FNDAQRQATKDAGVIAGLNVMRIINEPTAAAIAYGLDKKDGEKNVLVFDLGGGTFDVSLL 235
Bovine               FNDAQRQATKDAGTIAGLNVMRIINEPTAAAIAYGLDKREGEKNILVFDLGGGTFDVSLL  236
Human                FNDAQRQATKDAGTIAGLNVMRIINEPTAAAIAYGLDKREGEKNILVFDLGGGTFDVSLL  235
Mouse                FNDAQRQATKDAGTIAGLNVMRIINEPTAAAIAYGLDKREGEKNILVFDLGGGTFDVSLL  236
                     *************.************************::****:***************

Aedes_aegypti        TIDNGVFEVVATNGDTHLGGEDFDQRVMDHFIKLYKKKKGKDIRKDNRAVQKLRREVEKA 295
Aedes_albopictus     TIDNGVFEVVATNGDTHLGGEDFDQRVMDHFIKLYKKKKGKDIRKDNRAVQKLRREVEKA 295
Bovine               TIDNGVFEVVATNGDTHLGGEDFDQRVMEHFIKLYKKKTGKDVRKDNRAVQKLRREVEKA  296
Human                TIDNGVFEVVATNGDTHLGGEDFDQRVMEHFIKLYKKKTGKDVRKDNRAVQKLRREVEKA  295
Mouse                TIDNGVFEVVATNGDTHLGGEDFDQRVMEHFIKLYKKKTGKDVRKDNRAVQKLRREVEKA  296
                     ****************************:*********.***:*****************

Aedes_aegypti        KRALSSSHQVRIEIESFYEGDDFSETLTRAKFEELNMDLFRSTMKPVQKVLEDADMNKKD 355
Aedes_albopictus     KRALSSSHQVRIEIESFYEGDDFSETLTRAKFEELNMDLFRSTMKPVQKVLEDADMNKKD 355
Bovine               KRALSSQHQARIEIESFYEGEDFSETLTRAKFEELNMDLFRSTMKPVQKVLEDSDLKKSD  356
Human                K-ALSSQHQARIEIESFYEGEDFSETLTRAKFEELNMDLFRSTMKPVQKVLEDSDLKKSD 354
Mouse                KRALSSQHQARIEIESFFEGEDFSETLTRAKFEELNMDLFRSTMKPVQKVLEDSDLKKSD  356
                     * ****.**.*******:**:*********************************:*::*.*

Aedes_aegypti        VDEIVLVGGSTRIPKVQQLVKEFFNGKEPSRGINPDEAVAYGAAVQAGVLSGEQDTEAIV 415
Aedes_albopictus     VDEIVLVGGSTRIPKVQQLVKEFFNGKEPSRGINPDEAVAYGAAVQAGVLSGEQDTEAIV 415
Bovine               IDEIVLVGGSTRIPKIQQLVKEFFNGKEPSRGINPDEAVAYGAAVQAGVLSGDQDTGDLV  416
Human                IDEIVLVGGSTRIPKIQQLVKEFFNGKEPSRGINPDEAVAYGAAVQAGVLSGDQDTGDLV  414
Mouse                IDEIVLVGGSTRIPKIQQLVKEFFNGKEPSRGINPDEAVAYGAAVQAGVLSGDQDTGDLV  416
                     :**************:************************************:***  :*
```

```
Aedes_aegypti        LLDVNPLTMGIETVGGVMTKLIPRNTVIPTKKSQIFSTASDNQHTVTIQVYEGERPMTKD 475
Aedes_albopictus     LLDVNPLTMGIETVGGVMTKLIPRNTVIPTKKSQIFSTASDNQHTVTIQVYEGERPMTKD 475
Bovine               LLDVCPLTLGIETVGGVMTKLIPRNTVVPTKKSQIFSTASDNQPTVTIKVYEGERPLTKD  476
Human                LLHVCPLTLGIETVGGVMTKLIPSNTVVPTKNSQIFSTASDNQPTVTIKVYEGERPLTKD  474
Mouse                LLDVCPLTLGIETVGGVMTKLIPRNTVVPTKKSQIFSTASDNQPTVTIKVYEGERPLRKD  476
                     **.* ***:************** ***:***:*********** ****:*******: **

Aedes_aegypti        NHLLGKFDLTGIPPAPRGIPQIEVSFEIDANGILQVSAEDKGTGNREKIVITNDQNRLTP 535
Aedes_albopictus     NHLLGKFDLTGIPPAPRGIPQIEVSFEIDANGILQVSAEDKGTGNREKIVITNDQNRLTP 535
Bovine               NHLLGTFDLTGIPPAPRGVPQIEVTFEIDVNGILRVTAEDKGTGNKNKITITNDQNRLTP  536
Human                NHLLGTFDLTGIPPAPRGVPQIEVTFEIDVNGILRVTAEDKGTGNKNKITITNDQNRLTP  534
Mouse                NHLLGTFDLTGIPPAPRGVPQIEVTFEIDVNGILRVTAEDKGTGNKNKITITNDQNRLTP  536
                     *****.************:*****:****.****:*:********::**.**********

Aedes_aegypti        EDIERMIKDAERFADDDKKLKERVEARNELESYAYSLKNQLGDKDKLGAKVADDDKATME 595
Aedes_albopictus     EDIERMIKDAERFADDDKKLKERVEARNELESYAYSLKNQLGDKDKLGAKVADDDKAKME 595
Bovine               EEIERMVNDAEKFAEEDKKLKERIDTRNELESYAYSLKNQIGDKEKLGGKLSSEDKETME  596
Human                EEIERMVNDAEKFAEEDKKLKERIDTRNELESYAYSLKNQIGDKEKLGGKLSSEDKETME  594
Mouse                EEIERMVNDAEKFAEEDKKLKERIDTRNELESYAYSLKNQIGDKEKLGGKLSSEDKETME  596
                     *:****::***:**::*******:::***************:***:***.*::.:** .**

Aedes_aegypti        EAIDEKIKWLDENQDADSEDYKKQKKELEDVVQPIIAKLYASTGGSPPPTADD-EDLKDE 654
Aedes_albopictus     EAIDEKIKWLDENQDADSEDYKKQKKELEDVVQPIIAKLYASTGGSPPPTAGEDDDLKDE 655
Bovine               KAVEEKIEWLESHQDADIEDFKAKKKELEEIVQPIISKLYGSAG  --PPPTSEEEAADKDE 654
Human                KAVEEKIEWLESHQDADIEDFKAKKKELEEIVQPIISKLYGSAG  --PPPTGEEDTAEKDE 652
Mouse                KAVEEKIEWLESHQDADIEDFKAKKKELEEIVQPIISKLYGSGG  --PPPTGEEDTSEKDE 654
                     :*::***:**:.:**** **:* :*****::*****:***.* *  ****. :    ***

Aedes_aegypti        L 655
Aedes_albopictus     L 656
Bovine               L 655
Human                L 653
Mouse                L 655
                     *
```

Figure 9-1: Protein sequence alignment of GRP78

GRP78 sequences were obtained from GenBank and aligned using the Clustal Omega tool from EMBL-EBI (ANO39920.1, ABF18258.1, CAA05361.1, NP_001068616.1, CAA61201.1). Sequence identity, when compared to human GRP78, is as follows. Aedes aegypti = 81.40%, Aedes albopictus = 81.71%, Bovine = 98.02%, Mouse = 97.86%.

```
YFV_NS1          -QGCAINFGKRELKCGDGIFIFRDSDDWLNKYSYYPEDPVKLASIVKASFEEGKCGLNSV 59
DENV-3_NS1       --GCVINWKGKELKCGSGIFVTNEVHTWTEQYKFQADSPKRLATAIAGAWENGVCGIRST 58
ZIKV_NS1         DVGCSVDFSKKETRCGTGVFVYNDVEAWRDRYKYHPDSPRRLAAAVKQAWEDGICGISSV 60
JEV_NS1          -TGCAIDITRKEMRCGSGIFVHNDVEAWVDRYKYLPETPRSLAKIVHKAHKEGVCGVRSV 59
WNV_NS1          -TGCAIDISRQELRCGSGVFIHNDVEAWMDRYKYYPETPQGLAKIIQKAHKEGVCGLRSV 59
                   ** ::   :* :** *:*: .: . * ::*.:  : *  **  :  : ::* **: *.

YFV_NS1          DSLEHEMWRSRADEINAIFEENEVDISVVVQDPKNVYQRGTHPFSRIRDGLQYGWKTWGK 119
DENV-3_NS1       TRMENLLWKQIANELNYILWENNIKLTVVVGDIIGVLEQGKRTLTPQPMELKYSWKTWGK 118
ZIKV_NS1         SRMENIMWRSVEGELNAILEENGVQLTVVVGSVKNPMWGGPQRLPVPVNELPHGWKAWGK 120
JEV_NS1          TRLEHQMWEAVRDELNVLLKENAVDLSVVVNKPVGRYRSAPKRLSMTQEKFEMGWKAWGK 119
WNV_NS1          SRLEHQMWEAVKDELNTLLKENGVDLSVVVEKQEGMYKSAPKRLTATTEKLEIGWKAWGK 119
                   :*: :*.   .*:* :: ** :.::*** .  .    . : :      :  .**:***

YFV_NS1          NLVFSPGRKNGSFIIDGKSRKECPFSNRVWNSFQIEEFGTGVFTTRVYMDAVFEYTIDCD 179
DENV-3_NS1       AKIVTAETQNSSFIIDGPNTPECPNASRAWNVWEVEDYGFGVFTTNIWLKLREMYTQLCD 178
ZIKV_NS1         SHFVRAAKTNNSFVVDGDTLKECPLKHRAWNSFLVEDHGFGVFHTSVWLKVREDYSLECD 180
JEV_NS1          SILFAPELANSTFVVDGPETKECPDEHRAWNSMQIEDFGFGITSTRVWLKIREESTDECD 179
WNV_NS1          SILFAPELANNTFVVDGPETKECPTQNRAWNSLEVEDFGFGLTSTRMFLKVRESNTTECD 179
                   ..     *.:*::**    ***   *.**   :*:.* *:  * :::.     :  **

YFV_NS1          GSILGAAVNGKKSAHGSPTFWMGSHEVNGTWMIHTLEALDYKECEWPLTHTI-GTSVEES 238
DENV-3_NS1       HRLMSAAVKDERAVHADMGYWIES-QKNGSWKLEKASLIEVKTCTWPKSHTLWSNGVLES 237
ZIKV_NS1         PAVIGTAVKGKEAVHSDLGYWIES-EKNDTWRLKRAHLIEMKTCEWPKSHTLWTDGIEES 239
JEV_NS1          GAIIGTAVKGHVAVHSDLSYWIES-RYNDTWKLERAVFGEVKSCTWPETHTLWGDGVEES 238
WNV_NS1          SKIIGTAVKNNLAIHSDLSYWIES-RLNDTWKLERAVLGEVKSCTWPETHTLWGDGILES 238
                   ::.:**:.. : *..  :*: * . *.:* :.     : * * ** :**:   .: **

YFV_NS1          EMFMPRSIGGPVSSHNHIPGYKVQTNGPWMQVPLEVKREACPGTSVIIDGNCDGRGKSTR 298
DENV-3_NS1       DMIIPKSLAGPISQHNYRPGYHTQTAGPWHLGKLELDFNYCEGTTVVITENCGTRGPSLR 297
ZIKV_NS1         DLIIPKSLAGPLSHHNTREGYRTQMKGPWHSEELEIRFEECPGTKVHVEETCGTRGPSLR 299
JEV_NS1          ELIIPHTIAGPKSKHNRREGYKTQNQGPWDENGIVLDFDYCPGTKVTITEDCGKRGPSVR 298
WNV_NS1          DLIIPVTLAGPRSNHNRRPGYKTQNQGPWDEGRVEIDFDYCPGTTVTLSESCGHRGPATR 298
                 ::::* ::.** * **   **:.*  ***    : :  : * **.* :   *. ** : *

YFV_NS1          STTDSGKVIPEWCCRSCTMPPVSFHGSDGCWYPMEIRPRKTHESHLVRSWVTAGEI 354
DENV-3_NS1       TTTVSGKLIHEWCCRSCTLPPLRYMGEDGCWYGMEIRPINEKEENMVKSLVSAGSG 353
ZIKV_NS1         STTASGRVIEEWCCRECTMPPLSFRAKDGCWYGMEIRPRKEPESNLVRSMVTA--- 352
JEV_NS1          TTTDSGKLITDWCCRSCSLPPLRFRTENGCWYGMEIRPVRHDETTLVRSQVDAFNG 354
WNV_NS1          TTTESGKLITDWCCRSCTLPPLRYQTDSGCWYGMEIRPQRHDEKTLVQSQVNA--- 351
                 :** **::* :****.*::**: :  ..**** ***** .  *  :*:* * *
```

Figure 9-2: Protein sequence alignment of flavivirus NS1

NS1 sequences were obtained from GenBank and aligned using the Clustal Omega tool from EMBL-EBI (ANC90426.1, AFN80339.1, AAA81554.1, AGO04419.1, AFX61608.1).